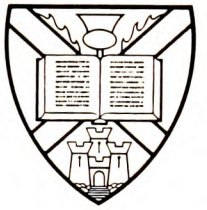

AN EXPERIMENTAL AND ANALYTICAL INVESTIGATION OF THE BEHAVIOUR OF REINFORCED CONCRETE BEAMS SUBJECTED TO COMBINED BENDING AND TORSION

Thesis submitted for the degree of

Doctor of Philosophy

of the

University of Edinburgh

by

Daniel R. Fairbairn, B.Sc.

April, 1967.

CONTENTS

	Page
SYNOPSIS	1
1. INTRODUCTION	3
2. REVIEW OF PREVIOUS INVESTIGATIONS	8
2.1 General	8
2.2 Introduction	8
2.3 Elastic torsion theory	9
2.4 Plastic torsion theory	11
2.5 Combined bending and torsion	12
3. TORSION THEORY FOR A RECTANGULAR SECTION	18
3.1 General	18
3.2 Introduction	18
3.3 St. Venant theory	19
3.4 Membrane theory	22
3.5 Approximate expressions	25
3.6 Plastic theory-sand-heap analogy	25
3.7 Conclusions	26
4. THE BEHAVIOUR OF A REINFORCED CONCRETE BEAM PRIOR TO CRACKING	29
4.1 General	29
4.2 Introduction	29
4.3 Moment of resistance to pure bending	30
4.4 Moment of resistance to pure torsion	36
4.5 Angle of crack	37
4.6 Conclusions	46
5. ULTIMATE LOAD DESIGN	48
5.1 General	48
5.2 Introduction	48

	Page
5.3 Ultimate equilibrium method of design	49
5.4 Design equations for ultimate moment	53
5.5 Ellipse theory	65
5.6 Conclusions	72
6. CALCULATIONS FOR ULTIMATE MOMENTS	76
6.1 General	76
6.2 Introduction	76
6.3 Ultimate moment calculations	77
6.4 Summary of results	85
6.5 Conclusions	89
7. EXPERIMENTAL INVESTIGATION	92
7.1 General	92
7.2 Introduction	92
7.3 Preliminary investigation	93
7.4 Series C, Series D	95
7.5 Series B	104
7.6 Summary of observations	107
7.7 Conclusions	109
8. GRID-FRAMES	112
8.1 General	112
8.2 Introduction	112
8.3 Equilibrium method	113
8.4 Ultimate load method	118
8.5 Conclusions	120
9. CONCLUSIONS	123
9.1 Summary	123
9.2 General conclusions	123
9.3 Future research	130

		Page
ACKNOWLEDGEMENTS		132
REFERENCES		133
APPENDIX A	Angle of inclination of the compression fulcrum	138
APPENDIX B	Torsion moment factor	140
APPENDIX C	Calculations for ultimate moment	142
APPENDIX D	Experimental data	148
APPENDIX E	Computer programmes	151

NOTATION

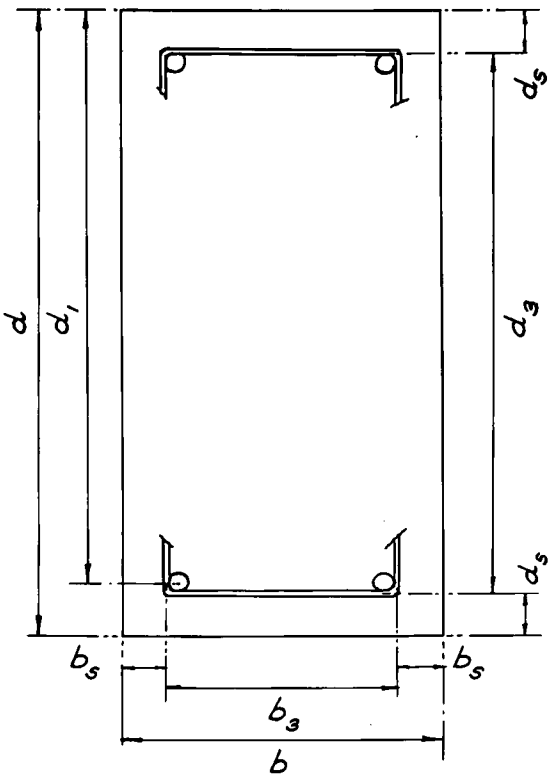

f'_c	ultimate compressive strength of concrete in bending
f_L	yield stress of the longitudinal steel
f_T	yield stress of the transverse steel
A_L	area of longitudinal steel
A_T	area of transverse steel
S	spacing of the transverse steel
t	wall-thickness of hollow beam
n	depth of neutral-axis below top surface of beam
q.d	depth of neutral-axis prior to cracking
d(1 - j)	depth of neutral-axis at ultimate
$\ell_a = g.d$	moment lever arm
f_t	tensile stress of concrete
f_c	compressive stress of concrete

f_p	maximum principal stress
ε_c	compressive strain of concrete
ε_t	tensile strain of concrete
C	compressive force in concrete
T	tensile force in concrete
E	Modulus of Elasticity
E_T	Modulus of Elasticity in bending
E_C	Modulus of Elasticity in compression
G	Shear Modulus of Elasticity
μ	Poisson's ratio
I	Moment of inertia about axis of bending
J	Polar moment of inertia
C_b	bending moment constant
γ	torsion moment constant
$k = d/b$	geometric constant
τ	torsional stress
α	angle of crack up to neutral-axis
ψ	angle of crack above neutral-axis
β	angle of inclination of compression fulcrum at ultimate
θ	angle of crack across top surface of beam at failure
M_b	bending moment
M_t	torsion moment
$\phi = M_b/M_t$	ratio of bending moment to torsion moment
M_u	ultimate resistance of beam subjected to bending
T_u	ultimate resistance of beam subjected to torsion

SYNOPSIS

The application of loads normal to the plane of a reinforced concrete grid-frame produces combinations of bending moment and torsion moment in the beams due to the monolithic connection of longitudinal and transverse members. The torsion moments are of secondary importance in practice and are neglected for working load design according to C.P.114 (1957). Two outstanding exceptions, however, are the design of edge-beams for Waterloo Bridge and the balcony of the Royal Festival Hall, in London. The effect of torsion moments at ultimate load is to reduce the ultimate bending capacity of the beam so that consideration must be given to this reduction in calculation of the design load factor. The study is therefore concerned with the evaluation of moments at the ultimate load stage.

The extraction of the main longitudinal beam from the grid, together with the transverse beam connection, permits investigation only of the effect of the combined moments on the longitudinal beam and calculation of its ultimate moment capacity under a known torsion moment applied through the transverse beam connection. A mechanism of failure is assumed whereby only the ultimate applied loads are considered and the Principle of Least Work is applied to rotation of the beam about a compression fulcrum along the neutral-axis. An expression is derived which is independent of the combination of load increments up to ultimate, and is equally true for bending or torsion moment.

An investigation is also made of the crack behaviour of the beam since the resolution of bending moments and torsion moments about the inclined neutral-axis at the ultimate stage is shown to be a function of the initial angle of crack. A necessary part of the

study, therefore, is concerned with the early stages of loading prior to cracking and the resistance of the beam is shown to be determined by the properties of the concrete subjected to the individual bending and torsional stresses. Cracking is then propogated at an angle across the beam section as the concrete attains its maximum tensile strength and the ultimate values are defined at the stage when the failure crack intercepts the neutral-axis on the vertical sides of the beam.

An experimental investigation is carried out to justify the assumptions made in the theoretical analysis of the beam and to give a comparison between calculated and practical values of ultimate moment. The results of other studies are included in this comparison.

Finally, the experimental and analytical investigation is extended to consider the analysis of a reinforced concrete frame. A mathematical method is outlined for evaluation of moments at working load and the theory derived in the main part of the study is discussed for the solution at ultimate load.

CHAPTER 1

INTRODUCTION

The design of reinforced concrete beams is largely determined by the applied bending moment and any secondary effects due to torsion are usually considered to be negligible. As a result, research has been largely concerned with the effects of bending of beams and few studies, in comparison, have dealt with the problem of torsion. Further, the application of mathematical theory to the rectangular section subjected to torsional stresses is complex so that design-formulae have not been readily evolved. A review of current Codes of Practice in twenty-two countries by Fisher and Zia[1]* shows that only sixteen specify torsion design requirements and of those only half give more than permissable stresses. C.P.114 (1957) contains no recommendation for torsion design. An interesting point, emerging from the Fisher Review, is that many codes which have adopted an ultimate strength approach are still based on the classical elastic theory of St. Venant.

Few examples are available in practice where the torsion moments control design of the main beam. Two outstanding exceptions, however, are the design of the box-section used in Waterloo Bridge, London, and the triangular girders supporting the balcony of the Royal Festival Hall, London.

With the development of the principle of ultimate load design in reinforced concrete, investigation into combined loading has become necessary in order to assess the value of ultimate bending moment to be used in evaluation of the design load factor.

* Numbers in parenthesis denote references at the end of the thesis.

Research into problems of combinations of bending and shear or axial load has again preceded investigations of beams subjected to combined bending and torsion. It seems likely that new design concepts[2,3,4], at present being discussed with a view to proposals for a new Code of Practice for reinforced concrete design will impose greater responsibility on calculating the value of load factor to be used in assessing an overall design factor.

The main application of combinations of bending and torsion moment is to longitudinal and transverse reinforced concrete beams connected together monolithically in a frame which is loaded normally to its plane. In this case, the longitudinal beams are subjected to primary bending moments due to the applied loading and to secondary torsion moments induced by the transverse beams at the rigid beam-to-beam, or, beam-column-beam connections.

This particular load application forms the basis of the present study. The author feels that even though the torsional effect is secondary and has not been included in the design of the beam at working load, a more realistic load factor is obtained for the design if the torsion moment is considered in calculating the ultimate moment. In order to simplify the problem, only the longitudinal beam is considered in this study and the application of torsional load is simulated by transmitting the torsion moment through concrete arms rigidly fixed to the beam.

An analytical investigation is made to calculate the ultimate bending moment of a reinforced concrete beam subjected to combined bending and torsion moments at ultimate. An expression is derived which is equally true for evaluation of an ultimate torsion moment given a known applied bending moment and vice-versa although the former application is less common in practice. The

expression is independent of the sequence of applying the loads and depends only on the values of moment at ultimate, this stage being defined by the maximum loads resisted by the beam, and more exactly by a limiting condition of crack propogation in the eventual failure zone.

An extensive research programme has been carried out recently in U.S.S.R. and the theory given for a specified failure mechanism at ultimate has been adopted and modified by the author. This ultimate equilibrium theory enables equilibrium conditions to be applied to the rotation of the beam about a compression hinge which forms in the cracked area. The initial part of the author's investigation is therefore concerned with the propogation of cracks in a reinforced concrete beam and, in particular, from initial application of load up to the loads causing initial cracking of the concrete, and the final part with the load stage from initial cracking up to the formation of the final failure crack.

It is shown that during the initial load stages and prior to cracking, the resistance of the beam is determined by the properties of the concrete only and an expression is derived for the angle of crack in terms of the bending and torsional stresses of concrete. The mathematical theory for evaluation of the torsional stress of a rectangular section is examined and both elastic and plastic deformations are considered for application to the behaviour of plain concrete. Assumptions for the stress-strain relationship of the concrete under both bending and torsion loads must then be made.

The second part of the theoretical investigation considers the behaviour of the beam beyond initial cracking to the ultimate

load stage so that redistribution of stress occurs as the lower fibres of the concrete reach the maximum tensile strength and the crack extends across the beam. An expression for the crack development at ultimate, determined by the propogation of the crack up to the neutral-axis position, is then used to derive general design equations. Therefore, although only the final values of applied load are used at the ultimate stage, the design equation also includes an expression relating the nature of the crack behaviour under the combined loads applied up to ultimate.

The exact mathematical analysis of the failure mechanism as given by Lessig[5] is overelaborate for working design procedure and the author attempts to simplify the expression by making assumptions without introducing inaccuracies of magnitude greater than those accepted in the working design. Further flexibility is achieved by eliminating the dependence of the expression on the load ratio so that the load condition is only introduced as a final consideration in the design.

Some thought is given to the practical application of the theoretical equation derived for calculating the ultimate moment, and the presentation of data in chart form, covering a range of material properties, is considered; for example, variations in concrete strengths according to mix design. However, a necessary restriction on the range of properties for a given section is in the use of under-reinforced design only, so that the yield stresses of the reinforcement can be used in the design equation and failure is brought about by crushing of the concrete in the compression zone of the beam. This condition is satisfied by balanced designs for working moments and only in exceptional cases is beam failure due to fracture of the steel. Chinenkov[6] showed in the Russian tests that 99% of the beams tested failed according to

the mechanism considered in this investigation.

An experimental investigation on model reinforced concrete beams and simulating the longitudinal beam of a frame system with transverse arms applying the torsion load is carried out to justify the assumptions made in the theoretical analysis. Results are also used from other practical studies to illustrate the application of the derived equations and give a comparison of practical and calculated moments at ultimate.

The final part of the study introduces the problem of the inter-connection of beams as elements of a rigid frame, and theoretical methods are considered for both working and ultimate load. The effects of the transverse beam members on the longitudinal beams and the transmission of moments by means of the monolithic connections is examined in relation to the theories put forward for the simpler longitudinal element considered earlier.

The application of combined bending and torsion moments is therefore examined for all stages of load, and a particular study is made of the beam at ultimate and the effect of varying the torsion moment on the ultimate capacity of the beam in bending.

The restraining effect of the in-situ slab has not been included in this study and consideration has not been given to shear effects, which would exist at all times. The author feels, however, that research into the problem at present under examination has not been extensive and that simplifications made at this stage are justified with a view to further development of the theory taking these additional factors into account.

CHAPTER 2

REVIEW OF PREVIOUS INVESTIGATIONS

2.1 General:

It is proposed to outline previous investigations into the problem of combined bending and torsion for both elastic and plastic behaviour and follow the development of theory from the circular to the rectangular section. Also, as solutions to the problem of torsion have been more difficult to obtain than for bending acting alone, it is proposed to include only the investigations into the torsion problem and finally investigations into combinations of torsion and bending for both working and ultimate load conditions.

2.2 Introduction:

Before attempting to investigate analytically the behaviour of a non-homogeneous material such as concrete subjected to either bending or torsion stresses, certain basic assumptions must be made with regard to stress-strain relationships for the concrete subjected to the different loadings. It is proposed to review in this Chapter theoretical, empirical and experimental investigations that have been carried out to examine in particular the behaviour of concrete subjected to torsional stresses so that a basis may be formed for examination of the behaviour of concrete in the beam from initial application of the loads through to the ultimate stage. It is shown in Chapter 4 that prior to cracking, the behaviour of a reinforced beam subjected to combined bending and torsion is determined only by the resistance of the concrete to the individual bending and torsion stress. It has been accepted that while solutions are available for the properties of concrete subjected to bending only, a review of previous studies

is required to assess the resistance of concrete to torsion especially for rectangular sections. Further, since this investigation is to be concerned with the behaviour of the beam at all load stages, some thought is given to the change in properties that may occur at a load stage defined by initial cracking of the concrete.

Finally, it is proposed to review the work that has already been carried out on the problem of combined bending and torsion at the ultimate load stage of a reinforced or prestressed beam and the extension of this theory to the evaluating of the ultimate moment of beams forming units or elements of a grid-frame system in which bending and torsion moments are produced by beams framing in to the monolithic joint of a reinforced concrete frame loaded normal to the plane.

2.3 Elastic Torsion Theory:

(a) Circular Section:- The theory for the application of torsion to an elastic, isotropic circular section is long established and full accounts are given in most textbooks[7]. This theory has been used for plain concrete and an expression obtained for the moment of resistance in terms of the diameter of the circle and the maximum torsional shear stress of the concrete occurring at the surface layer. However the expression is dependent on two assumptions, namely that the circular boundary remains undistorted, and that cross-sections remain plane and rotate as is absolutely rigid.

Experimental investigations carried out to study the distribution of shear stress over a circular section of plain concrete include work by MORSCH[8], ANDERSEN[9] and MARSHALL and TEMBE[10]. Morsch's tests give first evidence of the now familiar forty-five degree failure crack due to diagonal tension; Andersen's tests include strain measurements on the basis of an elastic

approach and Marshall compares the ultimate tensile strength of the concrete to a value of stress given by the average for elastic and plastic stress distribution.

(b) Rectangular Section:- The original assumptions made for the circular section are no longer true due to warping of the rectangular section and introduction of an additional axial stress. The theoretical method derived by ST. VENANT[11] and later expressed by LOVE[12] is essentially the derivation of a mathematical expression for the stress function, ϕ, and differentiating to obtain the shear stresses τ_{xz} and τ_{yz}. TIMOSHENKO and GOODIER[13] have developed the approach based on PRANDTL'S Membrane Theory[14]. In both cases, however, the theoretical equations involve hyperbolic terms with resultant complexity of the final expressions. Simplifications have all been based upon using the maximum, or minimum, values of τ[15]. As the application of the theory to rectangular sections forms part of the investigation of the properties of concrete at initial stages of loading, the author has included the more detailed study of St. Venant's Theory in Chapter 3.

A large number of experimental and empirical studies have been carried out on rectangular plain concrete sections, and at the same time as those investigations for circular sections. In addition, the practical application of including reinforcement in the section must be considered. BACH and GRAF[16] were probably first to investigate the effects of various reinforcements and deduced an expression for maximum moment in terms of the maximum shearing stress occuring at the mid-point of the longer side. ANDERSEN[9] suggests for square sections a parabolic distribution of shearing stress and derives a relationship between the length

of side and radius of the equivalent circle using BACH'S formula. RAUSCH[17] confines his original theory to spiral reinforcement with application to column design, and assumes that both the steel and concrete behave elastically within the stresses permitted by the Code of Practice for spiral reinforcement.

More recently however COWAN[18] has extended the theories of Rausch by applying the principle of strain energy and comparing the energy stored in the reinforcement and the concrete under compression against the work done by the torsion moment, modifying the theory for the more practical case of longitudinal reinforcement using the St. Venant Principle.

In general however the experimental and empirical studies of YOUNG, SAGAR, and HUGHES[19], MIYAMOTO[20], TURNER and DAVIES[21], and MARSHALL and TEMBE[10] all indicate a non-elastic behaviour and equate the torsional strength of the section to the tensile strength of the concrete. Nevertheless the extensive studies carried out by Cowan do indicate that some elastic behaviour takes place and that design equations based upon elastic theory give satisfactory results over a specified load range defined by Cowan's "visco-elastic" limit.

2.4 Plastic Torsion Theory:

The development of a plastic theory and the experimental representation of torsional stress distribution for a cylindrical or prismatic bar is given by NADAI[22] using a sand heap analogy. This concept is considered in more detail in Chapter 3 for its application to the rectangular plain concrete section.

Experimental evidence has been gathered by MARSHALL[23] to show that an expression based upon the assumption that concrete is fully plastic gives a satisfactory explanation for the value of

torsional shear stress at ultimate, and more recently ERNST[24] has included a plastic equation for evaluation of torque capacity for reinforced sections. The general opinion is that near ultimate load, redistribution of stress takes place over the cross section and by assuming uniform torsional stress, simpler formulae can be evolved. This conclusion is substantiated by Marshall's work[10] on crack observation by using strips of plaster to investigate location of the first crack, which is not located at the mid-point of the longer side as is suggested by an elastic stress distribution. NYLANDER[25], basing his statements on a large series of tests, indicates for T-sections in particular, that the uniform stress at ultimate is the maximum torsional strength of the concrete.

The relation between any change from an elastic to a plastic condition and the formation and development of internal cracks has been studied by EVANS[26] for beams subjected to bending load, and by KAPLAN[27] who shows experimentally, using sophisticated strain measuring techniques, that cracking is initiated at loads considerably less than ultimate and suggests concrete strain as the criterion. Evans outlines changes in strain distribution both before and after cracking.

2.5 Combined Bending and Torsion:

The application of the studies mentioned above to the problem of combined bending and torsion indicates that differentation must be made between the initial and final stages of applied load, so that development of formulae has proceeded as for the studies of bending or torsion acting alone.

(a) Elastic Theory-Circular Section:- The general theory given by TIMOSHENKO[7] includes a mathematical theory for the application of combined bending and torsion to circular sections, in which an

expression is derived for the stress in terms of an equivalent bending moment.

Rectangular Section:- BORG and GENARO[28] show how the elastic theories of St. Venant and Prandtl can be applied to structural steel sections on the assumption that rotation takes place about the shear-centre of the section, and specify in each case the degree of restraint against warping. The combined action of bending and torsion is then considered in frame analysis using moment distribution techniques in two planes and combining the individual solutions by super-position. The main studies using an elastic approach for reinforced concrete are by Cowan[29] and, in particular, a theory is given using Rankine's Maximum Principal Stress criterion and Coulomb's Internal Friction criterion for problems of combined stress. The experimental investigation is primarily concerned with the types of failure of the beam rather than the ultimate values of the combined loading, but Cowan indicates a correlation of the proposed theory up to the "visco-elastic" limit.

(b) Plastic Theories - Rectangular Section:- The theoretical application to reinforced concrete beams must take into account the non-homogeneous nature of the concrete. Most studies, as a result, introduce the concept of plastic behaviour at some stage of the applied loading. NYLANDER[25] first introduced the problem of combined bending and torsion to reinforced concrete frames and on the assumption of full plasticity at failure; FISHER[30], investigating the criterion for failure for variable combinations of bending and torsion, reviews most of the evidence obtained from previous studies of the problem of torsion acting alone, and previously discussed in sections 2.3 and 2.4; while RAO[31]

investigates the problem theoretically by assuming that rupture takes place at the stage where the layer of concrete at the centre of gravity of the shear stress diagram reaches the value of ultimate shear stress, and concludes that correlation is obtained for non-uniform stress distribution in evaluating the ultimate strength of the concrete.

The most comprehensive study, however, and the one to be adopted by the author, is given by LESSIG[32], CHINENKOV[6], LYALIN[33], GVOZDEV[34] and YUDIN[35]. The theory is commonly referred to as the Ultimate Equilibrium Method in which design formulae are developed for the combined moments at ultimate by assuming failure of a reinforced concrete beam due to yielding of the reinforcement crossing the crack about which failure takes place. Two types of failure-crack are considered in the experimental investigation, but in all but one test, failure occurs due to rotation about a compression-hinge acting along the line of inclination of a horizontal neutral-axis and intercepting the two vertical sides of the beam. This mechanism of failure is discussed in more detail in Chapter 5. An exact mathematical analysis of the Principle of Least Work applied to the failure-zone at ultimate load by LESSIG[5] gives complicated equations which are later modified by YUDIN[35] by assuming a constant neutral-axis depth. Experimental studies by CHINENKOV[6], LYALIN[33] and GVOZDEV[34] give good correlation with theory and there is no doubt in the author's mind that the equilibrium approach to the problem of combined bending and torsion gives a more realistic picture of the failure mechanism than any other. As a result, further studies have been undertaken to investigate the principle.

SARKAR[36] has applied the theory to hollow rectangular reinforced beams and calculates the depth of the neutral-axis for bending acting alone, then reduces this value by $\sqrt{2}$ for combined bending and torsion, assuming a constant horizontal angle of inclination of 45°. Sarkar also simplifies the expression for length of crack by assuming the angle of crack above the neutral-axis to be 45°. BOAZ[37] confirms the requirement of considering the combined effects of the applied bending and torsion loads and shows for the range of loadings investigated experimentally that agreement is not possible using individually calculated moments. For these values, Boaz used the A.S.C.E. - A.C.I. recommendations for ultimate flexural load and an expression for ultimate torsion related to the St. Venant constants and a value for ultimate tensile strength.

GESUND, SCHUETTE, BUCHANAN and GRAY[38] also extend the ultimate equilibrium principle by using design sections to ensure yielding of both longitudinal and transverse steel, but including in the ultimate moment equations expressions for the resistance of the longitudinal reinforcement due to dowel action and due to bending of the bars. A modified failure scheme is also considered whereby an S-shaped hinge is formed on the top surface of the beam and intercepts the vertical side cracks which are perpendicular at the bottom and horizontal towards the top of the vertical sides of the beam.

(c) Prestressed concrete:- Experimental investigations into the application of combined bending and torsion to prestressed concrete T-beams by REEVES[39] and to prestressed concrete I-beams by GARDENER[40] indicate the need for further research in this field. Both studies are concerned with variations in the sequence of

applied loads and its effect on ultimate strength. ROWE[41] had reported earlier on this subject and suggested the possible use of interaction curves. He also emphasised the importance of the bearing support to ensure rotation about the centroidal-axis and stated that failure of a prestressed beam under combined load is sudden and explosive.

(d) Grid Frames:- The final field of investigation is the problem of combined bending and torsion occurring in grid frames loaded normally to the plane. REYNOLDS[42] calculates collapse loads for prestressed concrete grillages by assuming rotation about plastic-hinges and comparing values found by Lower Bound and Upper Bound techniques. By introduction of a sufficient number of bending and torsion hinges, normal or skew-grid frames are solved and without calculation of the hinge rotation. Reynolds assumes however that rotation of the transverse beams takes place at the joint, due to the form of prestressing, and this permits further simplification as there is zero torsional moment in the transverse members of the grillage.

GOUDA[43] presents a method for analysing and determining the actual stresses in beams and slabs monolithically connected and taking into consideration the effect of the torsional rigidity of each on the other. The necessary assumptions, however, are for an elastic, homogeneous condition and that the ends of the beam are rigidily fixed, so that the application is limited. The valuable work of BAKER[44, 45, 46] has not yet been extended to space-frames with resultant introduction of both bending and torsion moments. A large research programme on plastic-hinges[47, 48] has been carried out with application to reinforced concrete plane-frames and it remains to extend this research to space-frames.

It would seem, therefore, that future investigation will be concerned with these aspects, meanwhile, the author's own work is concerned with a reinforced beam as an element of the frame and subjected to both bending and torsion moments.

CHAPTER 3

TORSION THEORY APPLIED TO A RECTANGULAR SECTION

3.1 General:

Reference has been made in Chapter Two to the application of pure torsion to a rectangular section and to the complexity of the equations based on an exact mathematical treatment of this problem. The author has therefore included a separate Chapter for amplification and assessment of these equations so that a basis may be formed for investigation of the behaviour of concrete in Chapter Four.

3.2 Introduction:

It is proposed to outline in this Chapter the two main methods by which the application of the elastic torsion theory to a rectangular section has been developed firstly by St. Venant[11] and later adopted by Love[12], and secondly by Prandtl's Membrane Theory as given by Timoshenko and Goodier[13]. The degree of complexity of the equations due to the inclusion of hyperbolic terms has limited their application, and it is shown how computer programmes give solutions for specified sections. The main application of the original equations, however, has been in the form of expressions involving only the maximum stress values. This method of representation is given in most text-books on the subject and has been adopted by most investigators in applying elastic conditions to the rectangular section.

It is further proposed to outline the plastic theory applied to rectangular sections as developed by Nadai[22], using a sand-heap analogy, in view of the experimental evidence for non-elastic behaviour of concrete at later stages of loading. This theory is

used for derivation of an equation expressing the behaviour of a reinforced concrete beam subjected to combined bending and torsion prior to cracking.

3.3 St. Venant Theory:

St. Venant considers the problem of torsion of prismatical bars, by couples applied at the ends, using a semi-inverse method in which assumptions are made as to the deformation of the twisted bar, then equations derived to satisfy both the equilibrium and boundardy conditions.

Thus from Fig. 1.3:-

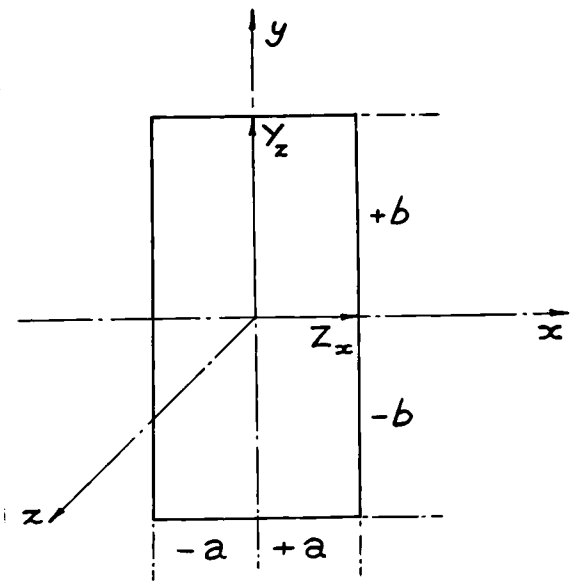

we have,

$$d^2u/dy^2 + d^2u/dx^2 = 0$$

$$du/dy = \Theta x \quad \text{for } y = \pm b, \quad -a \leq x \leq +a$$

$$du/dx = -\Theta y \quad \text{for } x = \pm a, \quad -b \leq y \leq +b$$

substituting $u = -\Theta y z + u'$

$$d^2u'/dy^2 + d^2u'/dx^2 = 0$$

(ii) $du'/dy = 2x$, for $y = \pm b$, $-a \leq x \leq +a$

$du'/dx = 0$, for $x = \pm a$, $-b \leq y \leq +b$

assume $u' = \sum A_m (e^{my} - e^{-my}) \sin mx$

and determine the constants by Fourier's Theorem so that

$$(iii)\quad u = \Theta a.b. \left[-\frac{y.x}{ab} + \frac{1}{2}\left(\frac{4}{\pi}\right)^2 \frac{a}{b} \sum_{n=1}^{\infty} \frac{(-1)^{n-1}}{(2n-1)^3} \cdot \frac{\sinh \frac{(2n-1)\pi y}{2a}}{\cosh \frac{(2n-1)\pi b}{2a.}} \sin \frac{(2n-1)\pi x}{2a} \right]$$

$$= \Theta a.b. \frac{1}{4}\left(\frac{4}{\pi}\right)^3 \sum_{n=1}^{\infty} \frac{(-1)^{n-1}}{(2n-1)^3} \left[\frac{a}{b} \frac{\sinh \frac{(2n-1)\pi y}{2a.}}{\cosh \frac{(2n-1)\pi b}{2a.}} \sin \frac{(2n-1)\pi x}{2a} - \frac{b}{a} \frac{\sinh \frac{(2n-1)\pi x}{2b}}{\cosh \frac{(2n-1)\pi a}{2b.}} \sin \frac{(2n-1)\pi y}{2b} \right]$$

$$(iv)\quad Y_z = G.\Theta \frac{\partial u}{\partial x}$$

$$= G\Theta b \left[\frac{a}{b}\left(\frac{4}{\pi}\right)^2 \sum_{n=1}^{\infty} \frac{(-1)^{n-1}}{(2n-1)^2} \frac{\sinh \frac{(2n-1)\pi y}{2a}}{\cosh \frac{(2n-1)\pi b}{2a.}} \cos \frac{(2n-1)\pi x}{2a} \right]$$

$$Z_x = G.\Theta \frac{\partial u}{\partial y}$$

$$= G.\Theta a \left[+2\frac{x}{a} - \left(\frac{4}{\pi}\right)^2 \sum_{n=1}^{\infty} \frac{(-1)^{n-1}}{(2n-1)^2} \cdot \frac{\cosh \frac{(2n-1)\pi y}{2a}}{\cosh \frac{(2n-1)\pi b}{2a.}} \sin \frac{(2n-1)\pi x}{2a.} \right]$$

Consider a standard rectangle, and introduce non-dimensional functions:-

$$k = a/b, \quad p = x/a, \quad q = y/b, \quad \text{then}$$

$$Y_z = -G.\theta b\left(\frac{4}{\pi}\right)^2 \sum_{n=1}^{\infty} \frac{(-1)^{n-1}}{(2n-1)^2} \cdot \frac{\sinh(2n-1)\frac{\pi}{2}\cdot p.k.}{\cosh.(2n-1)\frac{\pi}{2}\cdot k.} \cos.(2n-1)\frac{\pi}{2} q$$

$$\text{and } Z_x = G.\theta b.\left[2q - \left(\frac{4}{\pi}\right)^2 \sum_{n-1}^{\infty} \frac{(-1)^{n-1}}{(2n-1)^2} \cdot \frac{\cosh(2n-1)\frac{\pi}{2} pk}{\cosh.(2n-1)\frac{\pi}{2} k} \sin(2n-1)\frac{\pi}{2} q\right]$$

An identical solution is given by Love only introducing 'n + 1' to replace St. Venant's term in 'n', so that

$$Y_z = G.\theta b.\frac{16}{\pi^2} \sum_{n=0}^{\infty} \frac{(-1)^n}{(2n+1)^2} \cdot \frac{\sinh(2n+1)\frac{\pi}{2} p.k.}{\cosh(2n+1)\frac{\pi}{2} k} \cdot \cos(2n+1)\frac{\pi}{2} \cdot q$$

$$\text{and } Z_x = G.\theta b.\left[-2q + \frac{16}{\pi^2} \sum_{n=0}^{\infty} \frac{(-1)^n}{(2n+1)^2} \cdot \frac{\cosh(2n+1)\frac{\pi}{2} p.k.}{\cosh.(2n+1)\frac{\pi}{2} \cdot k.} \sin(2n+1)\frac{\pi}{2} q\right]$$

and these final expressions in Y_z and Z_x have been incorporated in a computer programme for solution, giving values as shown in Fig. 2.3 for grid points on the quarter cross-section. The programme and results are given in Appendix E.

$$Z = \frac{Q}{G.\theta b.} = \sqrt{\left[-2q + 4\left(\frac{2}{\pi}\right)^2 \sum_{n=0}^{\infty} \frac{(-1)^n}{(2n+1)^2} \cdot \frac{\cosh(2n+1)\frac{\pi}{2} p.k}{\cosh(2n+1)\frac{\pi}{2} \cdot k} \cdot \sin(2n+1)\frac{\pi}{2} q\right]^2 + \left[\frac{16}{\pi^2} \sum_{n=0}^{\infty} \frac{(-1)^n}{(2n+1)^2} \cdot \frac{\sinh(2n+1)\frac{\pi}{2} p.k}{\cosh(2n+1)\frac{\pi}{2} \cdot k} \cdot \cos.(2n+1)\frac{\pi}{2} \cdot q\right]^2}$$

$$\text{and, } \tan\theta = \frac{2q}{4\left(\frac{2}{\pi}\right)^2 \sum_{n=0}^{\infty} \frac{(-1)^n}{(2n+1)^2} \frac{\sinh(2n+1)\frac{\pi}{2} pk}{\cosh(2n+1)\frac{\pi}{2} k} \cos(2n+1)\frac{\pi}{2} q - \frac{\cosh(2n+1)\frac{\pi}{2} p.k. \sin(2n+1)\frac{\pi}{2} q}{\sinh(2n+1)\frac{\pi}{2} \cdot pk. \cos(2n+1)\frac{\pi}{2} q}}$$

where,

$$t\ell = {}^{Zx}/_{G\theta b}, \quad tm = {}^{Yz}/_{G\theta b}$$

$$Q = \sqrt{Y_z^2 + Z_x^2}$$

Fig. 2.3:-

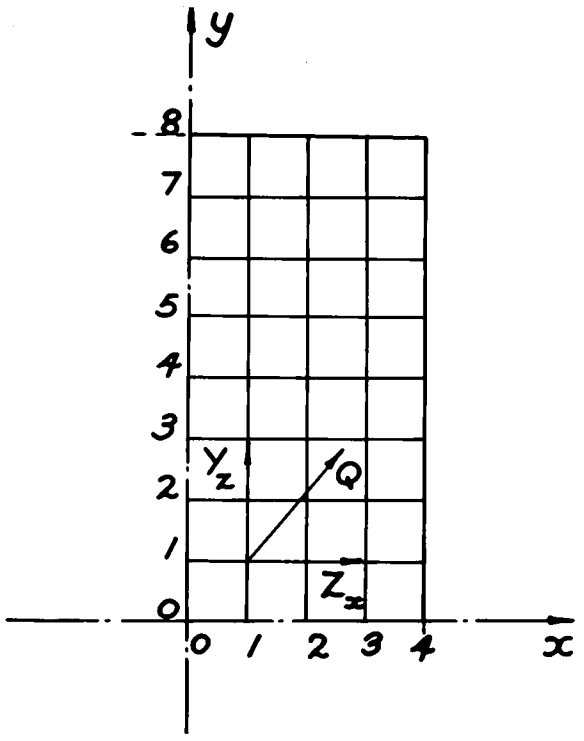

3.4 Membrane Theory:

A second approach to the problem is given by Timoshenko and Goodier using the membrane analogy developed by Prandtl in 1906, in which a homogeneous membrane supported at the edges with the same outline as the twisted cross-section is considered. This application is therefore true for both elastic conditions and beyond yield[14] since the membrane represents stress distribution over the elastic region and the stress over the plastic area is given by a surface of constant maximum slope corresponding to the yield stress.

Consider,

uniform tension at edges = s/unit length

and uniform lateral pressure = q/unit area

then, using the St. Venant rectangle.

$$\text{(i)} \qquad \frac{\delta^2 z}{\delta x^2} + \frac{\delta^2 z}{\delta y^2} = -\frac{q}{S}$$

$$\text{(ii)} \qquad z = \sum_{n=1,3,5,\cdots}^{\infty} b_n \cos\frac{n\pi x}{2a} \cdot Y_n$$

b_1, b_3, ... constant coefficients

Y_1, Y_3, ... functions of y

(iii)

to satisfy condition (i)

$$\frac{\delta z}{\delta x} = -\sum_{n=1,3,5,\cdots}^{\infty} b_n \frac{n\pi}{2a} \sin\frac{n\pi x}{2a} Y_n$$

$$\frac{\delta^2 z}{\delta x^2} = -\sum_{n=1,3,5,\cdots}^{\infty} b_n \frac{n^2\pi^2}{4a^2} \cos\frac{n\pi x}{2a} Y_n$$

$$\frac{\delta z}{\delta y} = \sum_{n=1,3,5,\cdots}^{\infty} b_n \cos\frac{n\pi x}{2a} \cdot Y_n'$$

$$\frac{\delta^2 z}{\delta y^2} = \sum_{n=1,3,5,\cdots}^{\infty} b_n \cos\frac{n\pi x}{2a} \cdot Y_n''$$

so that,

$$Y_n = \frac{16qa^2}{5\pi^3} \sum_{n=1,3,5,\cdots}^{\infty} \frac{1}{b_n n^3} (-1)^{\frac{n-1}{2}} \left[1 - \frac{\cosh\frac{n\pi y}{2a}}{\cosh\frac{n\pi b}{2a}} \right]$$

satisfying symmetry and zero deflection at $y = \pm b$

therefore from (ii)

general expression for deflection surface of membrane

$$z = \frac{16qa^2}{5\pi^3} \sum_{n=1,3,5,\cdots}^{\infty} \frac{1}{n^3} \cdot (-1)^{\frac{n-1}{2}} \left[1 - \frac{\cosh\frac{n\pi y}{2a}}{\cosh\frac{n\pi b}{2a}} \right] \cos\frac{n\pi x}{2a}$$

(iv)

by analogy, stress function is given by

$$\phi = \frac{32 G\Theta a^2}{\pi^3} \sum_{n=1,3,5,\cdots}^{\infty} \frac{1}{n^3} (-1)^{\frac{n-1}{2}} \left[1 - \frac{\cosh \frac{n\pi y}{2a}}{\cosh \frac{n\pi b}{2a}} \right] \cos \frac{n\pi x}{2a}$$

(v)

so that,

$$Y_z = -\frac{\partial \phi}{\partial x} = + \frac{16}{\pi^2} G\Theta a \sum_{n=1,3,5,\cdots}^{\infty} \frac{1}{n^2} (-1)^{\frac{n-1}{2}} \left[1 - \frac{\cosh \frac{n\pi y}{2a}}{\cosh \frac{n\pi b}{2a}} \right] \sin \frac{n\pi x}{2a}$$

$$Z_x = \frac{\partial \phi}{\partial y} = - \frac{16}{\pi^2} G\Theta a \sum_{n=1,3,5,\cdots}^{\infty} \frac{1}{n^2} (-1)^{\frac{n-1}{2}} \left[\frac{\sinh \frac{n\pi y}{2a}}{\cosh \frac{n\pi b}{2a}} \right] \cos \frac{n\pi x}{2a}$$

and for the standard rectangle

$$t\ell = \frac{Y_z}{G\Theta a} = \frac{16}{\pi^2} \sum_{n=1,3,5,\cdots}^{\infty} \frac{1}{n^2} (-1)^{\frac{n-1}{2}} \left[1 - \frac{\cosh \frac{n\pi q}{2k}}{\cosh \frac{n\pi}{2k}} \right] \sin \frac{n\pi p}{2}$$

$$tm = \frac{Z_x}{G\Theta a} = - \frac{16}{\pi^2} \sum_{n=1,3,5,\cdots}^{\infty} \frac{1}{n^2} (-1)^{\frac{n-1}{2}} \left[\frac{\sinh \frac{n\pi q}{2k}}{\cosh \frac{n\pi}{2k}} \right] \cos \frac{n\pi p}{2}$$

and,

$$Z = \sqrt{(t\ell)^2 + (tm)^2}$$

$$\tan \Theta = t\ell / tm$$

The above expressions and those given in section 3.3 differ essentially in the length of side 'a' or 'b' used, so that in comparing solutions in Z_x and Y_z, account must be taken of the factor 'b/a', equal to two in this case. Comments on these results are given in section 3.7.

3.5 Approximate Expressions:

Approximate expressions eliminating the hyperbolic terms have been developed by many authors by assuming a specified stress distribution over the sides of the rectangle and deriving an equation in terms of the maximum stresses, assumed to occur at the mid-points of the sides.

Seeley[49] uses Bach's Method and assumes a parabolic distribution with maximum stress at the mid-point of the longest side of the rectangle to simplify the St. Venant equations. The value for torsion moment is then given as

$$M_t = \alpha (2a)^2 (2b) \tau_{max}$$

and values of α are tabulated for 'b/a' varying between 1 and ∞.

Timoshenko[7] gives the same equation and almost identical α-values.

Approximate formulae are similarly obtained from the Membrane Theory by assuming that the maximum value of stress occurs at maximum slope of the membrane, and Timoshenko and Goodier by approximating the converging series in $\cosh \frac{n\pi b}{2a}$ give,

$$M_t = k_2 (2a)^2 (2b) \tau_{max}$$

Values of k_2 are given for variable 'b/a'.

The practical application is therefore one of expressing the maximum torque in terms of the maximum stress occurring at some specified location in the rectangular section. The consideration of maximum values introduces the concept of plastic behaviour.

3.6 Plastic Theory - Sand-Heap Analogy:

The condition of plasticity at which a shearing stress τ reaches the yield point of the material is given by a relation

between shear stress components τ_x and τ_y as,

$$\tau_x^2 + \tau_y^2 = k^2 = \text{constant}$$

The function F(x,y) is defined as the plastic stress function of the cross section, and at the points beyond yield

$$\left(\partial F/\partial x\right)^2 + \left(\partial F/\partial y\right)^2 = k^2$$

Finally, at every point along the region of plastic deformation

$$-\tau_y \,.\, dx + \tau_x . dy = \left(\partial F/\partial x\right)dx + \left(\partial F/\partial y\right)dy = 0$$

The plastic stress function can be considered to be a surface of constant maximum slope constructed over the edge of the cross section and analogous therefore to a sand-heap taking up a shape of slope equal to F and independent of the amount of twist.

The application to a rectangular section and complete plasticity is governed by the same rules as for the elastic torsion case so that, at any point on the surface, the resulting shear stress is given by the slope of the stress surface; the contour lines for constant F(x,y) are stress lines for the twisted section; and the torsion moment, M_t, is given as twice the volume contained by the surface, or, for the rectangle being considered,

$$M_t = 2F\iint (x,y)\, dx.dy.$$

$$= \tau_{max.}\left[\frac{(2a)^3}{3} + \frac{(2a)^2.(2b-2a)}{2}\right]$$

$$= \tau_{max.}(2a)^2\left[\, b - \frac{a}{3}\,\right]$$

3.7 Conclusions:

The results given in Appendix E are for solution by a KDF 9 Computer of the torsion stresses induced in a rectangular section, of 'b/a' ratio equal to two, using the elastic equations

outlined in Sections 3.3 and 3.4. The results obtained by the Membrane Theory approach are illustrated in Fig. 3.3. The following conclusions are therefore made on these results and the application of the various theories.

1. The results given by the two elastic methods of analysis are very similar and any differences are insignificant for representation as shown in Fig. 3.3.

2. Due to the rapid convergence of the hyperbolic expression in the St. Venant equations, a large number of terms in 'n' must be taken. Two sets of results are given, for n = 20 and for n = 40 and the difference between results for any given point is only introduced in the fourth decimal place. As a result, even for n = 40, the boundary condition is not yet satisfied at $x = \pm a$, and there is a residual stress at the corner point, although convergence is less rapid for this value.

3. The Membrane Theory gives equivalent results for n = 9, and boundary conditions are satisfied with zero stress at the corner. These results are plotted in Fig. 3.3 and the stress contours illustrate the basic principle of the theory first examined by Prandtl.

4. To study the problem of combined bending and torsion, additional computing is required to resolve the torsion stresses with the appropriate bending stress and evaluate the resultant stress in a third plane. The author's opinion is that this final stress distribution represents the stress condition in concrete at the early stages of loading.

5. The large amount of computation necessary for the elastic theory is avoided by considering only the maximum values of torsion stress. However, in applying maximum conditions to concrete, a

FIG. 3.3 :-

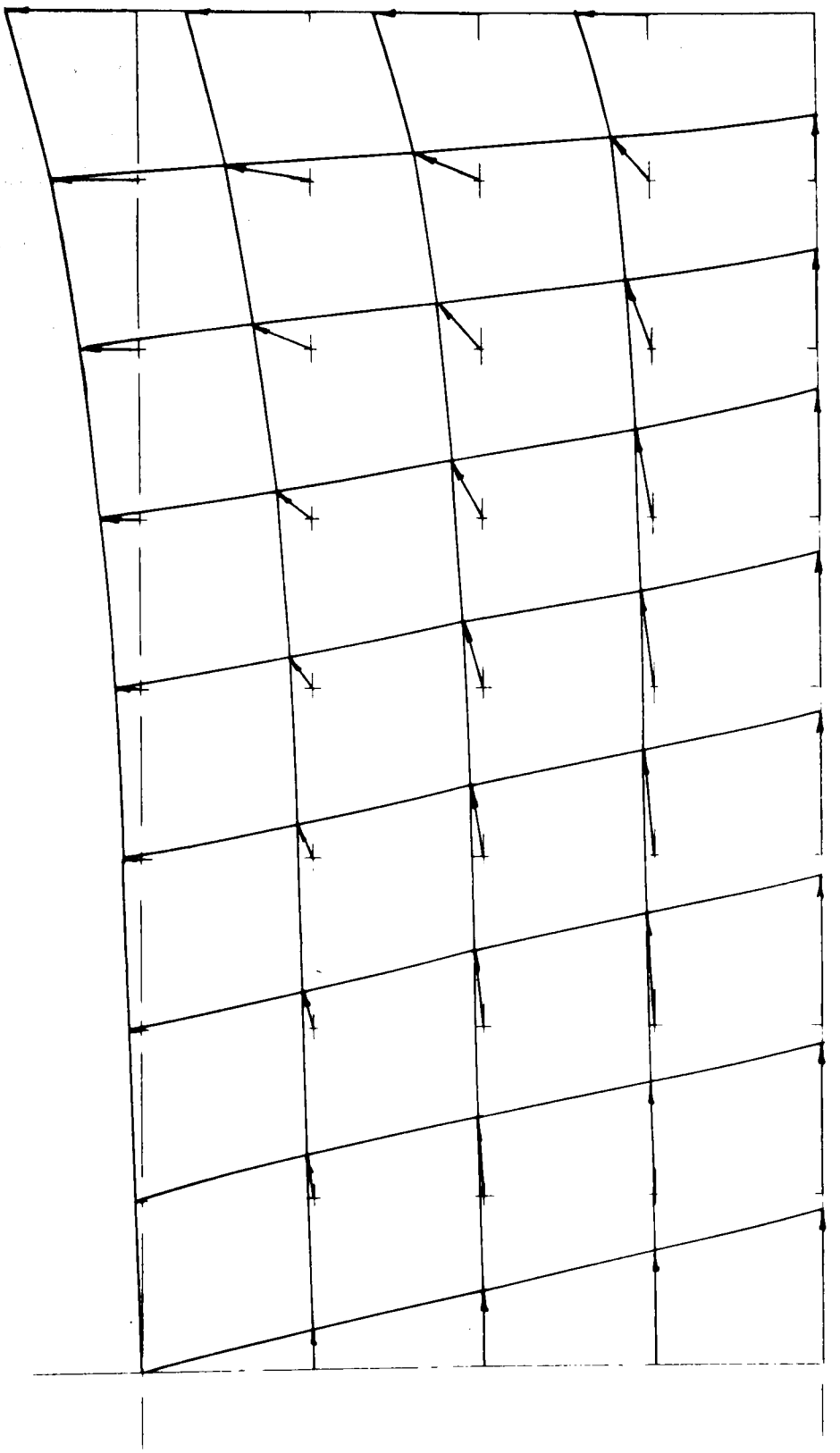

theory based on plastic behaviour must be investigated.

6. The author feels that for application of the torsion theory to rectangular sections of concrete, the equations developed by Nadai are more closely related to the behaviour of the section at maximum values of torsion stress. Also, the equations are much simpler in form, and it is proposed to adopt this theory for investigation in Chapter Four of the behaviour of a reinforced concrete beam prior to cracking.

CHAPTER 4

THE BEHAVIOUR OF A REINFORCED CONCRETE BEAM PRIOR TO CRACKING

4.1 General:

It is proposed to consider the resistance of reinforced concrete subjected to combined bending and torsion in two stages. Chapter 4 will deal with the range of combined loadings up to the initial cracking of the concrete. Chapter 5 is then concerned with combined loadings beyond the initial cracking stage up to the ultimate stage and will then deal with resultant failure of the beam.

4.2 Introduction:

In this Chapter, the resistance of the beam is defined by the concrete properties, and, in particular, the tensile strength of the concrete. Working on the basis of specified assumptions for stress distribution in the concrete, an expression is derived for the moment of resistance of the beam for pure bending and for pure torsion. An expression for the angle of crack is then found for the case of combined bending and torsion loading in terms of the original independent stresses.

A similar procedure has been developed by Evans and Sarkar[50] for hollow rectangular beams but due to initial differences in the value for the depth of the neutral axis, the subsequent expressions are of different form. The author shows that the angle of crack is the same for hollow and solid rectangular beams.

The design formulae to be developed in Chapter 5 for combined bending and torsion will be derived using the initial angle of crack in the concrete. It is shown in this Chapter that

the angle is determined only by considering the concrete stresses so that it is not necessary to consider any properties of the reinforcement at this stage. Finally a simplified expression for the angle of crack is derived in terms of the ratio of applied bending moment to applied torsion moment. The design expressions to be evolved in Chapter 5 are mainly concerned with strength properties of the concrete and steel, linear dimensions of the beam-section and trigonometrical terms involving the angle of crack and the angle of inclination of the compression hinge about which rotation eventually takes place. An expression for this angle is derived in terms of the angle of crack and a geometric property of the section.

4.3 Moment of Resistance to Pure Bending:

The resistance of a reinforced concrete beam to pure bending during the stage prior to cracking depends upon the nature of the stress-strain relationship assumed for the concrete. For this work a semi-plastic stress distribution has been adopted similar to that given by Cowan[51] and the assumed stress-strain relationship is represented by the following diagrams.

Fig. 1.4:-

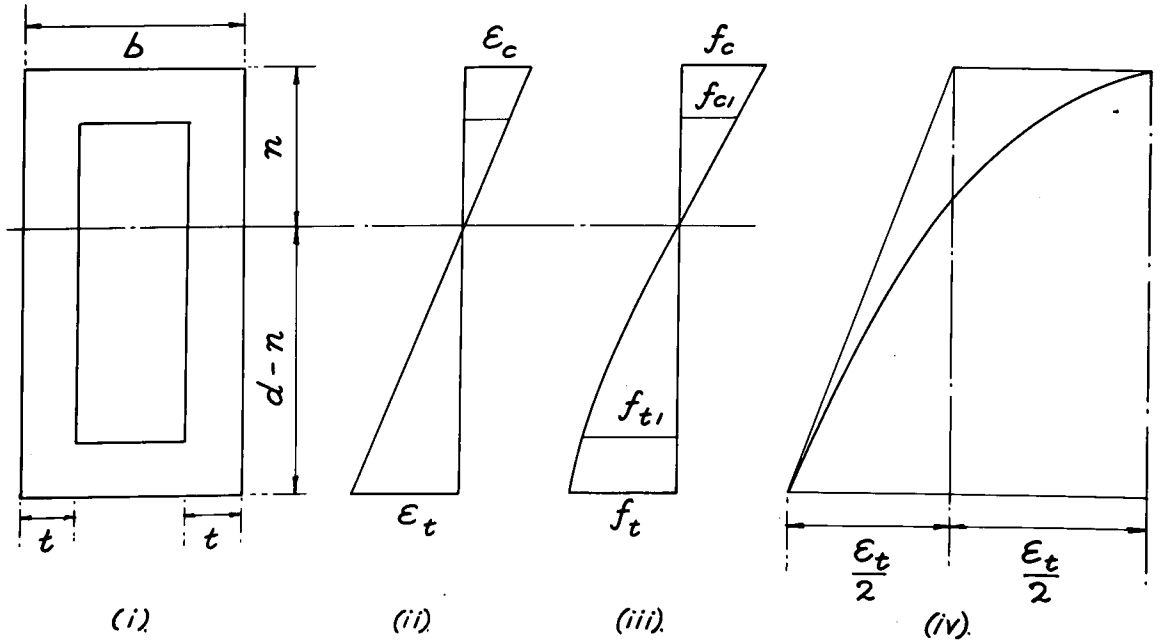

These relationships are used to determine the depth of the neutral axis, 'n', from the upper surface of the beam for (a) solid rectangular section (b) hollow rectangular section.

(a) solid rectangle - plain concrete

$$\frac{f_c}{f_t} = \frac{E_c \varepsilon_c}{\frac{1}{2} E_t \varepsilon_t} \qquad \text{fig. 1.4 (iv)}$$

$$\frac{f_c}{f_t} = \frac{2n}{d - n} \qquad \text{fig. (iii)}$$

equating resultant tensile and compressive forces,

$$\tfrac{2}{3} f_t \; b(d - n) = \tfrac{1}{2} f_c \; b \; n$$

so that $n = + 0.449 \; d$

(b) hollow rectangle - plain concrete

$$\frac{f_c}{f_t} = \frac{2n}{d - n}$$

equating resultant tensile and compressive forces

$$\tfrac{1}{2} f_c \; n \; t + \tfrac{1}{2} f_c \; n \; t \left[f_c - \frac{(f_c + f_{c_1})}{2} \right] (b - 2t)t$$

$$= \tfrac{2}{3} f_t \; (d - n) \; 2t + (b - 2t)t \; f_{t_1}$$

assume $f_{t_1} = f_t$ then

$$\frac{f_c}{f_t} = \frac{\frac{4}{3}(d - n) + (b - 2t)}{n + \frac{(b - 2t)(2n - t)}{2n}} - \frac{2n}{(d - n)}$$

solving for n, gives

$$2n^2 + n(8d + 9b - 18t) - (4d^2 + 3bt + 3bd - 6t^2 - 6td) = 0$$

assume $t = b/4$;

then, $t = d/4k$; $td = d^2/4k$; $t^2 = d^2/16k^2$; $tb = d^2/4k^2$

and, $n^2 + n \; \frac{d}{2} (8 + 9/2k) - \frac{d^2}{2} (4 + 3/8k^2 + 3/2k) = 0$

i.e. $n = \frac{d}{2} \left[- (4 + \frac{9}{4}/k) \pm \sqrt{24 + \frac{93}{16k^2} + \frac{21}{k}} \right]$

Evans and Sarkar have used the same stress-strain relationships for their work on hollow rectangular beams but their expression for 'n' differs from that given above by the author and therefore values of 'n', given for specific 'k' ratios (= d/b), are not the same. These expressions are now used to deduce values for lever arm, and finally an expression for the moment of resistance of the section. As a result, these expressions will differ from those of previous authors.

Table 1.4:

'n' - values (t = b/4)

d/b	1.0	1.25	1.5	2.0	3.0
n	0.435d	0.435d	0.435d	0.435d	0.435d

By inspection of Table 1.4, it is proposed to consider 'n' as constant for any value of 'k', within the given range of values, and for both solid and hollow rectangular sections.

Using the stress-strain diagrams of Fig. 1.4, and values for 'n' from above, an expression is now derived for the lever arm, 'l_a' of the section.

(a) solid rectangle - plain concrete

Fig. 2.4:-

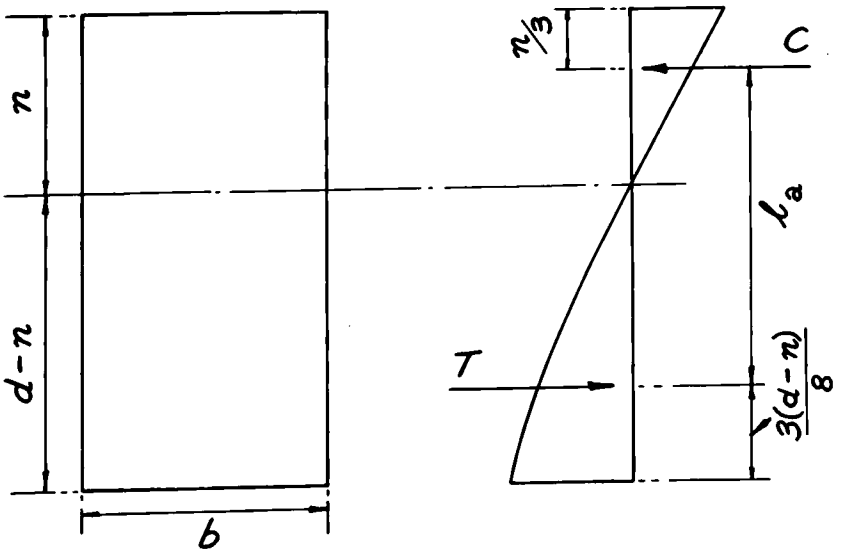

$$\ell_a = d - \frac{n}{3} - \frac{3}{8}(d - n)$$

$$= d - 0.15d - 0.375 \quad 0.551d$$

$$= 0.643d$$

(b) hollow rectangle - plain concrete

Fig. 3.4:-

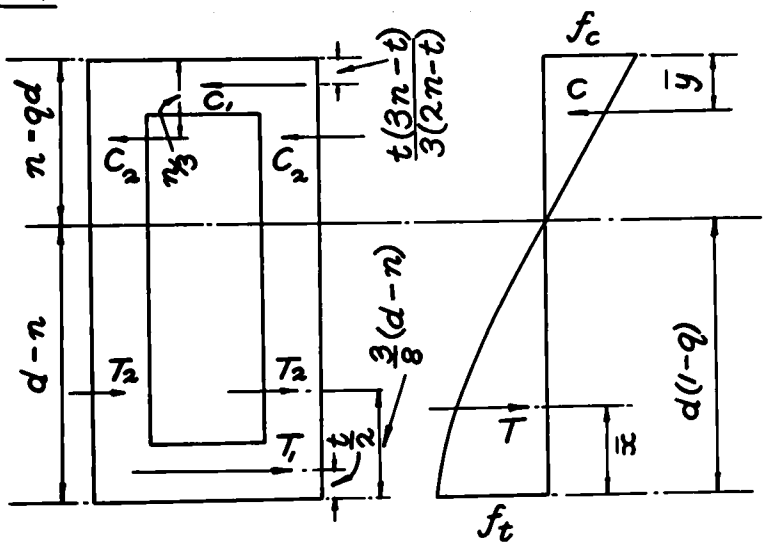

Compressive forces:-

$$C_1 = f_c \frac{n - \frac{t}{2}}{n}(b - 2t)t \; - f_c \frac{(2n - t)(b - 2t)t}{2n}$$

$$C_2 = f_c \, n \, t$$

so that

$$\bar{y} = \frac{f_c \frac{(2n-t)}{2n}(b-2t)t.\ \frac{t(3n\ t)}{3(2n\ t)} + f_c.nt\frac{n}{3}}{f_c \frac{(2n-t)}{2n}(b-2t)t \; + \; f_c.n.t.}$$

$$= \frac{(b-2t)t(3n-t) \quad + 2n^3}{3(2n-t)(b-2t) \quad + 6n^2}$$

assume t = b/4, then

$$t = \frac{d}{k} \; ; \quad tb = \frac{d^2}{4k^2} \; ; \quad t^2 = \frac{d^2}{16k^2}$$

and

$$\bar{y} = d\frac{(3q - \frac{1}{4k})\frac{1}{8k^2} + 2q^3}{\frac{3}{2k}(2q - \frac{1}{4k}) + 6q^2}$$

Tensile-Forces:-

$$T_1 = f_t(b - 2t)\,t$$

$$T_2 = \tfrac{2}{3} f_t(d - n)t \times 2$$

$$T = f_t\, t\left[\,4/3(d - n) + (b - 2t)\right]$$

and

$$\bar{x} = \frac{f_t(b-2t)\frac{t}{2} + \frac{2}{3}f_t(d-n).\,2.\,\frac{3}{8}(d-n)}{f_t(b-2t) + 4(d-n)}$$

$$= \frac{3}{2}\,\frac{(b - 2t)t + (d - n)^2}{3(b - 2t) + 4(d - n)}$$

assuming t = b/4 gives

$$\bar{x} = \frac{3}{2}\,d\left[\frac{\frac{1}{8k^2} + (1 - q)^2}{\frac{3}{2k} + 4(1 - q)}\right]$$

General expression for ℓ_a:-

$$\ell_a = d\left[1 - \left[\frac{(3q - \frac{1}{4k})\frac{1}{8k^2} + 2q^3}{\frac{3}{2k}(2q - \frac{1}{4k}) + 6q^2}\right] - \frac{3}{2}\left[\frac{\frac{1}{8k^2} + (1 - q)^2}{\frac{3}{2k} + 4(1 - q)}\right]\right]$$

This is a general expression for lever-arm in terms of 'q', the neutral-axis depth constant, and 'k', a geometric constant for the section, and for a given wall-thickness.

However, for the given 't' = b/4, using the evaluated n = 0.435d, the expression further simplifies as

$$\ell_a = d\left[1 - \left[\frac{(1.305 - \frac{1}{4k})\frac{1}{8k^2} + 0.164}{\frac{3}{2k}(0.870 - \frac{1}{4k}) + 1.134}\right] - 1.5\left[\frac{\frac{1}{8k^2} + 0.319}{\frac{3}{2k} + 2.260}\right]\right]$$

Table 2.4

ℓ_a - values (t = b/4)

d/b	1.0	1.25	1.50	2.0	3.0
ℓ_a	0.680d	0.697d	0.702d	0.707d	0.701d

The moment of resistance of the section prior to cracking is now derived in terms of the tensile force, T, and lever-arm, 'ℓ_a', as given in Figs. 2.4, 3.4. It is preferable to consider the moment in terms of the tensile properties of the concrete. In order to study the relative effects of combined bending and torsion it is necessary to exclude the effects of shear on the resistance of the beam. No consideration has been given to shear-resistance. However it has been shown[52] that the compressive stress of concrete under combined loading varies as the ratio of compressive stress to shear stress.

(a) solid rectangle - plain concrete

$$M_b = \tfrac{2}{3} f_t \, b \times 0.551d \times 0.643d$$

$$= f_t \frac{bd^2}{4.234} = f_t \frac{bd^2}{C_b}$$

(b) hollow rectangle - plain concrete

$$M_b = f_t \, t\left(\tfrac{4}{3}(d - n) + (b - 2t)\right) \ell_a$$

$$= f_t \, b \, d^2 \, \frac{(1 + 1.504k)}{2k} \, g/4$$

$$= f_t \left[\frac{bd^2}{\frac{8k}{g(1 + 1.504k)}} \right]$$

$$\text{i.e. } M_b = f_t \frac{bd^2}{C_b}$$

The Moment of Resistance to pure-bending is therefore a function of the geometrical properties of the section for both solid and hollow rectangular beams.

For the hollow rectangular section, the value of the constant C_b varies as 'k' given by the relation

$$C_b = \frac{8k}{g(1 + 1.504k)}$$ where g is given in Table 2.4 as $\ell_a = g.d$

The values of C_b tabulated in Table 3.4 are for the values of k considered in this thesis, and representative of practical design values.

Table 3.4

C_b values

k = d/b	1.0	1.25	1.5	2.0	3.0
solid rect.	4.234	4.234	4.234	4.234	4.234
hollow rect.	4.697	4.983	5.249	5.645	6.211

4.4 Moment of Resistance to Pure Torsion

As for pure bending, in investigating the resistance of the beam to pure torsion prior to cracking only the characteristics of the concrete need be considered. Several authors have investigated the stress-strain relationship for plain concrete subjected to pure torsion and in particular the case of the rectangular section. These studies[10, 21, 23], going as far back as 1934, but more recently an extensive study in America[53] all suggest a plastic distribution of torsional stress. This has been accepted in deriving the expression for moment of resistance of the section to pure torsion.

(a) solid rectangle - plain concrete

Using the sand-heap analogy developed by Nadai[22] for a rectangular cross-section, and outlined in Chapter 3 the moment of resistance in the completely plastic state is given by

$$M_t = \frac{(3k - 1)}{6k} \tau b^2 d$$
$$= \gamma \tau b^2 d$$

that is, the moment of resistance is a function of the geometrical properties of the section and the maximum torsional stress τ. Finally, the torsion constant γ is also a function of the 'k' ratio and the values given in Table 4.4 are for the range of k-values under consideration.

Table 4.4

γ values

d/b	(a)	(b)
1.0	0.333	0.291
1.25	0.367	0.308
1.50	0.389	0.319
2.00	0.417	0.333
3.00	0.444	0.347

(b) hollow rectangle - plain concrete

The application of Nadai's equation to hollow rectangular sections is given by considering the core to be negative and the values are included in Table 4.4 for t = b/4.

4.5 Angle of Crack:

The angle of crack in a reinforced concrete beam subjected to combined bending and torsion is now derived in terms of the individual bending and torsion stresses, f_t and τ. Cracking will occur in a plane normal to the direction of the principal tensile stress, so that the initial crack takes place at a point where the resolution of f_t and τ is a maximum, that is, at the bottom corner of the beam. Since a full plastic distribution of torsional stress has been assumed, maximum τ occurs along the longer length, namely the vertical side of the beam, and is constant.

These values for f_t and τ have been previously determined so that an expression for α, the angle of crack, is found.

Fig. 4.4 :-

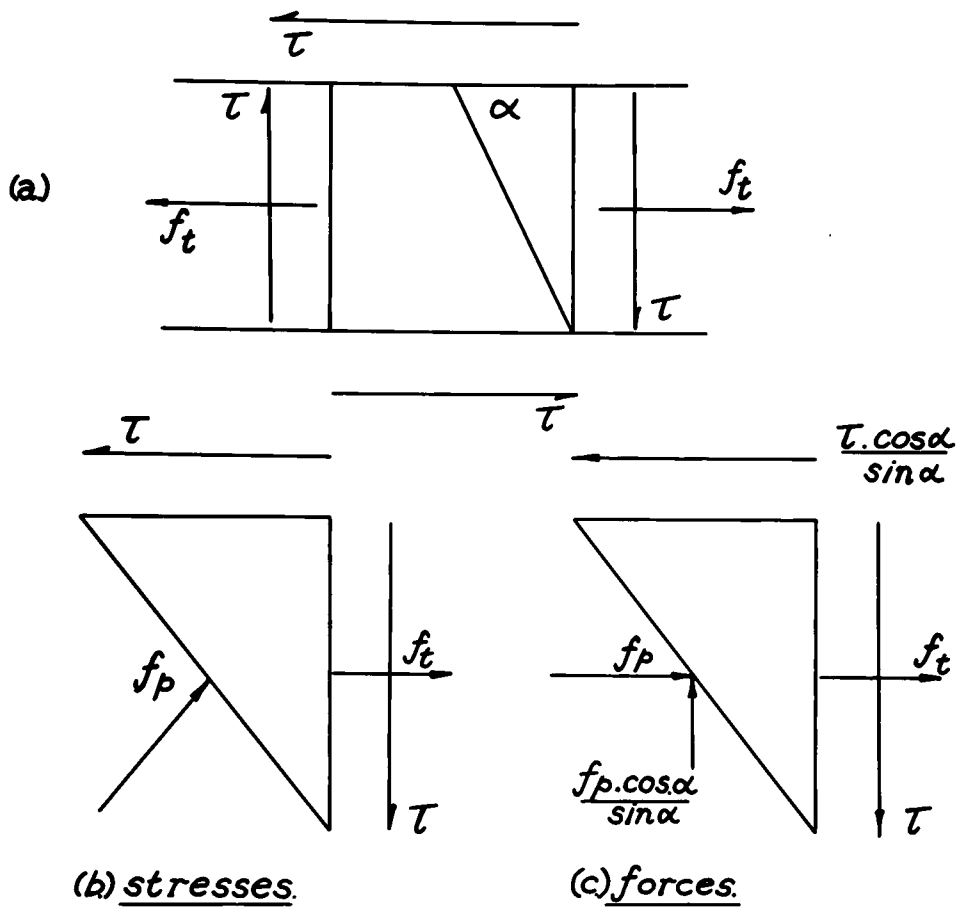

Considering the equilibrium of the wedge,

$$f_p + f_t = \frac{\tau \cos\alpha}{\sin\alpha} \qquad \ldots (1)$$

and,

$$f_p \frac{\cos\alpha}{\sin\alpha} = \tau \qquad \ldots (2)$$

Solve (1) and (2) and take maximum f_p then

$$f_p = \frac{1}{2}\left(f_t + \sqrt{f_t^2 + 4\tau^2}\right) \ldots (3)$$

and in direction opposite to that shown in Fig. 4.4(b).

In the above expression, f_t and τ have previously been found in terms of the geometrical properties of the beam section and the strength properties of the concrete.

$$f_t = \frac{C_b M_b}{b d^2} \quad ; \quad \tau = \frac{M_t}{\gamma b^2 d}$$

Substituting these values in equation (3) gives an expression for f_p in terms of the section characteristics and the applied bending moment and twisting moment as,

$$f_p = \frac{1}{2}\left[\frac{C_b M_b}{b d^2} + \sqrt{\left(\frac{C_b M_b}{bd^2}\right)^2 + 4\left(\frac{M_t}{\gamma b^2 d}\right)^2}\right]$$

where M_b and M_t are the respective bending moment and torsion moment being applied to the section at the load stage where cracking is initiated.

From fig. 4.4

$$\cot\alpha = \frac{\tau}{f_p} = \frac{\tau}{\frac{C_b.M_b}{2b.d^2} + \sqrt{\left(\frac{C_b.M_b}{2bd^2}\right)^2 + \left(\frac{M_t}{\gamma b^2 d}\right)^2}}$$

This expression for $\cot\alpha$ can be simplified by assuming a constant relation, ϕ, given by the ratio of applied bending-moment to applied twisting moment so that

$$\phi = \frac{M_b}{Mt} \quad \text{and}$$

$$\cot\alpha = \frac{1}{(\eta + \sqrt{\eta^2 + 1})}$$

where

$$\eta = \frac{C_b \phi \gamma b}{2d} = \frac{C_b \phi \gamma}{2k}$$

and is constant for a given section and specified combined loading ratio.

Having adopted a suitable beam shape, it is shown that the angle at which the concrete first cracks is largely determined by the ratio of applied bending moment to torsion moment. It has been observed[50] that any subsequent change, as is likely, in the ϕ ratio will not effect the propogation of the crack upwards, or across the bottom of the beam. The author intends to discuss this

point in the following Chapter in view of its importance with regard to calculations at ultimate load when the crack has fully traversed the cross-section; also, at a later stage with reference to experimental work carried out to examine the actual crack propogation. It can be mentioned here however that the influence of both longitudinal and transverse reinforcement must be considered in an investigation of crack propogation in a reinforced concrete beam beyond initial cracking.

The effect of varying the cross-section constant k and the ratio ϕ on the angle of crack α, is examined at this point for both solid and hollow rectangular sections with significant result as shown in Table 5.4 and Fig. 5.4.

Table 5.4

		ϕ	1.0	2.0	4.0	8.0
k = 1.25	$\cot \alpha$	S.R.	0.5561	0.3525	0.1937	0.0997
		H.R.	0.5591	0.3560	0.1961	0.1009
	α	S.R.	60-55	70-35	79-02	84-19
		H.R.	60-45	70-24	78-54	84-14
k = 2.00	$\cot \alpha$	S.R.	0.6488	0.4478	0.2610	0.1374
		H.R.	0.6339	0.4315	0.2487	0.1303
	α	S.R.	57-02	65-52	75-22	82-11
		H.R.	57-38	66-40	76-02	82-34
k = 1.50	$\cot \alpha$	S.R.	0.5921	0.3874	0.2177	0.1125
		H.R.	0.5873	0.3827	0.2139	0.1107
	α	S.R.	59-21	68-50	77-43	83-35
		H.R.	59-34	69-03	77-55	83-40

Applying limits to the expression for the special cases of pure torsion and pure bending gives $\cot \alpha = 1$ for $\phi = 0$, or $\alpha = 45^{\circ}$ as expected for the pure torsion case since the element considered

FIG. 5.4 :

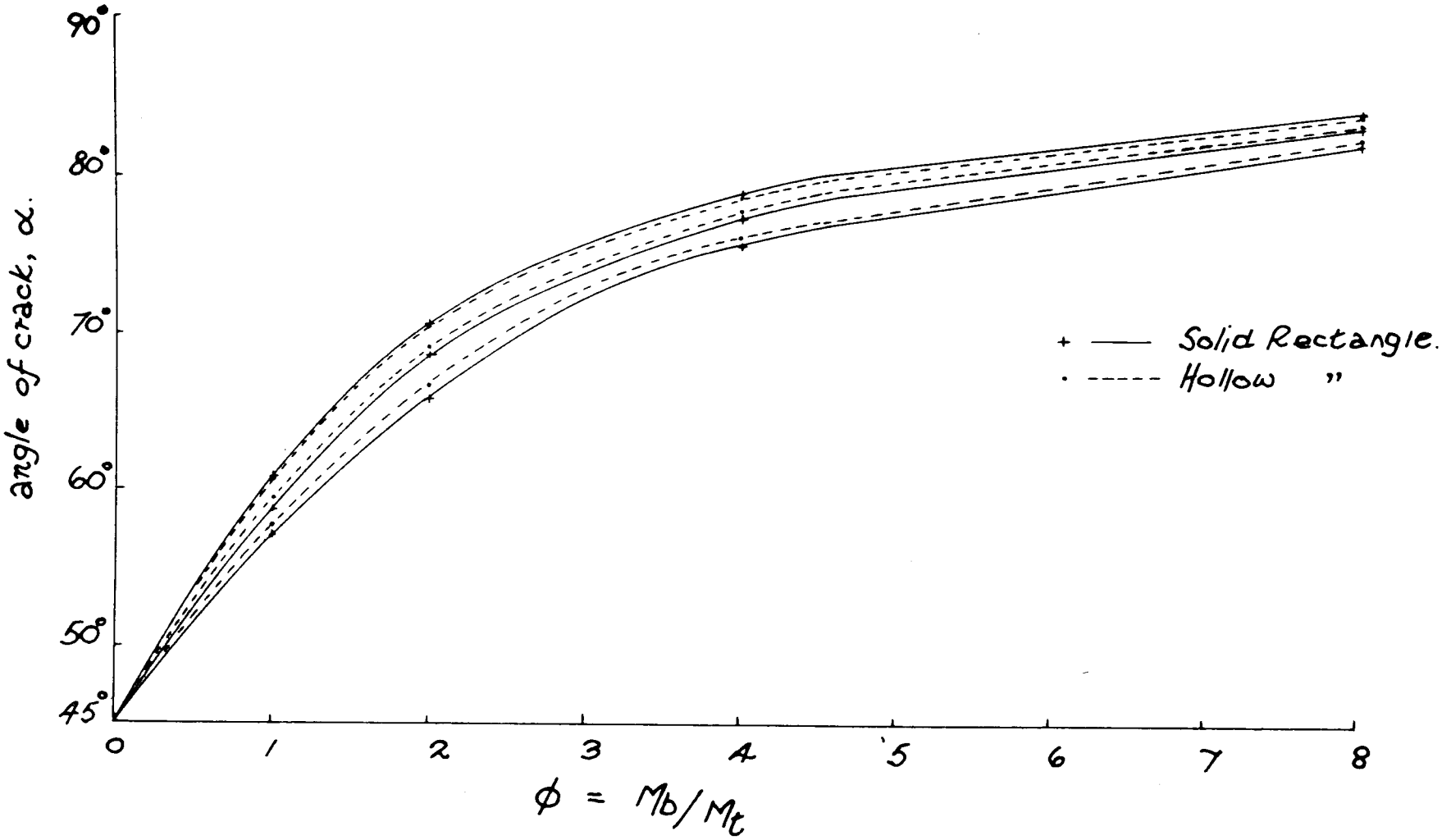
90°
80°
70°
60°
50°
45°
angle of crack, α.
0
1
2
3
4
5
6
7
8
φ = Mb/Mt
+ —— Solid Rectangle.
· ----- Hollow "

in Fig. 4.4 is now subjected to equal τ stresses, the resultant of which is a diagonal tensile stress causing fracture of the section at an angle of 45°; and for $\phi = \infty$, $\cot \alpha = 0$ or $\alpha = 90^{\circ}$ thus simulating the case of pure bending with a 90° fracture caused by bending stress f_t only.

The intermediate values of cot α for ϕ = 1.0, 2.0, 4.0, 8.0 have been tabulated in Table 5.4, and a graph of angle α plotted against ϕ is shown in Fig. 5.4.

Within the range of accuracies to which reinforced concrete designers usually work, the conclusion is that a single curve can be drawn from which values of initial angle of crack α can be found for any given ϕ ratio and any rectangle, solid or hollow, lying within the range of k-values considered.

Relation between α and β, α and θ:-

Fig. 6.4:-

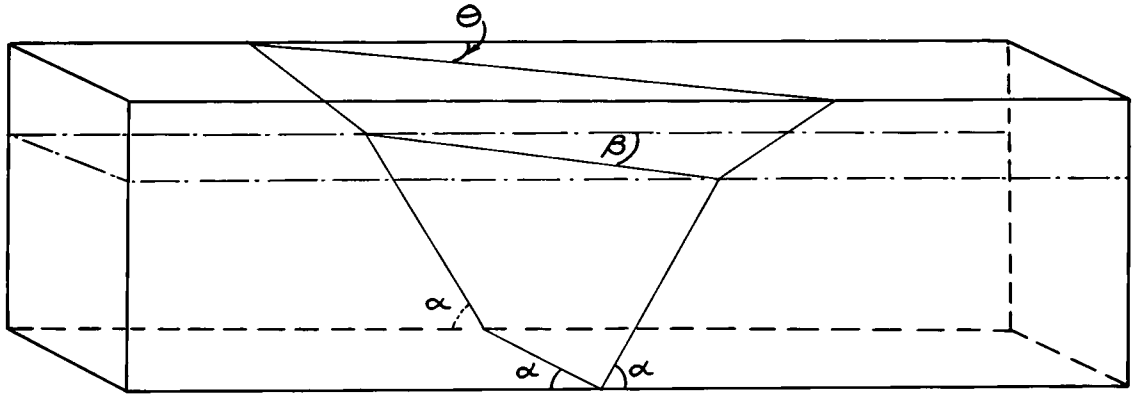

The angle, α, at which the crack propogates upwards and across the beam-section determines the values of angle β, or angle of inclination of the compression fulcrum, and angle θ, the angle at which the crack finally connects horizontally across

the upper surface of the beam to the vertical side cracks at failure. (Fig. 6.4).

The value of angle β is further determined by the neutral-axis position since it will be shown in Chapter 5 that rotation at ultimate load takes place about a compression fulcrum in the plane of the neutral-axis. The neutral-axis depth is no longer as previously calculated for angle α at initial cracking of the concrete, but the depth at ultimate load.

At the load-stage beyond initial cracking, the resistance of the beam to increasing tensile stress is provided by the reinforcement so that the neutral-axis depth 'n' remains constant for increasing steel-stress. At the same time, an increasing area of concrete reaches the tensile stress at which cracking is initiated so that the crack moves up the beam. The hypothetical stress-block is represented in diagrammatic form in Fig. 7.4 for pure bending. The addition of torsional stresses as in combined loading will increase the value of stress by an amount given by the component of torsional stress acting in the same direction as the bending stress. It is assumed, in the general case, that the bending-stress is the greater, corresponding to ϕ values greater than 2.

The change point occurs when the reinforcement reaches its yield stress. Any further increase in applied loading will be resisted by the beam by an increase in the length of the lever-arm with resultant decrease in the value of 'n'. The raising of the neutral-axis proceeds with continued loading, exposing an increasing depth of concrete to the critical cracking stress, so that crack propogation continues and at constant angle.

FIG. 7.4 :-

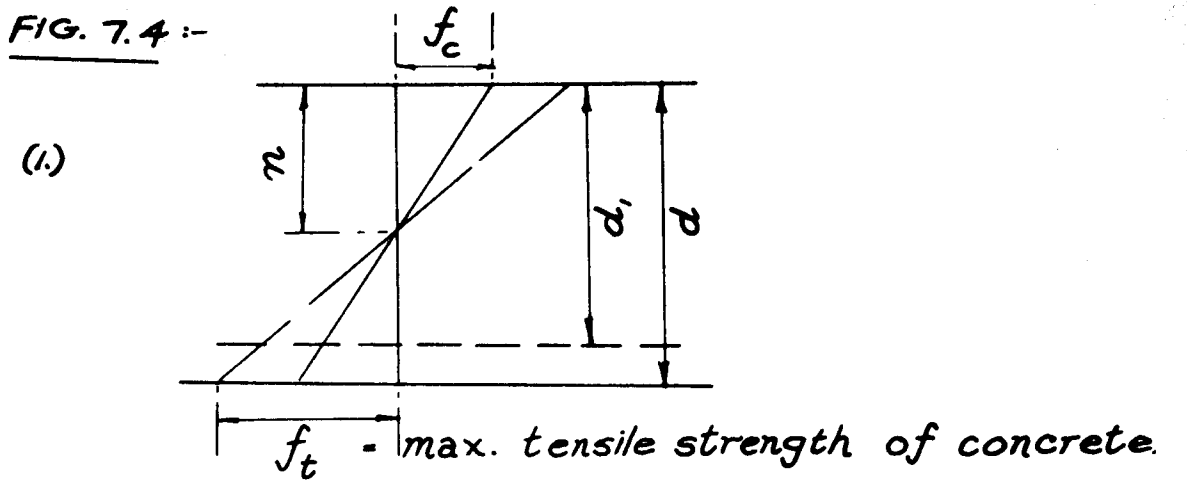
(1.)
f_c
n
d_1
d
f_t - max. tensile strength of concrete.
(2.)
n_2
height of crack
f_{ts} - hypothetical stress in steel.
(3.)
n_3
height of crack.
f_L
f_{cb}
(4.)
n_4
height of crack.
f_L

Ultimate load is reached when the area of concrete resisting the applied moments in compression is reduced to the point where the resistance of the beam in compression is equal to the applied moment. Failure is now reached due to crushing of the concrete in the compression zone at the upper surface of the beam.

Therefore, an expression for β is derived using the depth of the neutral-axis at ultimate load since any design equations deduced in Chapter 5 are for ultimate design. Assuming that values for α, the angle of crack on the beam face, and for 'n', the depth of the neutral-axis at ultimate load are known, the value of β is dependent upon the geometrical properties of the section. Now, applying the theory for the angle of crack and the crack propogation as developed in Fig. 8.4, an expression for β is found, given as

$$\cot \beta = \cot \alpha (2jk + 1)$$

The crack crosses the underside of the beam at angle α since the resultant stress remains constant across this length as far as the opposite face. At this point, due to a reversal in direction of the torsional stress, the crack continues up the beam at an angle α but in direction opposite to that on the front face.

In the limit, for $\phi = 0$, $\cot \alpha = 1$ and $j = 1$, and $\cot \beta$ is a function of 'k', not necessarily unity, so that pure torsion gives a β value not necessarily equal to 45°. This fact has been investigated experimentally and is reported in Chapter 7 and Appendix A but accepting 45° cracks up the front and back-faces of a beam subjected to pure torsion, the value of β is necessarily less than 45°. For $\phi = \infty$, both α and $\beta = 90^{\circ}$, thus agreeing with the practical case of pure bending.

FIG. 8.4

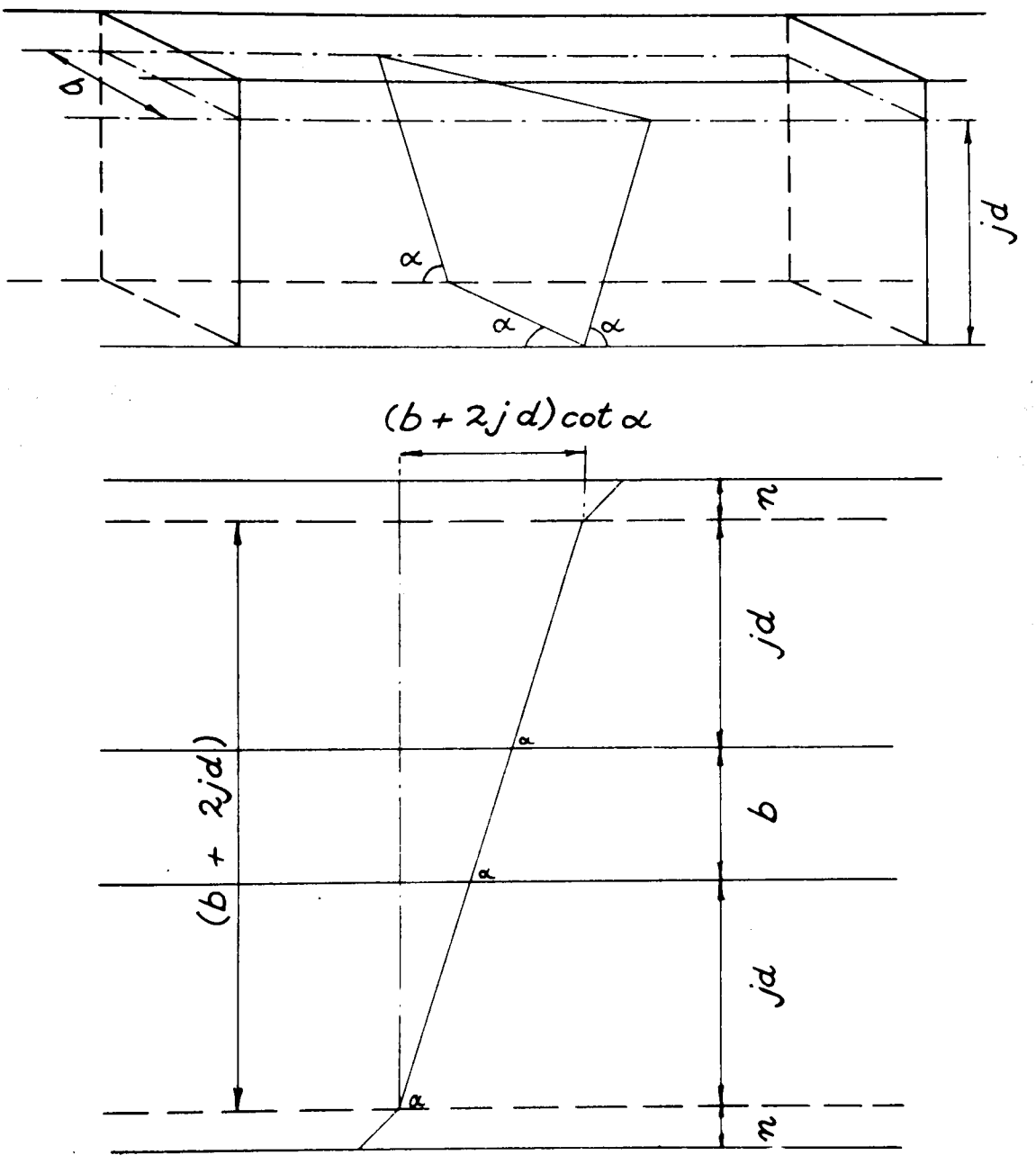

An expression can be similarly derived for θ, although this angle is of less significance in the design concept. The values of θ and β are theoretically not the same although towards ultimate this difference is reduced as the position of the neutral-axis tends towards the upper surface of the beam.

Although the general principle for calculation of the angle of crack, α, is acceptable, some thought is now given to its complex form particularly as in the final design equation it is intended to include $\cot\alpha$, and also $\sin\beta$, $\cos\beta$, $\operatorname{cosec}\beta$, expressed in terms of $\cot\alpha$, thus introducing square-root terms. The nature of the $\cot\alpha$ against ϕ plot does not enable results to be taken readily. Further, with a view to a general design equation, it is desirable to use a general expression for $\cot\alpha$ and hence the corresponding β terms.

A graph of $\log\cot\alpha$ against $\log\phi$ is shown in Fig. 9.4. The graph falls essentially into three parts according to ϕ value:-

(a) $\phi < 2$

(b) $\phi > 2, < 8.$

(c) $\phi > 8.$

This breakdown agrees with a practical assessment of ϕ in which ϕ values less than two give predominant torsion conditions, ϕ values lying between two and eight can be considered as combined loading, and ϕ values larger than eight produce essentially a pure bending condition.

Consider the equation of the graph to be

$$\log\cot\alpha = \log k + n\log\phi$$

so that

$$\cot\alpha = k\phi^{n}$$

FIG. 9.4:-

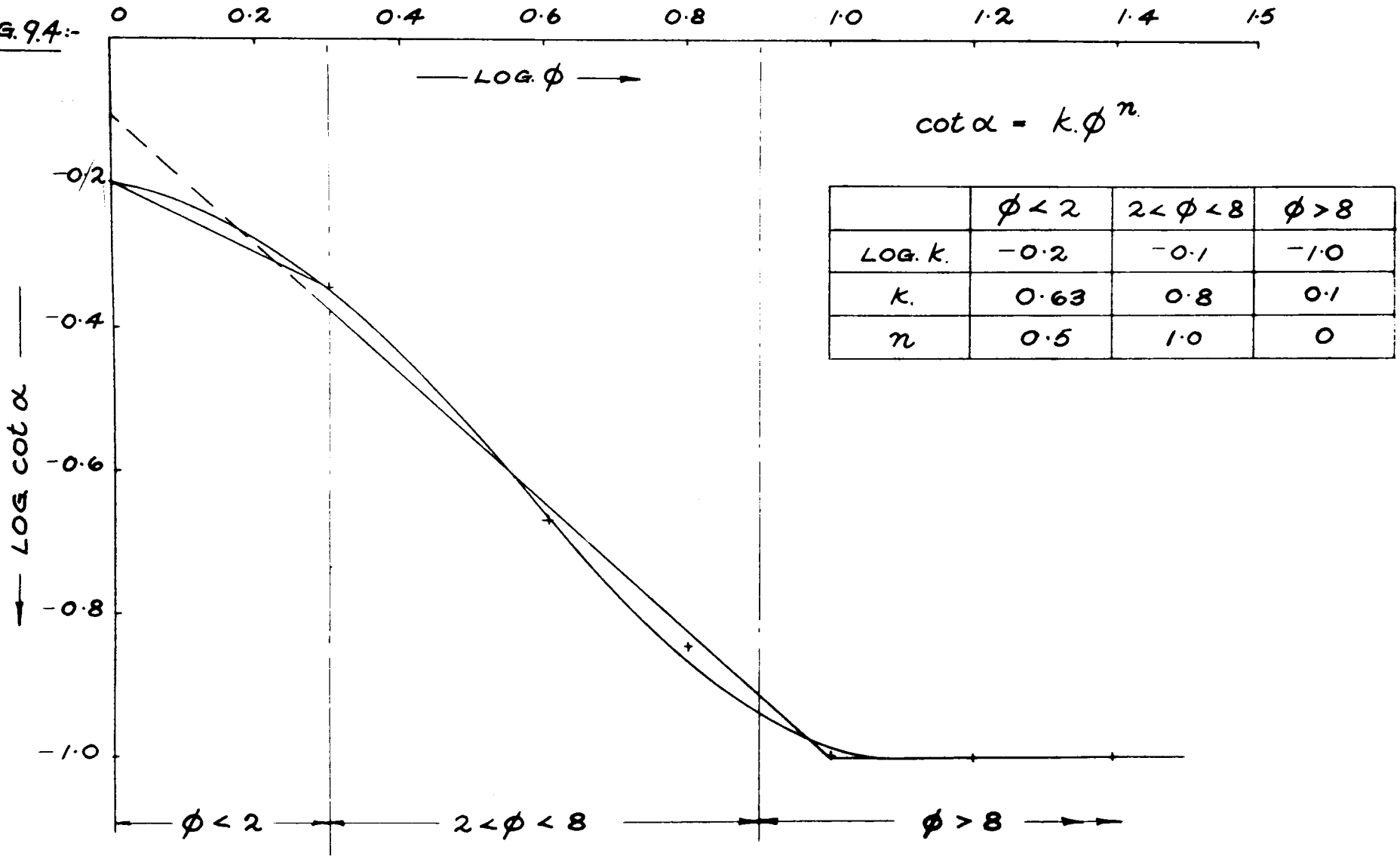

	φ < 2	2 < φ < 8	φ > 8
LOG. k.	−0·2	−0·1	−1·0
k.	0·63	0·8	0·1
n	0·5	1·0	0

(a) $\underline{\phi < 2}$:- from fig. 9.4.

$\log k = -0.2 = \bar{1}.8$

n = gradient of straight line $= -0.5$

so that $\cot \alpha = 0.63/\sqrt{\phi}$

(b) $\underline{2 < \phi < 8}$:-

$\log k = \bar{1}.9$

n = gradient $= -1.0$

so that $\cot \alpha = 0.8/\phi$

(c) $\underline{\phi > 8}$:-

Beyond ϕ values of eight, the plot of $\cot \alpha$ changes, and as values of α are now greater than eighty degrees, a large increase in ϕ will produce a relatively small increase in $\cot \alpha$. Therefore, to retain as simple an expression as possible, $\cot \alpha$ is considered to be constant over this region and given by

$$\cot \alpha = 0.1$$

Using these approximate expressions for $\cot \alpha$, values, comparable to those given in Table 5.4, are evaluated as shown in Table 6.4

ϕ	$\cot \alpha$	α
1.0	0.63	57°-48'
2.0	(a) 0.416	67°-24'
	(b) 0.400	68°-24
4.0	0.315	72°-30'
8.0	(b) 0.1	84°-42'
	(c) 0.1	84°-42'
10.0	0.1	84°-42'

Although slight discrepancies are incurred at change points, this does not affect the final design equations as shown in Chapter 5. A comparison between theoretical and practical values is made in Chapter 7.

4.6 Conclusions:

The behaviour of a reinforced concrete beam during the period from initial application of the load up to initial cracking of the beam, is determined only by the properties of the concrete. At this stage, the maximum tensile strength of the concrete is reached. Behaviour of the beam beyond cracking will then depend primarily upon the reinforcement.

Although it is the author's intention to study the effects of combined bending and torsion on the beam, it is necessary to consider the resistance of the concrete to pure bending and to pure torsion. The exact nature of the assumptions made as to whether concrete behaves elasto-plastically, semi-plastically or completely plastic, influences the conclusion drawn for this initial pre-cracking stage. The conclusions given in this Chapter are based on the assumptions that the concrete behaves visco-elastically in bending and plastically in torsion.

Since only concrete properties are being considered, differences in the moments of resistance of a solid rectangular section and a hollow rectangular section of the same shape to pure bending are to be expected. However, in both cases, the depth of the neutral axis and the length of the lever arm remain constant and proportional to depth. The moments of resistance can then be expressed as functions of the tensile strength of the concrete and the geometrical properties of the section in terms of constant 'k'.

For pure torsion, the equations of Nadai have been accepted for the solid rectangular section and modified to include hollow sections. In both cases, the moment of resistance is determined by the maximum torsional stress and the geometrical properties of the section.

The angle of crack formed on the sides of the beam is derived by considering the combined tensile and torsion stresses resulting from the applied bending and torsion moments. This crack forms at right angles to the maximum principal stress and therefore at the bottom corner of the beam. The propogation upwards and across the beam is at a constant angle, determined by the moments of resistance constants for the concrete, the geometrical properties of the section and the ratio of the applied bending to torsion moment. For design purposes the angle of crack can be considered to be dependent only on this ratio for both solid and hollow rectangular sections.

It is finally concluded that the angle about which rotation of the section takes place along the neutral axis due to combined bending and torsion at the ultimate stage can be related to the angle of cracking of the section up to the neutral axis depth at this stage. Consequently, the angle of rotation is also determined by the ratio of applied bending moment to torsion moment. An extensive study has been made of the problem of deriving an expression for β and Appendix A has been included on this subject. However, it is the author's opinion that the most satisfactory available expression for β has been adopted.

CHAPTER 5

ULTIMATE LOAD DESIGN

5.1 General:

This Chapter deals with the behaviour of a beam at ultimate load, that is, immediately prior to failure. A value can be obtained for the ultimate resistance of the section when subjected to both bending and torsion. This value is then compared with design preporties of the section at working load. The working design may, or may not, have included the torsion moment. Nevertheless by comparing the working design moment with the ultimate design moment as given in this Chapter, a more realistic load-factor is obtained.

5.2 Introduction

In considering the equilibrium of the cracked section of a reinforced concrete beam at ultimate load, values for the resistance of the beam can be found on the basis of the resistance of the concrete in the compression zone together with the moments provided by each unit of reinforcement, longitudinal or transverse, intercepted by the crack.

The concept of this design procedure is largely due to work carried out in Russia[5, 6, 32, 33, 34, 35], as reported in Chapter 2 and now referred to as the Ultimate Equilibrium Method. This method is said to reproduce most accurately the actual behaviour of the reinforced concrete structure. The disadvantage of the Russian approach is the complexity of the design equations, mainly due to an exact mathematical treatment of the failure mechanism. Further study has been carried out in Leeds[50] to express these design equations more simply, assuming a constant depth of neutral-axis over the area of the crack.

It is proposed in this Chapter to introduce further simplifications based on the conclusions drawn in Chapter 4 for the angle of crack and angle of inclination of the compression fulcrum. The Russian theory and more recent studies have been mentioned briefly in Chapter 2.

It is further intended to derive a new expression for the ultimate bending load, given any specific applied torsional load. The main disadvantage of the ultimate equilibrium method and any subsequent modified theory is that the ratio of applied bending moment to torsional moment is used in the design equation. Thus, the solution is dependent on the $\emptyset$ ratio remaining constant during the load stage from working to ultimate load. It is proposed to develop new design equations to allow for the substitution of any torsional-moment and, in particular, the torsion moment being applied at the ultimate stage.

The first part of the Chapter is concerned with the fundamental principles of the ultimate equilibrium design concept. The latter parts of the Chapter will deal with the author's own developments to obtain new design equations for both solid and hollow rectangular sections and with either longitudinal only, or longitudinal and transverse reinforcement.

5.3 Ultimate Equilibrium Method of Design:

The general case of the ultimate equilibrium theory applied to a reinforced concrete beam, reinforced both longitudinally and transversely and subjected to combined bending moment and torsion moment will be considered. Although two failure schemes are possible, only the more likely case of a horizontal neutral-axis crossing the vertical sides of the beam as shown in Fig. 1.5 will be considered.

Fig. 1.5:-

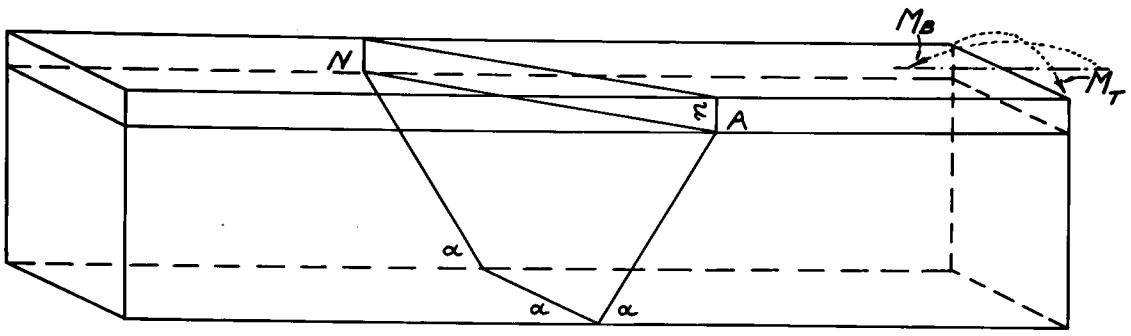

The following assumptions are made. Rotation takes place about the neutral axis NA inclined at an angle to the longitudinal axis of the beam. NA is therefore considered as the compression plastic hinge. All steel components, longitudinal or transverse, passing through the crack-area contribute to the resistance of the beam. For this purpose, it is necessary to assume a constant spacing of the transverse steel over the length of the crack. Further, it is assumed that all the reinforcement passing through the crack has reached its yield-stress at ultimate load. Finally, the effect of any steel in the compression zone, also the tensile strength of the concrete, is neglected. It is therefore a necessary part of this analysis to provide an under-reinforced design and thus ensure that the reinforcement reaches its yield-stress.

The derivation of the design equation then follows on the basis of The Principle of Least Work, and in particular, that the sum of the external moments due to bending and torsion is equal

to the sum of the internal moments acting normal to the neutral-axis.

The location of the neutral-axis is fixed by considering the equilibrium of the projections of the internal and external forces on the axis normal to the plane of the compression zone.

The application of these principles to the beam being considered is shown in fig. 2.5. This application has been made recently to hollow rectangular beams[50].

Equating external forces and internal forces normal to the compression hinge gives

$$f_c' \; b \; n \; \mathrm{cosec}\,\beta = f_L \; A_L \; \sin\beta + \frac{f_T \; A_T}{S} \; b_3 \; \cot\alpha \; \cos\beta$$

so that

$$n = \frac{f_L . A_L \sin\beta + \frac{f_T A_T}{S} b_3 . \cot\alpha . \cos\beta}{f_c' . b . \mathrm{cosec} . \beta}$$

Equating external and internal moments about the centre of gravity of the compression zone and normal to the compression hinge gives

$$M_b \sin\beta + M_t \cos\beta = \tfrac{1}{2} f_c' \; n^2 b \; \mathrm{cosec}\,\beta + f_L \; A_L \; (d_1 - n) \; \sin\beta$$
$$+ \frac{f_T \; A_T}{S} \; b_3 \; \cot\alpha \cos\beta (d - d_s - n)$$
$$- \frac{f_T A_T}{S} \; d_3 (j \cot\alpha' + (1-j)\cot\psi') \left[d(j \cot\alpha + (1-j)\cot\psi) \right.$$
$$\left. + b_3 \cot\alpha - b_3 \cot\beta \right]$$

Despite the simplification of a horizontal neutral axis, the expression is still complex, especially the term for the vertical transverse steel moment of resistance. Furthermore, the expression for the internal moment of the beam is apparently reduced by the negative contribution of the moment of the vertical transverse steel. It is intended to consider this with a view

FIG. 2.5 :

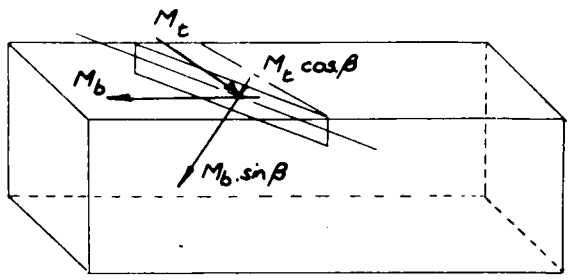

EXTERNAL MOMENTS.

$$= M_b \sin\beta + M_t \cos\beta$$

INTERNAL MOMENTS

1. concrete in compression

$$\text{moment} = f_c' (n.b.\operatorname{cosec}\beta).\frac{n}{2}$$
$$= \tfrac{1}{2} f_c' . b . n^2 \operatorname{cosec}\beta$$

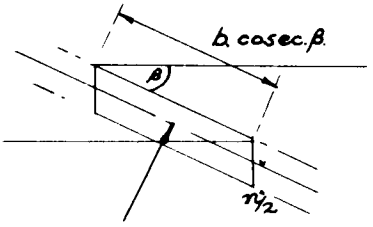

2. longitudinal steel.

$$\text{moment} = f_L . A_L (d_1 - n) \sin\beta$$
$$= f_L . A_L (d_1 - n) \sin\beta$$

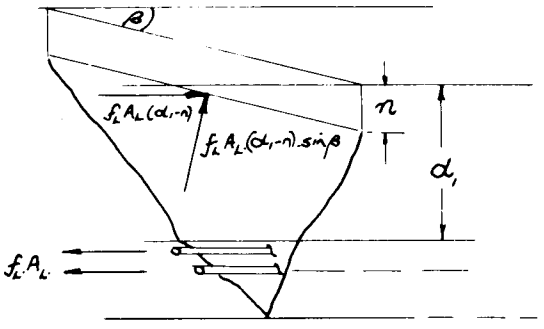

3. horizontal transverse steel.

area of transverse steel per unit length $= \frac{A_T}{S}$

area of transverse steel crossing crack $= \frac{A_T}{S} . b_3 . \cot\alpha$

$$\text{moment} = f_T . \left(\frac{A_T}{S} . b_3 . \cot\alpha\right)(d - d_s - n) \cos\beta$$
$$= \frac{f_T . A_T}{S} . b_3 . \cot\alpha . \cos\beta . (d - d_s - n)$$

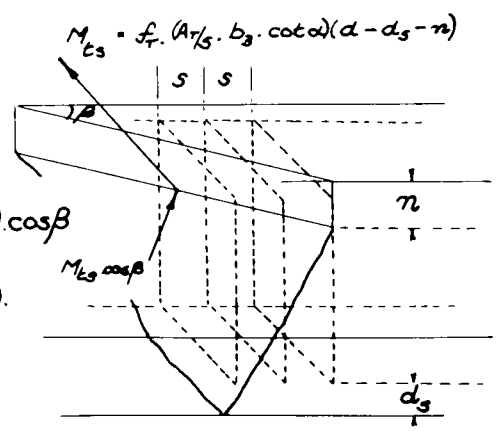

INTERNAL-MOMENTS - contin

4. vertical transverse steel.

The upward and downward forces F due to vertical transverse steel produce a couple of value $F \times \ell_a$ = distance between the equal forces on the vertical sides of the beam.

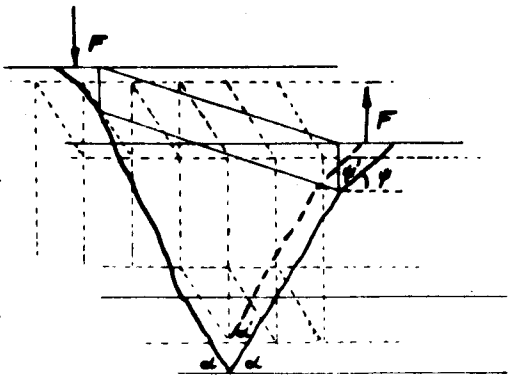

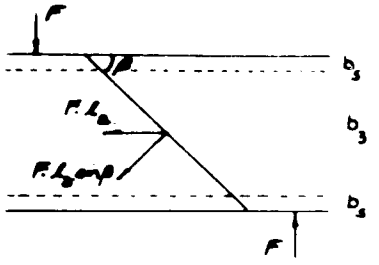

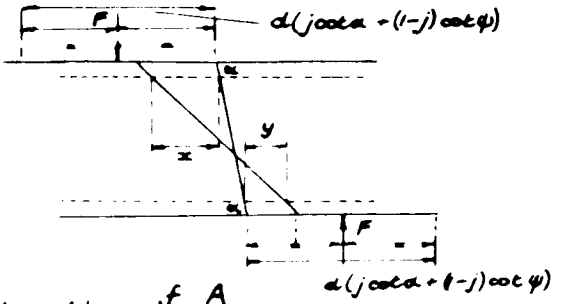

Area of transverse steel per unit length $= \frac{f_T A_T}{s}$

area along length of crack $= \frac{f_T A_T}{s} \cdot d_3 (j\cot\alpha' + (1-j)\cot\psi')$

where $\alpha' = 90° - b_3/b \cdot (90° - \alpha)$, $\psi' = \psi(2 - b_3/b)$

Lever-arm $= \frac{d}{2} \cdot (j\cot\alpha + (1-j)\cot\psi) + \frac{d}{2}(j\cot\alpha + (1-j)\cot\psi) - x - y$

$= d(j\cot + (1-j)\cot\psi) + b_3(\cot\alpha - \cot\beta)$

Moment due to vertical transverse steel =

$$\frac{f_T A_T}{s} \cdot d_3 (j\cot\alpha' + (1-j)\cot\psi')(d(j\cot\alpha + (1-j)\cot\psi) + b_3(\cot\alpha - \cot\beta))$$

Moment normal to neutral-axis =

$$-\frac{f_T A_T}{s} \cdot d_3 \cdot \sin\beta (j\cot\alpha' + (1-j)\cot\psi')(d(j\cot\alpha + (1-j)\cot\psi + b_3(\cot\alpha - \cot\beta))$$

to further simplification of the expression. Denoting M_t as a function of M_b and ϕ, the equation now reduces to

$$M_b = \frac{\phi}{\cos\beta + \phi \sin\beta} \left[\begin{array}{l} \frac{1}{2} f'_c . b . n^2 \operatorname{cosec}\beta + f_L A_L . \sin\beta (d_1 - n) \\ + \frac{f_T A_T}{s} . b_3 . \cot\alpha . \cos\beta (d - d_s - n) \\ - \frac{f_T . A_T}{s} d_3 \left[j \cot\alpha' + (1-j)\cot\psi' \right] \sin\beta \\ d \left[j\cot\alpha + (1-j)\cot\psi + b_3 (\cot\alpha - \cot\beta) \right] \end{array} \right]$$

A further simplification can be achieved by considering specific values of β such as 45° or 60°. It is shown, however, in Appendix A that variations in assumed values of β do produce significant differences in the calculated results for ultimate moment. A completely satisfactory value for β will only be found by analysis of the resultant stresses in the compression zone. Meanwhile, the author feels that it is more satisfactory to adopt a definite procedure for determining β. The expression for β derived in Chapter 4 can now be used to obtain a more direct expression.

However, the equation for ultimate bending moment given above can be evaluated for any specific ϕ ratio by substituting the details of the beam section, these details having been obtained by the normal design process for working load. The assumption[50] that $\alpha' = \alpha$, and $\psi' = \psi = 45^\circ$ provides further simplification without significant effect on the calculated result:-

$$M_b = \frac{\phi}{\cos\beta + \phi \sin\beta} \left[\begin{array}{l} \frac{1}{2} . f'_c . b . n^2 \operatorname{cosec}\beta + f_L A_L . \sin\beta (d_1 - n) \\ + \frac{f_T . A_T}{s} . b_3 . \cot\alpha . \cos\beta (d - d_s - n) \\ - \frac{f_T . A_T}{s} d_3 . \left[1 + j(\cot\alpha - 1) \right] \sin\beta \\ d \left[1 + j(\cot\alpha - 1) + b_3 (\cot\alpha - \cot\beta) \right] \end{array} \right]$$

5.4 Design Equations for Ultimate Moment

The conclusions from Chapter 4 with regard to angles α and β can now be included in order to simplify the ultimate equilibrium expression for ultimate moment. It is proposed to consider first the application to the simpler case of a rectangular section with longitudinal reinforcement only. The same principle can then be developed for the more general case of a rectangular section with longitudinal and transverse reinforcement.

The modified expressions for α and β are, in general,

$$\cot\beta = \cot\alpha(2jk + 1)$$

and for $\cot\alpha$, three expressions depending on the range of values of ϕ:-

$$\phi < 2 \qquad \cot\alpha = 0.63/\phi^{\frac{1}{2}}$$

$$2 < \phi < 8 \qquad \cot\alpha = 0.8/\phi$$

$$\phi > 8 \qquad \cot\alpha = 0.1$$

The theory is applicable to both solid and hollow rectangular sections, but it will be necessary to consider three design equations according to these limits. This procedure is not very satisfactory and at a later stage the author outlines a more general expression.

(a) Longitudinal reinforcement only

The modified ultimate equilibrium expressions for ultimate moment, M_b, and neutral axis depth, n, are

$$M_b = \frac{\phi}{\cos\beta + \phi\sin\beta}\left(\tfrac{1}{2} f_c' b n^2 \operatorname{cosec}\beta + f_L A_L \sin\beta(d_1 - n)\right)$$

and $$n = \frac{f_L A_L \sin^2\beta}{f_c' b}$$

so that, alternatively

$$M_b = \frac{\phi}{\cos\beta + \phi\sin\beta} f_L A_L \sin\beta(d_1 - {}^{n}/_{2})$$

Substituting values for β gives, for example,

(a) $\beta = 45^\circ$ $\qquad M_b = \dfrac{\phi}{1+\phi} f_L A_L (d_1 - \dfrac{f_L A_L}{4 f_c' b})$

(b) $\beta = 60^\circ$ $\qquad M_b = \dfrac{\sqrt{3}\,\phi}{1+\sqrt{3}\,\phi} f_L A_L (d_1 - \dfrac{3 f_L A_L}{8 f_c' b})$

(c) $\beta = 90^\circ$ $M_t = 0$, $\quad M_b = \frac{1}{2} f_c' b n^2 + f_L A_L (d_1 - n) = f_L A_L (d_1 - \dfrac{f_L A_L}{2 f_c' b})$

and this the pure bending case;

(d) $\beta = 45^\circ$ $M_b = 0$, $\quad M_t = f_c' b n^2 + f_L A_L (d_1 - n) = f_L A_L (d_1 - \dfrac{f_L A_L}{4 f_c' b})$

and this is the pure torsion case;

(e) or, in particular $\beta = \cot^{-1} (\cot \alpha (2jk + 1))$

The relevant trigonometrical functions are

$$\sin \beta = \frac{1}{\sqrt{1 + \cot^2 \beta}}$$

$$\cos \beta = \frac{\cot \beta}{\sqrt{1 + \cot^2 \beta}}$$

and $\operatorname{cosec} \beta = \sqrt{1 + \cot^2 \beta}$

It is also necessary, in addition to specifying a range of values for ϕ, to choose specific values for the geometric constant "k". For this purpose, values are chosen relating to practical design values.

One major assumption is made, namely with regard to the depth of the neutral-axis. It has already been shown (Ch. 4 Fig. 7.4) that the position of the neutral axis changes with increasing applied load from its position at initial cracking (Table 1.4) to an ultimate position given by equating forces

normal to the compression-hinge just prior to failure. It can be assumed therefore, that for the purposes of ultimate design, the value of n is very small compared to the depth of the section and so

take $j = 1$

β- values:- $\quad \phi < 2$

$$\cot\beta = \frac{0.63}{\sqrt{\phi}}(2k + 1)$$

$$\sin\beta = \frac{\sqrt{\phi}}{\sqrt{\phi + 0.4(2k + 1)^2}}$$

$$\cos\beta = \frac{0.63(2k + 1)}{\sqrt{\phi + 0.4(2k + 1)^2}}$$

$$\operatorname{cosec}\beta = \frac{\sqrt{\phi + 0.4(2k + 1)^2}}{\sqrt{\phi}}$$

so that, $$n = \frac{f_L A_L}{f_c' b} \frac{\phi}{\phi + 0.4(2k + 1)^2}$$

$$= \frac{f_L A_L}{f_c' b} \frac{\phi}{\phi + A} \qquad \ldots (1.5)$$

where $A = 0.4(2k + 1)^2$

and, $$M_b = \frac{\phi}{\phi + \frac{0.63}{\sqrt{\phi}}(2k + 1)} f_L A_L (d_1 - n/2)$$

$$= \frac{\phi}{\phi + \frac{B}{\sqrt{\phi}}} f_L A_L (d_1 - n/2) \qquad \ldots (2.5)$$

where $B = 0.63(2k + 1)$

$2 < \phi < 8$:-

$$\cot\beta = \frac{0.8}{\phi}(2k + 1)$$

$$\sin\beta = \frac{\phi}{\sqrt{\phi^2 + 0.64(2k+1)^2}}$$

$$\cos\beta = \frac{0.8(2k+1)}{\sqrt{\phi^2 + 0.64(2k+1)^2}}$$

$$\operatorname{cosec}\beta = \frac{\sqrt{\phi^2 + 0.64(2k+1)^2}}{\phi}$$

so that,

$$n = \frac{\phi^2}{\phi^2 + A} \frac{f_L A_L}{f_c' b} \qquad \ldots (3.5)$$

where $A = 0.64(2k+1)^2$

and, $$M_b = \frac{\phi^2}{\phi^2 + B} f_L A_L (d_1 - n/2) \qquad \ldots (4.5)$$

where $B = 0.8(2k+1)$

$\phi > 8$:- $\cot\alpha = 0.1$ $\sin\beta = \dfrac{1}{\sqrt{1 + 0.01(2k+1)^2}}$

$$\cos\beta = \frac{0.1(2k+1)}{\sqrt{1 + 0.01(2k+1)^2}}$$

$$\operatorname{cosec}\beta = \sqrt{1 + 0.01(2k+1)^2}$$

so that,

$$n = \frac{A \; f_L A_L}{f_c' b} \qquad \ldots (5.5)$$

where $A = \dfrac{1}{1 + 0.01(2k+1)^2}$

and, $$M_b = \frac{\phi}{\phi + B} f_L A_L (d_1 - n/2) \qquad \ldots (6.5)$$

where $B = 0.1(2k+1)$

Table 1.5 gives values of the constants A and B for a practical range of k-values from 2 to 1

ϕ		k-values 2.0	1.5	1.25	1.0
< 2	A	10.0	6.4	4.9	3.6
	B	3.15	2.52	2.205	1.89
> 2, < 8	A	16.00	10.24	7.84	5.76
	B	4.00	3.20	2.80	2.40
> 8	A	0.80	0.862	0.891	0.917
	B	0.50	0.40	0.35	0.30

The value k = 1 has been included in Table 1.5 as it is intended to include calculations in Chapter 6 for beams of square section.

(b) Longitudinal and transverse reinforcement

The same principles can now be applied to the general expression for ultimate moment of a reinforced concrete beam containing both longitudinal and transverse reinforcement and subjected to combined bending and torsion.

The assumption that j = 1 reduces the complicated expression representing the contribution of the vertical transverse steel moment of resistance in the ultimate equilibrium expression to the following

$$-\frac{f_T A_T}{S} d_3 \sin\beta \cot\alpha \,(d \cot\alpha + b_3 (\cot\alpha - \cot\beta)).$$

Finally assume $b_3 = b$ (the error introduced by this assumption is only of importance in beams with above average concrete cover for the reinforcement.) It is therefore proposed to develop the original equilibrium equation in the following simpler form:-

$$M_b \sin\beta + M_t \cos\beta = \tfrac{1}{2} f_c' b n^2 \operatorname{cosec}\beta + f_L A_L \sin\beta (d_1 - n)$$

$$+ \frac{f_T A_T}{S} b_3 \cot\alpha \cos\beta (d - d_s - n)$$

$$+ \frac{f_T A_T}{S} d\, d_3 \sin\beta \cot^2\alpha \qquad \ldots (7.5)$$

where $$n = \frac{f_L . A_L . \sin\beta + \frac{f_T . A_T}{S} . b_3 . \cot\alpha . \cos\beta}{f_c' . b . \text{cosec}\beta} \qquad \ldots (8.5)$$

n-values:-

$\phi < 2$:-

$$n = \frac{\frac{f_L A_L \sqrt{\phi}}{\sqrt{\phi + 0.4(2k+1)^2}} + \frac{f_T A_T}{S} b_3 \frac{0.63}{\sqrt{\phi}} \frac{0.63(2k+1)}{\sqrt{\phi + 0.4(2k+1)^2}}}{\frac{f_c' b \sqrt{\phi + 0.4(2k+1)^2}}{\sqrt{\phi}}}$$

$$= \frac{f_L . A_L . \phi + A . \frac{f_T . A_T}{S} . b_3}{(\phi + B) . f_c' . b} \qquad \ldots (9.5)$$

where $A = 0.4(2k + 1)$

$B = 0.4(2k + 1)^2$

$2 < \phi < 8$:-

$$n = \frac{\frac{f_L . A_L . \phi}{\sqrt{\phi^2 + 0.64(2k+1)^2}} + \frac{f_T . A_T}{S} . b_3 \frac{0.8}{\phi} \frac{0.8(2k+1)}{\sqrt{\phi^2 + 0.64(2k+1)^2}}}{\frac{f_c' b \sqrt{\phi^2 + 0.64(2k+1)^2}}{\phi}}$$

$$= \frac{f_L . A_L . \phi^2 + A . \frac{f_T . A_T}{S} b_3}{(\phi^2 + B) f_c' . b} \qquad \ldots (10.5)$$

where $A = 0.64(2k + 1)$

$B = 0.64(2k + 1)^2$

$\phi > 8$:-

$$n = \frac{\frac{f_L . A_L}{\sqrt{1 + 0.01(2k+1)^2}} + \frac{\frac{f_T A_T}{s} . b_3 \, 0.01(2k+1)}{\sqrt{1 + 0.01(2k+1)^2}}}{f_c' . b \sqrt{1 + 0.01(2k+1)^2}}$$

$$= \frac{f_L . A_L + A . \frac{f_T A_T}{s} . b_3}{B . f_c' . b} \qquad \ldots (11.5)$$

where $A = 0.01(2k + 1)$

$B = 1 + 0.01(2k + 1)^2$

The values of the constants are given in Table 2.5.

Table 2.5:

	k-values				
ϕ		2.0	1.5	1.25	1.0
< 2	A	2.0	1.6	1.4	1.2
	B	10.0	6.4	4.9	3.6
> 2, < 8	A	3.20	2.56	2.24	1.92
	B	16.00	10.24	7.84	5.76
> 8	A	0.50	0.40	0.35	0.30
	B	1.25	1.16	1.123	1.09

Three design equations for ultimate moment can now be obtained for the specified range of ϕ, with a table of constants for each equation. The expression now involves a larger number of terms and consequently more substitutions are required to produce the simplification achieved for sections with longitudinal reinforcements only. It is therefore proposed to derive an expression for one range of ϕ-values and to tabulate values for the other two.

For this purpose the most general application will be chosen, that is, for a range of ϕ-values between two and eight. In order to keep the expression as general as possible, the assumptions mentioned in dealing with the longitudinal reinforced section will be introduced at intermediate points in the development. To avoid unnecessary complexity, no substitution is made for "n" in terms of the derived ϕ expression.

$2 < \phi < 8$

$$M_b \frac{\phi}{\sqrt{\phi^2 + 0.64(2jk+1)^2}} + M_t \frac{\frac{0.8}{\phi}(2jk+1)}{\sqrt{\phi^2 + 0.64(2jk+1)^2}}$$

$$= \tfrac{1}{2} f'_c \, b \, n^2 \sqrt{\phi^2 + 0.64(2jk+1)^2}$$

$$+ f_L A_L (d_1 - n) \frac{\phi}{\sqrt{\phi^2 + 0.64(2jk+1)^2}}$$

$$+ \frac{f_T A_T}{S} b_3 \frac{0.8}{\phi} \frac{0.8(2jk+1)}{\sqrt{\phi^2 + 0.64(2jk+1)^2}} (d - d_s - n)$$

$$- \frac{f_T A_T}{S} d_3 \frac{\phi(j(0.8/\phi) + (1-j)\cot\psi')}{\sqrt{\phi^2 + 0.64(2jk+1)^2}} \left[d\left(j\frac{0.8}{\phi} + (1-j)\cot\psi'\right) + b\frac{0.8}{\phi}(1 - 2jk - 1) \right]$$

The assumptions made for the above expression are $b = b_3$, and $\cot\alpha' = \cot\alpha$. Now assume $j = 1$ and express M_t as M_b/ϕ then, multiplying throughout by $\phi \times \sqrt{\phi^2 + 0.64(2k+1)^2}$ gives

$$M_b \phi^2 + M_b \, 0.8(2k+1) = \tfrac{1}{2} f'_c \, b \, n^2(\phi^2 + 0.64(2k+1)^2) + f_L A_L (d_1 - n)\phi^2 + \frac{f_T A_T}{S} b_3 \, 0.64(2k+1)(d - d_s - n) + \frac{f_T A_T}{S} 0.64 \, dd_3$$

This may be replaced by

$$M_b = \frac{A\phi^2 + B}{\phi^2 + C} \qquad \ldots (12.5)$$

where,

$$A = \tfrac{1}{2} f'_c\, b\, n^2 + f_L\, A_L\, (d_1 - n)$$

$$B = D\, f'_c\, b\, n^2 + E\, \frac{f_T A_T}{S}\, b_3\, (d - d_s - n) + F\, \frac{f_T A_T}{S}\, d\, d_3$$

$$C = 0.8(2k + 1)$$

$$D = 0.32(2k + 1)^2$$

$$E = 0.64(2k + 1)$$

The above expression is now in the general form whereby, on the basis of the assumptions made, M_b can be given as a design-equation in terms of constants A, B, C, defined by the shape of the section together with the properties of the working design, that is the areas of steel, spacing of steel in both longitudinal and transverse sections and strength properties of concrete and steel at ultimate. The ultimate compressive strength of the concrete in bending is taken as two thirds of the cube strength and the longitudinal and transverse steel are assumed to have reached their respective yield-points. The derived expression is therefore only satisfactory for an under-reinforced design.

The values of constants C, D, E and F are tabulated as shown in Table 3.5.

$\underline{\phi < 2}$:-

Using the appropriate substitution for β and α, an expression for M_b is similary derived as

$$M_b = \frac{A\phi + B}{\phi + C/\sqrt{\phi}} \qquad \ldots (13.5)$$

where $A = \tfrac{1}{2} f'_c\, b\, n^2 + f_L\, A_L\, (d_1 - n)$

$$B = D\, f'_c\, b\, n^2 + E\, \frac{f_T A_T}{S}\, b_3\, (d - d_s - n) + F\, \frac{f_T A_T}{S}\, dd_3$$

$$C = 0.63(2k + 1)$$

$$D = 0.2(2k + 1)^2$$

$$E = 0.4(2k + 1)$$

and $$F = 0.4$$

The values for constants C, D, E, and F for the range of k-values being considered is given in Table 4.5.

Table 3.5:

	k-values			
	2.0	1.5	1.25	1.0
C	4.0	3.2	2.8	2.4
D	8.0	5.12	3.92	2.88
E	3.2	2.56	2.24	1.92
F	0.64	0.64	0.64	0.64

Table 4.5:

	k-values			
	2.0	1.5	1.25	1.0
C	3.15	2.52	2.205	1.89
D	5.00	3.20	2.45	1.80
E	2.00	1.60	1.40	1.20
F	0.4	0.4	0.4	0.4

$\phi > 8$:-

The corresponding design equation for ϕ-values greater than eight is similarly derived, and given as

$$M_b = \frac{A\,\phi}{\phi + B} \qquad \ldots (14.5)$$

where

$$A = C\,f'_c\,b\,n^2 + f_L A_L (d_1 - n) + D\,\frac{f_T A_T}{S}\,b_3\,(d - d_s - n) + E\,\frac{f_T A_T}{S}\,d\,d_3$$

$$B = 0.1\,(2k + 1)$$

$$C = \frac{(1 + 0.01(2k + 1)^2)}{2}$$

$$D = 0.01(2k + 1)$$

$$E = 0.01$$

The values of constants B, C, D and E for the range of values of k being considered is given in Table 5.5

Table 5.5:

	k-values			
	2.0	1.5	1.25	1
B	0.50	0.40	0.35	0.30
C	0.625	0.580	0.561	0.545
D	0.05	0.04	0.035	0.03
E	0.01	0.01	0.01	0.01

Using these design equations, and substituting the relevant constants for the given beam-shape, values of M_b are calculated for a specific applied torsion-moment, M_t. The application of these equations to the model reinforced concrete beams tested in the laboratory is reported on in Chapter 6, together with calculations based on experimental work carried out elsewhere[6,50,54,38].

In each case, values are available for M_b and M_t, measured experimentally as the applied bending and torsion moments at ultimate load, this stage being defined by the maximum loads resisted by the beam and not those causing complete failure. The $\emptyset$-value and design characteristics of the beam, namely concrete-strength, steel-strengths, areas and layout detail, are known so that M_b can be found from the expression and compared with the practical value. These calculations are presented in tabular form in Chapter 6, along with discussion and conclusions. Therefore the comments made at this point are only those which have an influence on the development of the subsequent design equations.

The objective throughout has been to establish a design equation from which a realistic value for ultimate moment can be obtained and used as the criterion for load-factor design of

a structure subjected to combined bending and torsion. Since the expressions given above are wholly dependent on the ϕ value, their application to previously obtained experimental results is straightforward. On the other hand, the more practical application to the design of a structure is only possible where some substitution for ϕ is made since in this case the ultimate loads are not known, indeed they are the subject of the investigation. It is necessary therefore to assume that any increase in the applied loads is such that the ϕ ratio remains constant and is therefore known at the ultimate stage. This further assumes that the ratio of bending-moment to torsion-moment at working-loads is known. Consider for example, the design of longitudinal and transverse floor beams subjected to combined bending and torsion due to uniformly distributed loading of the supported floor slab; then an increasing distributed load condition up to ultimate stage will satisfy the requirement for constant ϕ, and the ϕ value is therefore known from the working condition. However, any additional concentrated loading applied to the system during this range will upset the necessary condition.

The practical application of these design equations is consequently limited to the design moments M_b and M_t remaining proportionally constant throughout so that a correct evaluation at ultimate load can be made.

The author feels that such limitations are not a true reflection of the original principle of the ultimate equilibrium theory in which external and internal moments of the beam are equated at the ultimate load stage due to formation of the compression hinge and resultant rotation. It is the author's opinion therefore that the loading sequence up to ultimate should

not impose restrictions on the final design equations and only the values of the applied loads at the point where the hinge forms should be considered. An expression which allows for variation in either or both of the applied loadings, M_b, M_t, is not only desirable from a practical point of view but reflects the true nature of the failure mechanism. The derivation of this expression results from calculations of the M_b values using the three design equations given above applied to a given cross-section and over a range of ϕ values. This development is now covered in Section 5.5.

5.5 Ellipse Theory:

In an effort to overcome the disadvantage of having three design equations rather than one, the values for M_b are compared for a given beam-section by substitution of the ϕ value into the two relevant design equations at a change-point. Thus for a value for ϕ of 8, either the equation for $2 < \phi < 8$, or the equation for $\phi > 8$ can be used; similarly for (change-point) $\phi = 2$, values of M_b are compared for the given section. As a result, using the derived equations appropriate to the chosen design section, values for M_b and M_t can be calculated for a range of ϕ values lying within the limits of pure bending and pure torsion respectively, these limiting values being merely special values of the general case in which the angle of crack α and hence β are known,

that is, in particular for $\phi = \infty$ (pure bending)

$$\alpha = 90^\circ, \quad \cot \alpha = 0$$

$$\beta = 90^\circ, \quad \cot \beta = 0$$

so that the general expression reduces to

$$M_u = \tfrac{1}{2} f'_c \, b \, n^2 + f_L A_L \, (d_1 - n)$$

where $n = f_L A_L / f'_c \, b$

and, for ϕ = 0 (pure torsion)

$$\alpha = 45^{\circ}, \quad \cot\alpha = 1$$

$$\cot\beta = \cot\alpha\,(2k+1) = (2k+1)$$

$$\sin\beta = \frac{1}{\sqrt{1+(2k+1)^2}}$$

$$\cos\beta = \frac{(2k+1)}{\sqrt{1+(2k+1)^2}}$$

$$\operatorname{cosec}\beta = \sqrt{1+(2k+1)^2}$$

$$Tu\cos\beta = \tfrac{1}{2} f'_c\, b\, n^2 \operatorname{cosec}\beta + f_L A_L (d_1 - n)\sin\beta + \frac{f_T A_T}{S} b_3 \cos\beta (d - d_s - n) + \frac{f_T A_T}{S} dd_3 \sin\beta$$

$$\frac{Tu\,(2k+1)}{\sqrt{1+(2k+1)^2}} = \tfrac{1}{2} f'_c\, b\, n^2 \sqrt{(1+(2k+1)^2)} + \frac{f_L A_L (d_1 - n)}{\sqrt{1+(2k+1)^2}} + \frac{f_T A_T}{S} b_3 \frac{(d-d_s-n)(2k+1)}{\sqrt{(1+(2k+1)^2)}} + \frac{f_T A_T}{S} \frac{d\,d_3}{\sqrt{1+(2k+1)^2}}$$

multiply throughout by $\sqrt{1+(2k+1)^2}$

$$Tu = \frac{1}{(2k+1)} \left[\begin{array}{l} \tfrac{1}{2}(1+(2k+1)^2 f'_c\, b\, n^2 + f_L A_L (d_1 - n) \\ + (2k+1)\frac{f_T A_T}{S} b_3 (d-d_s-n) + \frac{f_T A_T}{S} d\, d_3 \end{array} \right]$$

$$= \frac{A.f'_c.b.n^2 + f_L.A_L(d_1-n) + B.\frac{f_T.A_T}{S}.b_3(d-d_s-n) + \frac{f_T A_T}{S} d d_3}{C}$$

where

$$n = \frac{\frac{f_L.A_L}{\sqrt{1+(2k+1)^2}} + \frac{f_T A_T}{S} b_3 \frac{(2k+1)}{\sqrt{1+(2k+1)^2}}}{f'_c.b\sqrt{1+(2k+1)^2}}$$

$$= \frac{f_L A_L + B \frac{f_T A_T}{s} b_3}{2 A f_c' b}$$

The values of constants A, B, and C are given in Table 6.5.

Table 6.5;

constant	k-values			
	2.0	1.5	1.25	1.0
A	13	8.5	6.625	5
B	5	4	3.5	3

Alternatively, the values for $\sin\beta$, $\cos\beta$, and $\operatorname{cosec}\beta$ can be evaluated directly and applied to the general equation.

The values of M_b and M_t, evaluated from the general expression for a given ϕ, are plotted to give the curve shown in Fig. 3.5. The plot is continuous with no interuptions indicated at the change-points for ϕ, and as this is a general statement curves can now be drawn for rectangular beams containing both longitudinal and transverse reinforcement or longitudinal reinforcement only, and for square beams. The examples chosen are for two types of rectangular beam of nominal design of section and a square section similar to those used in the American tests[38]. In order to facilitate calculation, nominal values are chosen for the section details.

In all cases, a continuous curve is obtained between the two limits of pure torsion and pure bending as derived from the general expression. It is proposed to examine the curve as an ultimate load curve for the given section, since on the basis of the assumptions made for the initial design equations, any combination of bending-moment, M_b, and torsion-moment, M_t, satisfying this equation lie on the curve.

FIG. 3.5 :-

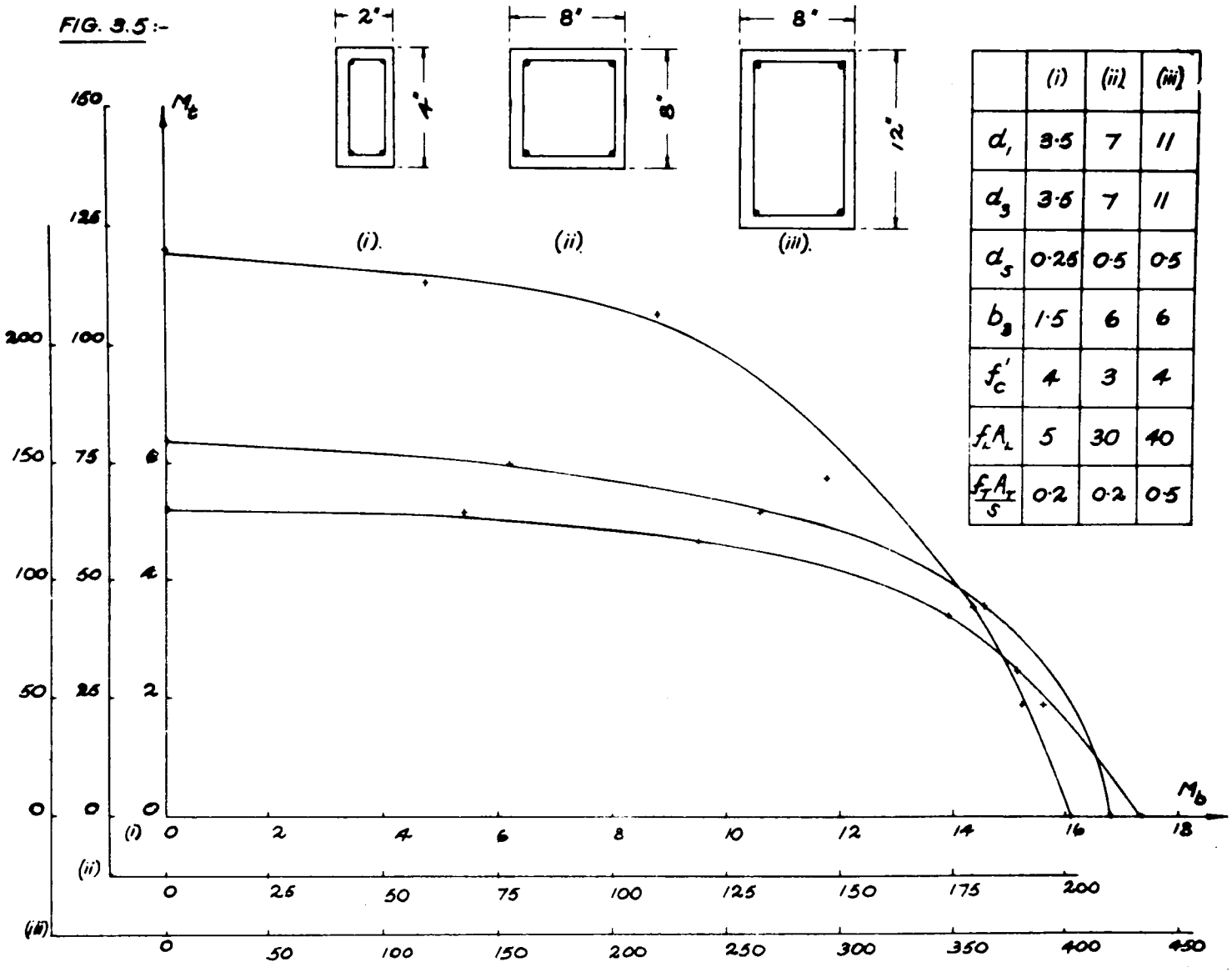

	(i)	(ii)	(iii)
d_1	3·5	7	11
d_3	3·5	7	11
d_5	0·25	0·5	0·5
b_3	1·5	6	6
f_c'	4	3	4
$f_L A_L$	5	30	40
$\frac{f_T A_T}{S}$	0·2	0·2	0·5

The main difference, however, between the previous design equations and the suggested ultimate load curve is with respect to the problem of the loading ratio. The curve is independent of this ratio so that the disadvantage of the design equations is overcome. Fig. 4.5 represents the condition in which the ultimate load curve is defined by the resistance of the beam in pure bending, M_u, the resistance in pure torsion, T_u, and any intermediate point, C, at which an ultimate moment of resistance, M_b, is given by the design equation for an applied torsion-moment at ultimate, M_t. In applying the previous design equations only route ABC can be considered or, rather route BC where B defines the arbitrary limit stated as working load, and so it is only necessary to assume constant ϕ-value beyond this stage. Using the ultimate load curve, the value of M_b is attained by any one of several routes ABC; ADC; AEC; simulating in practice the application of a constant applied loading, M_b/M_t; an initial torsion-moment, M_t, with increasing bending moment up to M_b; and an initial bending moment, M_b, with increasing torsion moment up to M_t. It can therefore be suggested that the calculated value, (M_b, M_t) is independent of the path taken in reaching the ultimate point, that is, the value is independent of the load sequence. This statement may also be true for a similar curve drawn through B defining the working load curve for the given section.

The assumption that the ultimate position (M_b, M_t) can be attained for any condition of applied loading lying within the limits defined by an initially applied M_t with an increasing bending moment up to value M_b, and an initially applied M_b with an increasing torsion moment up to value M_t, is dependent on the

FIG. 4.5 :- ULTIMATE LOAD CURVE

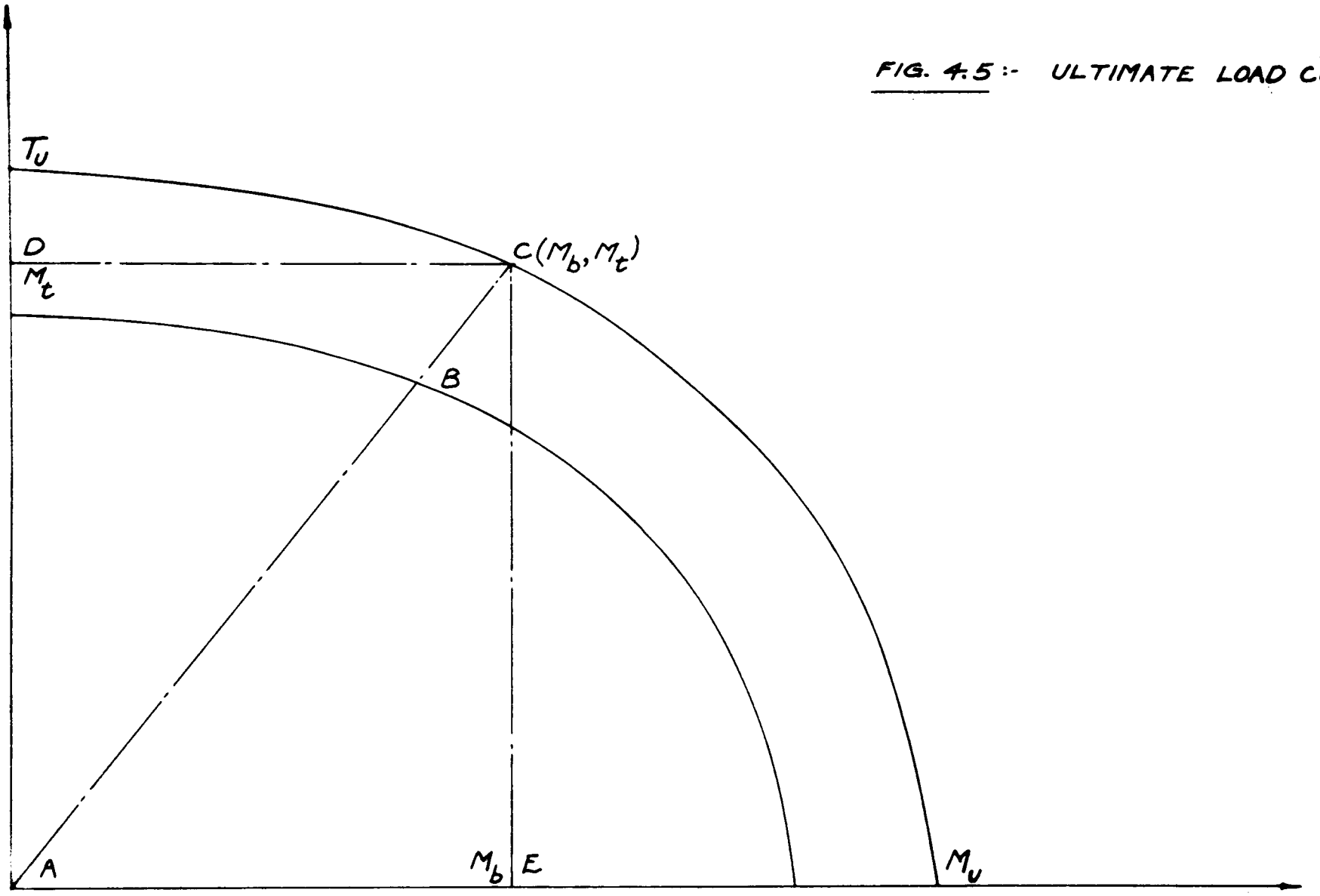

beam resisting wholly the applied moments. This is necessarily true but further research is necessary to examine the true value of the applied moment M_t. Some preliminary thoughts on this aspect are given in Appendix B where the inclusion of a factor, p_t, defined as M_t applied (actual) = p_t. M_t applied (as measured) in the design-equations is considered. However, for the remainder of this thesis it will be assumed that $p_t = 1$ so that any error in measurement of the applied loads will be included in the value of M_b, or M_t, as calculated from design equations using the ultimate load curve of Fig. 4.5.

The application of any one curve, for a particular beam section, is determined only by the design values used for calculation of the limiting conditions M_u and T_u and not by the loading sequence as before. A curve can therefore be drawn for each of the beams tested and from each curve the value of ultimate bending moment is found by the intersection of the ultimate load curve and the straight line defining the value of torsion moment applied to the section, and vice-versa.

A curve is plotted for each beam by substituting values of ϕ between the limits of $\phi = 0$ (T_u) and $\phi = \infty$ (M_u). The evaluation of ultimate moment for a given design section and variable applied loading requires a large amount of preliminary calculation and although the nature of this work is readily suited for a computer, it is preferable to present the theory as an algebraic equation for the curve, and this aspect is now investigated.

A suitable equation for the curve may be obtained in a number of ways, for example by expressing the equation as a polynomial in x, y and solving for the constants, as shown in

Fig. 5.5, by substituting values of $x = M_b$ and $y = M_t$ obtained from the design equations in β for a chosen ϕ value;

Fig. 5.5:-

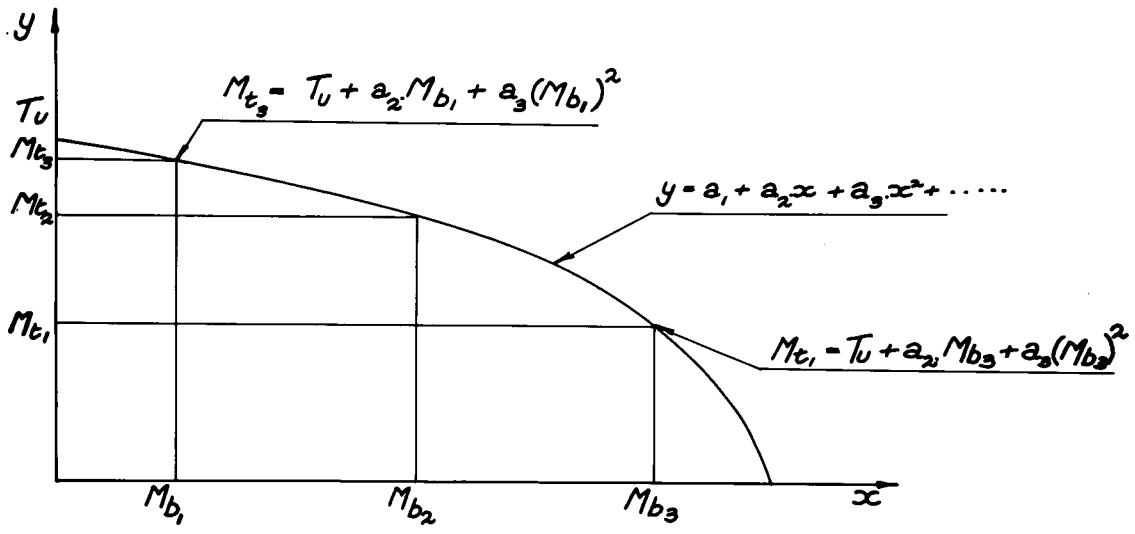

alternatively,

by selecting a particular curve of known equation and comparing values of M_b and M_t obtained from the chosen equation and those obtained from the original design equations. Fig. 6.5 shows the comparison obtained by choosing for the equation of the curve, the equation of an ellipse given by

$$x^2/a^2 + y^2/b^2 = 1, \text{ or, in particular}$$

$$(M_b/M_u)^2 + (M_t/T_u)^2 = 1$$

so that,

$$M_b = M_u \sqrt{1 - (M_t/M_u)^2} \qquad \ldots (15.5)$$

$$M_t = T_u \sqrt{1 - (M_b/M_u)^2} \qquad \ldots (16.5)$$

In Fig. 6.5 the three sections previously considered in Fig. 3.5 are shown and, for each, the M_b, M_t values are plotted between the ϕ-values defined by M_u and T_u together with an ellipse drawn for the same values of M_u and T_u, and using a

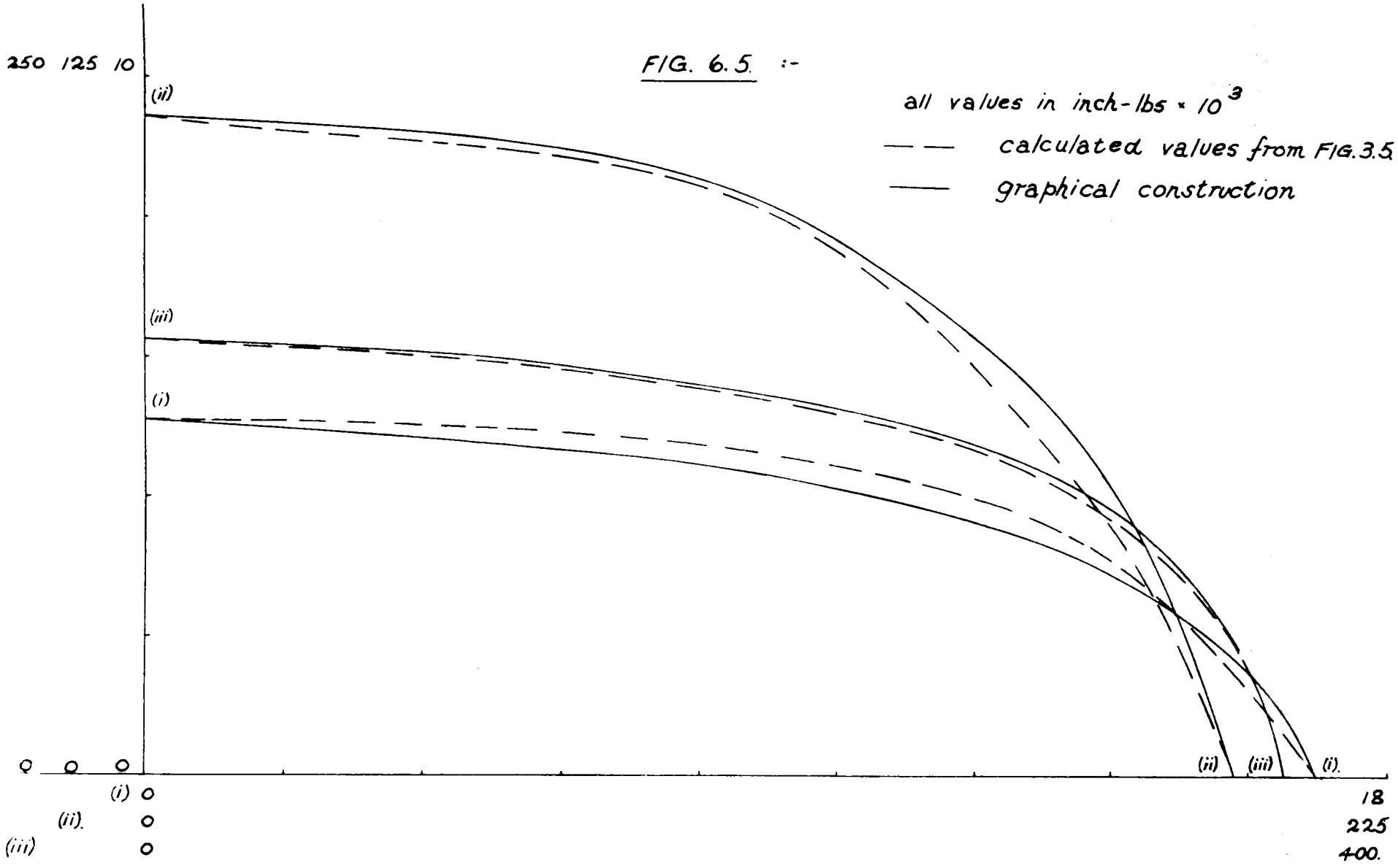
FIG. 6.5 :-
all values in inch-lbs × 10³
calculated values from FIG. 3.5
graphical construction
250 125 10
(ii)
(iii)
(i)
(ii)
(iii)
(i).
(i)
(ii).
(iii)
18
225
400.

graphical construction. In all three cases the difference between the two curves drawn for the same section is within the limits of accuracy accepted for the design of reinforced concrete.

Hence, given any applied torsion moment, M_t, the ultimate bending moment of a reinforced concrete section can be found in terms of M_t and the moments of resistance to pure bending and pure torsion, M_u and T_u. It is proposed to refer to this application as the Ellipse Theory, and the statement is equally true for a known applied bending moment.

Using this theory, values are calculated for the two series of beams tested in the laboratory as well as those of other investigators, as for the previous design equations. These calculations are given in Chapter 6.

For a given design section, two calculations are now necessary, namely for M_u and T_u. These values are substituted in the Ellipse theory and using these equations ultimate moments can be calculated for any chosen applied bending or torsion moment, and, in particular, the moment being applied to the beam under consideration. The ultimate moment and design working moment can then be compared to assess the load-factor of the design. Further calculation is required only for alteration in the design detail, for example a change in the pitch of the transverse reinforcement as this involves revised values for both working and ultimate moment. This form of calculation, in which a large number of factors are fixed and the final design depends upon a small number of variables lends itself to the use of computers. For illustration, consider a beam of fixed section-dimensions and so k-factor, recommended percentages of longitudinal and transverse steel based on sectional area, and 'economic design'

taking into account permissable stresses for working load and yield - stresses at ultimate; the detail dimensions are also preliminary fixed at this stage - any subsequent changes will be small and negligible in the calculation of M_u and T_u. The calculation for M_u and T_u, and hence the equation of the ellipse, is determined in this case by concrete strength so that a chart consisting of a series of ellipses can be drawn for a range of concrete compressive strengths. The designer then selects a suitable concrete mix for the given design in order to obtain the desired load factor.

Therefore, after preliminary calculations to fix the design details, the amount of additional calculation is kept to a minimum by using charts of ellipses for the various design sections under consideration. The author feels that the practical application of the Ellipse theory lies in this method of presentation. It is emphasised at this stage that the Ellipse theory has been developed on the basis of a balanced design so that at ultimate load the steel stresses have attained their respective yield points. Consequently, a limitation must be placed, on, for example in the above illustration, the range of concrete compressive strengths which can be used.

5.6 Conclusions:

The main objective of this Chapter, to reduce the original equation for ultimate load as given by the Russian Ultimate Equilibrium Method to a more straightforward expression is achieved by making a number of assumptions, some of which have been discussed in the conclusions for Chapter 4. Justification of the remaining assumptions will be investigated in Chapter 6 by obtaining a numerical comparison of values calculated from the

derived expressions with values obtained from experimental investigations. Nevertheless, certain comments are relevant at this stage.

The extensive work carried out by Messrs. Lessig, Yudin, Chinenkov, Gvozdev, and Lyalin has led to general acceptance of the Ultimate Equilibrium Theory for the design of reinforced concrete structures in U.S.S.R. In particular, its application to the problem of combined bending and torsion presents a more realistic picture of the mechanism of failure than any other method available, in that the formation of a plastic hinge along a line contained within the plane of the neutral-axis permits rotation and the application of two of the six equilibrium equations. A modification of the original equations using a neutral-axis depth constant over the cross-section has been adopted in this thesis.

The extension of these principles limits the application of any subsequent expressions to under-reinforced design, and further to a specified failure scheme in which the neutral-axis intercepts the vertical sides of the beam. A second failure scheme based on a vertical neutral-axis is less common in practice. However, these restrictions allow further simplification since the calculation for ultimate design now requires that reinforcement has attained its yield stress, and is therefore known. Finally, experimental techniques in the laboratory investigation must be taken to elliminate shear which otherwise will be included in the assessment of combined stresses.

The main assumption made in this Chapter is that the neutral-axis at ultimate load has moved sufficiently far up the

beam from its position at initial cracking as to consider the angle of crack to be of constant value throughout the area of the failure-zone. This allows simplification of the trigonometrical terms in β and also a much simpler term for the internal moment of resistance provided by the vertical transverse steel which permits further equations to be developed.

The three design equations given for ultimate moment are applicable to various shapes of beam section by substitution of appropriate constants and, for the specified k-ratio, evaluation of the moment is determined using the applied moment ratio. The applications of the equations are therefore limited and not suitable for a range of applied loads where the ratio of bending to torsion moment may be altered at any stage of the loading sequence.

The Ellipse Theory developed from these design equations is not dependent on a specified sequence of loading. The expression for the ultimate design moment depends only on the loads being applied at ultimate and the theory can be used for calculation of either the ultimate bending moment of a beam for a given applied torsion moment or the ultimate torsion moment of the beam when subjected to a given applied bending moment.

It is suggested that the practical application of the Ellipse Theory is in the form of a chart, consisting of a series of ellipses drawn for a constant beam section and selected variable such as concrete strength. By incorporating the moments at working load on the same chart, the value of load factor for the chosen section could then be found directly. The range of concrete strengths considered in this case must ensure that the design remains under-reinforced.

In view of previous studies carried out on structural steel sections[55] and in particular the representation of the combination of bending moment and torsion moment at full plasticity by an interaction curve corresponding to a lower bound solution[56], the concept of the Ellipse Theory for reinforced concrete beams subjected to combined bending and torsion is not unreasonable. Having accepted the expressions for calculating the limiting values in pure bending and in pure torsion, the development of the equation of the curve connecting these values and, at the same time, satisfying the condition for any intermediate combination of load, follows. Finally, an experimental investigation to justify these analytical procedures is made in Chapters 6 and 7.

CHAPTER 6

CALCULATIONS FOR ULTIMATE MOMENT

6.1 General:

In Chapters 4 and 5 the author has developed a number of design equations based on an initial assumption as to the mechanism of failure of a reinforced concrete beam subjected to combined bending and torsion and on subsequent assumptions introduced to obtain a simpler and more general design equation. It is also stated that these assumptions do not introduce errors of magnitude greater than the order of accuracy accepted in design. Numerical investigations are therefore made in this Chapter to justify the validity of these statements.

6.2 Introduction:

It is proposed to apply the design equations given in Chapter 5 to practical tests carried out in the laboratory in order to compare both the extent of calculation involved and the variation between practical and theorectical values obtained for each test using the different design equations. As the number of tests carried out is considered to be insufficient to enable general conclusions to be made, it is further proposed to include in this Chapter the results of experimental studies carried out recently in other laboratories. In selecting these results it has been necessary to exercise the limitations specified in Chapter 5 with respect to the design being under-reinforced so that, in all cases, values of yield stress for the reinforcement, whether longitudinal or transverse, can be used. On the other hand, it is possible by selection to cover the range of geometrical constant "k" considered in the general expressions, these being true for both solid and hollow sections.

The application of the design-equations will be made according to their sequence of development in Chapter 5, so that equations 7.5, 8.5, which are derived initially from the ultimate equilibrium method and modified only in the vertical transverse steel term are dealt with first and will be referred to as Design Equation A. The derived equations 1 - 6.5 and 9 - 14.5, expressing the trigonometrical terms as functions of the moment ratio, are referred to as Design Equation B and finally the design equations 15.5, 16.5, based upon the ellipse theory, are referred to as Design Equation C and dealt with last.

A general description is given of the calculation procedures to illustrate differences in the three methods, and general conclusions are given for the tabulated results of all tests.

6.3 Ultimate Moment Calculations:

The practical data necessary for application of the design-equations can be classified into the following. First, information is required on the details of the working-design of the reinforced concrete section, as will be available from the design drawings of the structural member. This is, in effect, the real objective of the study, namely to make use of this data to deduce the load factor of the design by comparing the ultimate-moment, so derived, with the working-moment for the design. Second, with particular application in this case to the laboratory tests, information is required on the ratio of bending-moment and torsion-moment at ultimate. This information in practice is only necessary for design equations A and B.

It is not proposed to include in this Chapter details of the design of the sections being considered, as this is

available by reference to the study quoted. Details of the author's design are given in Chapter 7 and Appendix D, Table 3.D, and therefore it is felt sufficient to mention the particular study under investigation and obtain results for the design-equations under consideration.

(a) Design Equation A:-

Design equation A is obtained from the general expressions 7.5, 8.5 derived in the previous Chapter.

$$n = \frac{f_L A_L . \sin\beta + \frac{f_T A_T}{s} b_3 \cot\alpha . \cos\beta}{f'_c . b . \operatorname{cosec}\beta} \qquad \ldots (A1)$$

and, $$M_b = \frac{\phi}{\cos\beta + \phi . \sin\beta} \left[\begin{array}{l} \frac{1}{2} f'_c . b . n^2 \operatorname{cosec}\beta \\ + f_L A_L \sin\beta (d_1 - n) \\ + \frac{f_T A_T}{s} b_3 . \cot\alpha . \cos\beta (d - d_5 - n) \\ + \frac{f_T A_T}{s} d . d_3 . \sin\beta . \cot^2\alpha . \end{array} \right] \qquad \ldots (A2)$$

The results of an experimental study carried out at Leeds on hollow beams[50] to investigate a similar expression have been used by the author to examine Design Equation A.

The general calculation procedure for a given beam-design is as follows:-

1. For the ϕ ratio, find the value of α from Fig. 5.4.
2. For the given beam section constant, "k",
   $\cot\beta = \cot\alpha\,(2k + 1)$, hence β, and $\sin\beta$, $\cos\beta$ and $\operatorname{cosec}\beta$.
3. Calculate the neutral-axis depth 'n', from equation A 1.
4. Calculate M_b from equation A 2, using the value of 'n' from 3.
5. Calculate M_t since $M_t = M_b/\phi$.

A numerical example is given in Appendix C. Hence, by substitution of the appropriate data, values for the ultimate bending and torsion moment are calculated and compared with the applied moments as shown in Table 1.6. The same equation is applicable to the author's own Series of tests, D/2, and the calculated and practical results are given in Table 2.6.

The application of the equation to beams with longitudinal reinforcement only is obtained by modification of the general equation so that

$$n = \frac{f_L A_L \sin^2\beta}{f_c' b}$$

and,

$$M_b = \frac{\phi}{\cos\beta + \phi \sin\beta} f_L A_L \sin\beta (d_1 - n/2)$$

The author's Series of tests, C/2, are used to examine this equation. The calculation procedure is as already described and calculated and practical values are given in Table 3.6.

(b) Design Equation B:- This equation is developed by the author using previously derived expressions for the angle of crack, α, and the angle of inclination of the compression hinge, β, and substituting these values in Design Equation A, so that the equation for ultimate moment, M_b, can now be expressed in terms of the ratio of bending to torsion moment, ϕ. It is proposed to apply this equation to all the available test results. The general calculation procedure for a given beam section is as follows:-

1. According to the given ϕ ratio and section constant, "k", select the appropriate equations for 'n' and M_b.(Section 5.4).
2. Substituting the details of the working design section, calculate 'n'.
3. Substituting the value of 'n' from 2, calculate M_b.
4. Calculate M_t since $M_t = M_b/\phi$.

Table 1.6:- all values in in.lbs. x 10^3

Beam	ϕ	Bending-moment, M_b		F_b = 2/1	Torsion-Moment, M_t		F_t = 4/3
		applied 1	theo. 2		applied 3	theo. 4	
1	0	-	-	-	44.1	52.76	1.20
2	1.97	66.8	62.5	0.94	33.9	31.7	0.94
3	3.69	75.3	73.4	0.97	20.4	19.9	0.97
4	5.20	81.6	83.6	1.02	15.7	16.1	1.02
5	6.174	81.5	81.8	1.00	13.2	13.2	1.00
6	∞	84.5	87.3	1.03	-	-	-
7	0	-	-	-	36.1	52.8	1.46*
8	3.72	79.6	31.6	1.02	21.4	21.9	1.02
9	4.65	85.1	93.5	1.10	18.3	20.1	1.10
10	5.28	91.3	96.2	1.05	17.3	18.2	1.05
11	6.67	94.0	96.4	1.03	14.1	14.4	1.03
12	∞	105.6	93.9	0.89	-	-	-
13	0	-	-	-	51.3	66.9	1.30*
14	1.97	82.1	88.5	1.08	41.7	44.9	1.08
15	3.71	111.0	107.0	0.96	29.9	28.8	0.96
16	5.21	122.0	127.2	1.04	23.4	24.4	1.04
17	6.36	126.0	125.5	1.00	19.8	19.7	1.00
18	∞	143.0	129.8	0.91	-	-	-

Table 2.6:- all values in in.lbs.x 10^3

Beam	ø	Bending Moment, M_b applied 1	Bending Moment, M_b theo. 2	F_b = 2/1	Torsion Moment, M_t applied 3	Torsion Moment, M_t theo. 4	F_t = 4/3
D/2/1*	12.86	9.913	14.227	1.43*	0.771	1.106	1.43*
D/2/2*	3.04	5.345	12.110	2.27*	1.760	3.983	2.27*
D/2/3	5.96	15.047	14.475	0.96	2.525	2.429	0.96
D/2/4	0	-	-	-	4.295	6.328	1.47*
D/2/5	7.08	13.860	15.045	1.08	1.957	2.125	1.08
D/2/6	4.665	13.399	13.575	1.01	2.873	2.910	1.01
D/2/2/R	8.08	14.250	14.713	1.03	1.763	1.839	1.03

Table 3.6:- all values in in.lbs.x 10^3

Beam	ø	Bending-Moment, M_b applied 1	Bending-Moment, M_b theo. 2	$F_b = \frac{2}{1}$	Torsion-Moment, M_t applied 3	Torsion-Moment, M_t theo. 4	F_t = 4/3
C/2/1	10.92	4.435	5.162	1.16	0.406	0.473	1.16
C/2/2	11.18	9.240	9.380	1.01	0.826	0.839	1.01
C/2/3	8.98	13.921	14.424	1.04	1.568	1.606	1.04
C/2/4	6.03	11.614	12.746	1.10	1.925	2.114	1.10
C/2/5	∞	9.240	9.778	1.06	-	-	-
C/2/6	3.56	8.911	11.832	1.33*	2.505	3.323	1.33*

An example of this procedure is given in Appendix C.

The design equation for each test series varies according to the beam section and loading ratio used. Consider first the application to beams with longitudinal reinforcement only.

(i) Author's Series C/2:- C/2/1 (plain concrete) and C/2/5 (pure bending) are considered separate.

C/2/4, C/2/6:-

$$n = \frac{\phi^2}{\phi^2 + 16} \frac{f_L A_L}{f'_c b}; \qquad M_b = \frac{\phi^2}{\phi^2 + 4} f_L A_L (d_1 - n/2)$$

C/2/2, C/2/3:-

$$n = \frac{0.8 f_L A_L}{f'_c b}; \qquad M_b = \frac{\phi}{\phi + 0.5} f_L A_L (d_1 - n/2)$$

The calculated and practical values are tabulated in Table 4.6.

(ii) American beams[54]:-

Beams 1, 2:- pure bending

Beams 3, 4:-

$$n = \frac{\phi}{\phi + 3.60} \frac{f_L A_L}{f'_c b}; \qquad M_b = \frac{\phi}{\phi + \frac{1.69}{\sqrt{\phi}}} f_L A_L (d_1 - n/2)$$

Beams 5 - 8:-

$$n = \frac{\phi^2}{\phi^2 + 5.76} \frac{f_L A_L}{f'_c b}; \qquad M_b = \frac{\phi^2}{\phi^2 + 2.40} f_L A_L (d_1 - n/2)$$

Beams 9, 10:-

$$n = \frac{\phi^2}{\phi^2 + 16} \frac{f_L A_L}{f'_c b}; \qquad M_b = \frac{\phi^2}{\phi^2 + 4} f_L A_L (d_1 - n/2)$$

The calculated and practical values are tabulated in Table 5.6.

Design Equation B is similarly applied to beams with longitudinal and transverse reinforcement.

Table 4.6:- in.lbs x 10^3

Beam	ø	Bending-Moment, M_b		$F_b = \frac{2}{1}$	Torsion-Moment, M_t		$F_t = \frac{4}{3}$
		applied 1	theo. 2		applied 3	theo. 4	
C/2/1	10.92	4.435	5.746	1.29	0.406	0.526	1.29
C/2/2	11.18	9.240	9.641	1.04	0.826	0.862	1.04
C/2/3	8.98	13.921	14.335	1.03	1.568	1.596	1.03
C/2/4	6.03	11.614	12.594	1.08	1.925	2.088	1.08
C/2/5	∞	9.240	9.778	1.06	-	-	-
C/2/6	3.56	8.911	12.216	1.37*	2.505	3.431	1.37*

Beam C/2/5 was tested for a different span length to the other beams.

Table 5.6:- all values in in.lbs.x 10^3

Beam	ø	Bending-Moment, M_b		$F_b = \frac{2}{1}$	Torsion-Moment, M_t		$F_t = \frac{4}{3}$
		applied 1	theo. 2		applied 3	theo. 4	
1	0	-	-	-	36	25	0.69*
2	0	-	-	-	39	45	1.15*
3	1	58	39	0.67*	58	39	0.67*
4	1	64	69	1.08	64	69	1.08
5	2	86	123	1.43*	43	61	1.43*
6	3	108	156	1.44*	36	52	1.44*
7	3	177	159	0.90	59	53	0.90
8	4	195	175	0.90	48.75	43.875	0.90
9	2	83	159	1.91*	41.5	79.3	1.91*
10	4	156	243	1.56*	39	61	1.56*

(iii) Author's Series D/2:-

All beams except D/2/4 (pure torsion):-

$$n = \frac{f_L A_L \cdot \phi^2 + 3{\cdot}2 \frac{f_T A_T}{S} b_3}{(\phi^2 + 16) f_c' \cdot b}$$

$$M_b = \frac{1}{\phi^2 + 4} \left[\left[\frac{1}{2} f_c' \cdot b n^2 + f_L A_L (d_1 - n) \right] \phi^2 + 8 f_c' \cdot b \cdot n^2 + 3{\cdot}2 \frac{f_T A_T}{S} \cdot b_3 (d - d_3 - n) + 0{\cdot}64 \frac{f_T A_T}{S} d \cdot d_3 \right]$$

The calculated and practical values are tabulated in Table 6.6.

(iv) Leeds Beams[50]:- Beams 1, 6, 7, 12, 13 and 18 are special cases.

Beams 2 - 5:-

$$n = \frac{f_L A_L \cdot \phi^2 + 2{\cdot}24 \frac{f_T A_T}{S} b_3}{(\phi^2 + 7{\cdot}84) f_c' \cdot b}$$

$$M_b = \frac{1}{\phi^2 + 2{\cdot}8} \left[\left[\frac{1}{2} f_c' \cdot b \cdot n^2 + f_L A_L (d_1 - n) \right] \phi^2 + 3{\cdot}92 f_c' \cdot b \cdot n^2 + 2{\cdot}24 \frac{f_T A_T}{S} b_3 (d - d_5 - n) + 0{\cdot}64 \frac{f_T A_T}{S} d \cdot d_3 \right]$$

Beams 8 - 11:-

$$n = \frac{f_L A_L \phi^2 + 2{\cdot}56 \frac{f_T A_T}{S} b_3}{(\phi^2 + 10{\cdot}24) f_c' \cdot b}$$

$$M_b = \frac{1}{\phi^2 + 3{\cdot}2} \left[\left[\frac{1}{2} f_c' \cdot b \cdot n^2 + f_L A_L (d_1 - n) \right] \phi^2 + 5{\cdot}12 f_c' \cdot b \cdot n^2 + 2{\cdot}56 \frac{f_T A_T}{S} b_3 (d - d_5 - n) + 0{\cdot}64 \frac{f_T A_T}{S} d d_3 \right]$$

Beams 14 - 17:-

$$n = \frac{f_L A_L \phi^2 + 3{\cdot}2 \frac{f_T A_T}{S} \cdot b_3}{(\phi^2 + 16) f_c' \cdot b}$$

Table 6.6:- all values in in.lbs.x 10^3

Beam	β	Bending-Moment, M_b applied 1	theo. 2	$F_b = \frac{2}{1}$	Torsion-Moment, M_t applied 3	theo. 4	$F_t = \frac{4}{3}$
D/2/1	6.43	9.913	14.426	1.46*	1.54	2.243	1.46*
D/2/2	3.04	5.345	12.028	2.25*	1.760	3.996	2.25*
D/2/3	5.96	15.047	14.523	0.96	2.525	2.44	0.96
D/2/4	0	-	-	-	4.295	6.150	1.43*
D/2/5	7.08	13.860	15.133	1.09	1.957	2.14	1.09
D/2/6	4.665	13.399	13.967	1.04	2.873	2.99	1.04
D/2/2/R	8.08	14.250	14.780	1.04	1.763	1.83	1.04

$$M_b = \frac{1}{\phi^2+4}\left[\left[\frac{1}{2}f_c'.b.n^2 + f_L A_L (d_1-n)\right]\phi^2 + 8f_c'.b.n^2 + 3{\cdot}2\frac{f_T A_T}{s}b_3(d-d_5-n) + 0{\cdot}64\frac{f_T A_T}{s}d.d_3\right]$$

The calculated and practical values are given in Table 7.6.

(v) American Beams[38]

Beams 1 - 2

$$n = \frac{f_L A_L \phi + 1{\cdot}2\frac{f_T A_T}{s}b_3}{(\phi + 3{\cdot}6)f_c'.b.}$$

$$= \frac{1}{\phi + \frac{1{\cdot}89}{\sqrt{\phi}}}\left[\left[\frac{1}{2}f_c'.b.n^2 + f_L A_L.(d_1-n)\right]\phi + 1{\cdot}8f_c'.b.n^2 + 1{\cdot}2\frac{f_T A_T}{s}b_3(d-d_5-n) + 0{\cdot}4\frac{f_T A_T}{s}d.d_3\right]$$

Beams 3 - 8

$$n = \frac{f_L A_L \phi^2 + 1{\cdot}92\frac{f_T A_T}{s}b_3}{(\phi^2 + 5{\cdot}76)f_c'.b.}$$

$$M_b = \frac{1}{\phi^2+2{\cdot}4}\left[\left[\frac{1}{2}.f_c'b.n^2 + f_L A_L(d_1-n)\right]\phi^2 + 2{\cdot}88f_c'.b.n^2 + 1{\cdot}92\frac{f_T A_T}{s}b_3(d-d_5-n) + 0{\cdot}64\frac{f_T A_T}{s}d.d_3\right]$$

Beams 9 - 12

$$n = \frac{f_L A_L \phi^2 + 3{\cdot}2\frac{f_T A_T}{s}b_3}{(\phi^2+16)f_c'.b}$$

$$M_b = \frac{1}{\phi^2+4}\left[\left[\frac{1}{2}f_c'.b.n^2 + f_L A_L(d_1-n)\right]\phi^2 + 8f_c'.b.n^2 + 3{\cdot}2\frac{f_T A_T}{s}b_3(d-d_5-n) + 0{\cdot}64\frac{f_T A_T}{s}d.d_3\right]$$

Table 7.6:- all values in in.lbs. x 10^3

Beam	ø	Bending-Moment, M_b applied 1	theo. 2	$F_b = \frac{2}{1}$	Torsion-Moment, M_t applied 3	theo. 4	$F_t = \frac{4}{3}$
1	0	-	-	-	44.1	52.8	1.20*
2	1.97	66.8	60.3	0.90	33.9	30.6	0.90
3	3.69	75.3	73.5	0.98	20.4	20.0	0.98
4	5.20	81.6	82.0	1.00	15.7	15.7	1.00
5	6.174	81.5	80.2	0.98	13.2	12.9	0.98
6	∞	84.5	87.3	1.03	-	-	-
7	0	-	-	-	36.1	52.8	1.46*
8	3.72	79.6	81.4	1.02	21.4	21.8	1.02
9	4.65	85.1	91.9	1.08	18.3	19.8	1.08
10	5.28	91.3	96.3	1.05	17.3	18.2	1.05
11	6.67	94.0	96.9	1.03	14.1	14.5	1.03
12	∞	105.6	93.9	0.89	-	-	-
13	0	-	-	-	51.3	66.9	1.30*
14	1.97	82.1	89.1	1.08	41.7	45.0	1.08
15	3.71	111.0	108.9	0.98	29.9	29.3	0.98
16	5.21	122.0	128.1	1.05	23.4	24.6	1.05
17	6.36	126.0	132.4	1.05	19.8	20.8	1.05
18	∞	143.0	129.8	0.91	-	-	-

The calculated and practical values are given in Table 8.6.

(vi) Russian Beams[6]

Series 1:- except beam 23 (pure torsion)

$$n = \frac{f_L A_L . \phi^2}{(\phi^2 + 10{\cdot}24) f_c' . b}$$

$$M_b = \frac{1}{\phi^2 + 3{\cdot}2} \left[\left[\tfrac{1}{2} . f_c' . b . n^2 + f_L A_L (d_1 - n) \right] \phi^2 + 5{\cdot}12 f_c' . b n^2 + 0{\cdot}64 \frac{f_T A_T}{s} d . d_3 \right]$$

The calculated and practical values are given in Table 9.6.

Series 2:-

Beams 1, 2:-

$$n = \frac{f_L A_L + 0{\cdot}4 \frac{f_T A_T}{s} b_3}{1{\cdot}16 f_c' . b}$$

$$M_b = \frac{1}{\phi^2 + 0{\cdot}4} \left[0{\cdot}58 f_c' . b . n^2 + f_L A_L (d_1 - n) + 0{\cdot}04 \frac{f_T A_T}{s} b_3 (d - d_5 - n) + 0{\cdot}01 \frac{f_T A_T}{s} d . d_3 \right]$$

Beams 3 - 13:-

$$n = \frac{f_L A_L \phi^2 + 2{\cdot}56 \frac{f_T A_T}{s} b_3}{(\phi^2 + 10{\cdot}24) f_c' . b}$$

$$M_b = \frac{1}{\phi^2 + 3{\cdot}2} \left[\left[\tfrac{1}{2} f_c' . b . n^2 + f_L A_L (d_1 - n) \right] \phi^2 + 5{\cdot}12 f_c' . b . n^2 + 2{\cdot}56 \frac{f_T A_T}{s} b_3 (d - d_5 - n) + 0{\cdot}64 \frac{f_T A_T}{s} d . d_3 \right]$$

The calculated and practical values are given in Table 10.6.

(c) Design Equation C:- Design Equation C can now be developed from the equation of the curve obtained by plotting the M_b values against the M_t values as given by Design Equation B. It has been shown in Chapter 5 that, over the range of accuracies to which a

Table 8.6:- all values in in.lbs. $\times 10^3$

Beam	ø	Bending-Moment, M_b		$F_b = \frac{2}{1}$	Torsion-Moment, M_t		$F_t = \frac{4}{3}$
		applied 1	theo. 2		applied 3	theo. 4	
1	1	79	91	1.15	79	91	1.15
2	1	102	117	1.15	102	117	1.15
3	2	122	136	1.11	61	67	1.11
4	2	134	154	1.15	67	74	1.15
5	3	147	155	1.05	49	51	1.05
6	3	168	164	0.98	56	55	0.98
7	4	173	166	0.96	42.25	40.56	0.96
8	4	176	173	0.98	44	43	0.98
9	2	120	163	1.36*	60	82	1.36*
10	4	176	235	1.33*	44	58	1.33*
11	2	138	178	1.29*	69	89	1.29*
12	4	213	241	1.13	53.25	60.17	1.13

Table 9.6:- all values in kg.cms. $\times 10^5$

Beam	ϕ	Bending-Moment, M_b		$F_b = \frac{2}{1}$	Torsion-Moment, M_t		$F_t = \frac{4}{3}$
		applied 1	theo. 2		applied 3	theo. 4	
1	5	5.6	5.38	0.96	1.12	1.07	0.96
2	5	5.6	5.76	1.03	1.12	1.15	1.03
3	5	4.8	5.34	1.11	0.96	1.07	1.11
4	5	5.2	5.58	1.07	1.04	1.11	1.07
5	5	5.2	5.28	1.01	1.04	1.05	1.01
6	5	5.2	5.03	0.97	1.04	1.01	0.97
7	5	5.2	5.78	1.15	1.04	1.20	1.15
8	5	6.4	6.49	1.01	1.28	1.29	1.01
9	5	6.4	6.75	1.05	1.28	1.34	1.05
10	5	6.4	6.97	1.09	1.28	1.39	1.09
11	3.33	4.4	4.77	1.08	1.32	1.43	1.08
12	4.3	5.6	5.21	0.93	1.32	1.23	0.93
13	3.33	4.8	5.02	1.05	1.44	1.51	1.05
14	3.33	4.0	4.77	1.19	1.20	1.43	1.19
15	3.33	4.2	4.80	1.14	1.26	1.44	1.14
16	2.5	4.0	4.93	1.23	1.60	1.97	1.23
17	2.5	3.8	3.99	1.05	1.52	1.60	1.05
18	2.5	3.3	4.40	1.33*	1.32	1.76	1.33*
19	2.64	3.6	4.14	1.15	1.36	1.56	1.15
20	2.5	3.4	4.20	1.23	1.36	1.67	1.23
21	2.5	3.6	4.50	1.25	1.44	1.80	1.25
22	2.5	4.8	5.68	1.18	1.92	2.27	1.18
23	0	-	-	-	1.28	2.10	1.64*

designer would assess his calculations, the equation of an ellipse given by

$$x^2/a^2 + y^2/b^2 = 1 \qquad \text{where}$$

x = applied bending-moment = M_b

y = applied torsion moment = M_t

$a = M_u$ = ultimate moment of resistance of the section to pure-bending

$b = T_u$ = ultimate moment of resistance of the section to pure-torsion,

is of the same form as the Design Equation B curve plotted for ϕ varying between 0 and ∞ .

Accepting this equation as the final Design Equation C, we have

$$M_b = M_u\sqrt{1 - M_t^2/T_u^2} \quad , \quad M_t = T_u\sqrt{1 - M_b^2/M_u^2}$$

where,

M_u:- $\quad n = f_L A_L / f'_c\, b$ ... C1

and $\quad M_u = \frac{1}{2}.f'_c.b.n^2 + f_L.A_L(d_1 - n)$ ... C2

T_u:-

$$T_u = \frac{f_L A_L.\sin\beta + \frac{f_T A_T}{s} b_3.\cos\beta}{f'_c.b.\operatorname{cosec}\beta} \qquad \text{... C3}$$

$$T_u = \frac{1}{\cos\beta}\left[\begin{array}{l} \frac{1}{2} f'_c.b.n^2.\operatorname{cosec}\beta + f_L A_L.\sin\beta(d_1 - n) \\ + \frac{f_T A_T}{s} b_3.\cos\beta(d - d_5 - n) + \frac{f_T A_T}{s}\sin\beta\, d.d_3 \end{array}\right] \qquad \text{... C4}$$

This is the general expression applicable to all beams for all ϕ values so that the equation is considerably more straightforward in its application.

The calculation procedure is as follows:-

(i) Calculate the resistance of the beam to pure bending using equations C1, C2, and substituting the details of the beam section.

Table 10.6:- all values in kg.cms. $\times 10^5$

Beam	ø	Bending-Moment, M_b applied 1	Bending-Moment, M_b theo. 2	$F_b = \frac{2}{1}$	Torsion-Moment, M_t applied 3	Torsion-Moment, M_t theo. 4	$F_t = \frac{4}{3}$
1	10	5.6	4.5	0.81	0.56	0.45	0.81
2	10	5.4	4.6	0.85	0.54	0.46	0.85
3	5	4.8	4.5	0.94	0.96	0.90	0.94
4	5	4.8	4.5	0.94	0.96	0.90	0.94
5	3.5	4.0	4.0	1.00	1.14	1.14	1.00
6	2.5	4.2	4.2	1.00	1.68	1.68	1.00
7	2.5	4.0	4.3	1.07	1.60	1.71	1.07
8	2.5	4.2	4.4	1.05	1.68	1.76	1.05
9	2.5	4.4	4.6	1.05	1.76	1.85	1.05
10	2.5	3.6	4.6	1.28*	1.44	1.84	1.28*
11	2.5	3.8	4.3	1.13	1.52	1.72	1.13
12	2.5	4.0	4.4	1.10	1.60	1.76	1.10
13	4.5	5.0	5.0	1.00	1.12	1.12	1.00

Table 11.6:- all values in in.lbs. $\times 10^3$

Beam	ø	Bending-Moment, M_b applied 1	Bending-Moment, M_b theo. 2	$F_b = \frac{2}{1}$	Torsion-Moment, M_t applied 3	Torsion-Moment, M_t theo. 4	$F_t = \frac{4}{3}$
C/2/1	10.92	4.435	-	-	0.406	-	-
C/2/2	11.18	9.240	9.421	1.02	0.826	0.940	1.14
C/2/3	8.98	13.921	14.096	1.01	1.568	1.651	1.05
C/2/4	6.03	11.614	11.301	0.97	1.925	1.839	0.955
C/2/5	∞	9.240	9.778	1.06	-	-	-
C/2/6	3.56	8.911	10.405	1.17	2.505	2.756	1.10

(ii) Calculate the resistance of the beam to pure torsion using equations C3, C4. For this, obtain the values for $\sin\beta$, $\cos\beta$, $\operatorname{cosec}\beta$, from tables using $\cot\beta = \cot\alpha(2k + 1) = (2k + 1)$ where 'k' is given for the beam section.

(iii) Either (a) using the values of M_u from (i) and T_u from (ii) construct an ellipse of equation

$$x^2/(M_u)^2 + y^2/(T_u)^2 = 1$$

this curve is now the general ultimate load curve applicable to any combined loading

or (b) using the design equations

$$M_b = M_u\sqrt{1 - M_t^2/T_u^2} \quad \text{or} \quad M_t = T_u\sqrt{1 - M_b^2/M_u^2}$$

substitute for M_u from (i), T_u from (ii) and the applied moment, M_t, (or M_b) to calculate the ultimate moment M_b (or M_t).

An example of this procedure is given in Appendix C. As the loading condition is introduced as a final step in the calculation, the equations cover all conditions including pure-bending and pure-torsion.

The design equation is now used to calculate the results of all the tests considered and these values together with those measured experimentally are given in Tables 11.6, 12.6, 13.6, 14.6, 15.6, 16.6, and 17.6.

6.4 Summary of results:-

It is proposed to use as a basis for comparison of the values calculated by the different design equations, the values F_b, defined as the ratio of theoretical ultimate bending moment to actual ultimate bending moment and F_t, defined as the ratio of theoretical to actual ultimate torsion moment. It has been stated in Chapter 5 that the beam necessarily resists the moments

Table 12.6:- all values in in.lbs. × 10^3

Beam	ø	Bending-Moment, M_b		$F_b = \frac{2}{1}$	Torsion-Moment, M_t		$F_t = \frac{4}{3}$
		applied 1	theo. 2		applied 3	theo. 4	
1	0	-	-	-	36	25	0.69
2	0	-	-	-	39	45	1.15
3	1	58	**	-	58	31	0.53*
4	1	64	54	0.84	64	63	0.98
5	2	86	133	1.55*	43	58	1.35*
6	3	108	147	1.36*	36	52	1.44*
7	3	177	89	0.5*	59	23	0.39*
8	4	195	143	0.82	48.75	25	0.57*
9	2	83	218	2.63*	41.5	61	1.47*
10	4	156	230	1.47*	39	54	1.64*

Table 13.6:- all values in in.lbs. × 10^3

Beam	ø	Bending-Moment, M_b		$F_b = \frac{2}{1}$	Torsion-Moment, M_t		$F_t = \frac{4}{3}$
		applied 1	theo. 2		applied 3	theo. 4	
D2/1	6.43	9.913	15.036	1.52*	0.771	4.175	5.41*
D2/2	3.04	5.345	15.051	2.82*	1.760	5.158	2.93*
D2/3	5.96	15.047	15.257	1.02	2.525	2.666	1.06
D2/4	0	-	-	-	4.295	6.150	1.43*
D2/5	7.08	13.860	15.077	1.09	1.957	2.821	1.44*
D2/6	4.665	13.399	14.014	1.05	2.873	3.362	1.17
D2/2/R	8.08	14.250	14.686	1.03	1.763	2.279	1.29*

Table 14.6:- all values in in.lbs.x 10^3

Beam	ø	Bending-Moment, M_b		$F_b = \frac{2}{1}$	Torsion-Moment, M_t		$F_t = \frac{4}{3}$
		applied 1	theo. 2		applied 3	theo. 4	
1	0	-	-	-	44.1	50.4	1.14
2	1.97	66.8	66.2	0.99	33.9	33.5	0.99
3	3.69	75.3	81.1	1.07	20.4	27.4	1.34*
4	5.20	81.6	83.9	1.03	15.7	19.9	1.27*
5	6.174	81.5	81.3	1.00	13.2	12.5	0.95
6	∞	84.5	87.3	1.03	-	-	-
7	0	-	-	-	36.1	47.2	1.46*
8	3.72	79.6	79.8	1.00	21.4	27.9	1.30*
9	4.65	85.1	95.3	1.12	18.3	31.0	1.69*
10	5.28	91.3	99.1	1.08	17.3	28.0	1.61*
11	6.67	94.0	98.4	1.05	14.1	21.8	1.55*
12	∞	105.6	93.9	0.89	-	-	-
13	0	-	-	-	51.3	92.2	1.30*
14	1.97	82.1	116.6	1.42*	41.7	60.1	1.44*
15	3.71	111.0	115.8	1.04	29.9	34.0	1.15
16	5.21	122.0	133.0	1.09	23.4	36.5	1.56*
17	6.36	126.0	135.9	1.08	19.8	33.3	2.14*
18	∞	143.0	129.8	0.97	-	-	-

Table 15.6:- all values in in.lbs. $\times 10^3$

Beam	ø	Bending-Moment, M_b		$F_b = \frac{2}{1}$	Torsion-Moment, M_t		$F_t = \frac{4}{3}$
		applied 1	theo. 2		applied 3	theo. 4	
1	1	79	141	1.79*	79	152	1.45*
2	1	102	152	1.49*	102	156	1.53*
3	2	122	159	1.30*	61	94	1.55*
4	2	134	167	1.25	67	125	1.87*
5	3	147	163	1.11	49	71	1.45*
6	3	168	168	1.00	56	57	1.02
7	4	173	170	0.97	42	37	0.85
8	4	176	177	1.00	44	47	1.06
9	2	120	222	1.84*	60	89	1.48*
10	4	176	245	1.39*	44	75	1.72*
11	2	138	241	1.75*	69	119	1.73*
12	4	213	252	1.18	53	65	1.21

Table 16.6:- all values in kg. cms. $\times 10^5$

Beam	ø	Bending-Moment, M_b		$F_b = \frac{2}{1}$	Torsion-Moment, M_t		$F_t = \frac{4}{3}$
		applied 1	theo. 2		applied 3	theo. 4	
1	5	5.6	4.5	0.80	1.12	0.54	0.48*
2	5	5.6	5.0	0.90	1.12	0.84	0.75*
3	5	4.8	4.9	1.03	0.96	1.03	1.07
4	5	5.2	5.1	0.98	1.04	0.99	0.96
5	5	5.2	4.7	0.90	1.04	0.75	0.72*
6	5	5.2	4.2	0.81	1.04	0.48	0.46*
7	5	5.2	5.5	1.06	1.04	1.24	1.19
8	5	6.4	6.0	0.93	1.28	0.98	0.76
9	5	6.4	6.4	1.00	1.28	1.26	0.98
10	5	6.4	6.5	1.01	1.28	1.32	1.03
11	3.33	4.4	3.7	0.85	1.32	1.12	0.85
12	4.3	5.6	4.0	0.71	1.32	0.53	0.40*
13	3.33	4.8	4.0	0.84	1.44	1.18	0.82
14	3.33	4.0	4.3	1.08	1.20	1.32	1.10
15	3.33	4.2	4.2	1.00	1.26	1.26	1.00
16	2.5	4.0	4.9	1.23	1.60	1.89	1.18
17	2.5	3.8	2.3	0.61*	1.52	1.20	0.78
18	2.5	3.3	4.2	1.26*	1.32	1.52	1.15
19	2.64	3.6	4.0	1.10	1.36	1.46	1.07
20	2.5	3.4	3.7	1.10	1.36	1.45	1.07
21	2.5	3.6	4.7	1.30*	1.44	1.80	1.25*
22	2.5	4.8	4.6	0.95	1.92	1.87	0.97
23	0	-	-	-	1.28	2.10	1.41*

Table 17.6:- all values in kg. cms. $\times 10^5$

Beam	ø	Bending-Moment, M_b		$F_b = \frac{2}{1}$	Torsion-Moment, M_t		$F_t = \frac{4}{3}$
		applied 1	theo. 2		applied 3	theo. 4	
1	10	5.6	**	-	0.56	**	-
2	10	5.4	**	-	0.54	**	-
3	5	4.8	**	-	0.96	**	-
4	5	4.8	**	-	0.96	**	-
5	3.5	4.0	3.5	0.87	1.14	0.52	0.46*
6	2.5	4.2	3.9	0.93	1.68	1.55	0.92
7	2.5	4.0	4.1	1.02	1.60	1.63	1.02
8	2.5	4.2	4.3	1.03	1.68	1.73	1.03
9	2.5	4.4	3.9	0.88	1.76	1.69	0.96
10	2.5	3.6	4.1	1.14	1.44	1.67	1.16
11	2.5	3.8	4.2	1.12	1.52	1.72	1.13
12	2.5	4.0	4.4	1.10	1.60	1.82	1.13
13	4.5	5.0	4.75	0.95	1.12	0.81	0.72*

being applied to the section and therefore by definition $F_b = F_t = 1$. These values are tabulated in Table 18.6.

Table 18.6:-

	F_b F_t	(i)	(ii)	(iii)	(iv)	(v)	(vi)	(vii)
A	F_b	1.07	-	1.02	1.00	-	-	-
	F_t	1.07	-	1.02	1.00	-	-	-
B	F_b	1.10	0.96	1.03	1.00	1.07	1.09	1.02
	F_t	1.10	0.96	1.03	1.00	1.07	1.09	1.02
C	F_b	1.05	0.83	1.05	1.03	1.08	0.93	1.00
	F_t	1.06	1.06	1.10	1.03	1.03	0.93	1.01

The numbers refer to the sequence of tests as given for Design Equation B. Any difference from unity can be considered as consisting of either an error introduced in measurement of the applied moments in the experimental investigation or the error resulting from differences between the simplified design equation and the expression obtained from the exact mathematical analysis of the failure mechanism. It will be assumed that any difference greater than 0.25 indicates an experimental error greater than normal and this result will not be used in assessing the accuracy of the design equations. For example, the bond failure of beam D/2/1 which gives F_b values of 1.43, 1.46, and 1.52 for the three design equations respectively has not been included in Table 18.6 so that general conclusions can be made.

Both design equations A and B depend upon an initially known ratio of applied bending moment to torsion moment so that calculation is based on the assumption that the values of F_b and

F_t are the same. Thus, in Table 1.6 and 7.6 for beam 4, the value of ϕ is given as 5.20 and used for evaluation of M_b. M_t is then found directly to be $M_b/5.20$ so that $F_b/F_t = \phi/\phi = 1$.

In Design Equation C, the M_b and M_t values are evaluated independently and further use can be made of the F_b/F_t ratio in assessing the validity of the practical values. The calculations given for Design Equation C are those obtained by substitution of both M_b and M_t, the respective applied bending and torsion moments, since in the experimental investigations both these values are known at ultimate. These values are illustrated in Fig. 1.6.

Fig. 1.6:-

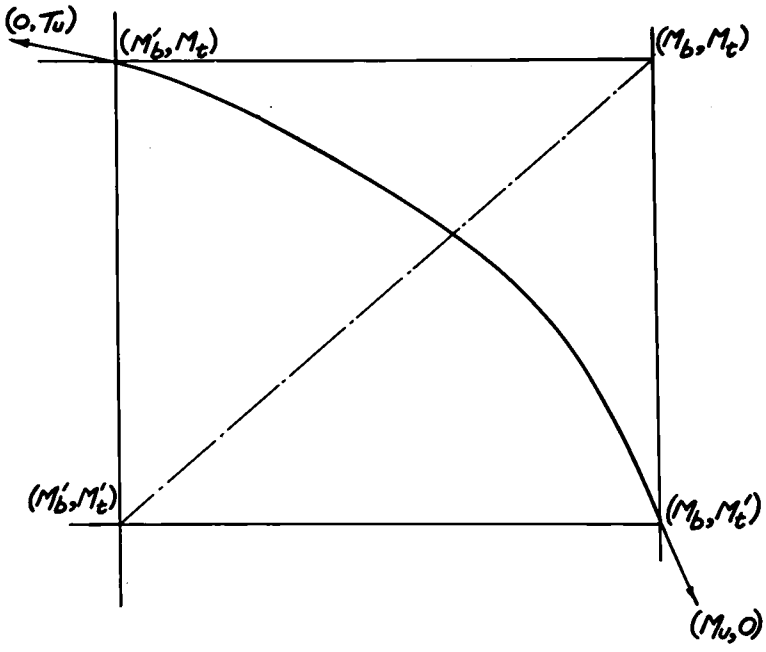

Due to errors in measurement, the applied moments at ultimate (M_b, M_t) are not necessarily on the elliptical curve defined by M_u and T_u. Thus, substituting M_b in the design equation gives $M_t' = T_u\sqrt{1 - (M_b/M_u)^2}$ and an ultimate value (M_b, M_t') on the curve. Similarly substituting for M_t gives $M_b' = M_u\sqrt{1 - (M_t/T_u)^2}$ and a second point on the curve (M_b', M_t).

In order to assess the accuracy of both equations the results given are for (M_b', M_t') so that the values $F_b = M_b'/M_u$, and $F_t = M_t'/M_u$ can be used independently. The true ellipse solution lying between (M_b', M_t') and (M_b, M_t) is not evaluated in this study since the differences are small. The practical application will be to calculation of say the ultimate bending moment, M_b, for a known applied torsion moment M_t so that in this case the values lie on the ellipse and only one of the design equations is used, that is, $M_b = M_u\sqrt{1 - (M_t/T_u)^2}$.

Considering again the bond failure in beam D/2/1, the F_b/F_t value is 1.52/5.41 = 0.28 indicating that the condition that ultimate moment is equal to applied moment is not satisfied. Compare the behaviour of beam D/2/3 which conforms to the predicted theoretical failure and has values of F_b/F_t from Table 13.6 of 1.02/1.06 = 1.

The results which have not been accepted on this basis as not complying with the theoretical mode of failure and not included in Table 18.6 are indicated thus *. Finally, the general application of Design Equation C can be used as a check that the design section conforms to the necessary requirement of being under-reinforced. An example of this is given by beams 1 - 4 of the Russian tests (Table 17.6) where the calculated moment of resistance to pure bending is less than the actual bending moment applied to the beam in combined loading so that the design equation cannot be applied. All beams exhibit extremely low concrete strengths so that the design again does not conform to the theoretical assumptions made for deriving the design equation.

6.5 Conclusions:-

The following conclusions are made for the three design equations derived in Chapter 5, and examined by application to a range of beam sections in this Chapter.

1. Design equations A and B necessarily use the ratio of applied bending to torsion moment in the calculation of ultimate moment M_b. The ϕ value must therefore be known and any error introduced in the calculation of M_b is included in the calculated value of M_t. The ratios of theoretical to applied moments must be equal for both as shown in Tables 1 - 10.6.

2. Using the F_b, F_t ratios for any series of results, a comparison of the relative accuracies of the three design equations can be made on the assumption that experimental errors are constant for any one series of tests. Thus, considering the Leeds tests, the F_b (and F_t) values of 1.00, 1.00, and 1.03 for the equations A, B, and C respectively do not indicate significant differences in the three expressions. It is concluded therefore that any error introduced in the progressive derivation of the design equations does not exceed the magnitude of error accepted in the design as a whole - in this case 3%, and 10% in general.

3. For Design Equation C, further use can be made of the F_b/F_t ratio, as the expression is not dependent on a F_b/F_t ratio of 1. This calculated ratio can therefore be used to ensure that the theoretical assumptions are satisfied since any violation of these assumptions, as may be caused by premature failure of the beam, is indicated by comparing the F_b/F_t value with unity.

4. The use of the three design equations is restricted to under-reinforced rectangular sections as the theory is based on the steel having reached its yield stress. Using Design

Equation C, the preliminary calculations to find the strength of the beam subjected to pure bending and pure torsion indicate that where these values are less than the applied moments, the condition is not satisfied.

5. Design Equation A includes trigonometrical terms which are evaluated in terms of the applied load ratio and prior to calculation of the ultimate moment, M_b. The author feels that the use of these terms introduces unnecessary computation. In addition, the use of the ϕ-value at an initial stage in the calculation restricts the application to the load ratio being considered.

6. In Design Equation B, direct substitution of the ϕ-value is made in evaluating M_b, thus overcoming one of the disadvantages of Design Equation A. However, in achieving this, the range of ϕ must be classified and as many as three different equations may be used in the calculations for one test series, for example, in calculating Table 5.6. Also, as for Design Equation A, the calculation for a given section is only applicable for the specified ϕ ratio.

7. Design Equation C is a general expression, applicable to a given section for all values of ϕ, and independent of trigonometrical terms. The initial calculation for the section is applicable to any specified loading and use can be made of graphs to elliminate further calculation for that section. As the loading condition is introduced as a final condition, this is the only expression in which the ratio of bending to torsion moment need not be known or maintained constant throughout the load-cycle.

It is the author's opinion that the design equation based upon an elliptical relationship between bending and torsion moments expressed as functions of the beam's resistance to pure bending and pure torsion, and on a failure mechanism whereby a hinge is formed at ultimate and rotation takes place about the neutral-axis, is of equal accuracy and the most flexible both for investigations into the problem and for practical application.

CHAPTER 7

EXPERIMENTAL INVESTIGATION

7.1 General:

Chapter 7 describes a Series of practical studies carried out to investigate the problem of combined bending and torsion. These tests have been referred to in Chapter 6 as Series C and D, and Series B will be considered in Chapter 8 with particular reference to the theoretical analysis of grid frames. The main objective is to investigate experimentally the application of the torsion moment by means of lengths of concrete arm framing into the main beam. It is proposed to rely on the results of other investigators to compare the application of the torsion moment by direct loading onto the main beam. The author feels that the former is the more realistic in the application of this theory to grid frame systems.

7.2 Introduction:

The experimental investigation is in three parts. A preliminary study of model reinforced micro-concrete beams, simulating a main beam framing into a column and secondary beam, is carried out to illustrate the effect of adding torsion to results for simple bending tests. The examination is then extended to model concrete beams of larger scale to provide more consistent results and, at the same time, the complex beam to column monolithic joint is simplified so that the effects of the torsion load being transmitted into the main beam by the secondary beams can be more easily studied. These two Series of tests, C and D, differ only in the form of reinforcement used and for each Series, the section design is kept constant in order to confine the

investigation to measuring the effect of varying the applied loading ratio. Special precautions are taken to maintain consistent concrete properties in all tests by precise batching and mixing so that the structural and not the material properties can be studied. The main criterion in the design of the beam section is that it should be under-reinforced, so that at ultimate the steel reinforcement has attained its yield stress and is therefore known.

Finally, the application to simple grid-frames is considered in Series B, in which four tests are made using a beam section identical to the one used for the Series C tests. In this Series however, the torsion moment is introduced by the secondary effect of the transverse beams of the grid and only direct bending load is applied to the main longitudinal beam under examination.

7.3 Preliminary Investigation

The purpose of this investigation is to make a rapid assessment of the methods of applying combined loading to a reinforced concrete beam, simulating in the laboratory as near as possible the location and behaviour of the beam in the actual structure. The results of these preliminary tests are useful in planning more extensive and comprehensive test systems to be used for Series B, C, and D.

(a) Mould and Section Design:- The section used is as shown in fig. 1.7 and the mould is constructed of hardboard which is sufficiently strong for this purpose.

(b) Materials:- The following materials were used:-

(i) mix proportions:- 1:1:3. = Ferrocrete cement: aggregate passing No. 25: aggregate passing No. 100.

(ii) water-cement ratio:- 0.7

(iii) reinforcement, longitudinal and transverse:- 1/16" diameter steel welding rod.

Fig. 1.7:-

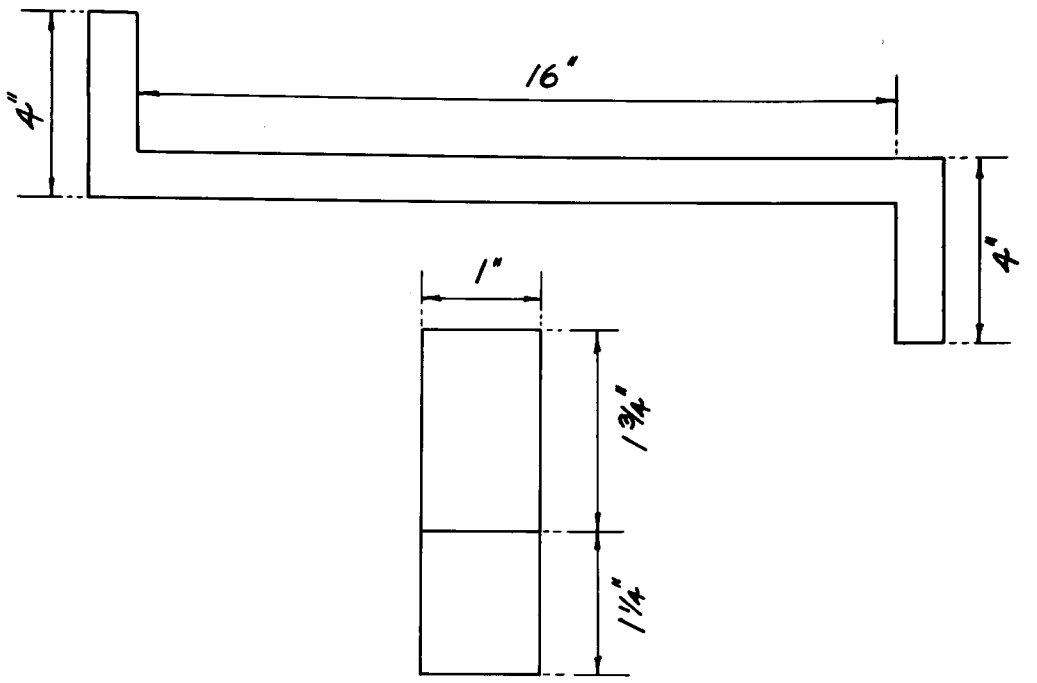

(c) Tests:- The beams were removed from the curing tank five days after casting, discs attached to the upper surface of the beam at two inch intervals along its span, and testing carried out at seven days by applying dead loads at the centre-point in pure bending, and in addition, dead loads on the arms at a distance of three inches from the centre-line of the beam for the combined bending and torsion case. Measurements of deflection were taken using dial gauges attached to magnetic bases mounted directly below the discs, for loads within the limit of proportionality and finally to failure. Observations of cracking in the beam were made, and graphs of deflection plotted against load are shown in Figs. 2.7, 3.7, 4.7, and 5.7.

FIG. 2.7:-

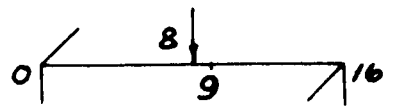

(a) BENDING ONLY

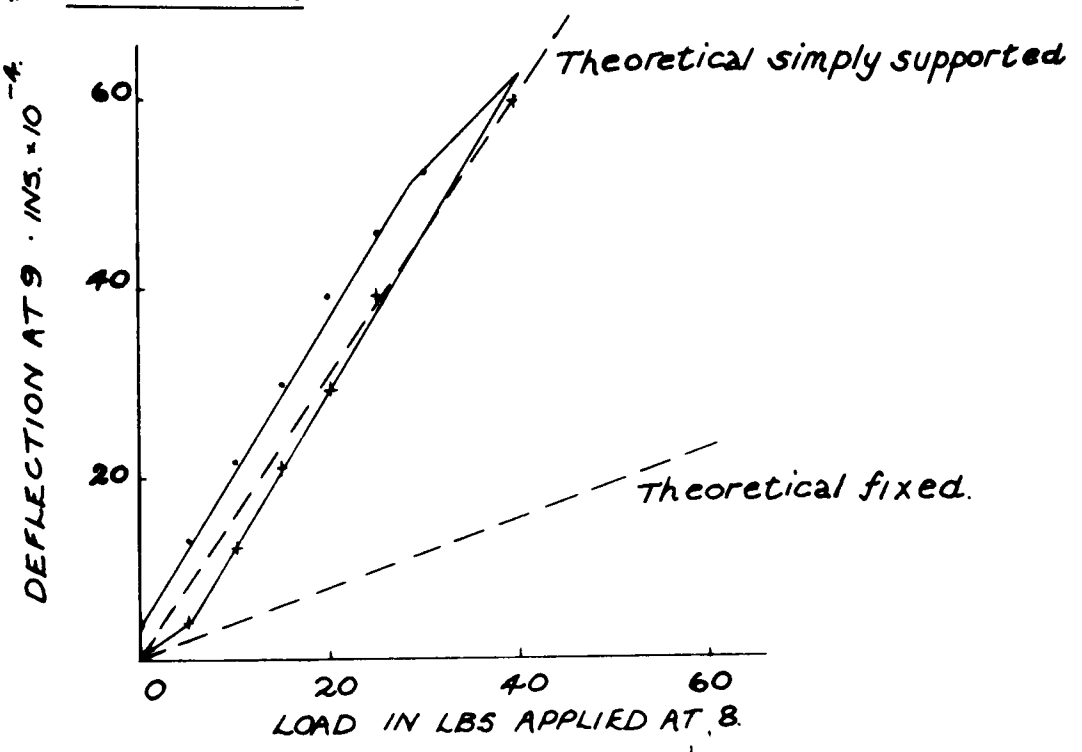

(b) BENDING + TORSION.

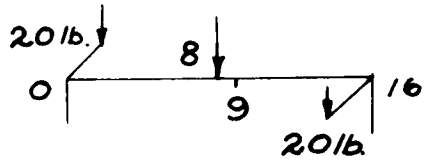

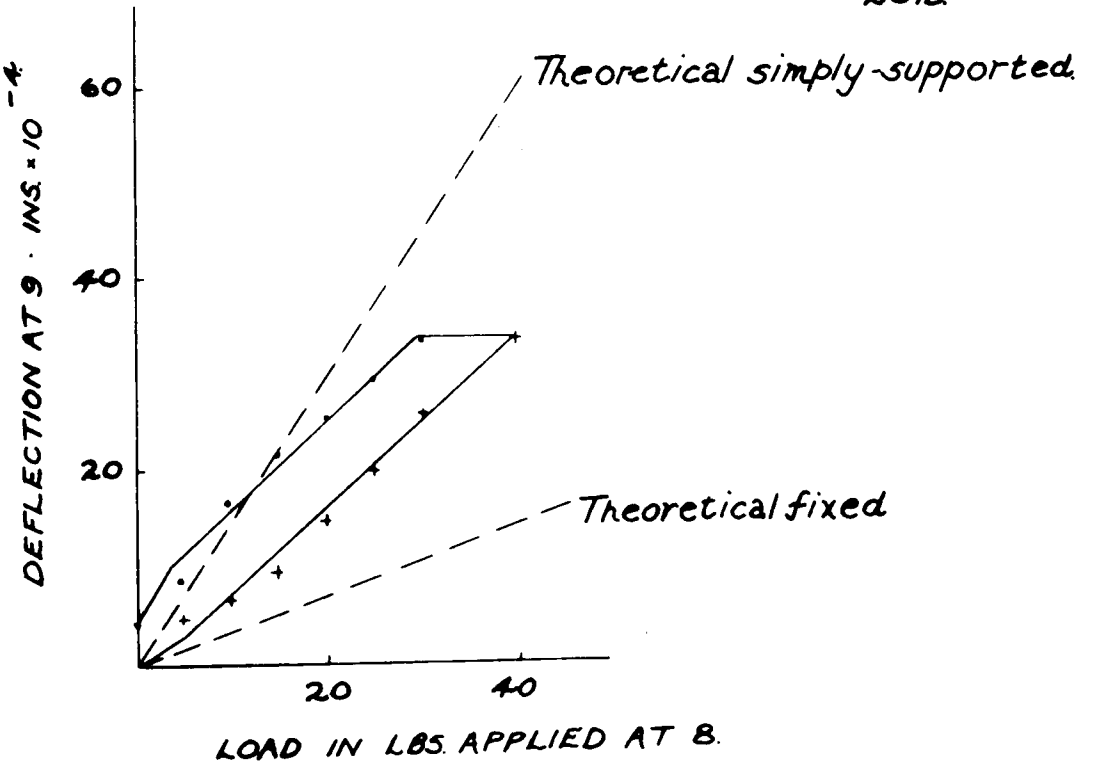

FIG. 3.7 :-

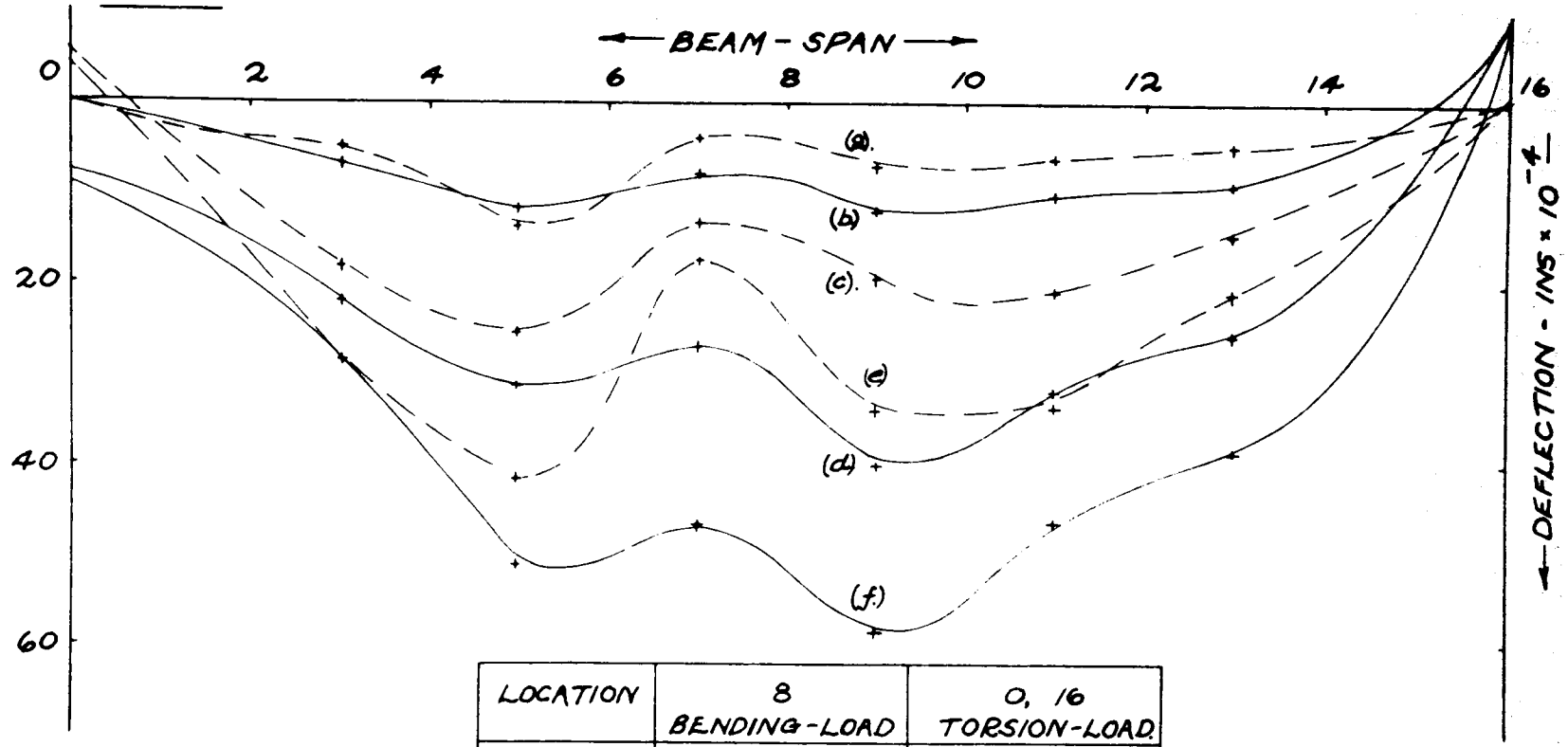

LOCATION	8 BENDING-LOAD	0, 16 TORSION-LOAD
(a).	10 lbs.	20 lbs.
(b).	10 "	0 "
(c).	25 "	20 "
(d).	25 "	0 "
(e).	40 "	20 "
(f).	40 "	0 "

FIG. 4.7:-

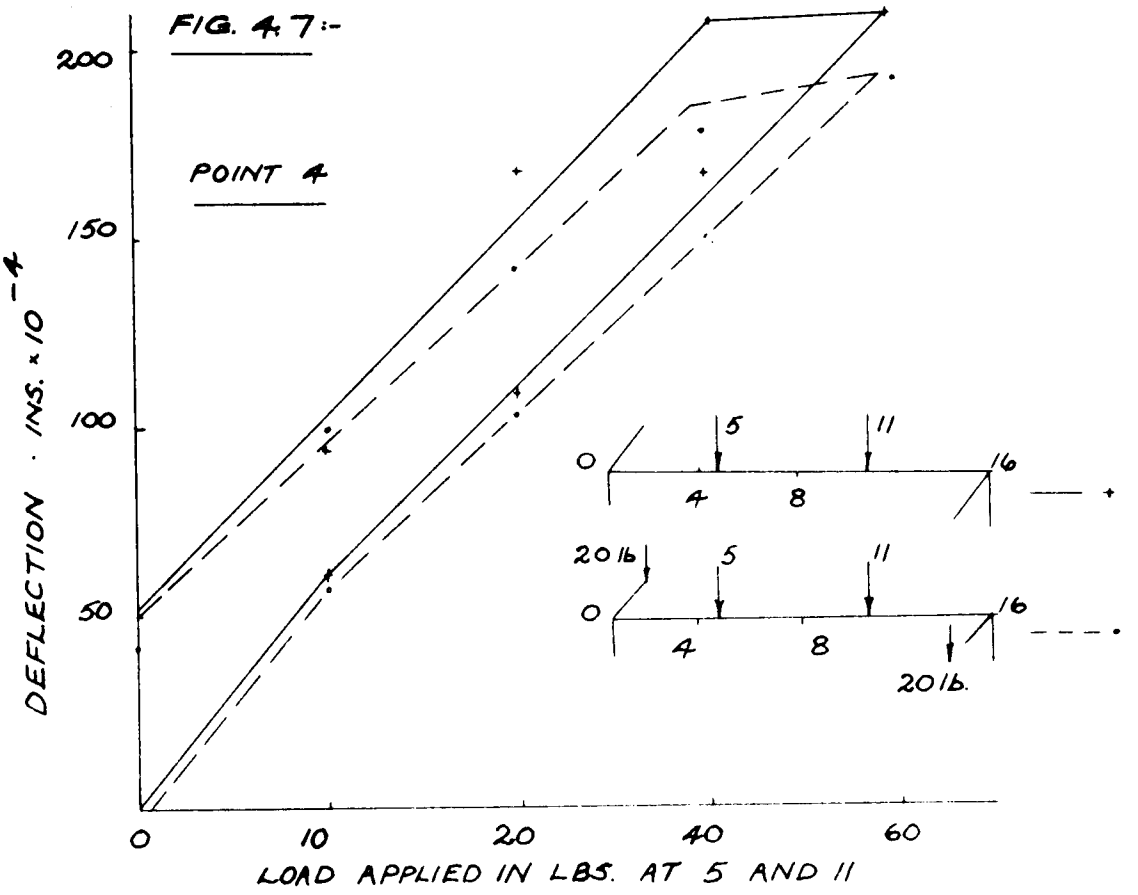
POINT 4
DEFLECTION · INS. × 10⁻⁴
200
150
100
50
0
10
20
40
60
LOAD APPLIED IN LBS. AT 5 AND 11
5
11
16
4
8
20 lb.

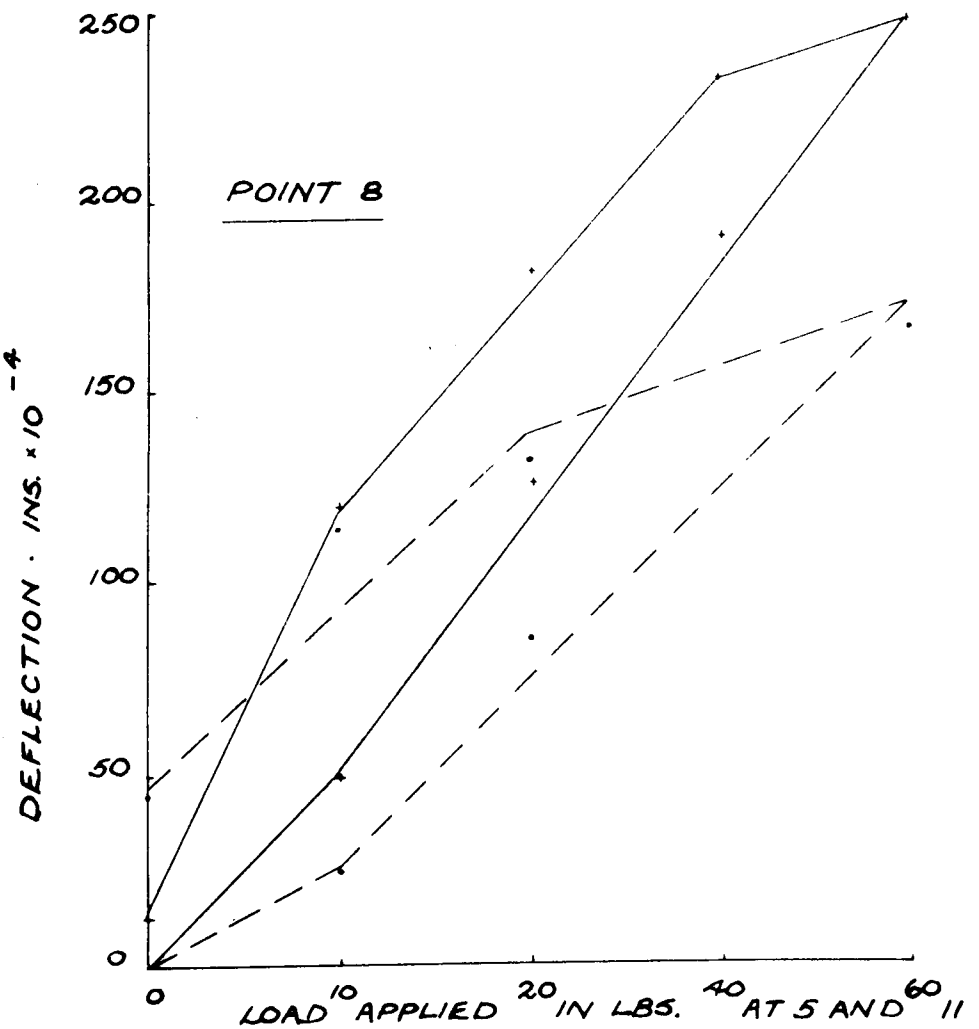
POINT B
DEFLECTION · INS. × 10⁻⁴
250
200
150
100
50
0
10
20
40
60
LOAD APPLIED IN LBS. AT 5 AND 11

FIG. 5.7:-

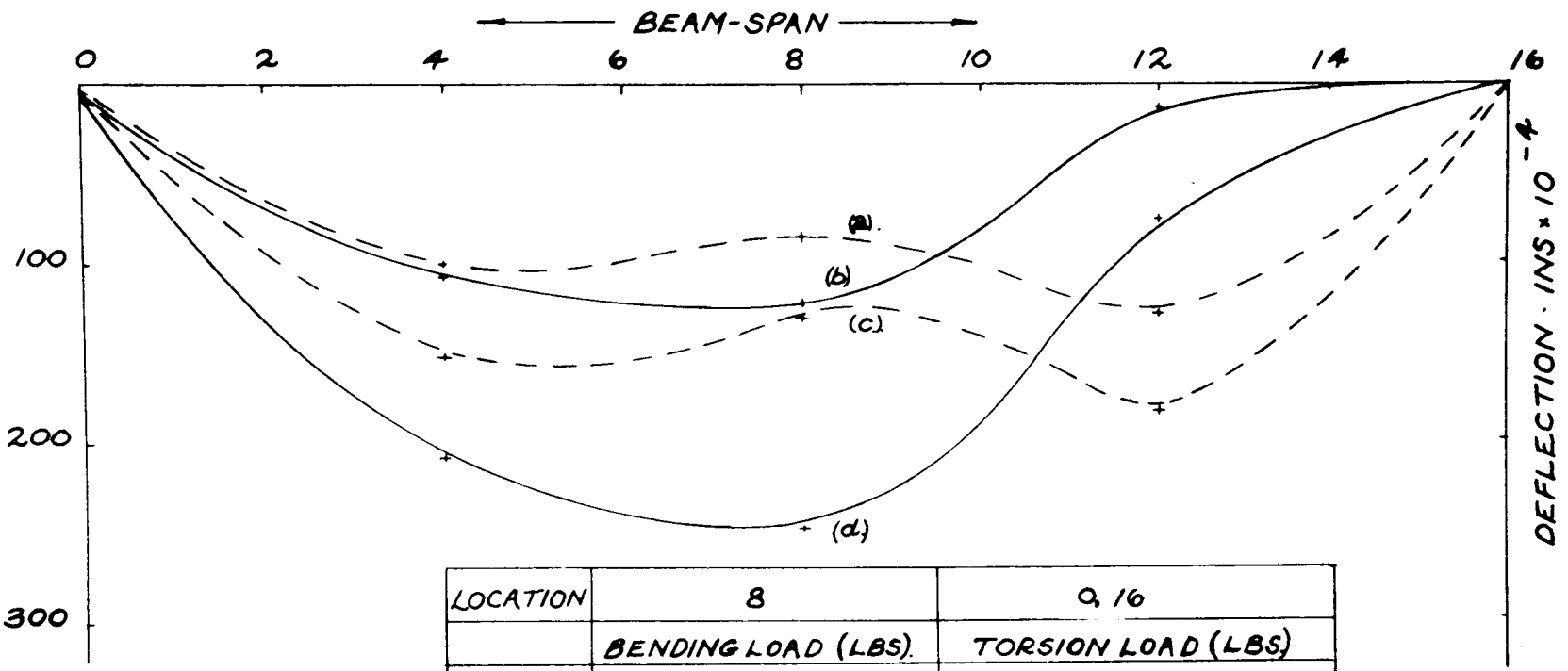

LOCATION	8	9, 16
	BENDING LOAD (LBS)	TORSION LOAD (LBS)
(a)	20	20
(b)	20	0
(c)	40	20
(d)	40	0

7.4 Series C, Series D:

Series C and D are discussed together since they differ only in the form of reinforcement used. These tests constitute the major part of the research programme. Differences between the two Series are only indicated where necessary and in general, materials, mould, testing arrangement, instrumentation and presentation of results are the same.

(a) Section design and Mould:-

The section design was calculated according to normal balanced design procedure and details are given in Table 3.D, Appendix D.

It is important that the design of the section conforms to the Design Code[57] at this stage so that it is only at ultimate load that the ultimate properties of the beam are taken into account. Thus these sections were adopted for testing and the mould designed accordingly.

A photograph of the mould is shown in plate 1.7, with steel reinforcement in place for Series D. The plan dimensions are given in Fig. 6.7.

At positions A and B in the mould, a half-inch diameter pipe was fixed to the reinforcement for application of the torsion moment through the loading arms. The mould was constructed of $\frac{1}{2}$" thick African Teak and attached to a baseboard by special springs. The complete Series of test beams was obtained using this mould. Nevertheless, variations in cross-section are unavoidable and micrometer measurements of the beam-section were taken over the length of span under examination, and in particular, at the failure zone. Provision was made in the mould construction at the left hand support point for the

inclusion of a steel shaft in the concrete during placing.

(Plate 2.7).

Fig. 6.7:-

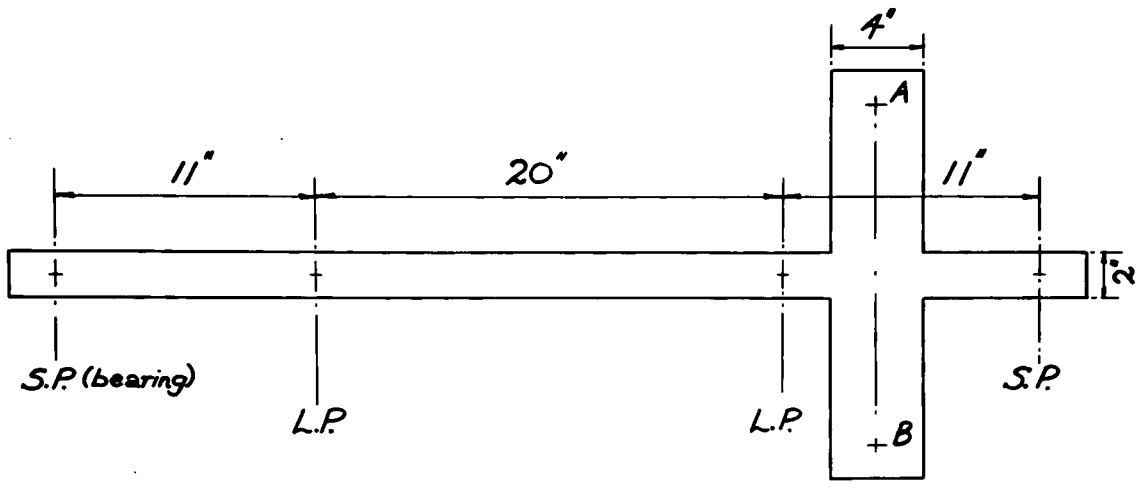

S.P. - support-point L.P. - loading-point

(b) Materials:-

Although an investigation of materials does not form part of this investigation, the author has devoted a considerable time to ensuring the production of consistent material properties for the beams for structural analysis. The summary of this work is given in two parts.

1. Concrete:-

The concrete materials used were Ferrocrete cement and Eddleston -$\frac{3}{8}$" aggregate. The mix proportions were designed for a rounded river gravel according to McIntosh and Erntroy[58] to give good workability - this is of special importance for Series D with close spacing of the transverse steel - and a concrete strength at twenty-eight days of 6,000 lbs/ins^2. Table 1.7 gives the mix proportions and aggregate grading required for one test,

Plate 1.7

Plate 2.7

including control-tests,[59] the results of which are summarised in Table 2.7.

Table 1.7:-

cement:- 25 lb. w/c = 0.55 water:- 13.75 lb. a/c = 4.05 aggregate:- 101.25 lb.			
No.	B.S Sieve size	Weight lbs.	Weight %
1	$\frac{3}{8}$" 3/16"	40.5	40.0
2	3/16" - no.7	14.25	14.08
3	no.7 - no.14	9.125	9.01
4	no.14 - no.25	9.125	9.01
5	no.25 - no.52	14.25	14.08
6	no.52 - no.100	11.00	10.86
7	no. 100	3.00	2.96
Total	-	101.25	100

For each batch, the aggregate was dried, broken down into its fractions by sieving and finally recombined at batching to conform to the proportions given in Table 1.7. This process occupied a considerable time but the author feels this was justified by the consistency of the control test results shown in Table 2.7. Also, Kaplan's study of strain measurement and crack behaviour of reinforced beams[27] shows that changes in aggregate volume effect the beam behaviour and it was considered important to eliminate this aspect in investigating the effects due only to changes in the ratio of applied loading.

The concrete was mixed in a two cubic-foot capacity "Cum-flow" type mixer for two minutes, then poured and vibrated into the mould and covered with damp hessian. The beam and

Table 2.7:-

Beam No.	Cube strength lbs/ins^2	Split. Load Tons	E_T lbs/ins^2 x 10^6	E_C lbs/ins^2 x 10^6	Mod. of Rupture lbs/ins^2
C/2/1	6,030	-	0.412	3.269	598.5
C/2/2	5,600	29.12	0.540	2.946	611.1
C/2/3	6,200	26.00	0.551	3.190	579.6
C/2/4	6,178	30.0	0.550	2.883	516.6
C/2/5	5,959	-	0.394	2.985	579.6
C/2/6	6,212	-	0.755	3.040	617.4
D/2/1	7,000	-	0.913	2.930	648.9
D/2/2	7,303	-	0.965	2.990	658.4
D/2/3	7,612	-	0.951	3.026	765.4
D/2/4	7,052	-	1.002	2.865	626.8
D/2/5	6,440	-	0.931	2.674	645.7
D/2/6	6,375	-	0.896	2.727	504.0
D/2/2/R	6,533	-	1.038	2.848	504.0

control specimen were demoulded after twenty-four hours then placed in a curing tank and water-cured at a constant temperature of 65°F for twenty-five days. The specimen were then removed from the water and air-dried prior to testing at twenty-eight days. Each beam was air-dried for twenty-four hours to remove surface moisture then prepared for testing. This procedure included rubbing-down the four faces of the beam with emery-paper, washing with acetone, filling the spores with durafix, marking the grid points and reference marks, attachment of "Demec" discs, dial-gauge discs, and measurement of the sectional dimensions.

2. Steel:-

The main property of the steel is its behaviour under stress and for these tests, it is essential that the steel is sufficiently ductile to maintain a constant stress beyond yield for increasing applied load up to ultimate beyond which failure is brought about due to crushing of the concrete in the compression zone. For this purpose, the properties of $\frac{1}{2}$" diameter black mild steel were found to be suitable and for each test, samples of each reinforcement were tested in a Hounsefield Tensometer to check that the required condition was satisfied and also to measure accurately the stress in the steel during the constant stress stage as this value is used in the design equation.

For the Series C beams, resistance strain gauges of gauge-factor, 2.0, and resistance, 50 ohms, were attached to the reinforcement, prior to placing the concrete, and rendered waterproof by covering the gauge with a water-repellant wax. Measurements of strain recorded on a Transducer Meter and balanced against an identical gauge set in an unstrained beam, gave readings of strain in the reinforcement as well as indicating that the condition of constant stress was reached prior to failure. The yield stresses of the steel used for the Series C beams varied between 30,000 and 50,000 lbs/sq. in. In the Series D tests however, better quality steel was used giving consistent yield stresses of 50,000 lbs/sq.in. and satisfying the condition of constant stress beyond yield under increasing applied load. Although samples were taken from each beam for testing in the tensometer, no strain gauge measurements were taken during the actual tests for Series D as it was considered more desirable to elliminate the effects of the strain gauge wire passing

internally along the beam. The use of $\frac{1}{8}$" diameter bright mild steel for the transverse reinforcement was not suitable as no definite yield point could be determined before rupture of the steel. Black mild steel of $\frac{1}{8}$" diameter was also unsuitable due to non-uniformity of the cross-section, so the bright mild steel was annealed at 900°C to give properties similar to those of the longitudinal steel and a consistent yield stress of 45,000 lbs/sq. in. Tensometer tests were taken for steel samples from each beam to ensure the necessary condition and measure accurately the values to be used for calculation. The spacing of the transverse steel was kept constant at two inches over the gauge length for beams D/2/1, 2 and 3, and $1\frac{1}{2}$" for the remainder.

The reinforcement used in the loading arms was designed to prevent failure as this part of the beam was not under investigation. In addition the transverse reinforcement was used to anchor the $\frac{1}{2}$" diameter piping in position during mixing (Plate 1.7). As beams D/2/1 and D/2/2 failed prematurely due to bond slip, the longitudinal steel in the remaining beams of the Series was cranked at 90° at both ends to prevent further failures of this kind.

(c) Testing Procedures

The main requirements in testing Series C and D were firstly the measurement of the applied loads and in particular the ultimate load, and secondly the measurement of the beam behaviour from initial application of the loads up to ultimate.

The test frame, shown in plates 3.7, 4.7, provided the support for the spherical rollers on which the beam was supported and the load frame against which the bending load was applied, by a hydraulically operated Black-Hawk jack of 5 ton capacity

Plate 3.7

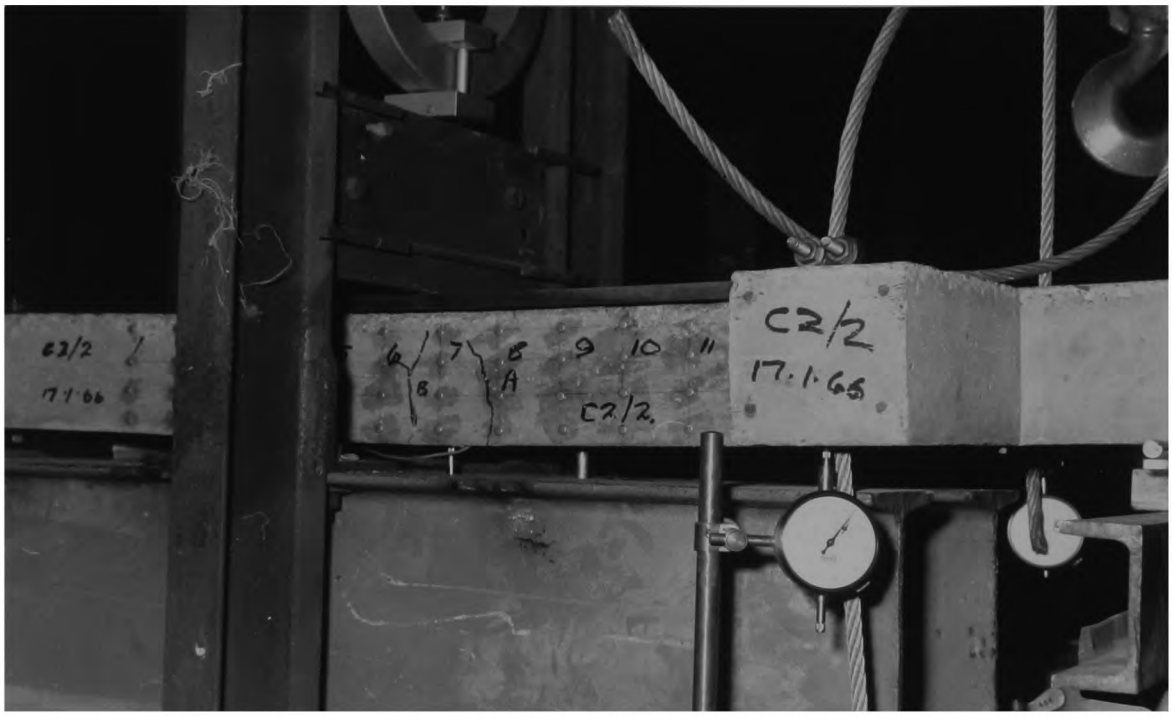

Plate 4.7

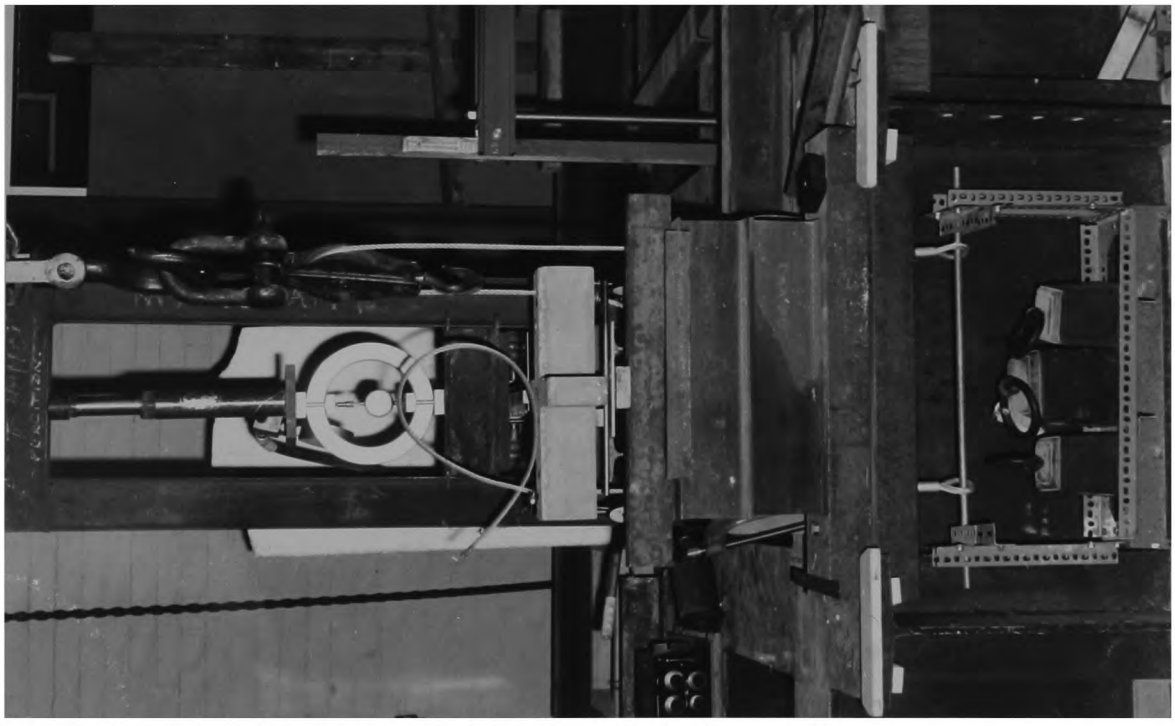

acting through a proving-ring on to a twenty-inch long loading bar placed centrally on the beam. The torsion moment was independently applied by dead weights transmitted through steel wires, one of which passed over a pulley, on to the concrete loading arms (Plate 5.7). The overturning moment was resisted by the left hand beam support in the form of a shaft passing through the concrete and held in the plane by two Skifco self-aligning bearings supported in plummer blocks bolted to the test frame (Plate 6.7). The torsion moment is therefore constant along the full length of the beam from the loading arms to the bearing support. Also, this length is not subjected to shear forces so that the investigation was in compliance with the assumptions made in Chapters 4 and 5. Although this method of loading is not as flexible as for example using a torsion machine, the author feels that it simulates more closely the practical application of torsion moment to the beam in the grid-frame system. The direct bending load was measured by taking readings on the dial gauge of the proving ring and using the calibration graph given in Fig. 7.7.

The experimental investigation also included the study of the actual behaviour of the beam under the applied loads from initial application of the load up to ultimate. For this, observations of the crack propogation were made at each load stage, and "Demec" readings taken at 2" intervals along the constant bending moment area. In addition, dial gauge readings were taken to record the vertical movement of the loading arms.

The pattern and sequence of cracking is of major importance in the study and details were recorded at every load stage to investigate the crack propogation as the loading increases to ultimate. The form of notation used was to mark the number of

Plate 5.7

Plate 6.7

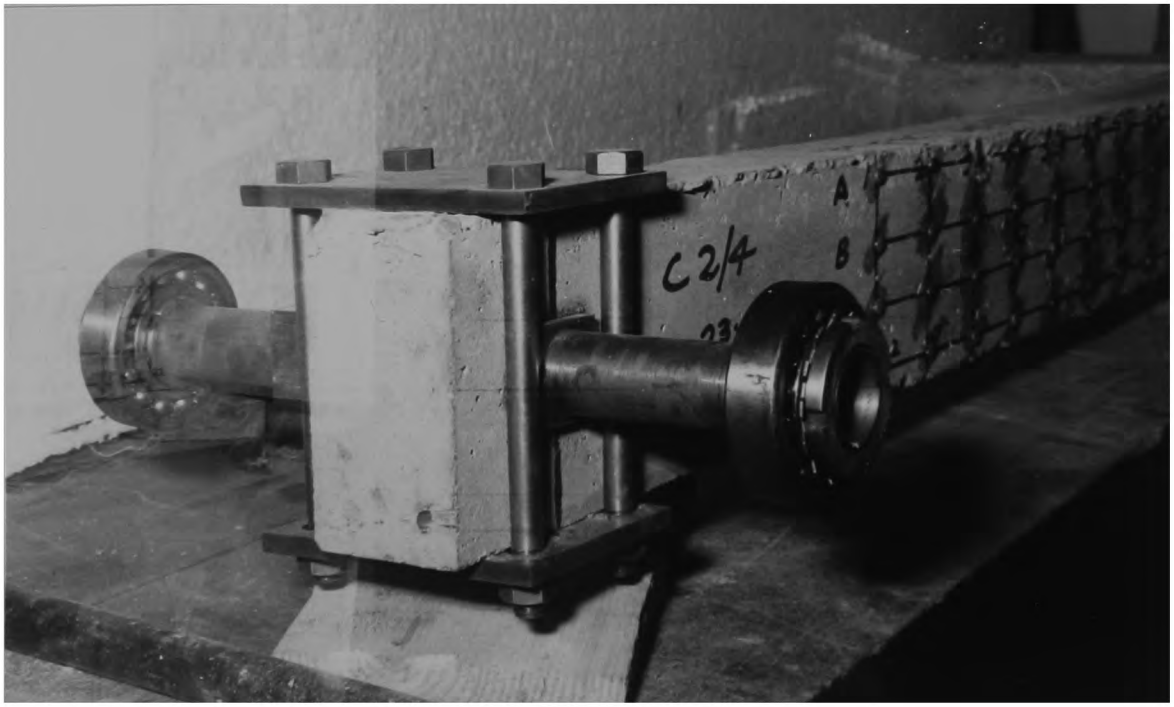

FIG. 7.7. CALIBRATION - CURVE

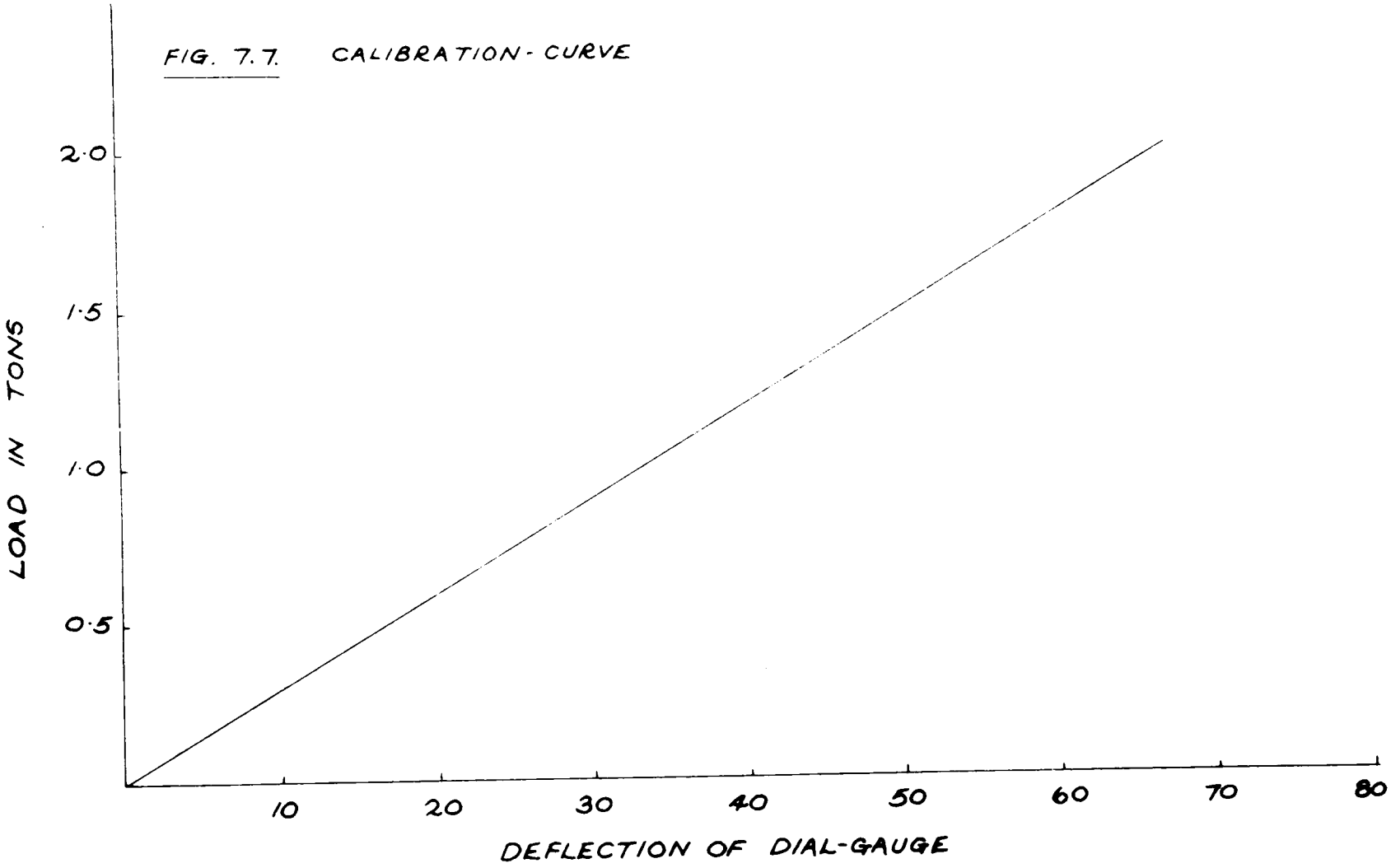

the load stage on the beam at the position where the crack had reached at that stage. The angles of crack were measured on completion of the test. In Series D, the initial micro-cracks were detected more quickly by coating the face of the beam with a thin layer of durafix so that visual detection of the breakdown in bond at the durafix-concrete interface was possible for lower surface strains than for visual cracking of the concrete. The position of the initial durafix cracks was indicated by adding the suffix 'd' to the load stage number. An example of the data recorded for beam D/2/6 is given in Table 1.D, Appendix D. Cracking of the concrete then followed at a later stage. This

Table 3.7:-

Beam	angle of crack in degrees	
	Practical	Theoretical
C/2/1	82	84
C/2/2	85	85
C/2/3	76	83
C/2/4	79	80
C/2/5	90	90
C/2/6	70	74
D/2/1	60	80½
D/2/2	70	72½
D/2/3	80	79¾
D/2/4	45	45
D/2/5	80	81½
D/2/6	75	77½
D/2/2/R	81	83¾

information is best presented by developing in the same plane photographs taken of the cracking on the four faces of each beam and is given in Plates 7, 8, 9, 10, 11, 12, 13, 14, 15, 16, 17, and 18.7. The practical values of the angle of the failure crack are compared with those given by Fig. 5.4 Chapter 4 in Table 3.7.

No measurements of the width of crack were possible but use was made of the "Demec" readings. The main object of this investigation was to study the effect of an applied torsion moment on the ultimate bending moment resisted by the beam, so that strain measurements were taken parallel to the longitudinal axis of the beam and only the component of the torsional stress acting in this direction is therefore included. Although an eight inch "Demec" has been used throughout, the setting of the discs at two inch intervals along the constant moment zone of the beam enabled readings to be taken within each gauge length. Thus, average strain measurements were obtained at three points, a, e and i, covering the length of beam under examination (Fig. 3.7, Plate 19.7) and the remaining measurements used to locate crack movement. The load-stage when initial cracking occurred and the concrete attained its maximum tensile strength was indicated by a large increment in the "Demec" readings at that point, and readings taken beyond this stage were used to give an estimate of the crack width since further increase in the gauge reading is related to the opening up of the crack. The effect of a particular crack could be assessed by examining consecutive readings at that point, for example in Fig. 8.7, a crack in the area 2-3 is indicated by the readings 'a' and 'b', and the reading 'c' is only affected by propogation of the crack into the area 3-4.

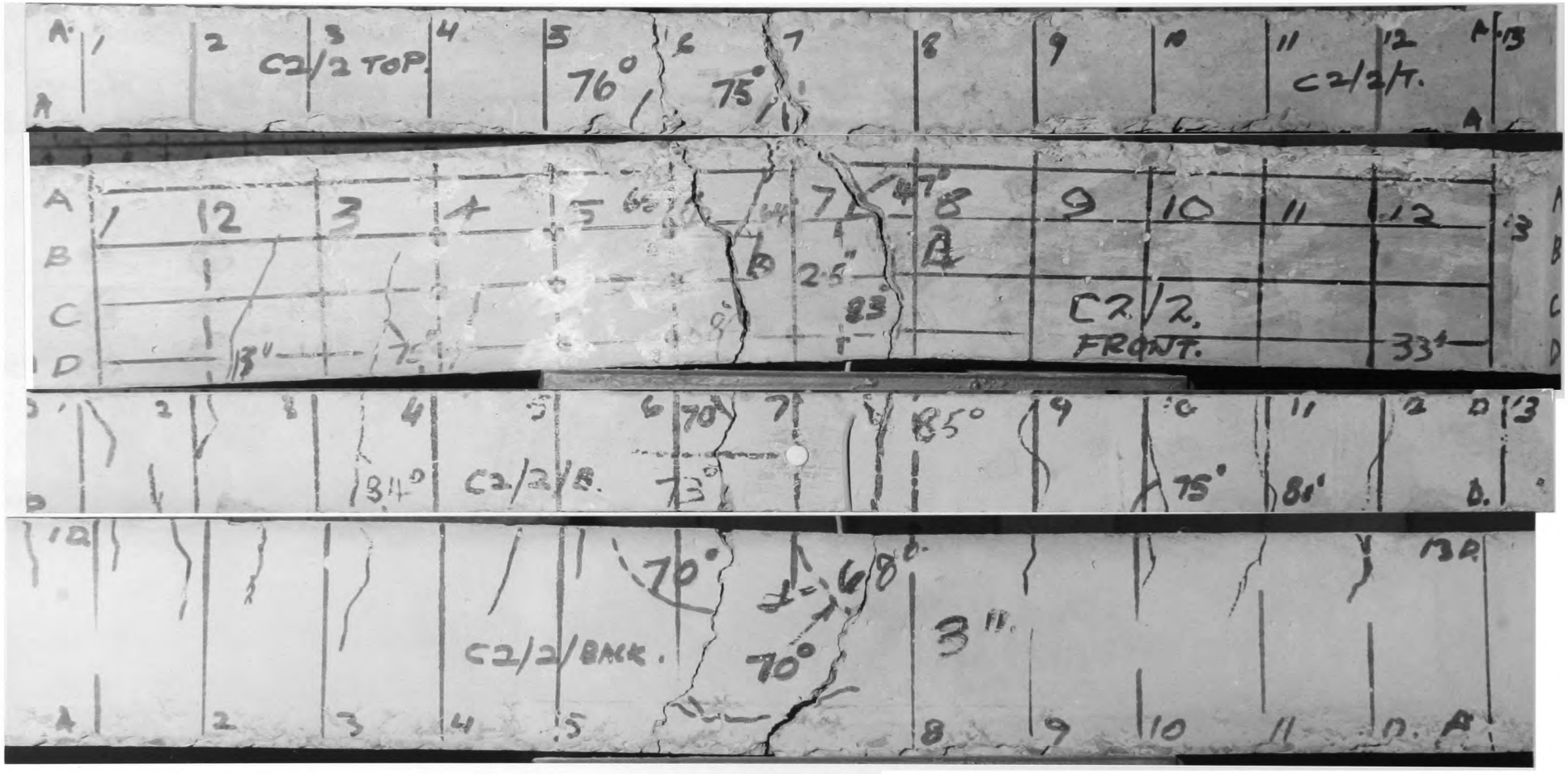
C2/2 TOP.
76°
75°
C2/2/T.
25"
83°
C2/2.
FRONT.
33"
13"
75°
70°
85°
75°
C2/2/B.
73°
C2/2/BACK.
70°
70°
3"

Plate 7.7. C/2/2

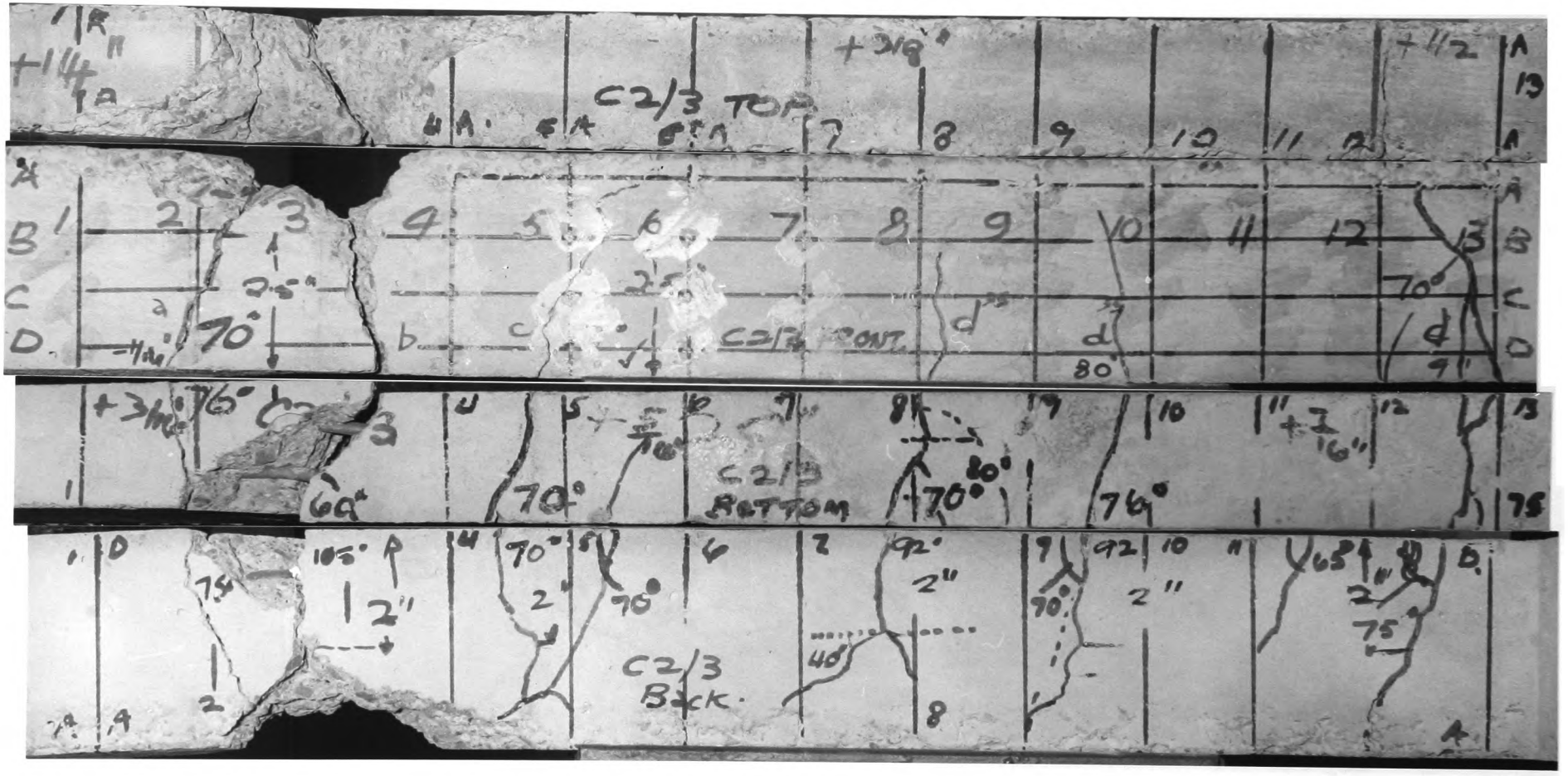

Plate 8.7. C/2/3

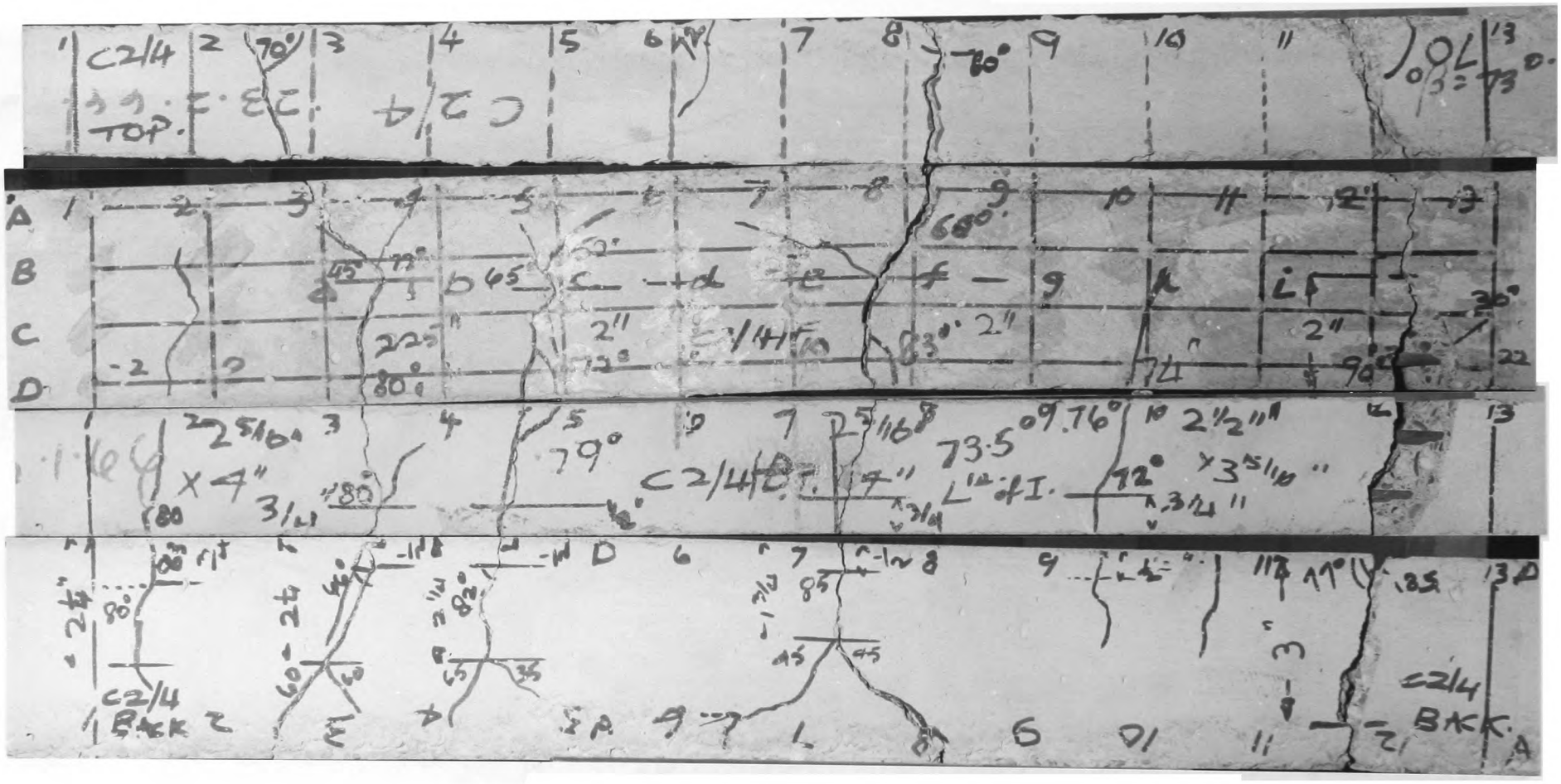

Plate 9.7. C/2/4

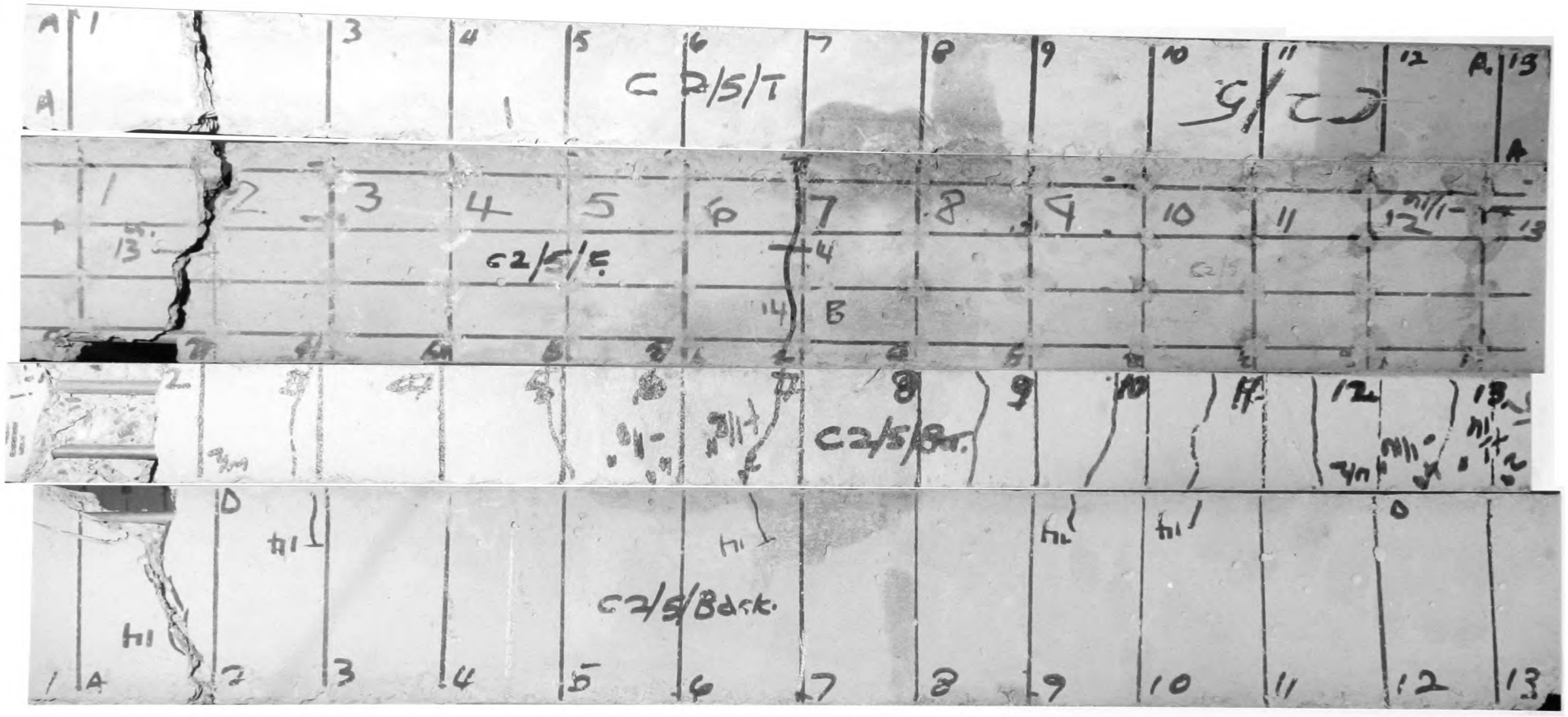

Plate 10.7. C/2/5

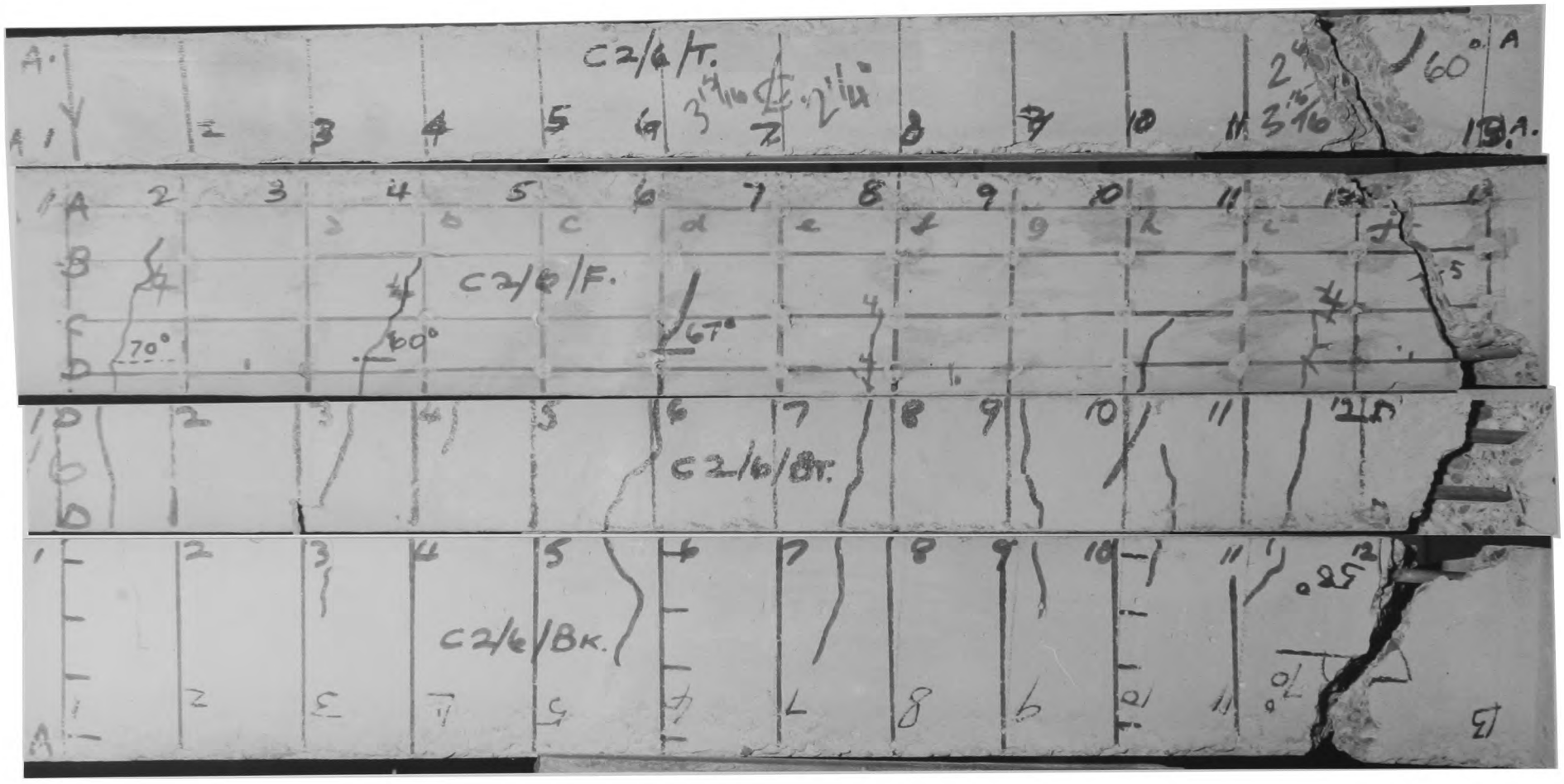

Plate 11.7. C/2/6

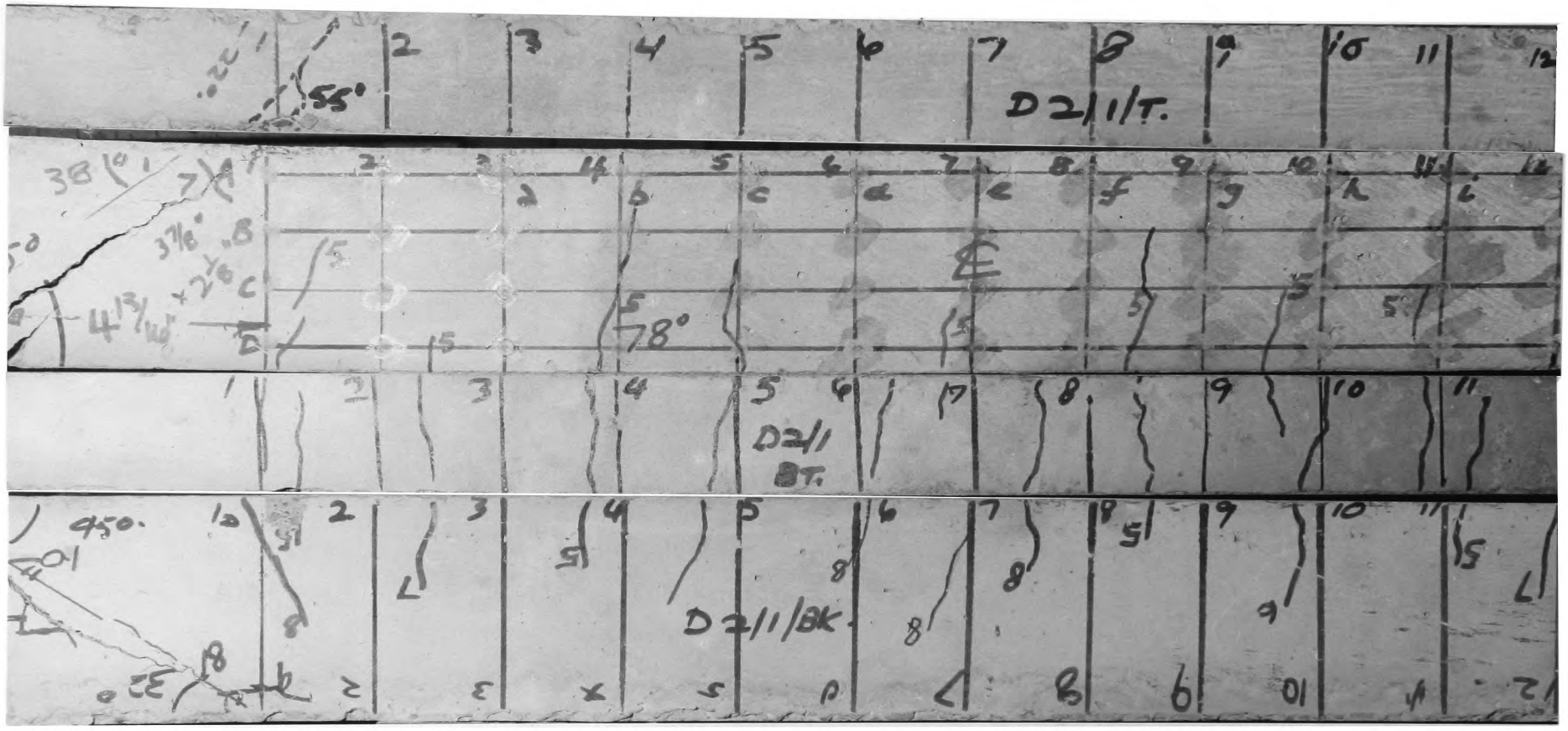

Plate 12.7. D/2/1

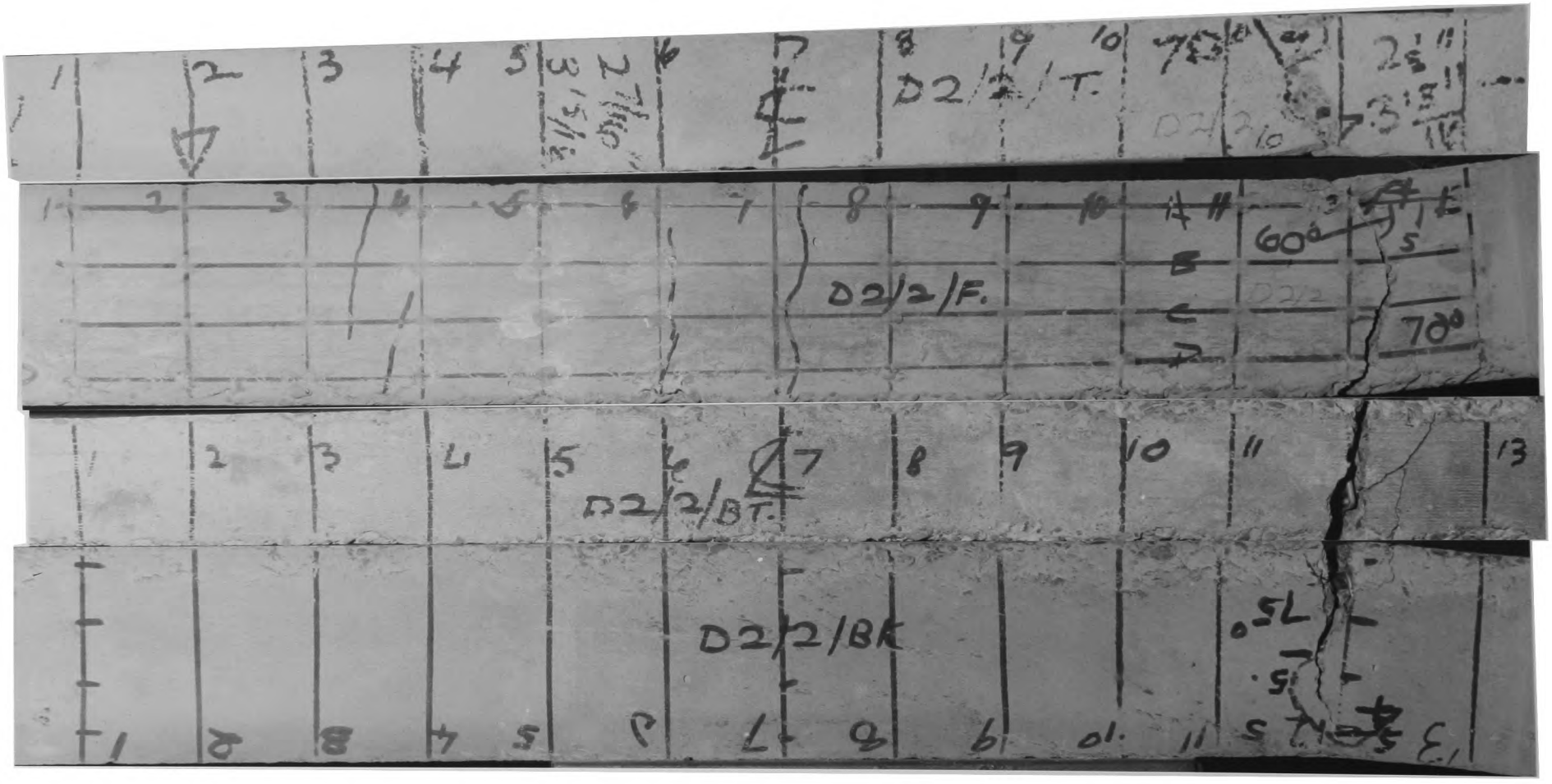

Plate 13.7. D/2/2

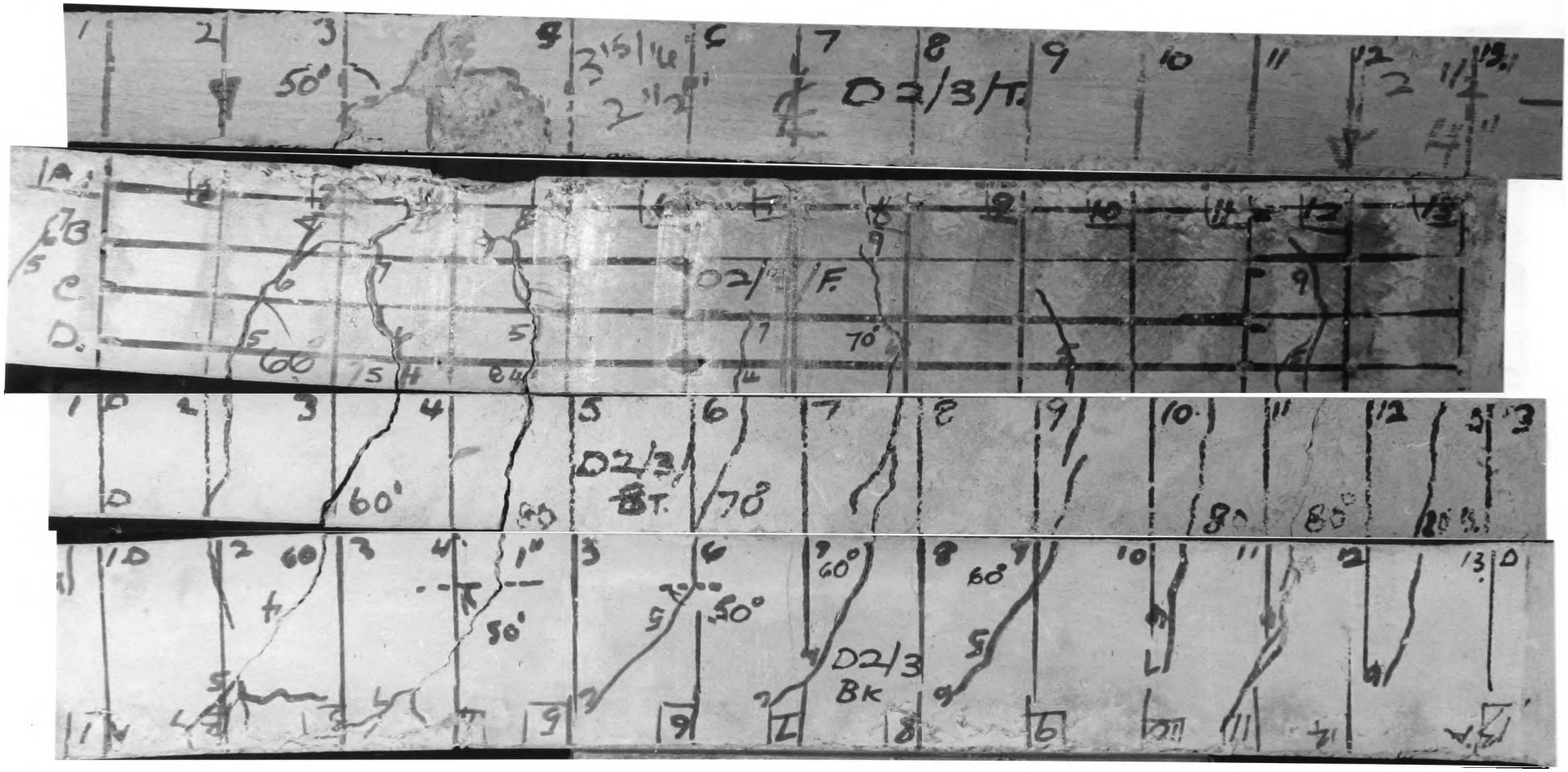

Plate 14.7. D/2/3

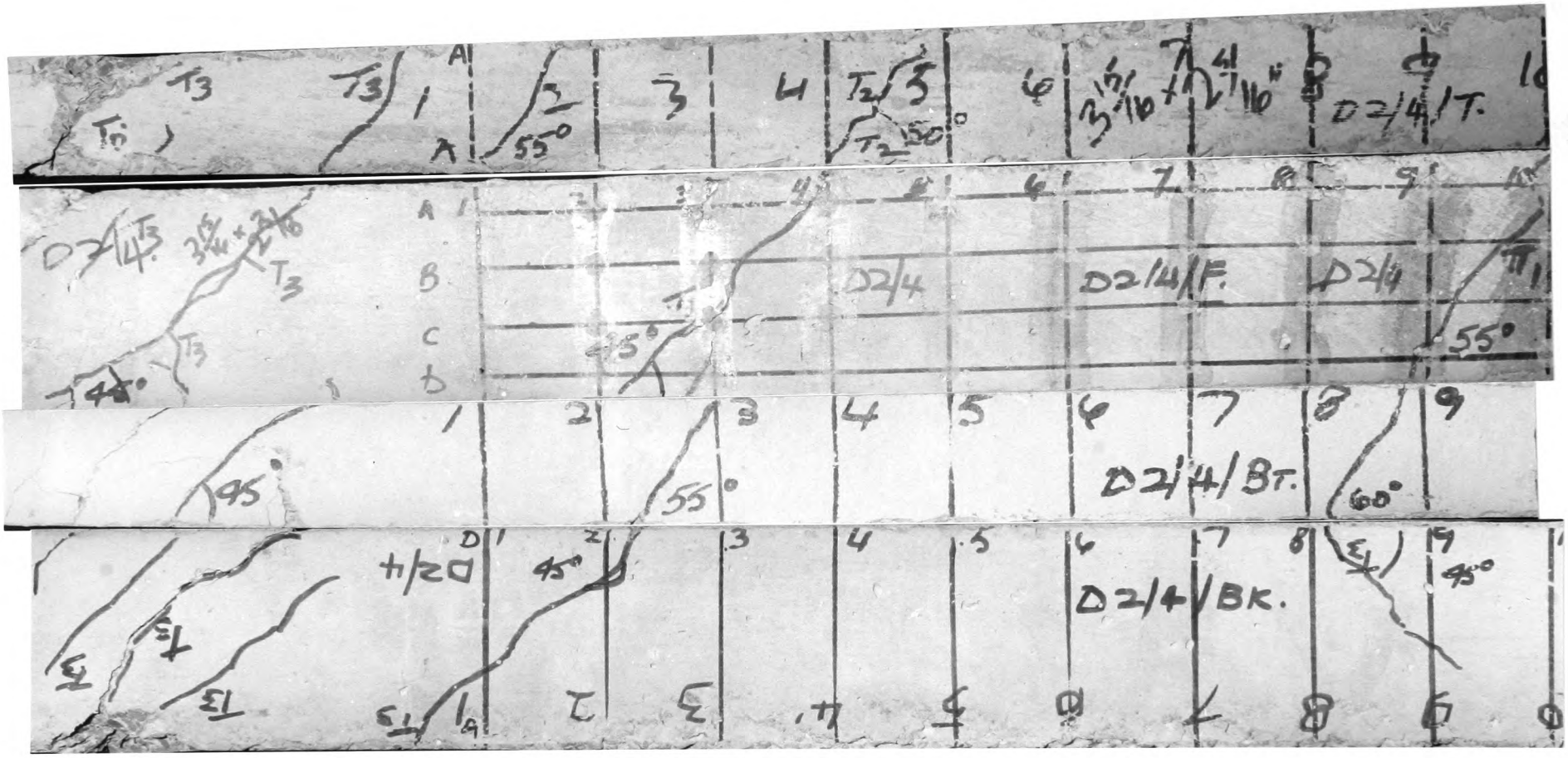

Plate 15.7. D/2/4

Plate 16.7. D/2/5

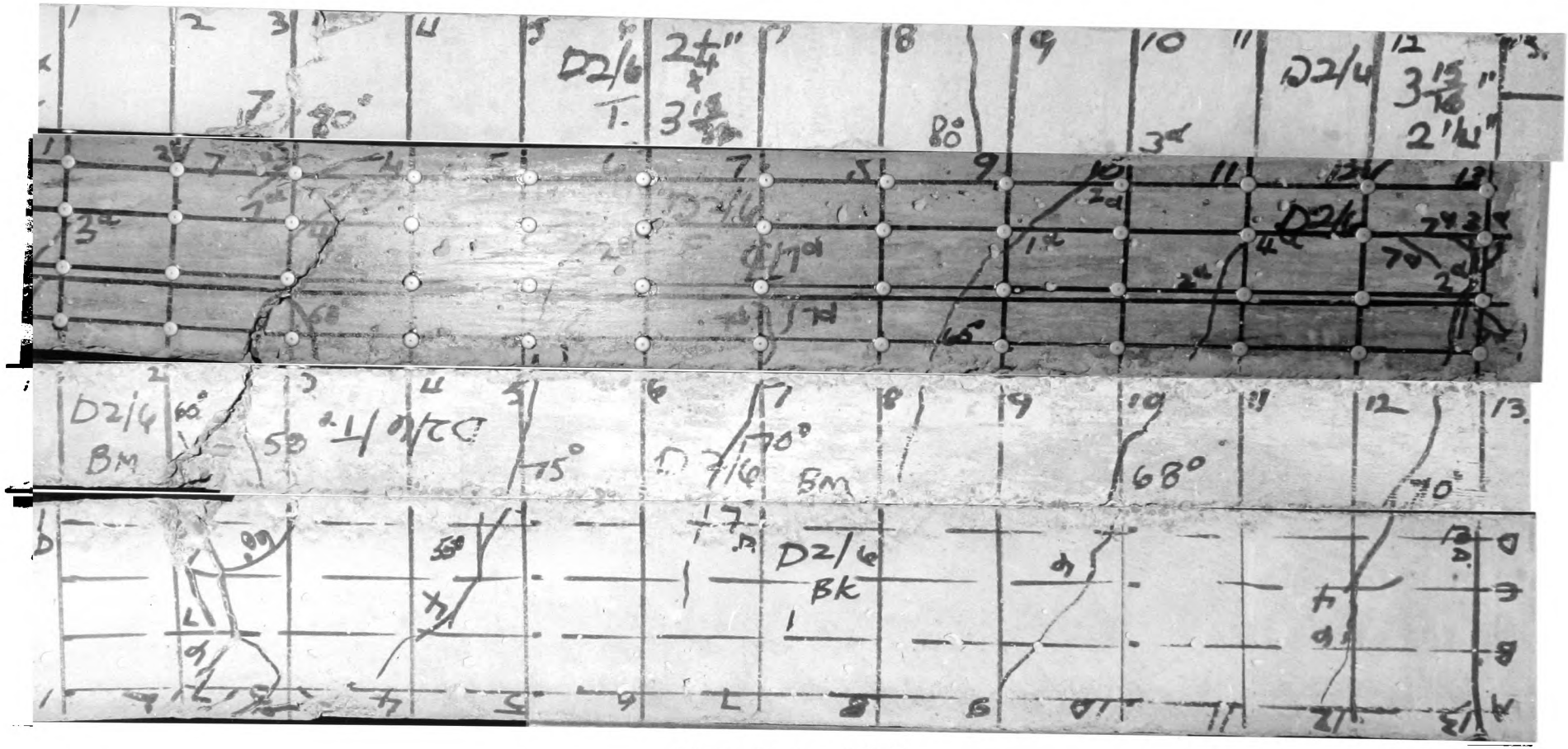

Plate 17.7. D/2/6

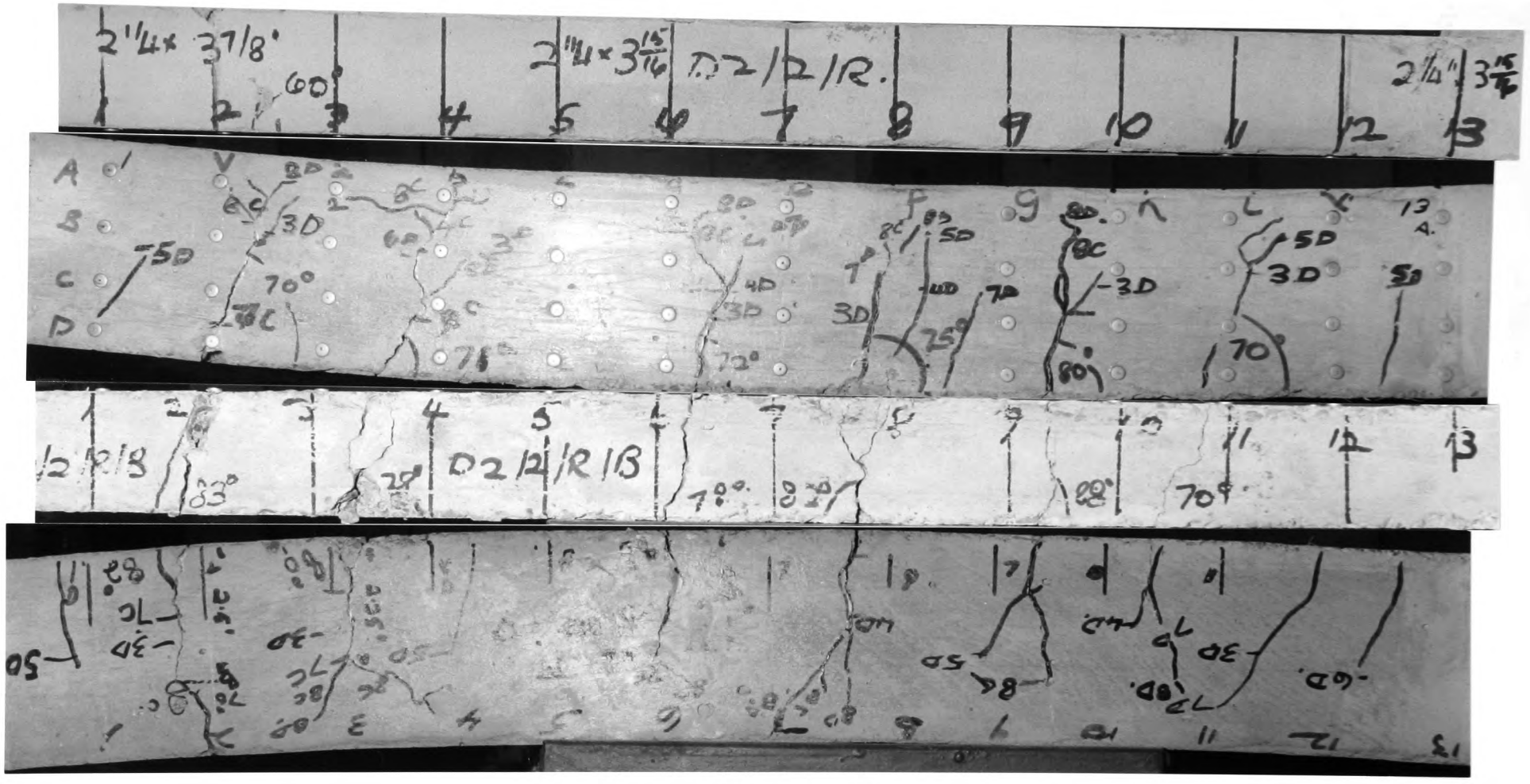

Plate 18.7. D/2/2/R

Similarly, the propogation upwards is traced using the readings a_A, a_B, b_B, b_C etc. The "Demec" readings have also been used to illustrate the upward movement of the neutral-axis with increasing load towards ultimate, and an example is included for Beam D/2/6 in Figs. 1.D, 2.D, Appendix D.

Initial "Demec" and dial gauge readings were taken prior to applying the torsion load and at every load stage, before and after observing and marking the crack propogation on the beam. Approximately ten minutes were required for this procedure at each load stage giving a total period of test of about 100 minutes and creep effects have not been included. The test load was maintained for up to 48 hours to investigate the load sustained by the beam after ultimate. Symmetrical application of the torsional load was checked by taking dial gauge and cathetometer readings at the ends of the loading arms (Plate 3.7).

7.5 Series B:-

The investigation procedure was similar to that used for Series C and D and only the essential differences are given.

(a) Section design and Mould:- As this investigation is an extension of the Series C and D tests, the same design section was used. The plan dimensions of the grid are shown in Fig. 9.7, and the mould used for the Series is shown in Plate 20.7. The mould was constructed so that during placing, the reinforcement could be inserted in the beam after pouring of the bulk of the concrete. This inversion of the mould produced a better finish for the upper face of the beams, and by screwing the ends of the transverse bars, the longer external formwork was held in position at the specified width during placing.

FIG. 8.7:-

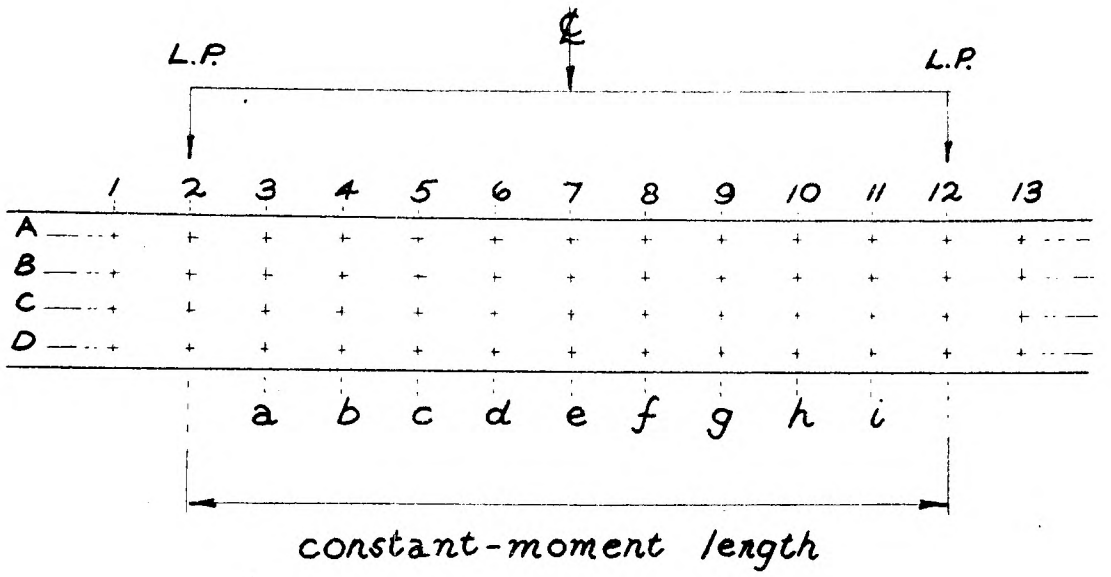
L.P.
℄
L.P.
1 2 3 4 5 6 7 8 9 10 11 12 13
A
B
C
D
a b c d e f g h i
constant-moment length

PL. 19.7:-

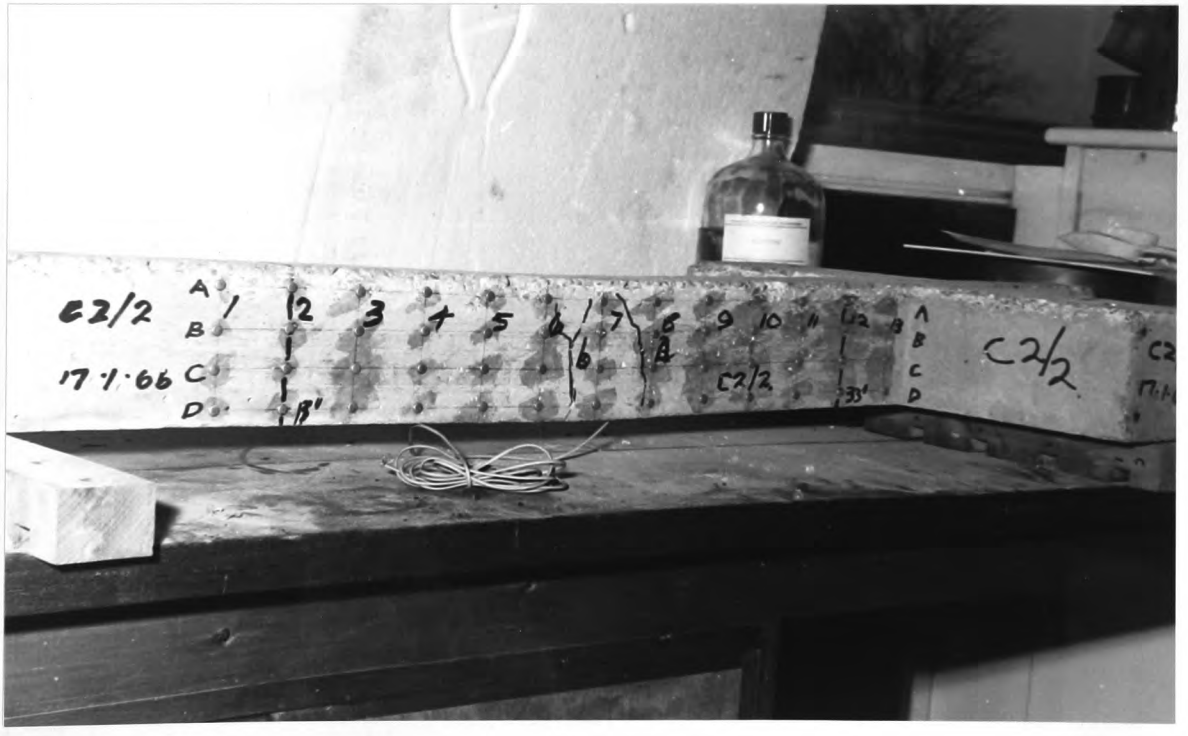
C2/2
17.1.66
A
B
C
D
1 2 3 4 5 6 7 8 9 10 11 12
C2/2
C2/2

FIG. 9.7:-

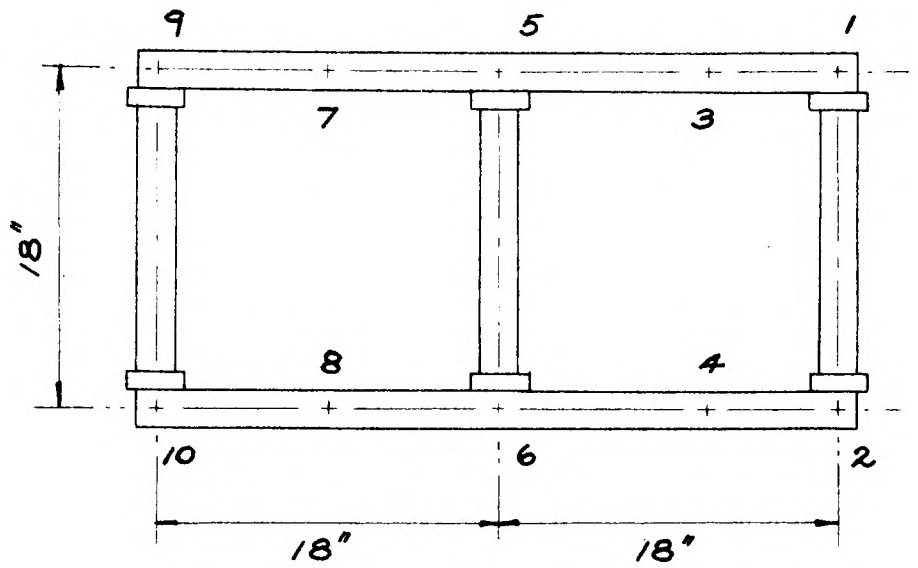

plan

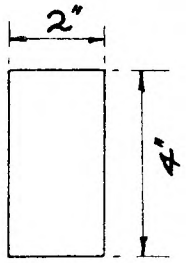

section

PL. 20.7.

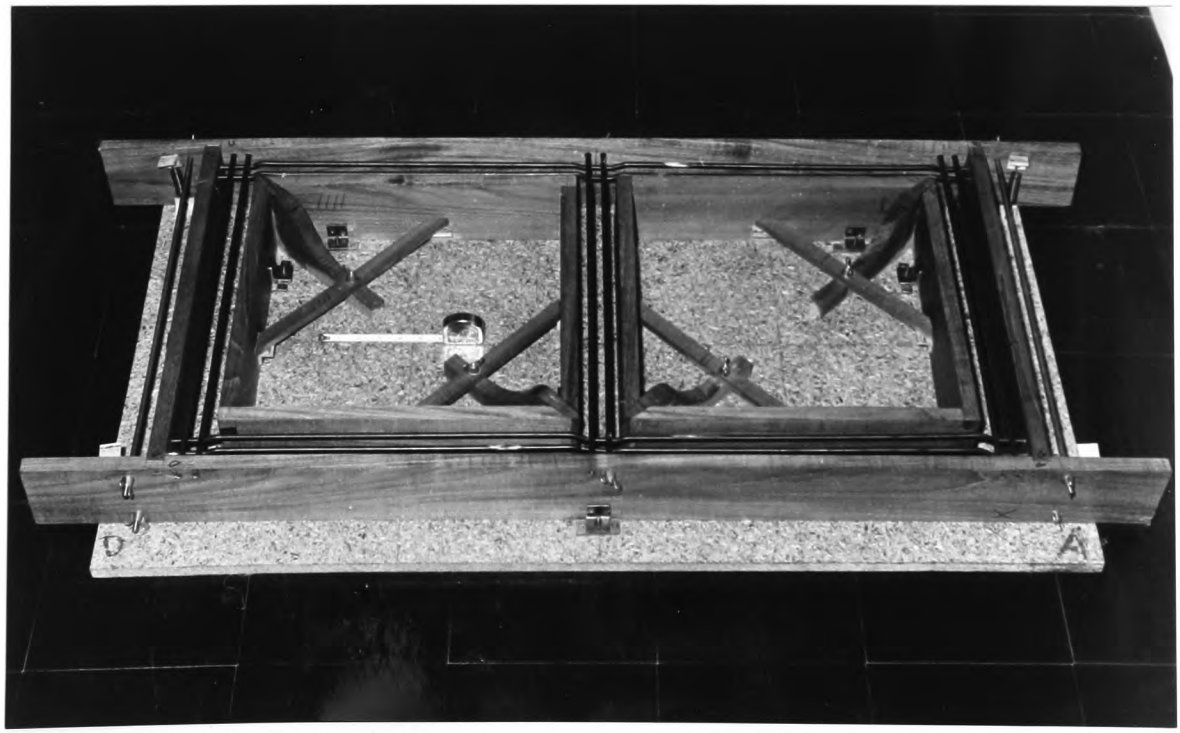

(b) Materials:- 1. Concrete:- The method of mix design used for Series C and D was repeated for Series B with adjusted weights of the various materials to give the extra volume of concrete required. The details are given in Tables 4.7 and 5.7.

Table 4.7:-

cement:- 30 lbs. w/c = 0.55 water:- 16.5 lbs. a/c = 4.05 aggregate:- 121.5 lbs.			
No.	B.S. Sieve	Weight lbs.	Weight %
1	3/8" - 3/16"	48.5	39.90
2	3/16" - no.7	17.0	14.00
3	no.7 - no.14	11.0	9.05
4	no.14 - no.25	11.0	9.05
5	no.25 - no.52	17.0	14.00
6	no.52 - no.100	13.5	11.12
7	no. 100	3.5	2.88
Total	-	121.5	100.00

Table 5.7:-

Beam No.	Cube strength lbs/ins^2	Split.Loads Tons	E_T lbs/ins^2 x 10^6	E_C lbs/ins^2 x 10^6	Mod. of Rupture lbs/ins^2
B/2/1	6,200	-	0.555	-	743
B/2/2	6,440	25.0	0.242	-	598
B/2/3	6,400	22.65	0.294	3.337	604.8
B/2/4	6,030	25.75	0.412	3.269	598.5

2. Steel:- The requirement for the properties of the steel are as for Series C and D, but due to there being reinforcement in the transverse beams, the longitudinal bars were bent up to pass over the transverse bars at the joints, as shown in Plate 20.7, in order to retain equal moments of resistance in all members of the grid.

(c) Testing Procedure:- The testing procedure was different from the procedure used for Series C and D as only the bending moment was applied directly to the grid-frame, the torsion moment being applied internally by the moments of resistance of the members of the frame acting in different planes at the joints. Thus, the torsion moment is transmitted by the transverse beam into the longitudinal beam as simulated by the loading arms in Series C and D but without applying the load directly.

The loading frame, shown in Plate 21.7, was designed to apply a direct compressive load of up to 20 tons on to the grid-frame by Losenhausenwerk hydraulic jacks, and the cross-beam and uprights designed to give variable positioning of the jack. For tests B/2/1 and 2, the load was applied at the central joint on one side of the frame, and for tests B/2/3 and 4 the load was applied equally to the same joint and at a point six inches along the transverse beam. The frame was supported at the four corners on two inch square metal plates seated on one inch spherical ball-bearings (Plate 22.7).

"Demec" readings were taken to give strain measurements along the outer face of the longitudinal beam subjected to the applied bending, similar to the procedure for Series C and D, and in addition, readings were taken along the central transverse beam. The general layout is shown in Fig. 10.7. The spacing

Plate 21.7

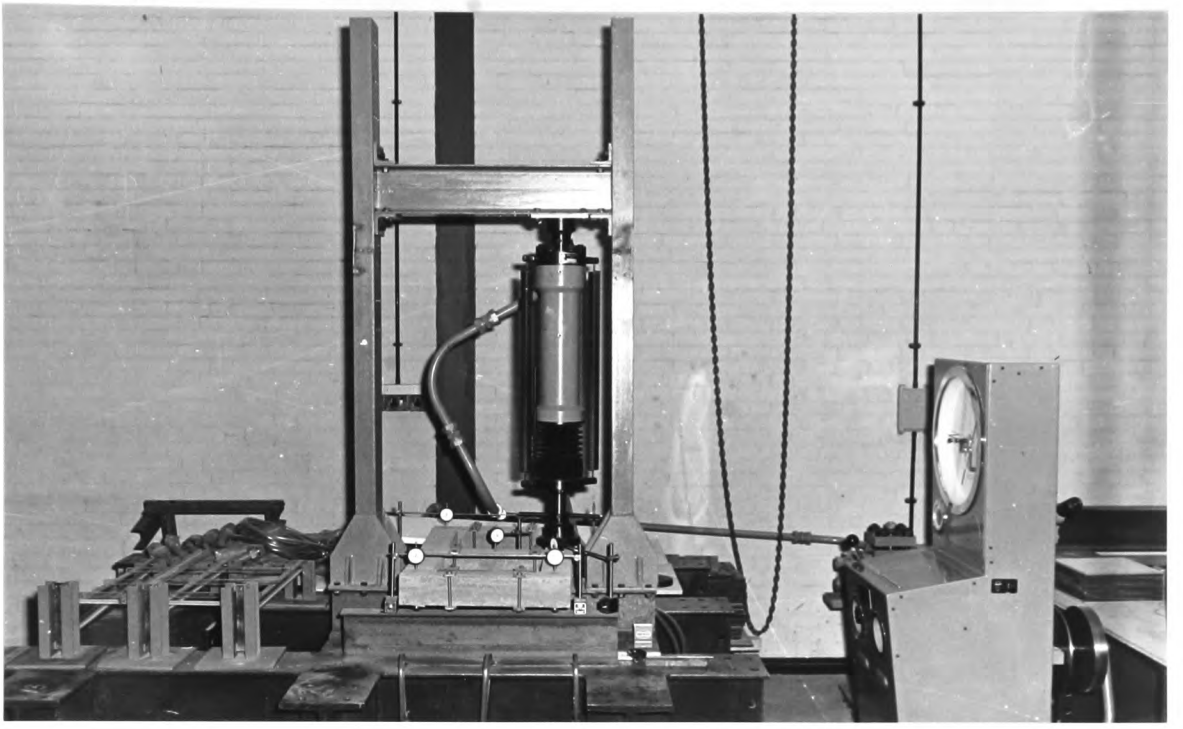

Plate 22.7

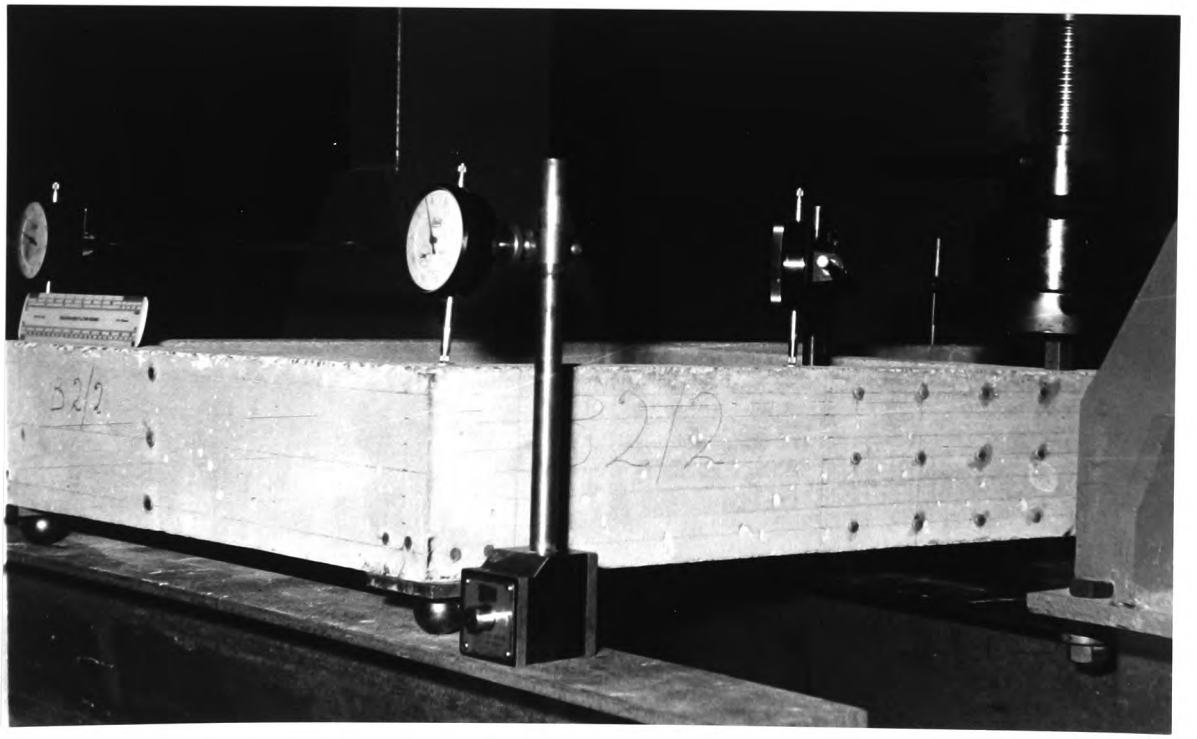

of the discs at two inch gauge and using an eight inch "Demec" gave information on crack initiation as in Series C and D. However, for this Series of tests, the main failure crack formed under the point of application of the load. "Demec" discs were placed at some supports and the unloaded joint to locate the subsidiary cracking (Plates 23.7, 24.7). Dial gauge readings were of greater importance in this Series with regard to the theoretical investigation to be outlined in Chapter 8, and discs were fixed to the upper surface of the frame at the locations numbered in Fig. 9.7. As the load-system in this Series does not produce a region of zero shear stress, clamps were used to prevent shear failure at the joints and the position of these clamps is shown in Fig. 9.7 and Plate 25.7. This technique was also found necessary by Reynolds in his work on pre-stressed concrete frames.(42)

7.6 Summary of Observations:

Each beam was subjected to a different ratio of applied bending to torsion moment so that the cracking behaviour differs for each test. An illustrated summary of the individual crack patterns has been given as developed views in Plates 7 - 18.7. The following observations were made for the four Series as a whole:-

1. The ultimate moment values from tests D/2/1 and D/2/2 have not been used for comparison with the analytical investigation as in both cases premature failure occurred due to bond slip. This non-conformity with the theoretical mechanism of failure has been discussed in Chapter 6 with application to design equation C.

Plate 23.7

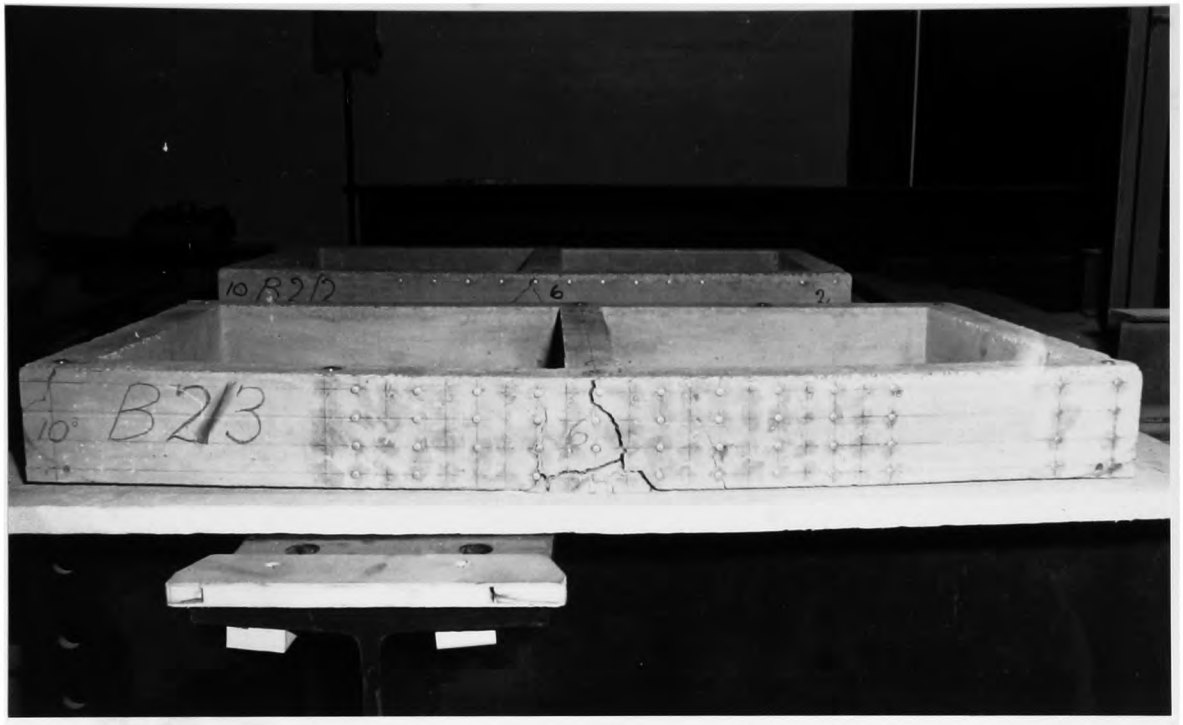

Plate 24.7

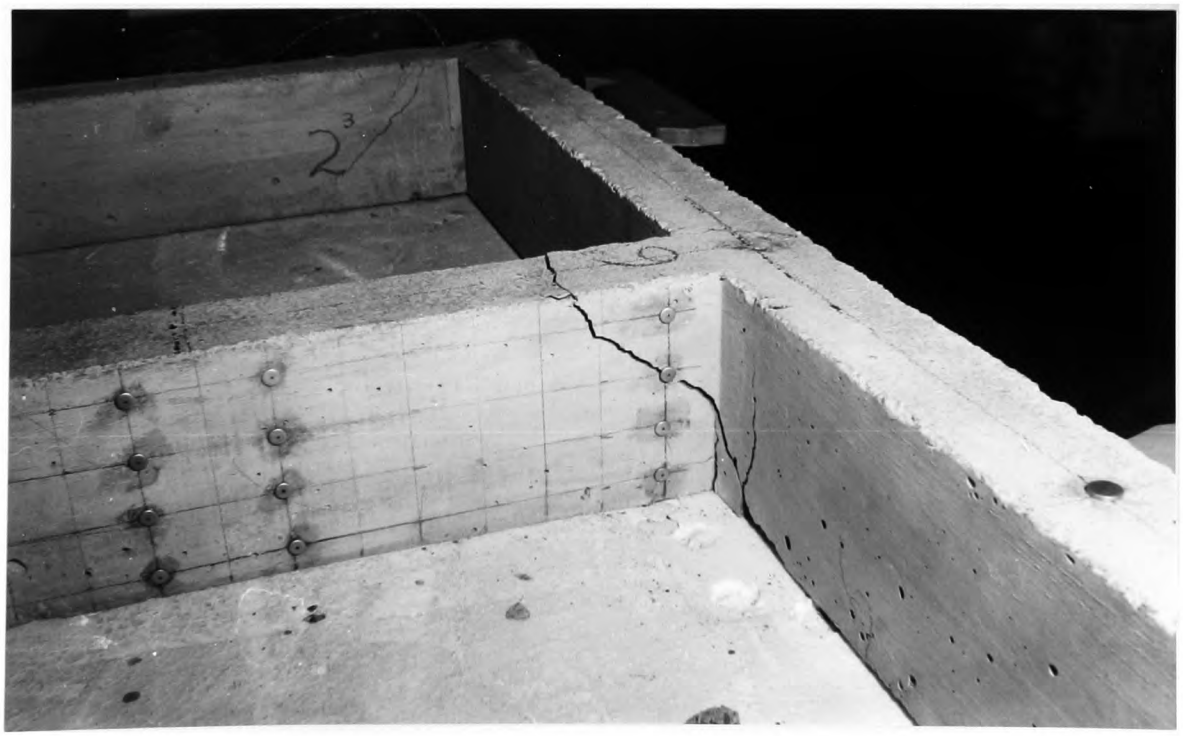

FIG. 10.7 :-

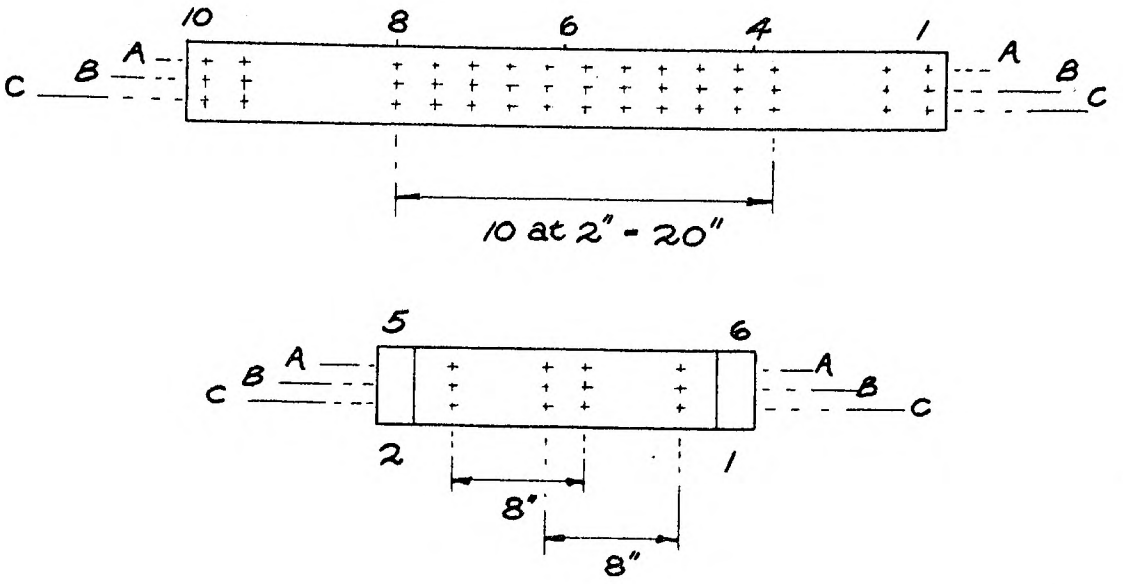

PL. 25.7 :-

2. The addition of a torsion moment produces an increased number of smaller cracks compared to the crack behaviour in a beam stressed only in bending.

3. No general sequence of crack formation was observed, but the initial crack observed does not form the final crack causing failure, the eventual failure crack forming at loads near to ultimate when cracking has already reached the upper parts of the beam elsewhere along the constant moment length.

4. With formation of the failure crack, propogation of the other cracks decreases as the failure crack moves rapidly over the cross section. This observation was confirmed by the "Demec" readings which increased only in the area of the failure crack beyond this stage.

5. The location of the failure crack varied in Series C and D, but for the majority of beams was immediately below one of the loading points for applied bending moment.

6. For the pure torsion case, although cracking occurred along the length of the beam, the main failure crack was located near the bearing support despite closer spacing of the transverse steel in this area.

7. The initial crack in all cases was observed on the same face and at the bottom of the beam. This face was consequently used as the side of the beam for crack observation. Readings of the dial gauges and cathetometer indicated that the torsion moment was applied symmetrically.

8. There is good agreement between practical values of α, measured from the beam, and theoretical values obtained from Fig. 5.4. These results are tabulated in Table 3.7, and the practical values given are the average of the mean line following the crack.

9. There was no sudden failure in the Series of tests, and a combined load of 75% ultimate was resisted by the beam for a period of up to 48 hours. In the test for beam C/2/3, the bending load was removed immediately after ultimate and prior to removal of the torsion-moment, with resultant rotation of the beam and failure (Plate 5.7).

10. The main failure crack for the four grids tested in Series B occurred under the applied load at the joint and was pyramoidal in shape (Plate 23.7). Increased loading beyond ultimate caused rotation of the beams and some of the corners to lift off the spherical seatings. Subsidiary cracks were less predictable and varied for each beam, occurring at some of the supports and the other central joint. As in Series C and D, no sudden failure occurred and a load of 75% of ultimate was resisted by the grid for up to 48 hours after.

7.7 Conclusions:

The following are the main conclusions for the experimental investigation of model reinforced concrete beams Series A, B, C and D:-

1. The total research programme was not extensive consisting of twenty tests of beams of dimensions not greater than two inches wide by four inches deep, and loading not exceeding two tons. Although these tests simulate practical load applications, the author feels that research on full scale beams would provide more information particularly with regard to the crack behaviour at early stages of loading when the micro-crack propogation in the model beams cannot be detected visually. Also, as crack widths are a criteria in the design for working load, measurement of crack width in the full scale beam could be made in addition

to locating the crack propogation at the various load stages.

2. The Series A tests, on a limited scale, provide a means of simulating the structural unit under consideration, that is, the transverse beam to column to longitudinal beam connection. It is essential for simplification of the problem at this stage to be able to extract the main component from the frame and examine the behaviour of the longitudinal beam.

3. Series C and D form the main part of the investigation to examine the effect of combined bending and torsion on the longitudinal beam with two arms simulating the transverse beam connections. The author feels that the application of the torsion moment through concrete arms, rigidly fixed to the main beam, is a necessary intermediate stage between the direct application by Torsion Machine and the practical application in the grid-frame. All measurements taken are for evaluation of the behaviour of the longitudinal beam to combined loading and no consideration is given to the transverse beam.

4. Series B is a preliminary investigation into the full problem using a simple grid with no fixities at the support and loads applied only at the joint under examination. In this case the effects on the beam system as a whole are considered although the resistance of the longitudinal beam forms the main part of the study.

5. In Series A, B, C and D, the use of uniform, identical beams produced by accurately measured quantities of materials and constant conditions of mixing, curing and preparation enables conclusions to be made on the effects of the variations of applied loading on the beam section.

The experimental investigation therefore forms an important part of the research programme. The assumptions made in the theoretical investigation, and necessary for deriving the various design equations, are examined by test and assessments are made of the accuracies attainable by comparing the experimental moments applied to the beams at ultimate with those calculated using the design equations given in Chapter 5.

CHAPTER 8

GRID-FRAMES.

8.1 General:

The previous Chapters have been concerned with the investigation of a longitudinal reinforced concrete beam subjected to combined bending and torsion and simulating a load condition brought about by other beams framing into the main member as in frame systems. In Chapter 8, it is proposed to first outline a method for solution of the bending and torsion moments in a grid-frame at working-load, and then to consider the application of the theory derived in the earlier parts of the investigation to the beams forming the grid-frame at a stage beyond working-load and up to ultimate.

8.2 Introduction:

The linear elastic analysis of a rigid jointed grid-frame structure loaded at right angles to the plane of the frame has been given by several authors, and in particular by Hendry and Jaeger[60] using a harmonic analysis method of solution and assuming a spread medium for the transverse beams; and by Lightfoot and Sawko[61, 62] using generalised slope-deflection equations. A general procedure, using the latter approach, is given by Livesley[63, 64, 65] for multi-beam systems and it is proposed to use this method for solution of the working-load moments in the reinforced concrete frames investigated experimentally by the author.

Beyond working-load, the method of analysis is related to the formation of plastic hinges and calculation of ultimate load is possible using the Lower and Upper Bound approach of

Greenberg and Prager[66,67] for an assumed mechanism of failure. Reynolds[68] has described this application to prestressed concrete frames on the assumption that joint rotation takes place and that the presence of bending has no effect on the torsion hinge and similarly torsion on the bending hinge.

The application of the expression obtained by the author for the ultimate bending moment of a beam subjected to combined bending and torsion is considered using the ratio of bending moment to torsion moment found from the elastic analysis.

A comparison of results for deflections at working-loads is given using theoretical values obtained by the elastic analysis and the practical values measured in the Series B tests. Finally, conclusions are given on the basis of this preliminary study for the behaviour of grid-frames at both working and ultimate loads.

8.3 Equilibrium Method:

A comprehensive account of the equilibrium method for the analysis of skeletal structures is given by Livesley[69]. It is proposed therefore to outline the application of this method to the grid-frames investigated by the author and indicate the extension of the basic theory to multi-beam systems with rigid joint connections. The main assumption made is that the structure is linear, that is the internal forces are linear functions of the applied loads, and so the principle of superposition can be applied. This method of solution is therefore for working-loads only.

The equilibrium method (or displacement method) considers displacement as the basic unknown and the general procedure is as follows:-

(a) Express the member end-loads in terms of the corresponding end-displacements. (by integration of the differential equation of extension, flexure or torsion.)

(b) Express the member end-displacements in terms of joint displacements using conditions of compatibility.

(c) Substitute the member end loads in equations for joint equilibrium. (gives the load-displacement equations of the structure, one equation per joint, relating a known load to an unknown displacement.)

(d) Solve for the unknown joint displacements.

(e) Use equilibrium equations to find the member end-loads.

This procedure is now applied to the grid-frame using the notation given in Fig. 1.8 and the sign convention defined by Livesley and shown in Fig. 2.8. The beams are assumed to have torsional stiffness, but warping effects are neglected. It is further assumed that there are no forces applied in the plane of the grillage and that no moments are applied about vertical axes, so that the displacement vector at each joint consists of a vertical displacement and rotation about two horizontal axes. In the generalised method given by Livesley, the special condition of supporting the corners of the grillage on spherical rollers is provided for by assuming each corner joint to consist of two nodes, one of which, joint R, is connected to the main structure and the other, joint S, to the support. The stiffness matrices are then formed for the grillage, with zero or null matrices to denote that there is no member connecting the two joints R and S at the supports. This apparent complication is necessary as the method developed by Livesley and adapted by Lightfoot and Sawko is for multi-beam systems making use of a general computer technique

FIG. 1.8 :-

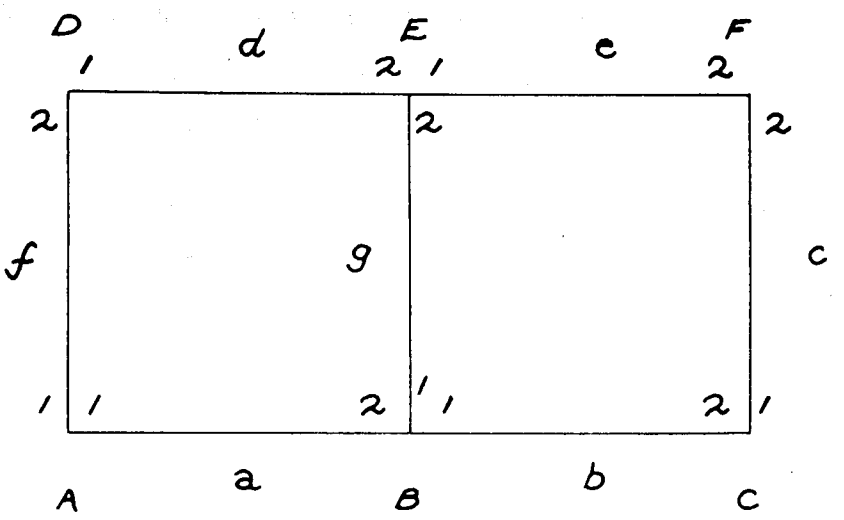

FIG. 2.8 :-

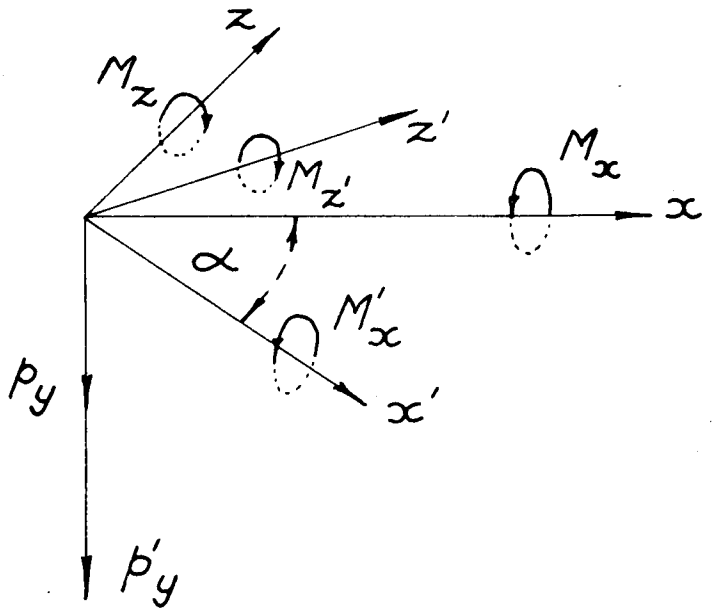

applicable to all conditions. Fixity at the corners, for example, is the most straightforward case with solution of a 3n x 3n, or (6 x 6) matrix for the frame being investigated, where n = number of joints; for the four corners supported on spherical rollers, the size of the matrix increases to (2s + n)3 x (2s + n)3 where s = number of supports and n = number of joints, = (30 x 30) in this case. The load displacement equations are then set up using the following conditions, for example at joint A:-

(i) $\theta_{xS_A} = \theta_{xR_A}$

(ii) $\theta_{zS_A} = \theta_{zR_A}$

(iii) $\delta_{yS_A} = 0$

The resultant matrix is non-symmetric and wasteful of computer storage space, and although the latter may not be important with the objective of a generalised procedure for all structural problems, further mathematical manipulation is required to remove the lack of symmetry.

The author, using the same approach but from first principles for the particular grillage under investigation, obtains the solution using the same conditions but with no imaginary dual node at the supports. The conditions reduce therefore to:-

(i) $\delta_{yA} = 0$

and the size of the matrix to (2s + 3n) x (2s + 3n) or 14 x 14 in this case.

A Computer programme and results for the two load conditions applied in Series B are given in Appendix E. This method can now be used for grillages with any combination of beam system by increasing the size of the matrix, and for any load condition by including the appropriate applied moments and applied loads at

the joints in the right-hand side of the equations. Thus, for B/2/3 and 4 in which the loads are applied at the joint B and six inches along the transverse beam 'g', the values which are substituted are the direct load, consisting of applied load and reaction, at B; the direct load, equal to the reaction, at E, and the fixing moments acting at B and E due to the load applied on the transverse beam and six inches from B.

Each grid-frame is analysed in the same way and a summary of the analysis is now given for the solution of B/2/1 and B/2/2:- The expression relating the unknown displacement vector, 'd', and the known loading condition, 'p', in terms of the stiffness matrix of the beam system is given in Fig. 3.8; the calculations for the matrix are given in Tables 1.8, 2.8 and 3.8, and the final values are included in the general Computer programme in Appendix E.

The solution of the simultaneous equations is obtained on a KDF 9 Computer and these values, which are tabulated in Table 4.8, are now substituted in the equation for each beam member relating end-load to end-displacement. An example of this procedure is given for member 'g':-

(i):- $p_{Eg} = K_{21g} \cdot d_B + K_{22g} \cdot d_E$

$$\begin{vmatrix} M_{Ex} \\ p_{Ey} \\ M_{Ez} \end{vmatrix} = \begin{vmatrix} 1.186 & -0.197 & 0 \\ 0.197 & -0.022 & 0 \\ 0 & 0 & -0.309 \end{vmatrix} \begin{vmatrix} 1.9547 \\ 64.8093 \\ 0 \end{vmatrix} + \begin{vmatrix} 2.372 & 0.197 & 0 \\ 0.197 & 0.022 & 0 \\ 0 & 0 & 0.309 \end{vmatrix} \begin{vmatrix} 1.9547 \\ 23.8636 \\ 0 \end{vmatrix}$$

i.e.,

$$M_{Ex_g} = 2.3183 - 12.7670 + 0 + 4.6365 + 4.7011 + 0 = -1.1112$$

$$p_{Eyg} = 0.3851 + 1.4258 + 0 + 0.3851 + 0.5250 + 0 = -0.1306$$

$$M_{Ez_g} = 0 + 0 + 0 + 0 + 0 + 0 = 0$$

FIG. 3.8

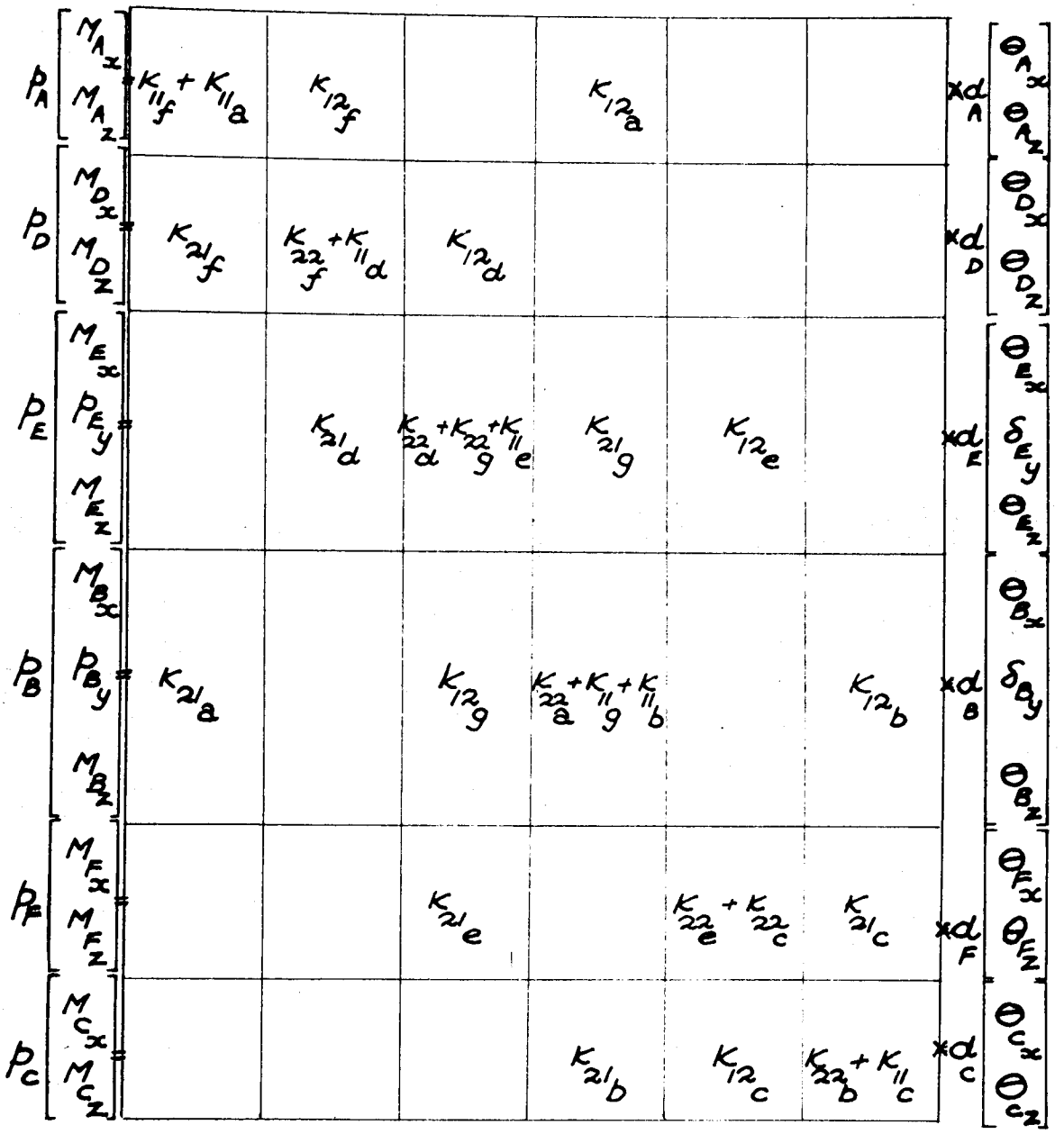

The values for these stiffness-matrices $\times 10^6$ are given in the Computer programmes.

TABLE 1.8:-

$$K_{11} = \begin{bmatrix} \cos^2\alpha \frac{GJ}{L} + \sin^2\alpha \frac{4EI}{L} & -\sin\alpha \frac{6EI}{L^2} & \sin\alpha\cos\alpha\left(\frac{GJ}{L} - \frac{4EI}{L}\right) \\ -\sin\alpha \frac{6EI}{L^2} & \frac{12EI}{L^3} & \cos\alpha \frac{6EI}{L^2} \\ \sin\alpha\cos\alpha\left(\frac{GJ}{L} - \frac{4EI}{L}\right) & \cos^2\alpha \frac{6EI}{L^2} & \sin^2\alpha \frac{GJ}{L} + \cos^2\alpha \frac{4EI}{L} \end{bmatrix}$$

$$K_{12} = \begin{bmatrix} -\cos^2\alpha \frac{GJ}{L} + \sin^2\alpha \frac{2EI}{L} & \sin\alpha \frac{6EI}{L^2} & \sin\alpha\cos\alpha\left(-\frac{GJ}{L} - \frac{2EI}{L}\right) \\ -\sin\alpha \frac{6EI}{L^2} & -\frac{12EI}{L^3} & \cos\alpha \frac{6EI}{L^2} \\ \sin\alpha\cos\alpha\left(-\frac{GJ}{L} - \frac{2EI}{L}\right) & -\cos\alpha \frac{6EI}{L^2} & -\sin^2\alpha \frac{GJ}{L} + \cos^2\alpha \frac{2EI}{L} \end{bmatrix}$$

$$K_{21} = \begin{bmatrix} -\cos^2\alpha \frac{GJ}{L} + \sin^2\alpha \frac{2EI}{L} & -\sin\alpha \frac{6EI}{L^2} & \sin\alpha\cos\alpha\left(-\frac{GJ}{L} - \frac{2EI}{L}\right) \\ \sin\alpha \frac{6EI}{L^2} & -\frac{12EI}{L^3} & -\cos\alpha \frac{6EI}{L^2} \\ \sin\alpha\cos\alpha\left(-\frac{GJ}{L} - \frac{2EI}{L}\right) & \cos\alpha \frac{6EI}{L^2} & -\sin^2\alpha \frac{GJ}{L} + \cos^2\alpha \frac{2EI}{L} \end{bmatrix}$$

$$K_{22} = \begin{bmatrix} \cos^2\alpha \frac{GJ}{L} + \sin^2\alpha \frac{4EI}{L} & \sin\alpha \frac{6EI}{L^2} & \sin\alpha\cos\alpha\left(\frac{GJ}{L} - \frac{4EI}{L}\right) \\ \sin\alpha \frac{6EI}{L^2} & \frac{12EI}{L^3} & -\cos\alpha \frac{6EI}{L^2} \\ \sin\alpha\cos\alpha\left(\frac{GJ}{L} - \frac{4EI}{L}\right) & -\cos\alpha \frac{6EI}{L^2} & \sin^2\alpha \frac{GJ}{L} + \cos^2\alpha \frac{4EI}{L} \end{bmatrix}$$

Table 2.8:-

I $ins.^4$	E $lbs/ins.^2$	J $ins.^4$	G $lbs/ins.^2$	L ins.	L^2 $ins.^2$	L^3 $ins.^3$	μ -
10.666	1×10^6	13.333	0.417×10^6	18	324	5832	0.2

Table 3.8:-

2EI/L lbs ins	4EI/L lbs ins	$6EI/L^2$ lbs	$12EI/L^3$ lbs/ins	GJ/L lbs ins
1.186	2.372	0.197	0.022	0.309

all values $\times 10^6$

Table 4.8:-

Joint	θ_x rads.	δ_y ins.	θ_z rads.
A	0.156	0	5.031
D	0.156	0	2.333
E	1.955	23.864	0
B	1.955	64.809	0
F	0.156	0	-2.333
C	0.156	0	-5.031

all values are for unit load (lb.), $\times 10^{-6}$

(ii) $p_{Bg} = K_{11_g} \cdot d_B + K_{12g} \cdot d_E$

$$\begin{vmatrix} M_{Bxg} \\ p_{Byg} \\ M_{Bzg} \end{vmatrix} = \begin{vmatrix} 2.372 & -0.197 & 0 \\ -0.197 & 0.022 & 0 \\ 0 & 0 & 0.309 \end{vmatrix} \cdot \begin{vmatrix} 1.9547 \\ 64.8093 \\ 0 \end{vmatrix} + \begin{vmatrix} 1.186 & 0.197 & 0 \\ -0.197 & -0.022 & 0 \\ 0 & 0 & -0.309 \end{vmatrix} \cdot \begin{vmatrix} 1.9547 \\ 23.8636 \\ 0 \end{vmatrix}$$

i.e.

$M_{Bx_g} = 4.6365 - 12.7674 + 0 + 2.3183 + 4.7011 + 0 = -1.1112$

$p_{By_g} = -0.3851 + 1.4258 + 0 - 0.3851 - 0.5250 + 0 = 0.1306$

$M_{Bz_g} = 0 + 0 + 0 + 0 + 0 + 0 = 0$

The calculated values for grillages B/2/1 and B/2/2 are given in Figs. 4.8, 5.8, 6.8; and for grillages B/2/3 and B/2/4 in Figs. 7.8, 8.8, 9.8, using the values for displacement vector, 'd', given in Tables 4.8 and 5.8 respectively. All values are calculated for a unit load in pounds and the values used for the elastic constants, G and E, are the average values from the control tests to simplify the amount of calculation; the values for I and J are for a rectangular concrete section and no account is taken of the effect of the reinforcement in this preliminary study.

Assuming the equilibrium theory to be true up to initial cracking of the beam, values of deflection can be compared and the practical and theoretical values, calculated using the measured applied load at cracking, are given for the Series B tests in Table 6.8. These results show a satisfactory correlation, despite the approximations made, and the values of applied load defining initial cracking of the beam are now assumed as the arbitrary limit of working load. Thus, using the values of internal

Table 5.8:-

Joint	θ_x rads.	δ_y ins.	θ_z rads.
A	0.488	0	9.336
D	-0.005	0	5.393
E	1.825	58.754	0
B	4.211	118.591	0
F	-0.005	0	-5.393
C	0.488	0	-9.336

all values are for unit load (lb.), x 10^{-6}

Table 6.8:-

Grillage	Joint Deflection (ins.)			
	3	5	6	8
B/2/1 theory	0.01425	0.0285	0.081	0.0405
practical	0.0092	0.0184	0.0736	0.0368
B/2/2 theory	0.0160	0.0321	0.0871	0.0436
practical	0.0200	0.0401	0.0992	0.0496
B/2/3 theory	0.0250	0.0500	0.1010	0.0505
practical	0.0283	0.0566	0.1142	0.0579
B/2/4 theory	0.0242	0.0483	0.0975	0.04875
practical	0.0216	0.0432	0.1044	0.0522

FIG 4.8

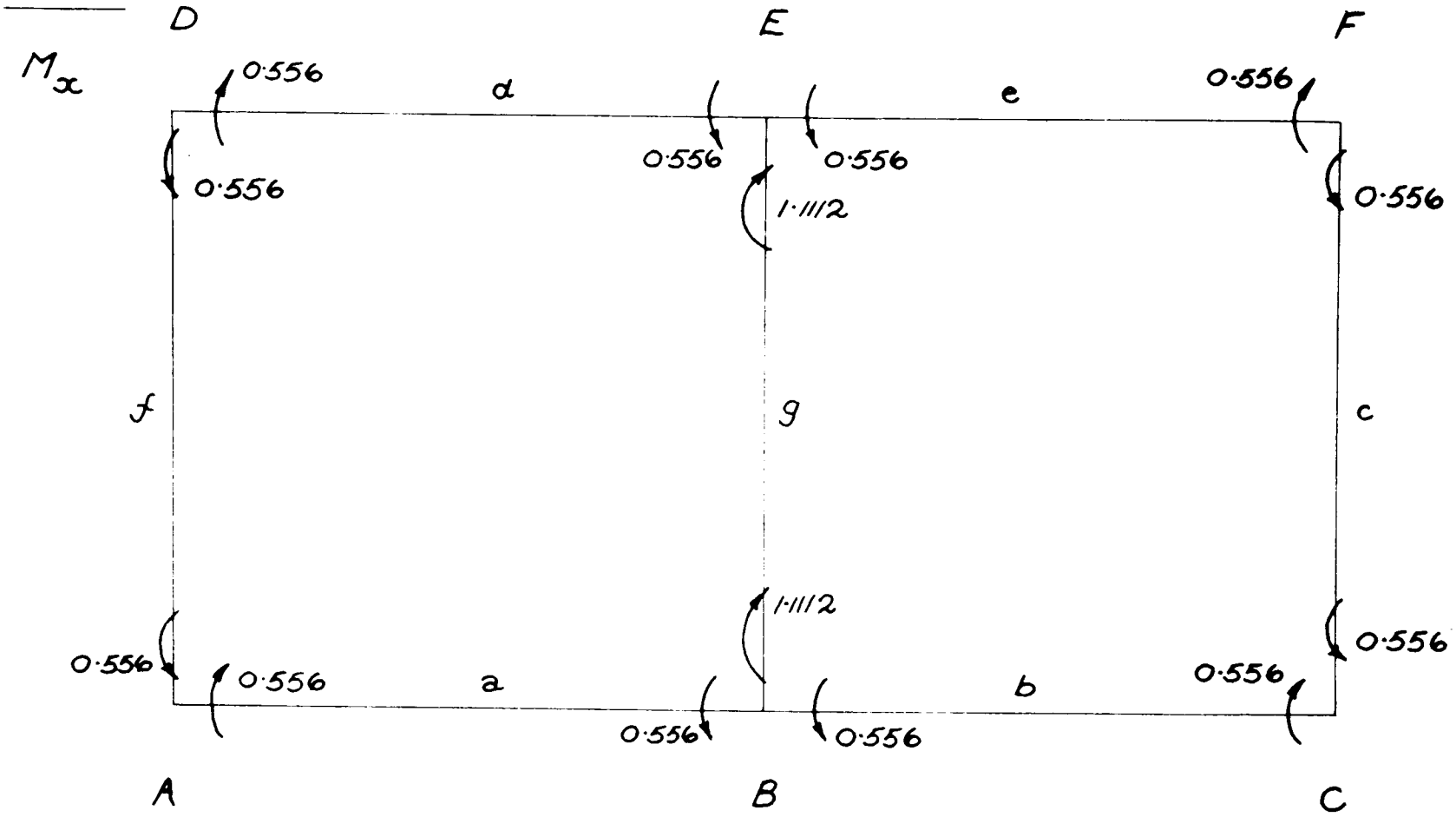
D
E
F
M_x
0·556
d
e
0·556
0·556
0·556
0·556
1·1112
0·556
f
g
c
1·1112
0·556
0·556
0·556
a
b
0·556
0·556
0·556
A
B
C

FIG. 5.8 :

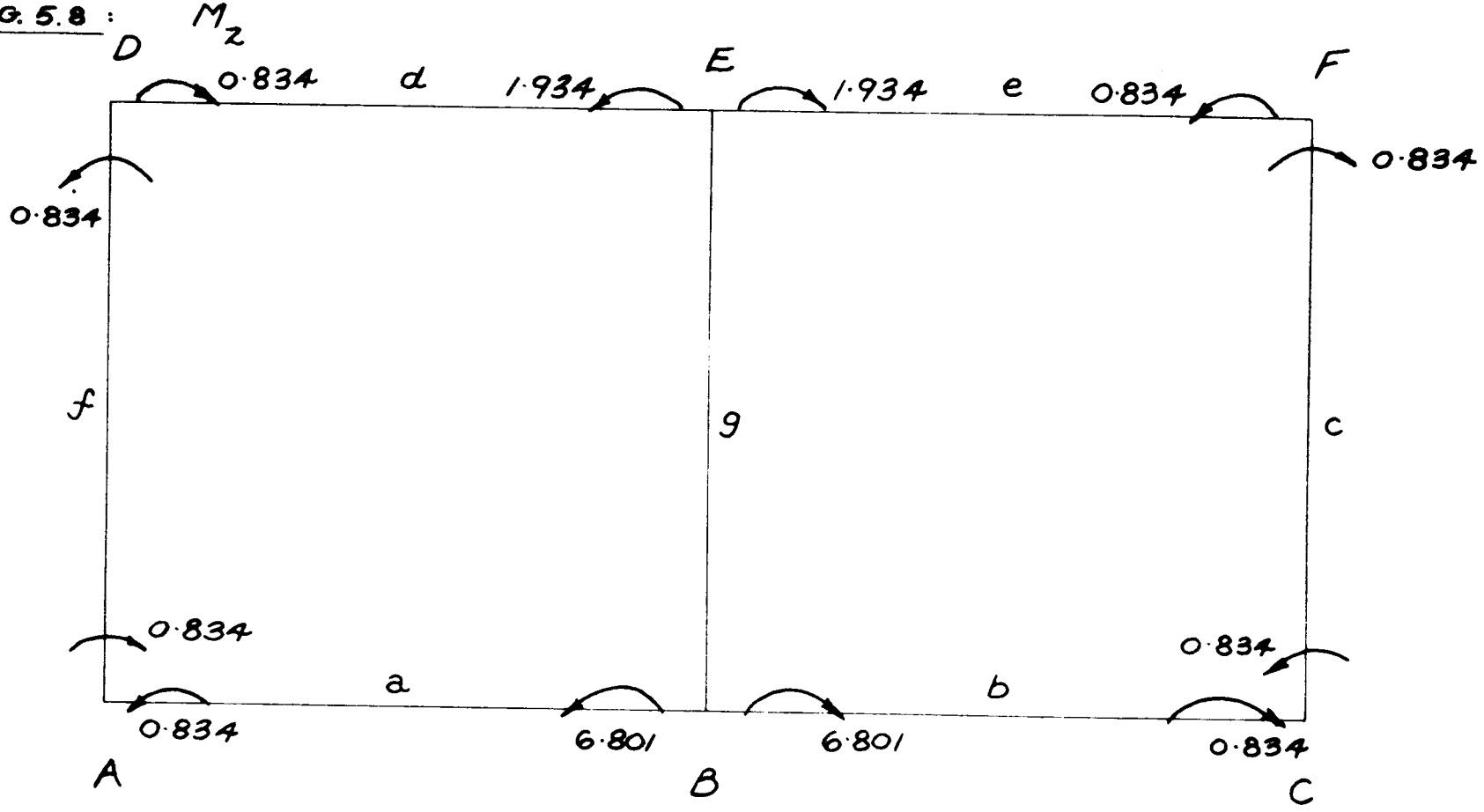
M_z
D
E
F
0·834
d
1·934
1·934
e
0·834
0·834
0·834
f
g
c
0·834
0·834
a
b
0·834
0·834
6·801
6·801
0·834
A
B
C

FIG 6.8 : p_y

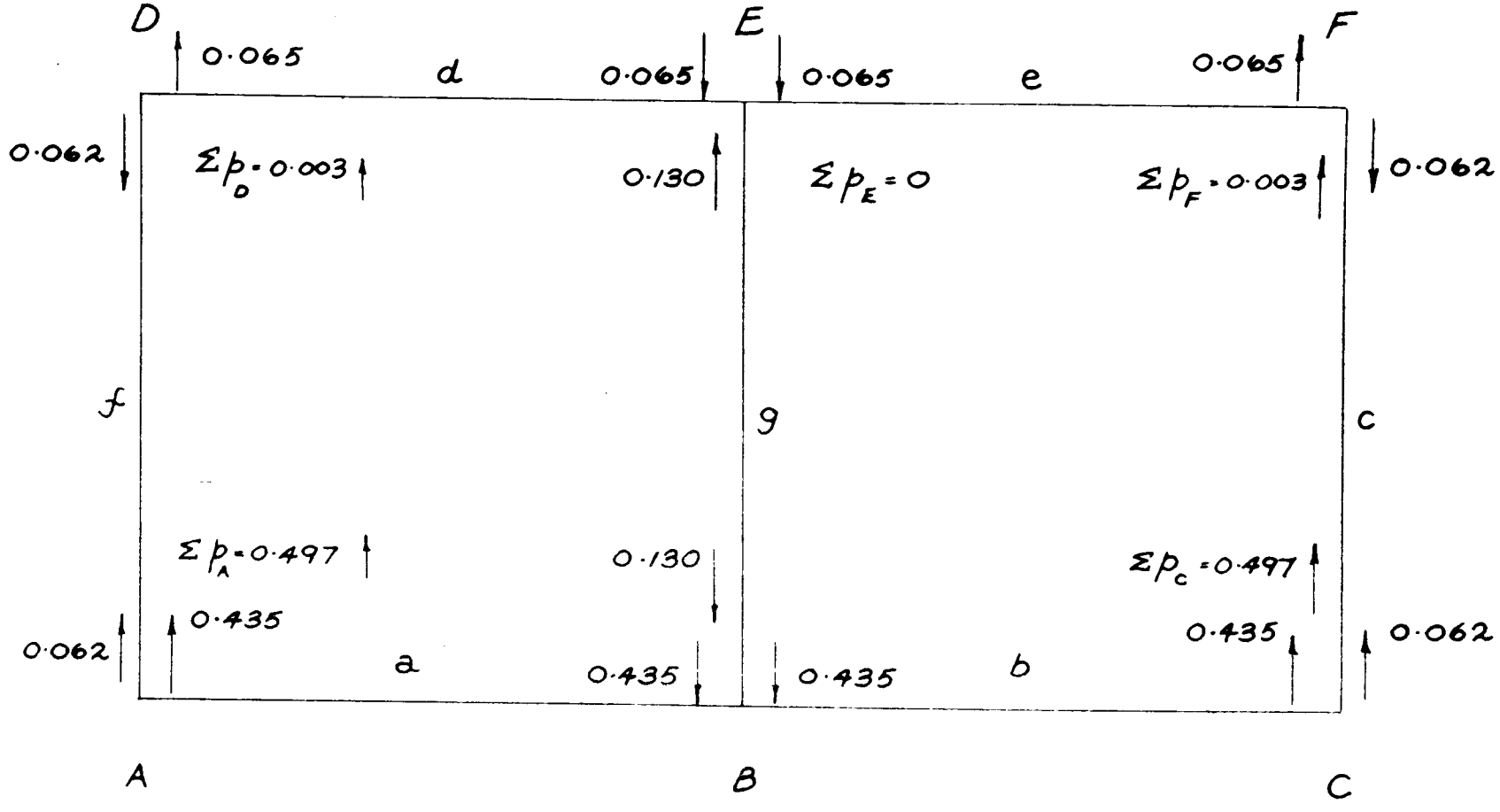

$\Sigma p_B = 0·130 + 0·87 = 1·0$

= applied-load

FIG. 7.8. : M_x

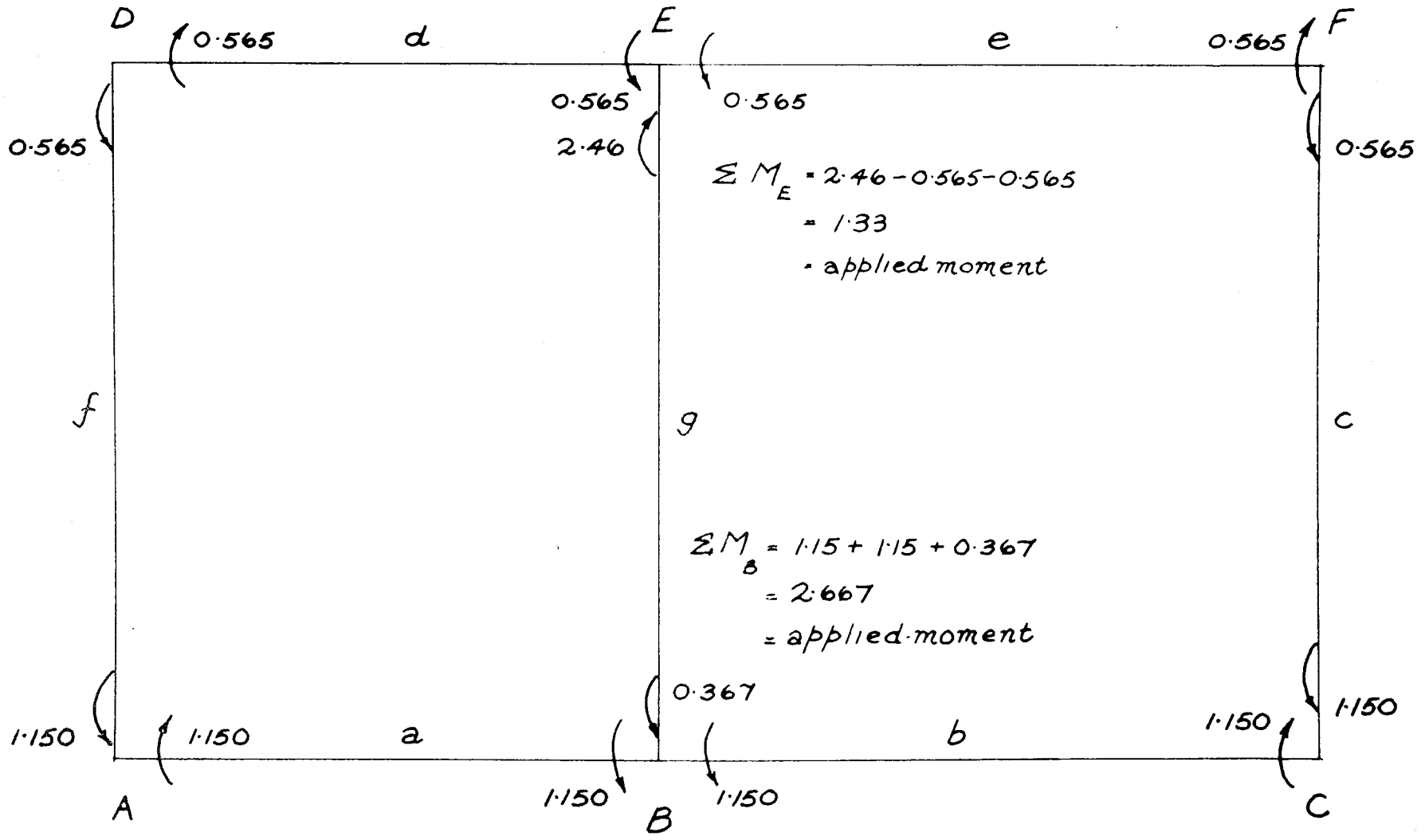
D
E
F
0·565
d
0·565
e
0·565
0·565
0·565
2·46
0·565
ΣM_E = 2·46 − 0·565 − 0·565
= 1·33
= applied moment
f
g
c
ΣM_B = 1·15 + 1·15 + 0·367
= 2·667
= applied moment
0·367
1·150
1·150
1·150
1·150
a
b
1·150
1·150
A
B
C

FIG. 8.8:- M_z

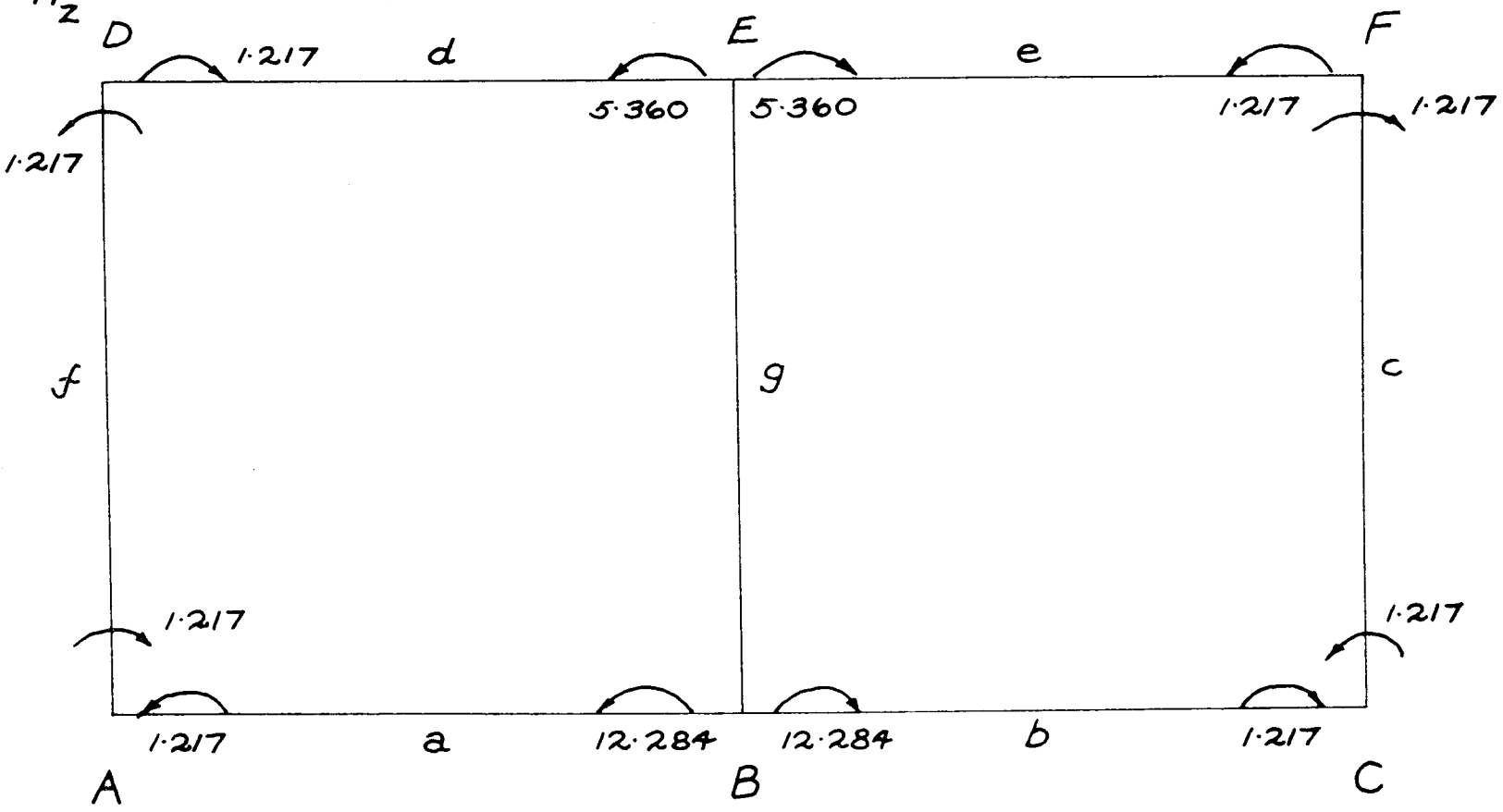
D
E
F
d
e
1·217
5·360
5·360
1·217
1·217
1·217
1·217
f
g
c
1·217
1·217
A
a
B
12·284
12·284
b
1·217
C

FIG. 9.8 :- p_y

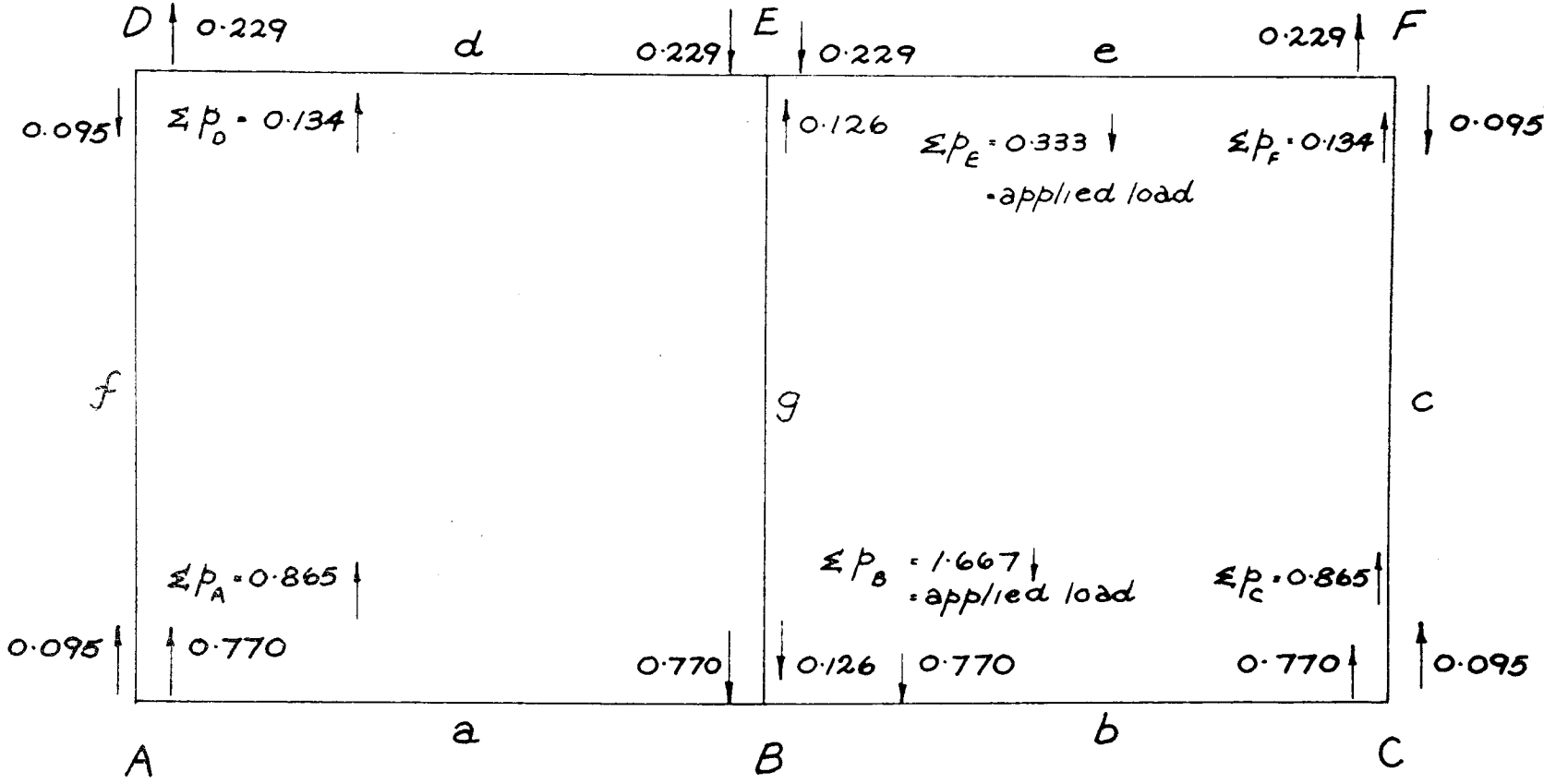

$$\Sigma_V = 2 - (2 \times 0.865 + 2 \times 0.134) = 0$$

bending moment and torsion moment given in Figs. 4-9.8, the beam sections can be designed to Code requirements.

Knowing the position of the maximum moments in the grid-frame, and assuming uniform cross-section, the location of plastic hinges can be specified for investigation of the grid-frame at ultimate load. Also, the application of the theory derived by the author for the failure mechanism in the longitudinal beam of a grid system at the location of the maximum combined moment can be considered, since the ratio of bending moment to torsion moment is also given at working load by the equilibrium method.

8.4 Ultimate Load Method:

An investigation of the behaviour of the grid-frame at ultimate load is now made on the basis of the solution given by the elastic analysis.

The limit-design method described by Greenberg and Prager utilises the formation of plastic hinges so that the ultimate load is calculated from the principle of virtual work by equating the work done by the ultimate load, P_u, in causing rotation of the structure to the work done by the plastic moments, M_p and T_p, acting at the hinges forming the mechanism. This upper bound solution is then used to examine the structure statically for calculation of a lower bound value for P_u. At the same time, the assumed values for M_p and T_p are checked to give a statically admissable system. The method is therefore dependent on an initial assessment of the location of the plastic hinges and the evaluation of the moments M_p and T_p for the beam system.

Reynolds illustrates this approach to prestressed concrete grillages but simplifies the problem by assuming rotation of the transverse beams at the joints. The range of grid-frames

investigated includes multi-beam grillages for both normal and skew systems.

The author's method for calculation of the ultimate bending and torsion moments of the component beams is now examined since evaluation of the ultimate moments is possible using the ratios of bending to torsion moment found from the elastic analysis. In particular, the application of the design equations derived in Chapter 6 can be considered for a failure mechanism occurring at the location of maximum combined moment in the frame and given by the working load solution.

The conclusions given in Chapter 6 suggest the use of Design Equation C as the most flexible of the three expressions, although for this application any one of the equations can be used since the ratio ϕ is taken as M_z/M_x and given by Figs. 4.8, 5.8; and 7.8, 8.8. Applying Design Equation C to grillages B/2/1 and B/2/2, the failure zone is taken at the joint B- this is substantiated by the experimental investigation as reported in Chapter 7.

The revised expression, in terms of $\phi = M_{Bz}/M_{Bx}$, is

$$M_{Bz_u} = \frac{\phi \cdot M_u \cdot T_u}{\sqrt{(T_u \cdot \phi)^2 + (M_u)^2}}$$

or,

for calculation of ultimate torque,

$$M_{Bx_u} = \frac{M_u \cdot T_u}{\sqrt{(T_u \cdot \phi)^2 + (M_u)^2}}$$

where M_u and T_u are, as defined in Chapter 6, the ultimate resistance moments of the beam to pure bending and pure torsion respectively.

For example, for grillage B/2/1, taking the average values of M_u and T_u for the Series, we have

$\phi = M_{Bz}/M_{Bx} = 6.8/0.556 = 12.23$

$M_u = 15.9; \quad T_u = 3.4;$

ultimate moment, $M_{Bz_u} = \dfrac{12.23 \times 15.9 \times 3.4}{\sqrt{(149.6 \times 11.56 + 250)}}$

$= 14.89$

cracking moment, $M_{Bzc} = 6.8 \times 1.255$

$= 8.53$

(all values expressed in inch-pounds x 10^3)

Thus, the design load factor for the grid-frame, using the above values is given as

$$M_{Bz_u}/M_{Bzc} = 14.89/8.53 = 1.63$$

The calculated values for Series B are given in Table 7.8

Table 7.8:-

Grillage	Cracking		Ultimate		Load Factor
	M_{zc}	M_{xc}	M_{zu}	M_{xu}	
B/2/1	8.53	0.69	14.89	1.21	1.63
B/2/2	9.14	0.74	14.89	1.21	1.75
B/2/3	10.42	0.97	15.00	1.40	1.40
B/2/4	10.01	0.94	15.00	1.40	1.49

all values in inch-lbs. x 10^3

8.5 Conclusions:-

Chapter 8 outlines the main application of the author's work to beams as elements of a grid-frame system. The investigation of a grid-frame at ultimate necessarily includes an initial elastic analysis and conclusions are given for a method of solution utilising a Computer to solve the simultaneous equations. Using

this information, the author's ultimate moment equation is applied to the solution at ultimate and preliminary conclusions made on a method for evaluating the design factor of the grid-frame. These conclusions are given as follows:-

1. The Equilibrium method is a well established technique and a powerful tool for the engineer in solving linear elastic problems associated with rigid jointed frames at working load. The method given by Livesley is extremely comprehensive but unnecessarily complicated for grillages, in particular the grid-frames tested by the author. A simpler expression has been used and gives a solution, the deflection values of which compare satisfactorily with values measured experimentally. The corresponding applied loads are then used to evaluate the internal bending and torsion moments for design at working load.

2. The information provided by an elastic analysis is utilised in the analysis of the grid-frame at ultimate load as follows:-

(a) The position of the maximum moment values occurring in the grid-frame indicate the location of potential plastic hinges at ultimate - these positions are required for analysis by the Greenberg-Prager limit design approach.

(b) Using a method of analysis derived by the author, the location in the grid-frame of the maximum combined moments defines the area of beam about which failure will take place. The design equation for ultimate moment is applied to this area using the ratio of bending moment to torsion moment calculated at working load to evaluate the ultimate bending moment of the beam and therefore of the grid system. The ultimate torsion-moment is similarly calculated.

3. A design load factor for the grid-frame is found by comparing the calculated value of ultimate moment to the working load moment given by the elastic analysis.

4. The application of the author's design equation is dependent on the ratio of bending to torsion moment remaining constant, that is, the theory assumes a uniform distributed load increase from working to ultimate load. For example in grillage B/2/1, only continued increase in the applied load at joint B can be considered.

5. The author's theory does not take into account the effects of shear which exists in the grid-frame at all times as shown by the elastic analysis. This, together with other points raised in the investigation are discussed in Chapter 9.

CHAPTER 9

CONCLUSIONS

9.1 Summary:

In Chapter 9 it is proposed to review the main conclusions given in detail in the previous Chapters so that an overall assessment can be made of the experimental and analytical investigation. These conclusions are classified into three main sections as follows:-

1. The study of a reinforced concrete beam during the initial stages of loading to establish a theory for the angle of cracking.

2. The study of a reinforced concrete beam at ultimate load to establish theory for calculating the ultimate bending moment of a beam subjected to a known applied torsion moment, or the ultimate torsion moment for a known applied bending moment, although the latter case is less common in practice.

3. The extension of this investigation to consider the moments in reinforced concrete grillages loaded normally to the plane of the grillage at ultimate. This study includes the analysis of the frame at working load.

Although sections 1 and 2 form the major part of the investigation, the author feels that the main application of these conclusions is to the study of the beam as a member of a frame system and section 3 thus illustrates the practical application of this study.

9.2 General Conclusions:

9.2.1 The following are the general conclusions for section 1, dealing with cracking of a reinforced concrete beam over a range of applied loading up to working load:-

1. The initial angle of crack depends on the following:-

(a) the ratio of applied bending moment to applied torsion moment.

(b) the stress-strain relationship for a rectangular section of plain concrete subjected to pure bending - in this study, a semi-plastic relation is assumed.

(c) the stress-strain relationship for a rectangular section of plain concrete subjected to pure torsion - in this study, a completely plastic relation is assumed.

2. The initial angle of crack is not dependent on the following:-

(a) the dimensions of the beam-section for the range of section investigated in this study, that is for ratios of depth/ breadth between two and one.

(b) whether the beam is hollow or solid

(c) the nature of the steel reinforcement.

3. For the stress-strain relations assumed in this investigation, and over the range of section up to "k" (= d/b) equal to three, the depth of the neutral-axis is constant for all "k" ratios during the stage of loading prior to initial cracking, this being true for both solid and hollow sections.

4. Prior to cracking,

(i) the moment of resistance of the beam to pure bending is defined by

(a) the maximum tensile strength of the concrete

(b) the geometric shape of the section

(ii) the moment of resistance of the beam to pure torsion is defined by

(a) the maximum torsional strength of the concrete

(b) the geometrical shape of the section .

and these statements are true for both solid and hollow sections.

9.2.2 The following are the conclusions for the behaviour of the beam beyond initial cracking:-

1. This investigation is restricted to beams of under-reinforced design; as a result, the position of the neutral-axis at ultimate differs from its position prior to cracking. At the load stage when the longitudinal reinforcement reaches its yield-stress, a condition of constant stress in the steel is assumed (this property having been specially selected for the steel used in the experimental investigation) so that further increase in the moment of resistance of the beam is achieved by increase in the length of the lever-arm with resultant decrease in the value of 'n'.

2. The ultimate stage is defined in this study by the load stage at which the neutral-axis intercepts the vertical side cracks on the front and rear faces of the beam. An expression for the horizontal angle of inclination of the neutral-axis at ultimate is then obtained in terms of (a) the vertical angle of crack

(b) the dimensions of the beam section

(c) the neutral-axis depth at ultimate

3. The mechanism of failure assumed in this study is that given by the Russian Ultimate Equilibrium Theory, whereby rotation in the failure area of the beam takes place about a fulcrum in the compression zone and along the neutral-axis, inclined at an angle to the longitudinal axis of the beam. The author is of the opinion that this mechanism agrees best with the actual behaviour of reinforced concrete beams subjected to combined bending and torsion.

4. The failure of the beam under investigation is caused by the raising of the neutral-axis and eventual crushing of the

concrete on the upper surface of the beam. Two failure schemes are possible and only the case of a horizontal neutral-axis is considered.

5. The theory based upon an exact mathematical analysis using the Principle of Least Work is complicated so that design equations and later modifications are complex and depend on a known value for the ratio of bending moment to torsion moment at ultimate, ϕ. A first simplification made by previous authors is to consider a constant value for 'n' over the section.

6. The author reduces the original equations further by using expressions derived in the first part of the study for the vertical angle of crack and the angle of inclination of the compression fulcrum. Three design equations are derived:-

(a) Design Equation A, obtained by assuming a constant angle of crack up to the neutral-axis depth at ultimate, gives a simplified expression for the transverse steel moment terms, but the equation is dependent on a known value for ϕ.

(b) Design Equation B, derived from A by using a relation between ϕ and α and hence β for a given section, contains no trigonometrical terms but is still dependent on ϕ, and in eliminating α, three equations must be considered over the specified range of ϕ. The assumption that the depth of the neutral-axis at ultimate is negligible compared to the depth of the section permits further simplification and calculations show that this assumption is justified for beams of under-reinforced design.

(c) Design Equation C overcomes the disadvantage of including ϕ in the expression since only one of the applied moments at ultimate need be known. This final expression therefore reflects the original concept of the ultimate equilibrium theory

since it is independent of the values of the applied loadings up to ultimate. The main advantages of this equation are:-

(i) the ϕ value is not used and so the equation is applicable to all loading conditions, including pure bending moment or pure torsion moment.

(ii) the load condition is applied as a final step in the calculation for ultimate moment so that the preliminary calculation may be used for the beam section subjected to a range of applied loadings.

(iii) the form of representation of the design equation as an ellipse allows the use of charts to extend the application to include variations in material properties such as, for example, concrete strength and selection of a moment capacity for in this case a specified mix proportion.

7. The application of the three design equations to the series of experimental investigations considered gives an assessment of the amount of calculation required for each; also, a comparison of results for ultimate moments, between the practical values measured from the tests and those calculated using the design equations, can be made. The following main conclusions are given:-

(a) Results of equal accuracy are obtained from the three design equations. Assuming that the experimental error in any one series of tests is constant (the conclusions are drawn from results in which differences between practical and theoretical values greater that 25% are not included), the assumptions made in progressive derivation of the three equations are valid within the range of accuracy accepted in reinforced concrete design.

(b) The three design equations can be applied to the experimental results considered in this study since both values of moment at ultimate are known. In the practical application to a beam subjected to a known torsion moment at ultimate, only design equation C can be used unless additional assumptions are made with regard to the nature of the load increments up to ultimate.

(c) For the experimental investigation, a check is made that the failure mechanism conforms to that assumed in the theoretical investigation by using design equation C to calculate both the ultimate bending and torsion moments since the ratios of theoretical to practical moments, F_b and F_t, are equal. A large difference therefore indicates a beam failure other than as specified in the theoretical investigation; for example, premature failure due to bond slip of the reinforcement does not satisfy this condition.

(d) The three design equations can be applied only to under-reinforced design sections. The preliminary calculation for design equation C includes evaluating the moments of resistance of the beam subjected to bending load only and to torsion load only so that a check is made at this stage on whether the theory is applicable to the given section.

9.2.3 The application of the theory derived in the main part of the study to grid-frames is discussed in Chapter 8, together with a method for solution of the moments in the frame at working load. The following conclusions are made:-

1. A solution for the elastic behaviour of a rigid jointed frame is necessary before applying existing ultimate load theories to the frame to calculate ultimate moment.

2. The equilibrium method, as outlined by Livesley, and using a Computer for solution of the simultaneous equations, provides an elastic analysis for skeletal structures in general and the application of this method to multi-beam systems is well established.

3. Applying the method to the grid-frames investigated experimentally by the author, the amount of computation is reduced to a minimum and theoretical values are obtained for the internal moments in the beam members. In addition, satisfactory agreement between practical and theoretical deflections at various points along the grid-frame is found at working load.

4. The elastic solution supplies the following information required for an ultimate load analysis:-

(a) Using the Greenberg-Prager limit design method, the position of the plastic hinges can be located more exactly.

(b) For the calculation of ultimate moments using the author's equations, the failure-zone about which the ultimate equilibrium principle is applied is located at the position of maximum combined bending and torsion moments; also, the ratio of the bending and torsion moments at that point is deduced at working load.

5. Using the latter approach, a value for load factor is found for each of the beams tested by comparing the working moment capacity of the beam given by the equilibrium method and the ultimate moment capacity of the beam given by the ultimate equilibrium method. This value thus defines the design factor for the grid-frame as a whole.

6. The author's experimental investigation of reinforced concrete frames is extremely limited and further study is required to investigate the behaviour of the rigid jointed frame loaded at

right angles to its plane at ultimate. Suggestions for future research are therefore given in Section 9.3.

9.3 Future Research:

The author's experimental and analytical investigation, and in particular the extension of the main theory to grid-frames, has raised a number of allied problems which require further study and these are now listed as suggestions for future research.

In the study of the beam behaviour prior to cracking and eventual formation of the failure crack, the author considers that these points are worthy of further study:-

(a) The angle of inclination of the compression fulcrum has not been defined in terms of the stress condition of the concrete in the compression zone. Further study is necessary to examine the compressive strength of the concrete subjected to combined stresses especially towards ultimate. The value of β is of importance for application of the ultimate equilibrium principle to reinforced concrete beams subjected to combined bending and torsion.

(b) A satisfactory theory for representing the combined bending and torsion moments at ultimate load has been developed. A similar theory may define the moment capacity of the beam at working load so that both relations could be represented on the same basis for load factor calculation. Also, the defining of the arbitrary limit of working load by width of crack will require further research on the formation of cracks in full scale beams.

The effects of shear have not been considered by the author. Morice and Lewis[70] have indicated that shear effects can be neglected for investigating the ultimate strength of prestressed concrete beams.

The author, however, is of the opinion that more research into the problem in reinforced concrete beams is required. As indicated in Chapter 8, shear effects are appreciable and cannot be eliminated as was possible in the Series C and D tests carried out by the author.

Finally, the problem of combined bending and torsion in grid-frames with rigid joints has only been introduced by the author. No attempt is made to assess accurately the stiffness property of the reinforced elements of the frame; only approximate values are used in the elastic analysis for G, J, I and E; and the effect of variable rigidity of the beams has not been investigated.

The final conclusion, therefore, is that only a preliminary study has been made into a problem which the author feels is an extremely interesting and worthwhile field of research.

ACKNOWLEDGEMENTS

The author wishes to express his appreciation to Professor A. W. Hendry for providing the opportunity and facilities for carrying out this research; to Dr. S. R. Davies for his supervision and enthusiasm throughout; to Mr. R. S. Elder and his technical staff for general assistance in the experimental investigation and to Mrs. M. Marshall for secretarial work and Miss Pauline Anderson for photographic work.

REFERENCES

1. G.P. FISHER, P. ZIA — Review of code requirements for torsion design, J. Am. Concr. Inst. 6, 1, 1966.

2. R.E. ROWE, W.B. CRANSTON, B.C. BEST — New concepts in the design of structural concrete, Struct. Engr., 43, 12, 1965.

3. Discussion on above paper, Struct. Engr., 44, 4, 1966.

4. Further Discussion on above paper, Struct. Engr., 44, 11, 1966.

5. N.N. LESSIG — Determination of the load-carrying capacity of reinforced concrete elements with rectangular cross-section under simultaneous action of flexure and torsion, P.C.A. Foreign Lit. Study No. 348, 1959.

6. YU. V. CHINENKOV — Study of the behaviour of reinforced concrete elements in combined flexure and torsion, P.C.A. Foreign Lit. Study No. 370, 1959.

7. S. TIMOSHENKO — Strength of Materials, Part 1, Van Nostrand, New York, 1956.

8. E. MORSCH — Der Eisenbetonbau, (translated by E.P. Goodrich), Engineering News Publ. Coy., New York, 1909.

9. P. ANDERSEN — Experiments with concrete in torsion, Proc. Am. Soc. civ. Engrs., 60, 5,6,8,10, 1934.

10. W.T. MARSHALL, N.R. TEMBE — Experiments on plain and reinforced concrete in torsion, Struct. Engr., 19, 4, 1941.

11. I. TODHUNTER, K. PEARSON — A History of the Theory of Elasticity and of the Strength of Materials, Vol. 2, Part 1, Cambridge University Press, 1893.

12. A.E. LOVE — A Treatise of a Mathematical Theory of Elasticity, Cambridge University Press, 1934.

13. S. TIMOSHENKO, J.N. GOODIER — Theory of Elasticity, McGraw-Hill, New York, 1951.

14. L PRANDTL — Membrane Analogy, Phys.Z., 4, 1903.

15. J. PRESCOTT — Applied Elasticity, Dover Publications, New York, 1946.

16. C. BACH
O. GRAF
Tests on the resistance of plain and reinforced concrete in torsion, Deutsche Ausschuss, Berlin, 1912.

17. E. RAUSCH
Design of Reinforced Concrete for Torsion and Shear, J.Springer, Berlin, 1929.

18. H.J. COWAN
An elastic theory for torsional strength of rectangular reinforced concrete beams, Mag. Concr. Res., 2, 4, 1950.

19. C.R. YOUNG
W.R. SAGAR
C.A. HUGHES
The torsional strength of rectangular sections of concrete, plain and reinforced, University Toronto Eng. Res. Bull., 3, 1922.

20. T. MIYAMOTO
Torsional strength of reinforced concrete, Conc. constr. Engng., 39, 11, 1927.

21. L. TURNER
V.C. DAVIES
Plain and reinforced concrete in torsion, Proc. Inst. civ. Engrs., Sel. Engr. paper No. 165, 1934.

22. W.T. MARSHALL
The torsional resistance of plastic materials with special reference to concrete, Conc. constr. Engng.,39, 4, 1944.

24. G.C. ERNST
Reinforced concrete in the plastic range, 3. Torsion, Univ. of Nebraska, Lincoln, 1956.

25. H. NYLANDER
Torsion and torsional restraint of concrete structures, Statens Kommitté för Byggnadsforsk[ning], Stockholm, 1945.

26. R.H. EVANS
Extensibility and modulus of rupture of concrete, Struct. Engr., 24, 12, 1944.

27. M.F. KAPLAN
Strains and stresses of concrete at initiation of cracking and near failure, J. Am.Concr. Inst., 60, 7, 1963.

28. S.F. BORG
J.A. GENARO
Advanced Structural Analysis, Van Nostrand, New York, 1959.

29. H.J. COWAN
Reinforced and Prestressed Concrete in Torsion, Arnold, London, 1965.

30. D. FISHER
The strength of concrete in combined bending and torsion, Ph.D. Thesis, University of London, 1950.

31. K.L. RAO
Ultimate strength of concrete sections in bending and torsion by extension of standard theory, Struct. Engr., 22, 7, 1944.

32. N.N. LESSIG — Determination of the load-bearing capacity of reinforced concrete elements with rectangular cross-section subjected to flexure and torsion, P.C.A. Foreign Lit. Study No. 371, 1959.

33. I.M. LYALIN — Experimental studies of the behaviour of reinforced concrete beams with rectangular cross-section subjected to the combined action of transverse shear, flexural and torsion moment, P.C.A. Foreign Lit. Study No. 402, 1959.

34. A.A. GVOZDEV — Design of Reinforced Concrete Structures, P.C.A. Foreign Lit. Study No. 398, 1961.

35. V.K. YUDIN — Determination of the load-bearing capacity of reinforced concrete elements of rectangular cross-section under combined bending and torsion, P.C.A. Foreign Lit. Study No. 377, 1962.

36. S. SARKAR — Study of combined bending, shear and torsion on a hollow reinforced concrete section, Ph.D. Thesis, University of Leeds, 1964.

37. I.B. BOAZ — Combined bending and torsion in concrete beams, M.S. Thesis, Institute of Virginia Polytechnic, 1962.

38. H. GESUND, F.J. SCHUETTE, G.R. BUCHANAN, C.A. GRAY — Ultimate strength in combined bending and torsion of concrete beams containing both longitudinal and transverse reinforcement, J. Am. Concr. Inst., 61, 12, 1964.

39. J.S. REEVES — Combined bending and torsion of prestressed T-beams, TRA/364, Cem. and Concr. Assoc., London, 1962.

40. R.P.M. GARDENER — The behaviour of prestressed concrete I-beams under combined bending and torsion, TRA/329, Cem. and Concr. Assoc. London, 1960.

41. R.E. ROWE — Discussion on Section 1, F.I.P., Third Congress, Berlin, 1958.

42. G.C. REYNOLDS — Strength of prestressed concrete grillage type bridges, M.Sc. Thesis, University of Adelaide, 1960.

43. M.A. GOUDA — Distribution of torsion and bending moments in connected beams and slabs, Ph.D. Thesis, University of London, 1960.

44. A.L.L. BAKER — The Ultimate Load Theory applied to the Design of Reinforced and Prestressed Concrete Frames, Concrete Publications, London, 1956.

45. INSTITUTION RESEARCH COMMITTEE — Ultimate load design of concrete structures, Proc. Inst. civ. Engrs., 21, 1962.

46. Discussion on above paper, Proc. Inst. civ. Engrs., 23, 1962.

47. W.W.L. CHAN — An investigation of the characteristics of plastic hinges in reinforced concrete, Ph.D. Thesis, University of London, 1954.

48. K. POOLOGASOUNDRA-NAYAGAM — An analytical and experimental investigation of the formation and behaviour of plastic hinges in prestressed and reinforced concrete frames, Ph.D. Thesis, University of London, 1959.

49. F.B. SEELY — Advanced Mechanics of Materials, Wiley and Sons, New York, 1932.

50. R.H. EVANS S. SARKAR — A method of ultimate strength design of reinforced beams in combined bending and torsion, Struct. Engr., 43, 10, 1965.

51. H.J. COWAN — The strength of plain and reinforced concrete under the action of combined stresses with particular reference to combined bending and torsion of rectangular sections, Mag. Concr. Res., 5, 14, 1953.

52. B. BRESLER K.S. PISTER — Failure of plain concrete under combined stresses, Proc. Am. Soc. civ. Engrs., 81, 674, 1955.

53. G.C. ERNST — Ultimate torsional properties of rectangular beams, J. Am. Concr. Inst., 29, 4, 1957.

54. H. GESUND L.A. BOSTON — Ultimate strength in combined bending and torsion of concrete beams containing only longitudinal reinforcement, J. Am. Concr. Inst., 61, 11, 1964.

55. J.F. BAKER M.C. HORNE J. HEYMAN — The Steel Skeleton, Vol. 2, Cambridge University Press, 1956.

56. S.S. GILL J.K. BOUCHER — An experimental investigation of plastic collapse of structural members under combined bending and torsion, Struct. Engr., 42, 12, 1956.

57. - - B.S. Code of Practice C.P.114 (1957), The structural use of reinforced concrete in buildings, British Standards Institution, London.

58. J.D. McINTOSH, H.C. ERNTROY — Design of concrete mixes with aggregate of $\frac{3}{8}$" maximum size, Research Report No. 4, Cem. and Concr. Assoc., London, 1955.

59. - - B.S. 1881 (1952) Methods of testing concrete, British Standards Institution, London.

60. A.W. HENDRY, L.G. JAEGER — The Analysis of Grid Frameworks and Related Structures, Prentice-Hall, New Jersey, 1958.

61. E. LIGHTFOOT, F. SAWKO — Structural frame analysis by electronic computer, Engineering, Lond., 187, 4863, 1959.

62. E. LIGHTFOOT, F. SAWKO — The analysis of grid frameworks and floor systems by the electronic computer, Struct. Engr., 38, 3, 1960.

63. R.K. LIVESLEY — Analysis of rigid frames by an electronic digital computer, Engineering, Lond., 176, 4572, 1953.

64. R.K. LIVESLEY, T.M. CHARLTON — Analysis of rigid frames by an electronic digital computer, Engineering, Lond., 177, 4595, 1954.

65. R.K. LIVESLEY — The application of an electronic digital computer to some problems of structural analysis, Struct. Engr., 34, 1, 1956.

66. H.J. GREENBERG, W. PRAGER — Limit design of beams and frames, Proc. Am. Soc. civ. Engrs., 77, Sep. No. 59, 1951.

67. Discussion on above paper, Proc. Am. Soc. civ. Engrs., 78, Sep. No. D-59, 1952.

68. G.C. REYNOLDS — The strength of prestressed concrete grillage bridges, TRA/268, Cem. and Concr. Assoc., London, 1957.

69. R.K. LIVESLEY — Matrix Methods of Structural Analysis, Pergammon Press, London, 1964.

70. P.B. MORICE, H.E.L. LEWIS — The strength of prestressed concrete continuous beams and simple plane frames, Proc. Symp. on the strength of concrete structures, Cem. and Concr. Assoc., London, 1956.

APPENDIX A

ANGLE OF INCLINATION OF COMPRESSION FULCRUM

The problem of evaluating β, the angle of inclination of the compression fulcrum, is now discussed in greater detail than in Chapter 4. The value for this angle is of particular importance in calculations for ultimate moment using the theory outlined in Chapter 5 of this thesis.

The author has adopted a geometric relation for β on the assumption that the inclined neutral-axis intercepts the vertical cracks on the sides of the beam at ultimate so that an expression is derived and given as

$\cot\beta = \cot\alpha(2jk + 1)$ where α = vertical angle of crack, and k = geometric constant = d/b; and for j = 1, $\cot\beta = \cot\alpha(2k+1)$ so that $\cot\beta > \cot\alpha$, and $\beta < \alpha$ since for the rectangular sections considered, k is always greater than unity. This is a necessary condition due to the change in direction of the vertical cracks on the front and back faces of the beam. The relative values of α and β are of particular significance in the expression for the internal moment provided by the vertical transverse steel since the sign of the moment will change, for example in the case of pure torsion, according to the value of β adopted.

The approach used by Evans and Sarkar[50] is based on the same principle as that given for evaluating α, that is by resolving the torsion stress, τ, and the compressive stress in bending, f_c, as shown in Fig. 1.A. to obtain the principal stress, f_p, acting normal to the fulcrum, and hence β. Using this approach, the value of β must lie between 45° and 90°, and for $\tau = f_c$, $\beta = 58.5^\circ$; therefore the two theories agree only for the case of pure bending since $\beta = \alpha = 90^\circ$.

Fig. 1.A

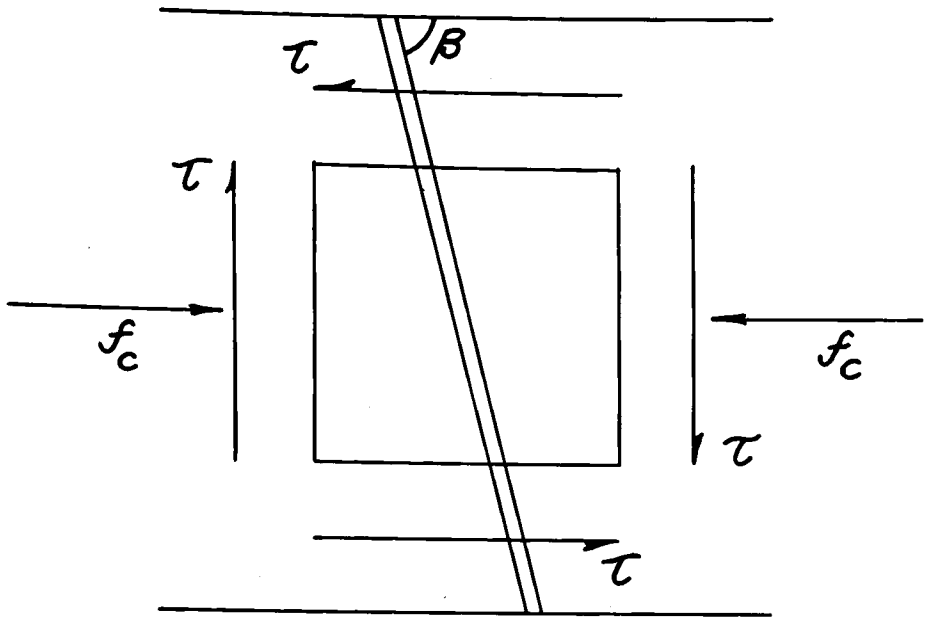

A true value for β will only be found by considering the stress condition in the compression zone at ultimate. Further research is necessary to investigate the condition of stress in the concrete in the compression zone at the stage when the fulcrum is formed.

The results given in Table 1.A and Table 2.A are for selected values of $\beta = 45^{\circ}$, 60° and the geometric expression adopted by the author, applied to calculations of ultimate moment for the Series C and D tests. Significant differences are shown, and for the pure torsion case, D/2/4, as mentioned above, a considerable difference is obtained due to the value of β given by the geometric expression being less than 45°.

Table 1.A:- values are in inch-lbs. x 10^3

Beam	ø	Ultimate Bending Moment, M_b			
		$\beta = 45^\circ$	$\beta = 60^\circ$	$\beta = \cot^{-1}(2k + 1)$	actual
C/2/1	10.92	8.013	6.084	5.746	4.435
C/2/2	11.18	9.473	9.678	9.380	9.240
C/2/3	8.98	11.998	12.298	14.424	13.921
C/2/4	6.03	12.603	13.191	12.746	11.614
C/2/5		-	-	9.778	9.240
C/2/6	3.56	12.683	14.028	11.832	8.911

Table 2.A:- values are in inch-lbs. x 10^3

Beam	ø	Ultimate Bending Moment, M_b			
		$\beta = 45^\circ$	$\beta = 60^\circ$	$\beta = \cot^{-1}(2k + 1)$	actual
D/2/1	6.43	14.067	14.558	14.227	9.913
D/2/2	3.04	15.115	14.197	12.110	5.345
D/2/3	5.96	14.362	14.935	14.475	15.047
D/2/4	0	13.244	-	6.328	4.295
D/2/5	7.08	14.805	15.222	15.045	13.860
D/2/6	4.665	13.761	14.504	13.575	13.399
D/2/2/R	8.08	14.487	14.806	14.713	14.250

APPENDIX B

TORSION MOMENT FACTOR

Appendix B deals with the statement made in Section 5.5, Chapter 5, regarding the torsion moment factor, 'p_t' and defined as

M_t applied (actual) = p_t x M_t applied (as measured).

In the Ellipse Theory, derivation of the ultimate load curve is dependent on the ultimate resistance of the beam to pure bending and pure torsion, or M_u and T_u respectively, and the equation of the curve is given as

$$(x/M_u)^2 + (y/T_u)^2 = 1$$

It is true to say, therefore, that at any intermediate point (x,y) on the curve, the resistance of the beam is defined by the ratio of x, the resistance to the applied bending moment, to y, the resistance to the applied torsion moment. This can now be applied as the Design Equation C in which the substitution of an applied torsion moment, y, given by M_t, into the equation enables calculation of the ultimate resistance bending moment, M_b. As a result, any error in the measurement of the applied torsion moment, M_t, will produce an error in the calculated result, M_b; similarly, for applied bending moment, an error in calculated M_t.

Or, since the beam resists only the effective moments being applied to it, the calculated result is in error when the measured applied and actual applied are not the same.

No definite conclusion can be made from the work covered in this investigation, but it is suggested that the variation in the F_t values are greater than those for F_b in Tables 10 - 16.6, and in particular, in those tests where application of the torsion moment is through loading arms rigidly fixed to the concrete; for example,

compare Series D, Table 12.6, in which the mean values for the Series, excluding beams D/2/1 and D/2/2, are $F_b = 1.05$ and $F_t = 1.28$, and the Russian beams, Table 16.6, in which the torsion load is applied directly to the beam, and the corresponding values are $F_b = 1.00$ and $F_t = 1.01$.

Further research is necessary and is proceeding in this field with the object of investigating the effect of the rigidity of the loading arms.

However, applying the factor 'p_t' to the Design Equation B gives the following modified equations, for $2 < \phi < 8$:-

$$n = \frac{f_L A_L \phi^2 + 0.64(p_t)^2(2k+1)\frac{f_T A_T}{S} b_3}{f'_c b(\phi^2 + 0.64(p_t)^2(2k+1)^2)}$$

$$M_b = \frac{1}{\phi^2 + 0.8 p_t (2k+1)} \left[\begin{array}{l} \left[\frac{1}{2} f'_c b n^2 + f_L A_L (d_1 - n)\right] \phi^2 \\ + 0.32(p_t)^2(2k+1)^2 f'_c b n^2 \\ + 0.64(p_t)^2(2k+1)\frac{f_T A_T}{S} b_3 (d - d_s - n) \\ + 0.64 (p_t)^2 \frac{f_T A_T}{S} d d_3 \end{array} \right]$$

Similarly, expressions are evolved for the whole range of ϕ, and in all cases the effect of p_t on the calculated M_b is dependent on the ϕ-value.

The effect of p_t is more clearly defined in the Ellipse Theory, and the modified expression for T_u is given as,

$$T_u = \frac{1}{(p_t(2k+1))} \left[\begin{array}{l} \frac{(1 + (2k+1)^2)}{2} f'_c b n^2 + f_L A_L (d_1 - n) \\ + (2k+1)\frac{f_T A_T}{S} b_3 (d - d_s - n) \\ + \frac{f_T A_T}{S} d d_3 \end{array} \right]$$

APPENDIX C

CALCULATIONS FOR ULTIMATE MOMENT

Calculations are given in Appendix C for a beam section selected from the Leeds series of tests, beam 5, as given in Tables 1.6, 7.6, 13.6, and in addition, results are given using the original equations[50].

The actual applied moments are, in inch lbs. x 10^3, $M_b = 81.5$; $M_t = 13.2$; so that $\phi = 6.17$, and $\phi^2 = 38.118$

(i) Design Equation 1 (original equation):-

The working details are given in Fig. 1.C

Fig. 1.C

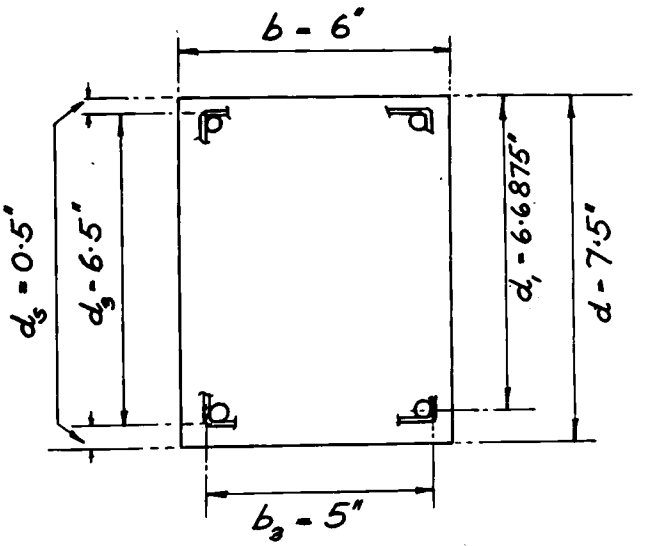

$f'_c = 5.056$; $f'_c b = 30.336$

$f_L.A_L = 12.98$ $\quad \frac{f_T.A_T}{S} = 0.564$

1. From Fig. 7.4, for $\phi = 6.17$, $\alpha = 83.8^\circ$

$\cot \alpha = 0.109$

2. Assume $\beta = 45^\circ$, then calculate $n = \dfrac{12.98 + 0.564 \times 5 \times 0.109}{2 \times 30.336}$

$= 0.219$ ins.

3. Calculate M_b, using the value of 'n' from '2'.

$$M_b = \frac{6.17}{7.17} \times \Big[\begin{array}{l} 30.336 \times 0.048 \\ + 12.98\ (6.6875 - 0.219) \\ + 0.307\ (7.5 - 0.5 - 0.219) \\ - 0.564 \times 6.5\ (0.6 \times 0.109 + 0.4) \\ \qquad (7.5 \times 0.446 + 6\ (0.109 - 1)) \end{array} \Big]$$

$$= \frac{6.17}{7.17}\ (1.455 + 83.961 + 2.089 + 3.164)$$

$$= \underline{78.066}$$

4. Calculate $M_t = 78.066/6.17 = \underline{12.65}$

(ii) Design Equation 2:-

This equation differs from Design Equation 1 only in the term for the vertical transverse steel, and is included to justify statements made in Section 5.4 of Chapter 4 and used in deriving the Design Equations A, B and C.

$\alpha' = 84.8^\circ$, $\cot\alpha' = 0.091$; $\psi = 52.5^\circ$, $\cot\psi = 0.767$

vertical transverse steel term:-

$$= 0.564 \times 6.5\ (0.6 \times 0.091 + 0.4 \times 0.767)$$
$$(7.5 \times 0.446 + 5\ (-0.891))$$

$$= 2.272$$

3. $M_b = \dfrac{6.17}{7.17} \times 88.777$

$$= \underline{76.437}$$

4. $M_t = 76.437/6.17 = \underline{12.4}$

(iii) Design Equation A:-

The calculation procedure outlined in Section 6.3(a), Chapter 6, is now applied to the same beam section, using equations 'A1' and 'A2'.

1. For $\phi = 6.17$, from Fig. 7.4, $\alpha = 83.8^{\circ}$, $\cot \alpha = 0.109$, $\cot^2 \alpha = 0.012$

2. 'k' for the given beam section $= 1.25$

$$\cot \beta = 0.109 \ (2 \times 1.25 + 1) = 0.382$$

hence,

$$\sin \beta = 0.934, \ \cos \beta = 0.357, \ \text{cosec} \ \beta = 1.07$$

3. Calcuate 'n' from equation 'A2'

$$n = \frac{12.98 \times 0.934 + 0.564 \times 5 \times 0.109 \times 0.357}{30.336 \times 1.07}$$

$$= 0.377 \text{ ins.}$$

4. From equation 'A1', using calculated 'n',

$$M_b = \frac{6.174}{0.357 + 5.767} \left[\begin{array}{l} 15.168 \times 0.142 \times 1.07 \\ + 12.98 \ (6.6875 - 0.377) \ 0.934 \\ + 0.307 \ (7.000 - 0.377) \\ + 0.564 \times 6.5 \times 7.5 \times 0.934 \times 0.012 \end{array} \right]$$

$$= \underline{81.797}$$

5. $M_t = \frac{81.797}{6.17} = \underline{13.26}$

(iv) Design Equation B:-

According to the procedure outlined in section 6.3(b), Chapter 6, and applying the equations given in section 6.3(iv), for the given beam section,

1. Select equations for $k = 1.25$, $\phi > 2, < 8$.

2. Calculate n:-

$$n = \frac{12.98 \times 38.118 + 2.24 \times 0.564 \times 5}{30.336 \ (38.118 + 7.84)}$$

$$= 0.359 \text{ ins.}$$

3. Calculate M_b, using calculated n:-

$$(38.118 + 2.8) \ M_b$$

$$= 15.168 \times 0.129 + 12.98 \ (6.6875 - 0.359) \ 38.118$$

$$+ 3.92 \times 3.914$$

$$+ 2.24 \times 0.564\ (7.500 - 0.500 - 0.359)$$

$$+ 0.64 \times 0.564 \times 7.00 \times 6.50$$

$$M_b = \underline{80.176}$$

4. $M_t = \frac{80.176}{6.17} = \underline{12.9}$

(v) Design Equation C :-

The calculation procedure outlined in general in Section 6.3(c), Chapter 6, is now applied to the beam section using the equations 'C1', 'C2', 'C3' and 'C4',

1. using equations 'C1' and 'C2',

$$n = \frac{12.98}{30.336} = 0.428 \text{ ins}; \quad n^2 = 0.183 \text{ ins}^2.$$

$$M_u = 15.168 \times 0.183 + 12.98\ (6.6875 - 0.4280)$$

$$= 84.024$$

2. for k = 1.25, cot α = 1

$$\cot \beta = 1(2 \times 1.25 + 1) = 3.5$$

$\sin \beta = 0.274$, $\cos \beta = 0.962$, $\text{cosec}\ \beta = 3.649$

using equations C3 and C4

$$n = \frac{12.98 \times 0.274 + 0.564 \times 5 \times 0.962}{30.336 \times 3.649}$$

$$= 0.057 \text{ ins.}$$

$$n^2 = 0.003 \text{ ins}^2.$$

$$T_u = \frac{1}{3.5}\Big[\ 6.625 \times 30.336 \times 0.003 + 12.98\ (6.6875 - 0.057)$$
$$+ 3.5 \times 0.564 \times 5\ (7.5 - 0.5 - 0.057)$$
$$+ 0.564 \times 7.5 \times 6\ \Big]$$

$$= 51.594$$

3. Applying the load condition,

$$M_t = 51.594 \sqrt{1 - (81.5/84.024)^2}$$

$$= \underline{12.537}$$

$$M_b = 84.024 \sqrt{1 - (13.2/51.594)^2}$$

$$= \underline{81.251}$$

or, alternatively, using the graphical construction, and an ellipse of equation,

$$x^2/(84.024)^2 + y^2/(51.594)^2 = 1$$

for, M_t = 13.2, M_b = 81.251

and for M_b = 81.5, M_t = 12.537

The latter application is general for any applied M_t, or M_b, for beam 5.

With reference to comments made in Chapter 6 and Fig. 1.6, the results for beam 5 are given below in the same form, where M_b = 81.5, M_b' = 81.251, M_t = 13.2, M_t' = 12.537.

Fig. 2.C:

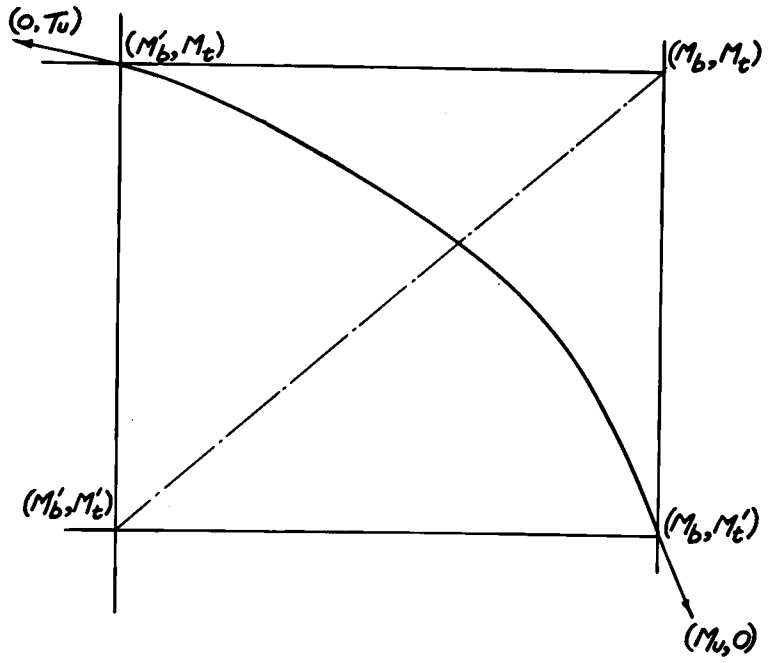

The results given for Design Equation C (81.251, 12.537) are for both M_t and M_b known respectively, so that both design equations are used. The final results now involve the errors in the substituted values so that the result does not lie on the ellipse as explained in Chapter 6. The values are however comparable with those given by the other design equations, as

shown in Table 1.C.

Table 1.C - summary of results.

M_b actual = 81.5		M_t actual = 13.2	
Design Equation	n	M_b	M_t
1	0.219*	78.066	12.65
2	0.219*	76.437	12.40
A	0.377**	81.797	13.26
B	0.359***	80.176	12.90
C	-	81.251	12.54

* $\beta = 45^{\circ}$

** $\beta = \cot^{-1}(2k + 1)$

*** $\beta = \cot^{-1}(2k + 1)$ expressed in terms of ϕ.

APPENDIX D

EXPERIMENTAL DATA

Appendix D contains a typical set of data for the series of tests carried out in the experimental investigation and reported on in Chapter 7. The data given is for beam D/2/6, and is representative of the information available for each of the test beams in Series B, C and D.

The large number of calculations and drawings concerned with the control-tests the final results of which are summarised in Tables 2.7 and 4.7 have not been included as these are of a standard form and dealt with by any text-book on concrete-technology[1].

The observations of crack-propogation and "Demec" readings taken for beam D/2/6 are given in Tables 1D and 2D respectively, and reference to this information has been made in Chapter 7. Fig. 1.D illustrates the increase in Demec readings with load and the effect of cracking of the concrete as it reaches the gauge length. Fig. 2.D is a plot of these readings over the constant moment length of the beam to assess the upward movement of the neutral axis. (Figs. 1.D and 2.D are included in the folder-pocket at the end of the thesis). As stated in Chapter 7, only locations 'a', 'e', and 'i' represent true average strain readings, and the remaining data is used to locate more exactly the crack propogation at different points along the beam. Table 1.D and Fig. 1.D thus correlate the sequence of cracking through the load stages up to ultimate.

[1] A.M. NEVILLE Properties of Concrete, Pitman, London, 1963.

Table 3.D gives details of the beam-sections as required for substitution in the various design equations used for calculating the ultimate moments of Series C and D in Chapter 6.

Table 1.D:-

Load stage	Front	Back
1. (D.L)	-	-
2. (T.L)	-	-
3. (0.15^T)	(i) $8\text{-}9^d$-B, i.e. crack in durafix, diagonal between 8 and 9, reaching B	-
4. (0.30^T)	(i) $8\text{-}9^d$, $9\text{-}10^d$ reaching A	
	(ii) $5\text{-}6^d$ reaching B	
	(iii) $0\text{-}1^d$ reaching B	-
	(iv) $12\text{-}13^d$ reaching C	
	(v) $10\text{-}11^d$ reaching C	
5. (0.45^T)	(i) $8\text{-}9\text{-}10^d$ - top of beam	
	(ii) $0\text{-}1^d$ - C/B	
	(iii) $3\text{-}4^d$ - B/A	-
	(iv) 2-3-4 - C/B	
	(v) 13 - C/B	
6. (0.6^T)	(i) 2-3-4 - B	(i) 12-C
	(ii) $10\text{-}11^d$ - B	(ii) 5-4-B
7. (0.75^T)	-	-
8. (0.9^T)	(i) 2-3-4-A	-
9. (1.05^T)	(i) major failure crack, 2-3-4 - top	(i) major failure crack 2-3-4- top

TABLE 2.D :

	LOAD-STAGE 1.				LOAD-STAGE 2				LOAD-STAGE 3			
	A	B	C	D	A	B	C	D	A	B	C	D
a	0	-20·2	-10·1	-20·2	-60·6	-30·3	-40·4	-111·1	-151·5	-20·2	+20·2	0
b	-60·6	-40·4	-10·1	+10·1	-60·6	-60·6	-10·1	+70·7	-131·3	-80·8	+40·4	+2020
c	-151·5	-20·2	-30·3	-60·6	-141·4	-10·1	-30·3	-30·3	-191·9	0	+10·1	+60·6
d	-90·9	-40·4	-20·2	-60·6	-101·0	-20·2	0	0	-151·5	-30·3	+10·1	+10·1
e	-30·3	-30·3	-20·2	-30·3	-20·2	-30·3	-10·1	-10·1	-50·5	-40·4	+90·9	+141·4
f	-10·1	-10·1	-10·1	+30·3	0	0	0	+10·1	+10·1	+70·7	+101·0	+181·8
g	-10·1	-20·2	+70·7	+30·3	0	-50·5	+101·0	+101·0	+30·3	+90·9	+222·2	+212·1
h	+202	+10·1	+10·1	+30·3	+10·1	+10·1	+50·5	+70·7	+10·1	+80·8	+111·1	+232·3
i	+10·1	0	-30·3	+10·1	+30·3	+202	-10·1	+70·7	+50·5	+70·7	+40·4	+101·0

	LOAD-STAGE 4				LOAD-STAGE 5				LOAD-STAGE 6			
	A	B	C	D	A	B	C	D	A	B	C	D
a	-181·8	-30·3	+90·9	+131·3	-232·3	+50·5	+262·6	+6262	-313·1	+141·4	+565·6	+1,141·3
b	-202·0	-60·6	+191·9	+333·3	-222·2	+10·1	+373·7	+7979	-313·1	+121·2	+696·9	+1,373·6
c	-252·5	+40·4	+141·4	+494·9	-262·6	+151·5	+353·5	+292·9	-353·5	+191·9	+686·8	+343·4
d	-202·0	-40·4	+80·8	+262·6	-262·6	-70·7	+90·9	+212·1	-373·7	-131·3	+101·0	+292·9
e	-101·0	-30·3	+292·9	+161·6	-151·5	-40·4	+363·6	+333·3	-242·4	-70·7	+404·0	+484·8
f	0	+111·1	+191·9	+252·5	-60·6	+101·0	+252·5	+424·2	-161·6	+80·8	+262·6	+525·2
g	-40·4	+40·4	+343·4	+333·3	-171·7	+50·5	+404·0	+555·5	-191·9	+90·9	+505·0	+787·8
h	+70·7	+111·1	+282·8	+444·4	-50·5	+101·0	+353·5	+565·6	-151·5	+101·0	+464·6	+787·8
i	+10·1	+141·4	+151·5	+454·5	-70·7	+131·3	+202·0	+464·6	-151·5	+161·6	+404·0	+767·6

TABLE 2D (contin.)

	LOAD STAGE 7				LOAD STAGE 8				LOAD STAGE 9			
	A	B	C	D	A	B	C	D	A	B	C	D
a	-414·1	+282·8	+1,010·0	+1,848·3	-535·3	+666·6	+2,009·9	+4,403·6	-1,373·6	+2,454·3	+6,979·1	+11,393
b	-414·1	+272·7	+1,181·7	+2,171·5	-515·1	+656·5	+2,181·6	+3,807·7	-1,191·8	+2,585·6	+7,302·3	+12,211
c	-424·2	+333·3	+1,141·3	+414·1	-505·0	+696·9	+2,100·8	+454·5	-949·4	+2,706·8	+7,261·9	+434·3
d	-474·7	-171·7	+121·2	+373·7	-545·4	-191·9	+151·5	+444·4	-595·9	-191·9	+791·9	+565·6
e	+343·4	-101·0	+444·4	+656·5	-414·1	-121·2	+505·0	+797·9	-484·8	-131·3	+535·3	+929·2
f	-262·6	+30·3	+303·0	+606·0	-333·3	+10·1	+333·3	+707·0	-373·7	-10·1	+363·6	+7,575
g	-292·9	+40·4	+545·4	+939·3	-363·6	+40·4	+606·0	+1,090·8	-414·1	0	+686·8	+1,2019
h	-252·5	+101·0	+515·1	+909·0	-333·3	+80·8	+565·6	+1,020·1	-404·0	+30·3	+535·3	+979·7
i	-212·1	+202·0	+595·9	+1,100·9	-323·2	+242·4	+828·2	+1,434·2	-353·5	+303·0	+1,060·5	+1,807·9

Table 3.D:-

dimension detail in ins.							in.lbs x 10^3				
Beam	b	b_3	d	d_3	d_s	d_1	$f_L A_L$	$\frac{f_T A_T}{s}$	f'_c b	M_u	T_u
C/2/1	$2\frac{1}{16}$	-	$4\frac{1}{16}$	-	-	-	-	-	-	5.162	-
C/2/2	$2\frac{1}{16}$	-	$4\frac{1}{16}$	-	-	$3\frac{1}{2}$	2.98	-	7.704	10.03	2.41
C/2/3	$2\frac{5}{16}$	-	$3\frac{15}{16}$	-	-	$3\frac{1}{2}$	4.90	-	9.553	15.89	3.42
C/2/4	$2\frac{1}{2}$	-	$3\frac{15}{16}$	-	-	$3\frac{1}{2}$	4.90	-	10.301	15.99	3.42
C/2/5	$2\frac{1}{8}$	-	$3\frac{7}{8}$	-	-	$3\frac{1}{2}$	2.98	-	8.446	9.778	-
C/2/6	$2\frac{3}{8}$	-	$3\frac{15}{16}$	-	-	$3\frac{1}{2}$	4.90	-	9.841	15.62	3.36
D/2/1	$2\frac{1}{8}$	$1\frac{3}{8}$	$3\frac{7}{8}$	$3\frac{1}{8}$	$\frac{5}{16}$	$3\frac{3}{8}$	4.9	0.3	9.922	15.33	5.48
D/2/2	$2\frac{1}{2}$	$1\frac{3}{8}$	$3\frac{15}{16}$	$3\frac{1}{8}$	$\frac{5}{16}$	$3\frac{7}{16}$	4.9	0.3	12.177	15.86	5.58
D/2/3	$2\frac{1}{2}$	$1\frac{3}{8}$	$3\frac{15}{16}$	$3\frac{1}{8}$	$\frac{5}{16}$	$3\frac{7}{16}$	4.9	0.3	12.694	17.12	5.58
D/2/4	$2\frac{3}{8}$	$1\frac{3}{8}$	$3\frac{15}{16}$	$3\frac{1}{8}$	$\frac{5}{16}$	$3\frac{7}{16}$	4.9	0.3	11.172	-	6.15
D/2/5	$2\frac{3}{16}$	$1\frac{3}{8}$	4	$3\frac{1}{8}$	$\frac{5}{16}$	$3\frac{1}{2}$	4.9	0.4	9.399	15.87	6.30
D/2/6	$2\frac{1}{4}$	$1\frac{3}{8}$	$3\frac{15}{16}$	$3\frac{1}{8}$	$\frac{5}{16}$	$3\frac{7}{16}$	4.9	0.4	9.562	15.59	6.58
D/2/2/R	$2\frac{1}{4}$	$1\frac{3}{8}$	$3\frac{7}{8}$	$3\frac{1}{8}$	$\frac{5}{16}$	$3\frac{3}{8}$	4.9	0.4	9.816	15.31	6.21

APPENDIX E

COMPUTER PROGRAMMES

Appendix E lists the computer programmes and results used in the study, and classified as follows:-

1. Torsion theory for a rectangular section

   (a) St. Venant

   Programme 1 - LOV 2, n = 20.

   Programme 2 - LOV 2, n = 40.

   (b) Membrane Theory

   Programme GOODTIM, n = 9.

These programmes have been referred to in Chapter 3.

2. Grid-Frames

   Programme MATRIX SOLVE - B/2/1 and 2.

   Programme MATRIX SOLVE - B/2/3 and 4.

These programmes have been referred to in Chapter 8.

All the above programmes, plus results, are included in the folder-pocket at the end of the thesis.

FIG. 2.D. · μ-strain (compression -ve). BEAM D/2/6. 28·7·66 :-

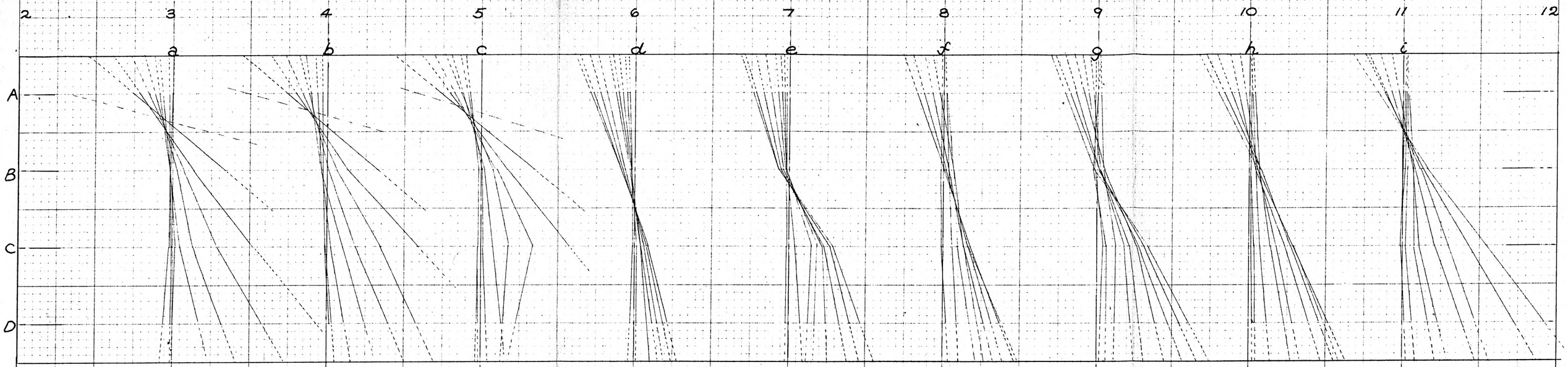

n values (ins)

LOAD STAGE			n_a	n_b	n_c	n_d	n_e	n_f	n_g	n_h	n_i
D.L.	1	-	-	2·9	-	-	-	2·9	1·8	-	2·9
T.L	2	-	-	2·9	-	-	-	2·9	1·8	-	3·0
	3	0·15	1·9	2·2	1·9	2·0	1·8	-	-	-	-
	4	0·30	1·7	1·8	1·3	1·9	1·6	-	-	-	-
	5	0·45	1·3	1·4	1·1	1·9	1·6	0·8	1·2	1·2	0·8
	6	0·60	1·2	1·2	1·1	1·9	1·7	1·1	1·2	1·3	1·0
	7	0·75	1·1	1·1	1·0	1·9	1·7	1·4	1·4	1·2	1·0
	8	0·90	0·9	0·9	0·9	1·9	1·7	1·4	1·4	1·2	1·0
	9	1·05.	0·8	0·8	0·8	1·9	1·7	1·5	1·5	1·3	1·0

FIG. 1.D μ-strain v. LOAD STAGE

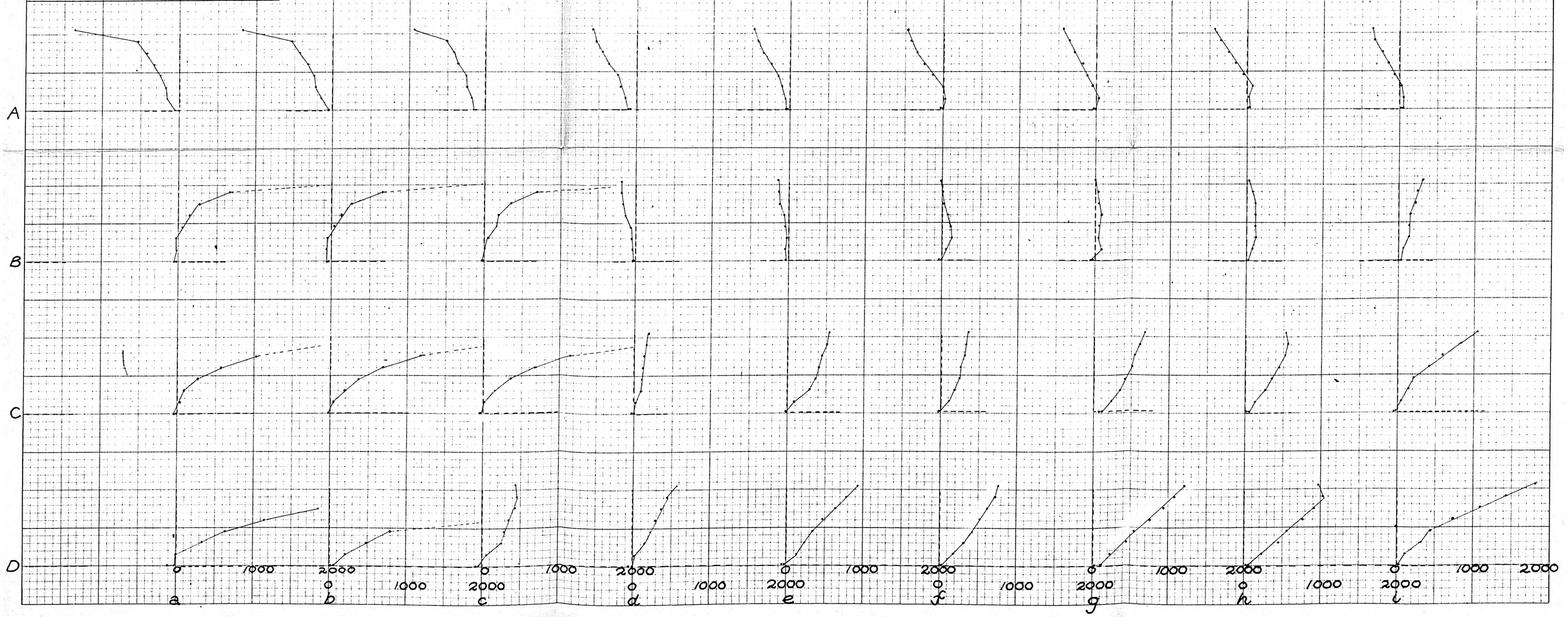

```
12/04/67   22.28.15
EDINBURGH UNIVERSITY ATLAS AUTOCODE    16/01/67

U EDIN. LP/3281   0000 FAIRBAIRN CIVIL ENG, GOOD TIM, n=9
     0   BEGIN
    46   END OF PROGRAM

PROGRAM (+PERM) OCCUPIES 2569 WORDS
PROGRAM DUMPED
COMPILING TIME   34 SEC /  8 SEC
    0.000000       0.000000         0.000000   LARGE
•000000      -0.121332          0.121332      0.000000
•000000      -0.320244          0.320244      0.000000
•000000      -0.715221          0.715221      0.000000
•000000      -1.486744          1.486744      0.000000

    0.440066       0.000000         0.440066   LARGE
•422809      -0.112178          0.437437     -3.769083
•360742      -0.296711          0.467089     -1.215804
•223343      -0.668567          0.704885     -0.334062
•000000      -1.410482          1.410482      0.000000

    0.911775       0.000000         0.911775   LARGE
•879764      -0.086009          0.883958    -10.228709
•763674      -0.228699          0.797184     -3.339206
•497148      -0.528074          0.725272     -0.941436
•000000      -1.214319          1.214319      0.000000

    1.363581       0.000000         1.363581   LARGE
•321592      -0.046631          1.322414    -28.341617
•167989      -0.124680          1.174625     -9.367883
•799167      -0.296791          0.852499     -2.692691
•000000      -0.849397          0.849397      0.000000

    1.779330       0.000000         1.779330   LARGE
07      0.000000         1.733807     LARGE
000000          1.566656     LARGE
    1.156318     LARGE
00     LARGE

0.000000   -0.056299   0.056299   0.000000   0
0.000000   -0.205108   0.205108   0.000000   0
0.000000   -0.483260   0.483260   0.000000   0
0.000000   -1.040244   1.040244   0.000000   0

0.435907   -0.052036   0.439002   -8.376950   0
0.398858   -0.189760   0.441697   -2.101902   0
0.303857   -0.449099   0.542236   -0.676593   0
0.117581   -0.982012   0.989026   -0.119735   0

0.904067   -0.039870   0.904946   -22.675557   0
0.835171   -0.145732   0.847790    -5.730849   0
0.655287   -0.348896   0.742381    -1.878175   0
0.278629   -0.801115   0.848186    -0.347802   0

1.353481   -0.021601   1.353653   -62.659588   1
1.262878   -0.079144   1.265355   -15.956732   1
1.021554   -0.191906   1.039424    -5.323198   0
0.463985   -0.476638   0.665181    -0.973452   0

1.768385   0.000000   1.768385   LARGE   1.7338   0.
1.670050   0.000000   1.670050   LARGE   1.566656   0.000000
1.405790   0.000000   1.405790   LARGE   1.156318   0.000000   0.0000
0.754872   0.000000   0.754872   LARGE   0.000000   0.000000

X0 YJ

X1 Y0      X1 Y1      X1 Y2

X2 Y0      X2 Y1      X2 Y2

STOPPED AT LINE  46
U EDIN. LP/3281   0000 FAIRBAIRN CIVIL ENG, GOOD TIM
```

newlines (5)

```
caption x 0 ≠ yj
newlines(4)
caption x1 ≠ y0; spaces(5); caption x1 ≠ y1; spaces(5); caption x1 ≠ y2
newlines(4)
caption x2 ≠ y0 ; spaces(5); caption x2 ≠ y1 ; spaces(5); caption x2 ≠ y:

end of program
```

4 8 4 8

***Z

1(b). PROGRAM GOODTIM, n = 9

```
***A
JOB
U EDIN, LP/3281   0000 FAIRBAIRN CIVIL ENG, GOOD TIM
COMPUTING 2000 INSTRUCTIONS
OUTPUT
0 LINE PRINTER 2000 LINES
STORE 25 BLOCKS
COMPILER AA


begin
real a,b,k,p,q,cosh,sinh,cosh1,tl,tm,l,m,z,tan,cs,sn,c
integer n,x,y,i,j
read (a,b,i,j)
k=a/b

cycle x=0,1,i
cycle y=0,1,j
tl=0; tm=0
p=x/a; q=y/b
cycle n=1,2,9

c=n*π/2
cosh=½(exp(c*q/k) + exp(-c*q/k))
sinh=½(exp(c*q/k) - exp(-c*q/k))
cosh1=½(exp(c/k)+ exp(-c/k))

sn = sin(c*p)
cs = cos(c*p)
l= (16/(π↑2))(1/(n↑2))((-1)↑((n-1)/2))(1-(cosh/cosh 1))(sn)
m=-(16/(π↑2))(1/(n↑2))((-1)↑((n-1)/2))(sinh/cosh 1)(cs)
tl=tl+l;  tm=tm+m;
z=sq rt((tl↑2)+(tm↑2))
->2  unless tm > -0.000001
tan=4000
-> 8
2: tan=(tl/tm)



8: ->50 unless n=9
print(tl,4,6)
spaces(2)
print(tm,4,6)
spaces(4)
print(z,4,6)
spaces(2)

->4  unless tan<3438
print(tan,4,6)

->6
4: caption $$ large

6: spaces(4)
50: repeat
    repeat

newlines(2)
```

1(a). PROGRAMME 1. - LOV 2, $n = 20$.

```
***A
JOB
CIE   003/00000000/  DR FAIRBAIRN  LOV2 N 20
COMPUTING 2000 INSTRUCTIONS
OUTPUT
0 LINE PRINTER 2000 LINES
STORE 25 BLOCKS


COMPILER AA
begin
real a,b,k,p,q,cosh,sinh,cosh1,tl,l,tm,m,z,tan,cs,sn,c,Tl,s
integer n,x,y,i,j
read (a,b,i,j)
k=a/b

cycle  x=0,1,i
cycle  y=0,1,j

tl=0;  tm=0;
p=x/a;  q=y/b;

cycle  n=0,1,20

c=((2*n+1)(π/2))
sinh=⅓(exp(c*k*p)-exp(-c*k*p))
cosh=½(exp(c*k*p)+exp(-c*k*p))
cosh1=½(exp(c*k)+exp(-c*k))
sn=sin(c*q)
cs=cos(c*q)
s=-(2*q)

l=(16/(π↑2))(((-1)↑n)/(((2*n)+1)↑2))((cosh*sn)/cosh1)
m=(16/(π↑2))(((-1)↑n)/(((2*n)+1)↑2))((sinh*cs)/cosh1)

tl=tl+l;  tm=tm+m;
->2 unless n=20
2:  repeat


Tl=tl+s
print(Tl,4,6)
spaces(2)
print(tm,4,6)
spaces(4)


z=  sq  rt ((Tl↑2) + (tm↑2))
print(z,4,6)
spaces(2)

->3 unless tm=0
tan=4000
->4

3:  tan=Tl/tm
print(tan,4,6)
4: caption $$$ large
```

```
12/04/67   21.53.52
EDINBURGH UNIVERSITY ATLAS AUTOCODE   16/01/67


CIE   003/00000000/  DR FAIRBAIRN  LOV2  n=20.
     0   BEGIN
    47   END OF PROGRAM

PROGRAM (+PERM) OCCUPIES 2541 WORDS
PROGRAM DUMPED
COMPILING TIME   12 SEC /  7 SEC
    0.000000       0.000000         0.000000      LARGE        -0.028149       0.000000         0.028149      LARGE        -0.06
0666       0.000000         0.060666      LARGE        -0.102554       0.000000         0.102554      LARGE        -0.160122
  0.000000         0.160122      LARGE        -0.241630       0.000000         0.241630      LARGE        -0.357609       0.0000
00         0.357609      LARGE        -0.520054       0.000000         0.520054      LARGE        -0.739432       0.000000
  0.739432      LARGE


    0.000000       0.223254         0.223254       0.000000   LARGE        -0.026018       0.221175         0.222700       -0.11
7637   LARGE        -0.056089       0.214626         0.221834      -0.261334   LARGE        -0.094880       0.202650         0.
223762      -0.468197   LARGE        -0.148355       0.183592         0.236041      -0.808069   LARGE        -0.224550       0.
155150         0.272936      -1.447307   LARGE        -0.334284       0.114892         0.353477      -2.909552   LARGE        -
0.491045       0.061952         0.494937      -7.926216   LARGE        -0.708000      -0.000000         0.708000   49600605094
0195564.180612   LARGE


    0.000000       0.450566         0.450566       0.000000   LARGE        -0.019935       0.446712         0.447157       -0.04
4626   LARGE        -0.043005       0.434560         0.436683      -0.098961   LARGE        -0.072866       0.412264         0.
418654      -0.176747   LARGE        -0.114350       0.376516         0.393497      -0.303705   LARGE        -0.174448       0.
322322         0.366502      -0.541222   LARGE        -0.264038       0.243254         0.359010      -1.085443   LARGE        -
0.400596       0.134068         0.422435      -2.988004   LARGE        -0.608125      -0.000000         0.608125   68210716682
22430.162131   LARGE


    0.000000       0.685392         0.685392       0.000000   LARGE        -0.010800       0.680342         0.680428       -0.01
5875   LARGE        -0.023315       0.664397         0.664806      -0.035093   LARGE        -0.039572       0.635041         0.
636272      -0.062314   LARGE        -0.062340       0.587596         0.590894      -0.106093   LARGE        -0.095953       0.
514379         0.523252      -0.186542   LARGE        -0.148394       0.403186         0.429628      -0.368055   LARGE        -
0.238209       0.235604         0.335042      -1.011054   LARGE        -0.416395      -0.000000         0.416395   65534837982
559.110969   LARGE


    0.000000       0.930519         0.930519       0.000000   LARGE         0.000430       0.924405         0.924405       0.00
0466   LARGE        -0.000358       0.906955         0.906955      -0.000394   LARGE        -0.000195       0.875936         0.
875936      -0.000222   LARGE         0.000647       0.823693         0.823693       0.000785   LARGE        -0.000367       0.
742555         0.742555      -0.000494   LARGE        -0.000738       0.619478         0.619479      -0.001192   LARGE
0.002210       0.418082         0.418088       0.005287   LARGE        -0.019296      -0.000000         0.019296   15292394683
.347083   LARGE


X0 YJ

X1 YJ

X1 YJ


STOPPED AT LINE  47
CIE   003/00000000/  DR FAIRBAIRN  LOV2
RUNNING TIME   13 SEC /  9 SEC
```

2. GRID-FRAMES.

```
***A
JOB
CIE  003/00000000/  D R FAIRBAIRN  MATRIX SOLVE  B/2/3 AND B/2/4
EXECUTION 30 SECONDS
COMPILER AA


begin
integer i,j,ctr,r,y
read(r,y)
begin
array A(1:y,1:y),B(1:y),X(1:y)
integer array  PERM (1:y)
routine spec MRLINEQ(array name A,B,X, integer array name PERM, integer n,Q)


comment  r is the number of matrices to be solved c
         y is the size of the matrix
ctr= 1
1: cycle i= 1,1,y
       cycle j= 1,1,y
       read  (A(i,j))
       repeat
repeat
cycle j= 1,1,y
read (B(j))
repeat

MRLINEQ(A,B,X,PERM,y,1)
caption ###### SOLUTION
newlines (2)
cycle i= 1,1,y
newline
print fl (X(i),7)
repeat


ctr= ctr + 1
if  ctr ≥ r then  ->2

-> 1



routine MRLINEQ(array name A,B,X, integer array name PERM, integer n,Q)
real AMAX,CHANGE
integer i,j,jMAX,s
switch ENTER(1:2)
if n>1then ->ENTER(Q)
if  n<0then->2
X(1)=B(1)/A(1,1)
return
2:caption MRLINEQ#data#fauult,n<0;stop
ENTER(1): cycle i=1,1,n-1
AMAX=0; jMAX=0
cycle j=i,1,n
if mod(A(j,i))<AMAX then ->1
AMAX=mod(A(j,i)); jMAX=j
1:repeat
PERM(i)=jMAX
cycle j=i,1,n
CHANGE=A(i,j)
A(i,j)=A(jMAX,j)
A(jMAX,j)=CHANGE
repeat
cycle j=i+1,1,n
A(j,i)=A(j,i)/A(i,i)
cycle s=i+1,1,n
A(j,s)=A(j,s)-A(i,s)*A(j,i)
repeat
repeat
repeat
ENTER(2):cycle i=1,1,n
X(i)=B(i)
repeat
cycle i=1,1,n-1

CHANGE=X(PERM(i))
X(PERM(i))=X(i)
X(i)=CHANGE
cycle j=i+1,1,n
X(j)=X(j)-A(j,i)*X(i)
repeat
repeat
X(n)=X(n)/A(n,n)

cycle i=n-1,-1,1
cycle j=i+1,1,n
X(i)=X(i)-A(i,j)*X(j)
repeat
X(i)=X(i)/A(i,i)
repeat
end
2:  end
end of program

***T

1   14
2.681 0 1.186 0 0 0 0 -0.309 0 0 0 0 0 0
0 2.681 0 -0.309 0 0 0 0 -0.197 1.186 0 0 0 0
1.186 0 2.681 0 -0.309 0 0 0 0 0 0 0 0 0
0 -0.309 0 2.681 0 -0.197 1.186 0 0 0 0 0 0 0
0 0 -0.309 0 2.99 0.197 0 1.186 -0.197 0 -0.309 0 0 0
0 0 0 -0.197 0.197 0.066 0 0.197 -0.022 0 0 0.197 0 0
0 0 0 1.186 0 0 5.053 0 0 -0.309 0 1.186 0 0
-0.309 0 0 0 1.186 0.197 0 2.99 -0.197 0 0 0 -0.309 0
0 -0.197 0 0 -0.197 -0.022 0 -0.197 0.066 0 0 0 0 0.197
0 1.186 0 0 0 0 -0.309 0 0 5.053 0 0 0 1.186
0 0 0 0 -0.309 0 0 0 0 0 2.681 0 1.186 0
0 0 0 0 0 0 0.197 1.186 0 0 0 0 2.681 0 -0.309
0 0 0 0 0 0 0 0 -0.309 0 0 1.186 0 2.681 0
0 0 0 0 0 0 0 0 0 0 0.197 1.186 0 -0.309 0 2.681
0 0 0 0 -1.333 0.333 0 2.667 1.667 0 0 0 0 0


*** Z
```

```
07/04/67   18.53.57
EDINBURGH UNIVERSITY ATLAS AUTOCODE   16/01/67


CIE  003/00000000/  D R FAIRBAIRN  MATRIX SOLVE  B/2/3 AND B/2/4
      0    BEGIN
      3       BEGIN
     27          ROUTINE MRLINEQ
     73          END OF ROUTINE
     74       END OF BLOCK
     75    END OF PROGRAM

PROGRAM (+PERM) OCCUPIES 2682 WORDS
PROGRAM DUMPED
COMPILING TIME    18 SEC /  10 SEC
      SOLUTION


 4.8777899₨ -1
 9.3356956₨  0
-5.4337453₨ -3
 5.3932764₨  0
 1.8250421₨  0
 5.8754538₨  1
-2.7356196₨-12
 4.2112979₨  0
 1.1859126₨  2
 7.9917384₨-12
-5.4337453₨ -3
-5.3932764₨  0
 4.8777899₨ -1
-9.3356956₨  0


STOPPED AT LINE  75
CIE  003/00000000/  D R FAIRBAIRN  MATRIX SOLVE  B/2/3 AND B/2/4.
RUNNING TIME    3 SEC /  2 SEC
```

1 (a). PROGRAMME 2 - LOV 2, $n = 40$.

```
***A
JOB
CIE   003/00000000/  DR FAIRBAIRN  LOV2 N40
COMPUTING 2000 INSTRUCTIONS
OUTPUT
0 LINE PRINTER 2000 LINES
STORE 25 BLOCKS


COMPILER AA
begin
real a,b,k,p,q,cosh,sinh,cosh1,tl,l,tm,m,z,tan,cs,sn,c,Tl,s
integer n,x,y,i,j
read (a,b,i,j)
k=a/b

cycle  x=0,1,i
cycle  y=0,1,j

tl=0;  tm=0;
p=x/a;  q=y/b;

cycle  n=0,1,40

c=((2*n+1)(π/2))
sinh=½(exp(c*k*p)-exp(-c*k*p))
cosh=½(exp(c*k*p)+exp(-c*k*p))
cosh1=½(exp(c*k)+exp(-c*k))
sn=sin(c*q)
cs=cos(c*q)
s=-(2*q)

l=(16/(π↑2))(((-1)↑n)/(((2*n)+1)↑2))((cosh*sn)/cosh1)
m=(16/(π↑2))(((-1)↑n)/(((2*n)+1)↑2))((sinh*cs)/cosh1)

tl=tl+l;  tm=tm+m;
->2 unless n=40
2:  repeat


Tl=tl+s
print(Tl,4,6)
spaces(2)
print(tm,4,6)
spaces(4)


z=  sq  rt ((Tl↑2) + (tm↑2))
print(z,4,6)
spaces(2)

->3 unless tm=0
tan=4000
```

```
07/04/67   18.51.28
EDINBURGH UNIVERSITY ATLAS AUTOCODE   16/01/67


CIE   003/00000000/  DR FAIRBAIRN  LOV2 , n=40.
     0   BEGIN
    47   END OF PROGRAM

PROGRAM (+PERM) OCCUPIES 2544 WORDS
PROGRAM DUMPED
COMPILING TIME   27 SEC /  8 SEC
    0.000000      0.000000      0.000000     LARGE      -0.028149      0.000000      0.028149     LARGE      -0.06
0666      0.000000      0.060666     LARGE      -0.102554      0.000000      0.102554     LARGE      -0.160122
  0.000000      0.160122     LARGE      -0.241630      0.000000      0.241630     LARGE      -0.357609      0.0000
00      0.357609     LARGE      -0.520054      0.000000      0.520054     LARGE      -0.739432      0.000000
  0.739432     LARGE


    0.000000      0.223254      0.223254      0.000000   LARGE      -0.026018      0.221175      0.222700      -0.11
7637   LARGE      -0.056089      0.214626      0.221834     -0.261334   LARGE      -0.094880      0.202650      0.
223762     -0.468197   LARGE      -0.148355      0.183592      0.236041     -0.808069   LARGE      -0.224550      0.
155150      0.272936     -1.447307   LARGE      -0.334284      0.114892      0.353477     -2.909552   LARGE      -
0.491045      0.061952      0.494937     -7.926216   LARGE      -0.708000     -0.000000      0.708000   49600665187
4631643.295288   LARGE


    0.000000      0.450566      0.450566      0.000000   LARGE      -0.019935      0.446712      0.447157      -0.04
4626   LARGE      -0.043005      0.434560      0.436683     -0.098961   LARGE      -0.072866      0.412264      0.
418654     -0.176747   LARGE      -0.114350      0.376516      0.393497     -0.303705   LARGE      -0.174448      0.
322322      0.366502     -0.541222   LARGE      -0.264038      0.243254      0.359010     -1.085443   LARGE      -
0.400596      0.134068      0.422435     -2.988004   LARGE      -0.608125     -0.000000      0.608125   68217398785
49124.114215   LARGE


    0.000000      0.685392      0.685392      0.000000   LARGE      -0.010800      0.680342      0.680428      -0.01
5875   LARGE      -0.023315      0.664397      0.664806     -0.035093   LARGE      -0.039572      0.635040      0.
636272     -0.062314   LARGE      -0.062340      0.587596      0.590894     -0.106093   LARGE      -0.095953      0.
514379      0.523252     -0.186542   LARGE      -0.148394      0.403186      0.429627     -0.368055   LARGE      -
0.238209      0.235605      0.335042     -1.011055   LARGE      -0.416395     -0.000000      0.416395   66030616934
876.888990   LARGE


    0.000000      0.930181      0.930181      0.000000   LARGE      -0.000048      0.924474      0.924474      -0.00
0051   LARGE      0.000093      0.907390      0.907390      0.000103   LARGE      -0.000135      0.875367      0.
875367     -0.000154   LARGE      0.000170      0.823719      0.823719      0.000207   LARGE      -0.000197      0.
743380      0.743380     -0.000265   LARGE      0.000209      0.618318      0.618318      0.000337   LARGE      -
0.000164      0.418284      0.418284     -0.000393   LARGE      -0.009885     -0.000000      0.009885   10219188829
.069025   LARGE


XO YJ

X1 YJ

XI YJ



STOPPED AT LINE  47
CIE   003/00000000/  DR FAIRBAIRN  LOV2
RUNNING TIME   19 SEC /  18 SEC
```

2. GRID-FRAMES.

```
***A
JOB
CIE  003/00000000/  D R FAIRBAIRN  MATRIX SOLVE  B/2/1 AND B/2/2
EXECUTION 30 SECONDS
COMPILER AA


begin
integer i,j,ctr,r,y
read(r,y)
begin
array A(1:y,1:y),B(1:y),X(1:y)
integer array  PERM (1:y)
routine spec MRLINEQ(array name A,B,X, integer array name PERM, integer n,Q)


comment  r is the number of matrices to be solved c
         y is the size of the matrix
ctr= 1
1: cycle i= 1,1,y
      cycle j= 1,1,y
      read  (A(i,j))
      repeat
repeat
cycle j= 1,1,y
read (B(j))
repeat

MRLINEQ(A,B,X,PERM,y,1)
caption $$$$$$ SOLUTION
newlines (2)
cycle i= 1,1,y
newline
print fl (X(i),7)
repeat


ctr= ctr + 1
if  ctr > r then  ->2

-> 1




routine MRLINEQ(array name A,B,X, integer array name PERM, integer n,Q)
real AMAX,CHANGE
integer i,j,jMAX,s
switch ENTER(1:2)
if n>1then ->ENTER(Q)
if  n<0then->2
X(1)=B(1)/A(1,1)
return
2:caption MRLINEQ$data$fauult,n<0;stop
ENTER(1): cycle i=1,1,n-1
AMAX=0; jMAX=0
cycle j=i,1,n
if mod(A(j,i))<AMAX then ->1
AMAX=mod(A(j,i)); jMAX=j
1:repeat
PERM(i)=jMAX
cycle j=i,1,n
CHANGE=A(i,j)
A(i,j)=A(jMAX,j)
A(jMAX,j)=CHANGE
repeat
cycle j=i+1,1,n
A(j,i)=A(j,i)/A(i,i)
cycle s=i+1,1,n
A(j,s)=A(j,s)-A(i,s)*A(j,i)
repeat
repeat
repeat
ENTER(2):cycle i=1,1,n
X(i)=B(i)
repeat
cycle i=1,1,n-1

CHANGE=X(PERM(i))
X(PERM(i))=X(i)
X(i)=CHANGE
cycle j=i+1,1,n
X(j)=X(j)-A(j,i)*X(i)
repeat
repeat
X(n)=X(n)/A(n,n)

cycle i=n-1,-1,1
cycle j=i+1,1,n
X(i)=X(i)-A(i,j)*X(j)
repeat
X(i)=X(i)/A(i,i)
repeat
end
2:  end
end of program

***T

1   14
2.681 0 1.186 0 0 0 0 -0.309 0 0 0 0 0 0
0 2.681 0 -0.309 0 0 0 0 -0.197 1.186 0 0 0 0
1.186 0 2.681 0 -0.309 0 0 0 0 0 0 0 0 0
0 -0.309 0 2.681 0 -0.197 1.186 0 0 0 0 0 0 0
0 0 -0.309 0 2.99 0.197 0 1.186 -0.197 0 -0.309 0 0 0
0 0 0 -0.197 0.197 0.066 0 0.197 -0.022 0 0 0.197 0 0
0 0 0 1.186 0 0 5.053 0 0 -0.309 0 1.186 0 0
-0.309 0 0 0 1.186 0.197 0 2.99 -0.197 0 0 0 -0.309 0
0 -0.197 0 0 -0.197 -0.022 0 -0.197 0.066 0 0 0 0 0.197
0 1.186 0 0 0 0 -0.309 0 0 5.053 0 0 0 1.186
0 0 0 0 -0.309 0 0 0 0 0 2.681 0 1.186 0
0 0 0 0 0 0.197 1.186 0 0 0 0 2.681 0 -0.309
0 0 0 0 0 0 0 -0.309 0 0 1.186 0 2.681 0
0 0 0 0 0 0 0 0 0 0.197 1.186 0 -0.309 0 2.681
0 0 0 0 0 0 0 0 0 1 0 0 0 0 0


*** Z
```

```
10/04/67   17.13.19
EDINBURGH UNIVERSITY ATLAS AUTOCODE   16/01/67


CIE  003/00000000/  D R FAIRBAIRN  MATRIX SOLVE  B/2/1 AND B/2/2.
     0   BEGIN
     3      BEGIN
    27         ROUTINE MRLINEQ
    73         END OF ROUTINE
    74      END OF BLOCK
    75   END OF PROGRAM

PROGRAM (+PERM) OCCUPIES 2682 WORDS
PROGRAM DUMPED
COMPILING TIME   21 SEC /  10 SEC
      SOLUTION


 1.5619413₁₀ -1
 5.0311233₁₀  0
 1.5619413₁₀ -1
 2.3333626₁₀  0
 1.9547013₁₀  0
 2.3863595₁₀  1
-4.5593660₁₀-13
 1.9547013₁₀  0
 6.4809303₁₀  1
 4.3729505₁₀-12
 1.5619413₁₀ -1
-2.3333626₁₀  0
 1.5619413₁₀ -1
-5.0311233₁₀  0


STOPPED AT LINE  75
CIE  003/00000000/  D R FAIRBAIRN  MATRIX SOLVE  B/2/1 AND B/2/2.
RUNNING TIME   3 SEC /  2 SEC
```